Stress and signalling in Arabidopsis in response to the pollutant 2,4,6-trinitrotoluene (TNT)

Emily Jane Johnston

Doctor of Philosophy

University of York

Biology

September 2015

Abstract

The explosive 2,4,6-trinitrotoluene (TNT) is a persistent and toxic pollutant. High levels of TNT and the water-mobile co-pollutant Royal Demolition Explosive (RDX) have accumulated at manufacturing waste sites and military training ranges. Due to the scale of these sites, phytoremediation could be the most cost-effective and environmentally-friendly means of cleaning up the pollution. Plant lines which are both tolerant to, and able to degrade explosives pollution, are therefore being developed.

Prior to this PhD research, it was identified that *Arabidopsis thaliana* L. (Arabidopsis) plants deficient in MONODEHYDROASCORBATE REDUCTASE 6 (MDHAR6; At1g63940) have hugely enhanced TNT tolerance. In Chapter 3, the means behind this enhanced TNT tolerance is investigated. Enzymatic analysis identified that purified MDHAR6 reduces TNT by one electron, to a TNT nitro radical which autoxidises, generating superoxide. Reactive superoxide can oxidise and damage protein, DNA and lipids. This reaction could also be inhibitory to plant development, due to the futile use of NADH.

In Chapter 4, the organelle-targeting of MDHAR6 is investigated; MDHAR6 is unusual in that dual targeting to mitochondria or plastids appears to be dependent on the transcription start site used. A further understanding of MDHAR6 location would provide useful insight as to the endogenous role of this enzyme. Preliminary experiments indicate that *MDHAR6* is more highly expressed in roots than leaves, and that a previously undescribed third transcription start site is dominant, encoding plastid-targeted MDHAR6.

The induction of detoxification genes following TNT treatment is explored in Chapter 5; the profile of detoxification genes induced following TNT treatment is similar to that following phytoprostane treatment, which requires class II TGACG-binding (TGA) factors. It is identified that induction of detoxification genes following TNT treatment also requires class II TGA factors, but the induction is not mediated by phytoprostanes.

Table of contents

List of figures

List of tables

Acknowledgements

A HUGE thank you to everyone who's helped and supported me over the last four years:

To Neil Bruce for all your advice, guidance and calming influence.

To Liz Rylott for your endless enthusiasm, and generous time given for discussing research.

To my Training Advisory Panel members, Louise Jones, Ian Graham and Antony Dodd, for also taking the time to guide me in this research.

To everyone in CNAP who have helped with my introduction to lab life. This has been an exceptionally enjoyable environment to learn and to work in, due to being filled with lovely people who take the time to support others around them.

I am very grateful to those who isolated and characterised the *mdhar6* mutants (Liz Rylott, Astrid Lorenz, Emily Beynon and Maria Budarina), to Luisa Elias for her kind assistance in using the AktaPurifier, and to Victor Chechik for help with the EPR spectrometry experiments. I am also grateful to Christiane Gatz, Robert Edwards and Ian Graham for providing seed lines used in this research.

Finally, a huge thank you to my fantastic family and friends for their tremendous support, particularly Billy Jones, Amy Sawtell, Dana Sabir and Lenka Havlickova.

Bruce Group, 2014

Author's declaration

I declare that the work presented in this thesis is my own original research, except where due reference has been given to collaborators and co-workers.

This thesis has not previously been presented for an award at this, or any other, University.

All sources are acknowledged as references.

Publications arising from this research

Johnston, E.J., Rylott, E.L., Beynon, E., Lorenz, E., Chechik, V., Bruce, N.C. (2015). Monodehydroascorbate reductase mediates TNT toxicity in Arabidopsis. *Science* 349, 1072-1075.

1 Introduction

1.1 THE EXPLOSIVE 2,4,6-TRINITROTOLUENE (TNT)

1.1.1 Chemical properties

The synthetic compound TNT (Figure 1) is a common energetic component of explosives, produced by combining toluene with nitric and sulphuric acids. The chemical properties of TNT are summarised in Table 1. Upon detonation, TNT decomposes exothermically, yielding CO_2, N_2, H_2, H_2O and C (Scheme 1). The activation energy required for these reactions is approximately 35 kcal.mol^{-1} in condensed phase, and 62 kcal.mol^{-1} in gas phase (Furman et al., 2014).

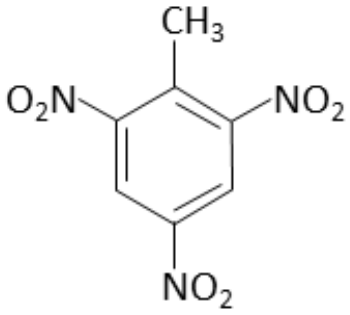

Figure 1: The chemical structure of TNT

Table 1: The chemical properties of TNT

Chemical Abstracts Service number 118-96-7. Reference; US. EPA (2014a).

Property	Value
Appearance at room temperature	yellow, ordourless, crystalline solid
Molecular weight	227.13 g/mol
Melting point	80.1 °C
Boiling point	240 °C
Ignition temperature	300 °C
Activation energy	34.18 kcal/mol
Water solubility at 20 °C	130 mg/L
Octanol-water partitioning coefficient (Log K_{OW})	1.6 (measured)
Soil organic carbon-water partitioning coefficient (K_{OC})	300 (estimated)

$$2\ C_7H_5N_3O_6 \rightarrow 3\ N_2 + 5\ H_2O + 7\ CO + 7\ C$$

$$2\ C_7H_5N_3O_6 \rightarrow 3\ N_2 + 5\ H_2 + 12\ CO + 2\ C$$

Scheme 1: Decomposition reactions of TNT

Reference; Furman et al. (2014).

1.1.2 History

German chemist Joseph Wilbrand was the first to synthesise TNT, in 1863 (Akhavan, 2004). Before the explosive properties of TNT were appreciated, the aromatic was manufactured for use as a yellow dye (US EPA, 2012).

Germany began using TNT in artillery shells instead of picric acid (2,4,6-trinitrophenol) in 1902 (Akhavan, 2004). This had great advantages; while picric acid is highly shock-sensitive, exploding upon impact, TNT is more stable, penetrating targets before explosion, hence having a greater destructive effect. The low melting point and thermal stability of TNT, is also more amenable to casting into shells. The US Army began using TNT in 1912, and by 1914, TNT was a standard explosive for all World War I armies (Akhavan, 2004).

Today, TNT remains one of the most common bulk explosives, used in military ordinance, and in mining and quarrying operations (Pichtel, 2012). As TNT does not contain enough oxygen to oxygenise all the carbon, it is commonly mixed with oxygen-rich compounds, to yield more explosive energy per kg than TNT alone. Examples of compositions containing TNT are included in Table 2.

Table 2: Compositions of military explosives containing TNT

RDX; Royal Demolition Explosive, i.e. 1,3,5-trinitroperhydro-1,3,5-triazine. HMX; High Melting Explosive, i.e. octahydro-1,3,5,7-tetranitro-1,3,5,7-tetrazocine. PETN; pentaerythitol tetranitrate. References; Akhavan (2004) and Pichtel (2012).

Name	Composition
Amatex	TNT, ammonium nitrate, RDX
Ammonal	TNT, ammonium nitrate, RDX
Anatols	TNT, ammonium nitrate
Baratol	TNT, barium nitrate
Composition B	RDX (60 %), TNT (39 %), wax (1 %)
Cyclotol	RDX, TNT, wax
HTA-3	HMX, TNT, aluminium
Minol-2	TNT (40 %), ammonium nitrate (40 %), aluminium (20 %)
Octol	HMX (75 %), TNT (25 %)
Pentolite	PETN (50 %), TNT (50 %)
Picratol	Picric acid (52 %), TNT (48 %)
Tetryol	Tetryl (70 %), TNT (30 %)
Torpex	RDX (40 %), TNT (40 %), aluminium (18 %)
Tritonal	TNT (80 %), aluminium (20 %)

1.1.3 Detrimental effects

Exposure to TNT has had toxic effects on all organisms tested, including earthworms (Lachance et al., 2004) and amphibians (Paden et al., 2011). In soil, TNT decreases the density and diversity of microbial communities (George et al., 2008, 2009; Travis et al., 2008a, 2008b), and limits the establishment of vegetation (Travis et al., 2008b).

Plants exhibit greatly stunted growth in the presence of low concentrations of TNT; on agar plates, roots of 7-day old Arabidopsis seedlings are approximately half as long in the presence of 2 µM TNT (Johnston et al., 2015). On soil, 300 mg TNT.kg soil^{-1} is lethal to Arabidopsis (Johnston et al., 2015). Generally, monocots are more tolerant to TNT than dicots (Gong et al., 1999).

The toxicity of TNT to people was discovered in World War I, during which time TNT poisoning was reported in >17,000 munitions factory workers, with >475 fatalities (US EPA, 2014a). The main toxicity symptom of TNT is hepatitis, however TNT is also rated a class C carcinogen by the US Environmental Protection Agency (EPA), causes hyperplasia of bone marrow and induces cataract formation (ATSDR, 1995).

Induction of neuronal damage following TNT exposure has also been reported in rats (Zitting et al., 1982). Kumagai et al. (2004) attribute this to the one electron reduction of TNT by neuronal nitric oxide synthase. This generates a TNT nitro radical, which autoxidises, producing superoxide. This group also identified that bovine lens ζ-crystallin similarly reduces TNT by one electron, which could be the cause of TNT-induced cataracts (Kumagai et al., 2000).

The cause of TNT toxicity to plants has been previously unknown.

1.2 EXPLOSIVES POLLUTION

1.2.1 Co-pollutants with TNT

As shown in Table 2, TNT is used in munitions in combination with other compounds, most commonly RDX. Energetic compounds are categorised as primary, secondary or tertiary, depending on sensitivity to detonation; primary explosives (e.g. silver azide, lead styphnate, mercury fulminate) are highly sensitive to detonation, and are commonly used to initiate detonation of secondary explosives (e.g. TNT, RDX, HMX, PETN, Tetryl, ammonium picrate). Tertiary explosives (e.g. ammonium nitrate with fuel oil), require primary and secondary explosive ignition for detonation. The structures of organic co-pollutants of TNT are shown in Figure 2. Along with TNT, RDX and perchlorate are high priority targets for remediation.

Royal Demolition Explosive (RDX)

The explosive properties of RDX were recognised in 1920, and after a manufacturing route was established, RDX began to be added to TNT in munitions during World War II, to increase explosive power (Akhavan, 2004). The nitramine has been found to cause convulsions (Burdette et al., 1988), is classified as a possible human carcinogen, and can damage the nervous system if inhaled or ingested (US EPA, 2014b). Although RDX can be degraded and used as a nitrogen source by some bacterial species (Chong et al., 2014), high levels of pollution persist (Pichtel, 2012). Unlike TNT, RDX has a low soil organic carbon-water partitioning coefficient (K_{OC} 1.80), and can readily leach into groundwater and aquifers; RDX has already been detected in the Cape Cod Aquifer (the sole-source drinking water aquifer near the Camp Edwards Massachusetts Military Reservation, US), prompting a high level of regulatory and public scrutiny (Clausen et al., 2004). This mobility makes RDX a high priority for explosives remediation (Rylott and Bruce, 2009).

Perchlorate

Perchlorate (ClO^{4-}) is both a naturally occurring and man-made salt, which is commonly used as an oxidiser in munitions, fireworks and vehicle airbag initiators, and is also found in herbicides and disinfectants (US EPA, 2014c). Perchlorate is used in >250 different munitions and >40 missile systems used by the US Department of Defense (Trumpolt et al., 2005), and migrates quickly from soil to groundwater. Perchlorate is now classed as a "persistent contaminant of concern" by the EPA (US EPA, 2014c), as perchlorate can disrupt thyroid function (ATSDR, 2008). Due to this, the US EPA has initiated a proposal for a national primary drinking water regulation for perchlorate (US EPA, 2014c).

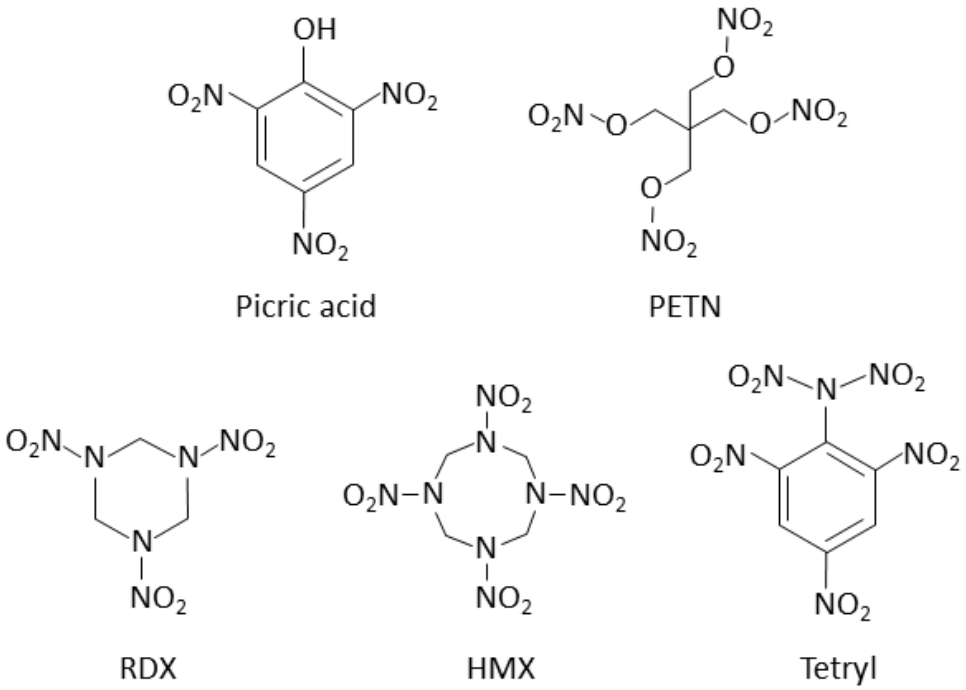

Figure 2: The chemical structures of TNT co-pollutants

PETN; pentaerythitol tetranitrate. RDX; Royal Demolition Explosive, i.e. 1,3,5-trinitroperhydro-1,3,5-triazine. HMX; High Melting Explosive, i.e. octahydro-1,3,5,7-tetranitro-1,3,5,7-tetrazocine. Tetryl; trinitrophenylmethylnitramine.

1.2.2 Lifetime health advisory limits

The US EPA publishes Soil Screening Levels for pollutants, as advisory target levels in clean-up programmes. The recommended screening levels for TNT, RDX, HMX and perchlorates are shown in Table 3.

Table 3: US EPA advisory screening levels for TNT and co-pollutants

Reference; US EPA (2015a). SSL; Soil Screening Level. Screening levels for picric acid not available.

Pollutant	Industrial SSL (mg.kg soil^{-1})	Residential SSL (mg.kg soil^{-1})	Tap water screening level (µg.L^{-1})
TNT	96	21	2.5
RDX	28	6	0.7
PETN	580	120	19
Tetryl	1,600	120	39
HMX	57,000	3,800	1,000
Perchlorate and perchlorate salts	820	55	14

1.2.3 Sites of contamination

Pichtel (2012) provides a comprehensive review of explosives pollution at manufacturing waste sites, military training ranges, and former conflict zones. Specific examples of polluted sites are provided in Table 4 and Table 5. In the US, TNT is present at >30 sites on the EPA National Priorities List (US EPA, 2014a). The presence of explosives pollution impedes the re-sale of land for industrial or residential purposes, and in some cases, the further use of land for military training (Clausen et al., 2004; Pichtel, 2012).

Historically, in many countries unlined lagoons were used for the disposal of wastewater from ordnance manufacturing and decommissioning (Pichtel, 2012). High concentrations of explosives have now accumulated at these sites (Table 4).

Military training ranges and former conflict zones are polluted with both unexploded ordinance (UXO) which malfunctioned upon firing, constituents of which can leak into the soil, and unexploded residues of ordinance which successfully detonated; for example, Taylor et al. (2004) estimate that up to 2 % of TNT in a high-order 155 mm howitzer round persists on soil after detonation. In surface waters, TNT undergoes rapid photolysis to degradation products including 1,3,5-trinitrobenzene (US EPA, 2014), however soil sampling at military live-fire ranges, which is often restricted to surface soils due to the risk of detonating UXO below ground, has identified TNT at high concentrations; in an extensive survey of energetic residue distribution across 27 military installations in the US and Canada, published by Pennington et al. (2006), the average concentration of TNT in soil was generally low (<2 $mg.kg^{-1}$), with the exception of live-fire bombing range impact areas, and soil near or beneath sites of partial (low-order) artillery ordnance detonation, where TNT concentration regularly reached >1,000 $mg.kg^{-1}$ (Table 6).

The US Department of Defense has used an estimated 10 million hectares of land for ordnance testing and military training (United States General Accountability Office, 2004). Clean-up estimates for this land have ranged from $16 billion to $165 billion (United States General Accountability Office, 2004).

Explosives pollution will continue to be an issue while manufacturing, training and use of ordnance in warfare is considered necessary.

Table 4: Examples of explosives-polluted waste sites from manufacturing operations

Site	Overview	Reference
Explosives Factory Maribyrnong, Victoria, Australia	A survey of the factory waste lagoon concluded there to be an estimated 5 tonnes of TNT-contaminated soil, relatively unchanged since TNT production ceased in 1944. The pollution included a near pure layer of TNT 10 – 15 cm below the soil surface, predicted to persist for 2,000 years.	Martel et al. (2007)
The Panex Plant, US	The solid waste management unit at this site is contaminated with TNT, RDX and HMX, with concentrations highest at 10 m depth, continuing to depths of 85 m. Contamination has also been detected offsite, threatening the Ogallala aquifer- the region's primary source of drinking water.	Pichtel (2012)
WerkTanne, Clausthal-Zellerfeld, Germany	Concentration of TNT ranged from <0.05 to 5,525 mg/kg in soil, and <0.05 to 62 mg/L in soil water, which had genotoxic effects in laboratory studies.	Eisentraeger et al. (2007)

Table 5: Estimated scale of explosives pollution at former conflict zones

Site	Overview	Reference
Iraq	An estimated 1,730 km^2 of affected land, including 20 million mines, numerous UXO sites, and many abandoned munitions sites.	Pichtel (2012)
Vietnam	An estimated 350,000 – 800,000 tonnes of ordnance contaminated soil, affecting approximately 7 – 8 % of the country.	Pichtel (2012)
Nagorno-Karabakh	Landmines and UXO are estimated to affect 37 million m^2 of arable land and 35 million m^2 of pasture, with 80,000 m^2 of vineyards rendered unusable.	Pichtel (2012)

Table 6: Distribution of TNT and RDX residues at live-fire military training ranges

Average concentration of energetics in soil samples for 27 military installations in the US and Canada are provided by Pennington et al. (2006). The minimum and maximum average values reported for TNT and RDX are shown in this table.

Soil sample origin	Average concentration for military installation minimum ($mg.kg^{-1}$)		Average concentration for military installation maximum ($mg.kg^{-1}$)	
	TNT	RDX	TNT	RDX
Hand grenade ranges	<0.01	<0.01	36	51
Adjacent to targets at anti-tank rocket ranges	0.04	<0.1	125	5.3
Near artillery targets	<0.001	<0.003	19	16
Near low-order detonations at artillery targets	<1	<1	143,000	678
Below low order detonations at artillery ranges	<0.001	<0.01	15,100	832
Live-fire bombing range impact areas	<0.01	<0.01	3,720	0.56
Demolition ranges where C4 used to detonate high order munitions	<0.01	<0.03	11.6	60.2

1.3 REMEDIATION OF TNT FROM POLLUTED SITES

Approaches to removing and destroying TNT pollution are presented below. For remediation from groundwater, enhancement of TNT transformation by indigenous microbial communities is a promising approach. For remediation from soil, the use of plants *in situ* could be the most cost-effective and environmentally-friendly solution.

1.3.1 *Ex situ* granular activated carbon treatment of groundwater and wastewater

Granular activated carbon adsorption is the most commonly used *ex situ* method for treating explosives-contaminated water in the US (US EPA, 2014a); water is pumped through vessels containing activated carbon, to which the dissolved organic contaminants adsorb, and are removed for disposal. This is a method for TNT removal rather than destruction.

1.3.2 *In situ* bioremediation in groundwater

The capacity of anaerobic and aerobic bacteria to reduce TNT to hydroxylamino-dinitrotoluene (HADNT) and amino-dinitrotoluene (ADNT) appears to be relatively widespread (Rylott et al., 2011b). Some bacterial flavoproteins from the Old Yellow Enzyme family additionally transform TNT, by hydride addition to the aromatic ring, forming monohydride-Meisenheimer or dihydride-Meisenheimer complexes. The hydride-Meisenheimer complexes can condense with HADNT to form stable diarylamines (Rylott et al., 2011b). It does not appear that TNT is mineralised by microbes; instead, the reduced TNT derivatives polymerise with each other and other organic compounds, to polymers with low solubility and toxicity (Pennington et al., 1995).

Considering that biodegradation of TNT may be limited by concentrations of substrates for co-metabolism, a recent field study at the Picatinny Arsenal in New Jersey, US, implemented a groundwater extraction-reinjection system, to distribute and mix cheese whey into groundwater (Hatzinger and Lippincott, 2012). Groundwater samples before the trial contained 5 – 190 µg/L TNT and 5 – 170 µg/L RDX. Four cycles of extraction-reinjection were carried out, and groundwater samples one year later contained TNT and RDX at levels below the detection limit (0.25 µg/L). This system appears to be a viable method for reducing levels of nitramine and nitroaromatic explosives in groundwater, utilising indigenous bacteria, at an estimated cost of $1.29 per gallon.

1.3.3 *Ex situ* incineration of soil

Low concentrations of TNT in soil can be destroyed by incineration (US EPA, 2014a), including by hot gas (260 °C steam), or rotary kiln incineration (temperatures 427 – 649 °C; FRTR, 2007a). Incineration of soil is associated with high costs, due to the need to remove (with care for UXO) and transport the soil, and to fuel the high temperatures required. Incineration also damages soil structure and microbial communities.

1.3.4 *Ex situ* composting of soil

Composting of soil and sludges to treat explosives pollution has been investigated by the US Department of Defense since the early 1980s (FRTR, 2007b). Composting has the benefits of, unlike incineration, providing enriched product, which can sustain vegetation, and has been effective in transforming and degrading energetic pollutants (FRTR, 2007b). As detailed earlier, TNT is not completely degraded by microbial communities; in a composting study with radiolabelled TNT by Pennington et al. (1995), over half of added radioactivity was recovered in the cellulose and humic fractions, and almost no radiolabelled CO_2 was produced. Similar to incineration, composting also shares the costs of removing and transporting soil.

1.3.5 *In situ* landfarming of soil

In landfarming, soil is excavated to specific plots, for periodical tilling to mix in nutrients, moisture and bacteria. This has been used extensively to treat soil contaminated with persistent organic pollutants such as polycyclic aromatic hydrocarbons (FRTR, 2007b), however landfarming for removal of explosives has had limited success (FRTR, 2007b).

1.3.6 *In situ* phytoremediation from soil and groundwater

Phytoremediation is the use of plants to remove contaminants from soil and/or groundwater through phytodegradation (degradation in the plant), rhizodegradation (degradation by microbial communities in the rhizosphere), phytosequestration (pollutant containment, preventing access to groundwater) or phytovolatization (release into the atmosphere through transpiration). Although TNT is phytotoxic, plants are able to detoxify TNT to a limited extent (discussed in 1.4.3), and pollutant-degrading capabilities can be enhanced by the use of genetic engineering to introduce specific combinations of transgenes, to appropriate plant species (Rylott et al., 2015).

With regards to explosives remediation, resilient and fast-growing grasses, with extensive root networks, are appropriate for use on military ranges. Poplar has been used previously to remediate groundwater pollution at US EPA Superfund sites (US EPA, 2015b), and could also

be used at site perimeters. Prior phytoremediation studies within Neil Bruce's group have focused on introducing RDX-degrading capabilities to plants; *Arabidopsis thaliana* L. (Arabidopsis) plants expressing RDX-degrading cytochrome P450 *XplA,* and reductase *XplB,* from *Rhodococcus rhodochrous* strain 11Y, together with *Enterobacter cloacae* nitroreductase *nfsI*, successfully remove RDX (the primary remediation target) from soil leachate (Rylott et al., 2011a). These microbial genes have now been transferred to switchgrass (*Panicum virgatum* Alamo), a native species at many US training ranges (Rylott et al., 2015).

The use of plants for *in situ* remediation is preferable to *ex situ* composting and incineration, as the high costs of soil removal are avoided, and military training operations could be continued on site while remediation is taking place. Even without engineered explosive-degrading capabilities, explosive-tolerant plants could have a huge impact on contaminated sites; plants are important for soil stabilisation, and diverse plant communities promote microbial diversity and density (Lange et al., 2015). Furthermore, there is extensive evidence that metabolites in root exudates promote microbial degradation of pollutants, either through stimulating microbial growth and diversity, and/or providing co-metabolites for degradation of organic pollutants (Singer et al., 2003).

1.4 DETOXIFICATION IN PLANTS

Although TNT is phytotoxic, plants are able to detoxify the nitroaromatic to a limited extent. Understanding endogenous TNT detoxification pathways in plants, and the limiting steps, is important for the development of robust lines for phytoremediation. The process of detoxification in plants, and TNT detoxification in Arabidopsis, is discussed below.

1.4.1 The process of detoxification in plants

The process of detoxifying xenobiotics (foreign compounds) and aberrant endogenous compounds in plants, can typically be categorised into three phases (Sandermann Jr., 1992).

Phase I: Activation

Functional groups are exposed or added to the xenobiotic, which allow progression into phase II. These reactions are most commonly catalysed by cytochromes P450 (P450s; 244 genes and 28 pseudogenes in Arabidopsis; Bak et al., 2011), carboxylesterases (20 genes in Arabidopsis; Marshall et al., 2003) and/or oxophytodienoate reductases (OPRs; 6 genes in Arabidopsis; Beynon et al., 2009).

Phase II: Conjugation

Polar metabolites are conjugated to the activated xenobiotic, which can increase solubility and stability, and decrease toxicity. Common conjugates are glutathione, conjugated by glutathione *S*-transferases (GSTs; 55 genes in Arabidopsis; Dixon and Edwards, 2010), glucose, conjugated by uridine diphosphate-glycosyltransferases (UGTs; 107 genes in Arabidopsis; Ross et al., 2001) and malonate, conjugated by malonyltransferases (MTs; 4 genes in Arabidopsis; TAIR, 2015).

Phase III: Sequestration

Conjugated xenobiotics are recognised by transporters (most commonly ATP binding cassette transporters; 136 genes in Arabidopsis; Verrier et al., 2008), which import the conjugate into the cell vacuole, where further modifications may take place (Phase IV). In some cases the xenobiotic may be exported to the apoplast, and become incorporated into cell wall components (Sandermann Jr., 1992).

1.4.2 Arabidopsis detoxification genes induced by TNT treatment

In order to identify early TNT-response detoxification genes, the products of which may have a role in TNT detoxification, Lorenz (2007) used an Affymetrix GeneChip microarray. Two-week old seedlings, in liquid ½ MS culture, were treated with 60 µM TNT or a control treatment (0.06 % DMF) for 6 h (full experimental details in 2.1.2). The microarray experiment was published by Gandia-Herrero et al. (2008).

Prior to the array, Lorenz (2007) had carried out preliminary tests to establish the most practical method of TNT treatment, with minimised general stress responses. Dosing seedlings in liquid culture was more practical than transferring seedlings to TNT-supplemented agar, as sterile conditions were more easily maintained, and the seedlings more evenly dosed. Whole seedlings were snap frozen in liquid nitrogen, to avoid the additional stress of wounding while separating tissues.

In a prior study by Ekman et al. (2003), two-week old seedlings growing in liquid ½ MS were treated with various concentrations of TNT (0, 5, 10, 15, 20, 25, 30 and 40 $mg.L^{-1}$), and five days after treatment, 15 $mg.L^{-1}$ (66 µM) TNT was judged to produce visual stress (leaf chlorosis and necrosis) without causing death, and considered an appropriate TNT concentration for studying transcriptome responses. Ekman et al. (2003) then used Serial Analysis of Gene Expression (SAGE) to identify transcriptome changes in roots of the two-week old seedlings treated with TNT for 24 h; in this method, cDNA is biotin-tagged, captured on a streptavidin column, then cleaved, leaving "tags" of approximately 11 nucleotides, which are then sequenced and annotated. Comparing the TNT treatment with a control treatment, Ekman et al. (2003) reported a five-fold increase in abundance of 242 tags, and a five-fold decrease of 287 tags.

Lorenz (2007) dosed two-week old seedlings in ½ MS with 60 µM TNT or a control treatment (0.06 % DMF) for 1, 2, 4, 6 or 24 h, and used semi-qPCR to measure the expression of seven of the TNT response genes identified by Ekman et al. (2003); a sucrose synthase (At5g20830), *GSTU24* (At1g17170), a tolB-related protein (At4g01870), *NAC102* (At5g63790), *CYP81D11* (At3g28740) and *GSTU8* (At3g09270). After 6 h 60 µM TNT treatment, induction of two of these genes (*GSTU24* and *CYP81D11*) was observed, and the 6 h time point was chosen for studying early transcriptome changes in response to TNT treatment. In response to 6 h 60 µM TNT treatment, Arabidopsis OPR, 12 P450, 15 UGT, 15 GST, 1 MT and 11 ABC transporter genes were induced over two-fold (Gandia-Herrero et al., 2008; Figure 3). The roles of the most upregulated OPRs, UGTs and GSTs in TNT detoxification have been investigated, as discussed below.

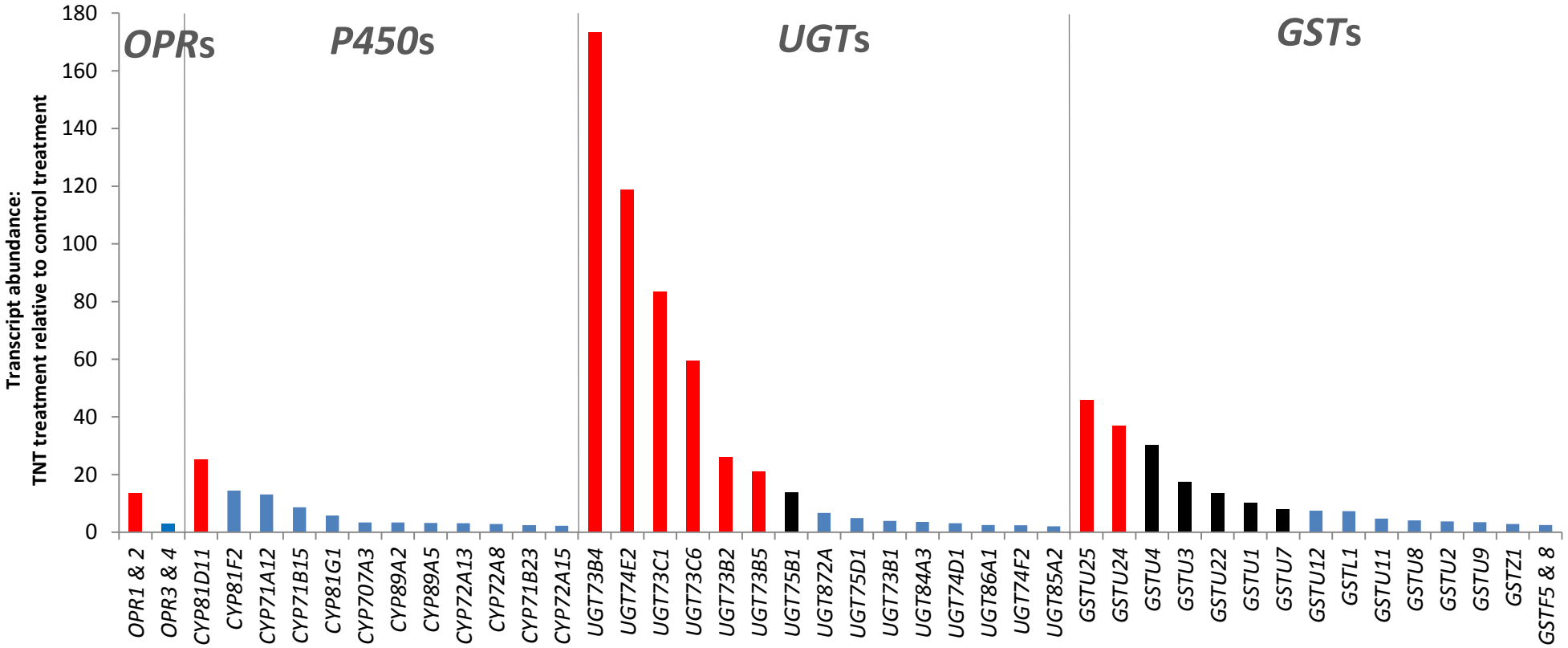

Figure 3: Phase I and II detoxification genes induced by 6 h 60 µM TNT treatment

Detoxification genes with >2-fold higher transcript abundance in 6 h 60 µM TNT-treated seedlings compared with control-treated seedlings (Gandia-Herrero et al., 2008). Red bars; enzyme has since been found to have activity towards TNT or TNT derivatives. Black bars; enzyme has been found not to have activity towards TNT or TNT derivatives. Blue bars; activity towards TNT and derivatives not yet tested. Where "&" between genes; microarray probe not specific to single gene.

1.4.3 Detoxification of TNT in Arabidopsis

Products of the most TNT-induced *OPR*, *UGT* and *GST* genes have been investigated for activity towards TNT.

Phase I (Activation) TNT-detoxification reactions

The enzymes OPR1, OPR2 and OPR3 reduce TNT to hydroxylaminodinitrotoluene (HADNT) and then aminodinitrotoluene (ADNT) *in vitro*, with OPR1 also generating hydride- and dihydride-Meisenheimer complexes (Beynon et al., 2009). These reactions are shown in Figure 4. Arabidopsis seedlings overexpressing *OPR1* or *OPR2* grow longer roots than wild type (WT) on 2 µM TNT ½ MS(A), and have greater overall biomass than WT in liquid media containing 200 µM TNT (Beynon et al., 2009).

Phase II (Conjugation) TNT-detoxification reactions

Six UGTs have been found to conjugate glucose to 2-HADNT and 4-HADNT (and to a lesser extent 2-ADNT and 4-ADNT) *in vitro* (Gandia-Herrero et al., 2008). These conjugates are shown in Figure 5, and have been identified in plant extracts and growth media. Increased levels of the conjugates were identified in extracts and growth media of both *UGT73B4* and *UGT73C1* overexpression lines, and *UGT73B4* overexpressing plants have increased root growth in the presence of TNT compared with WT (Gandia-Herrero et al., 2008).

The products of the two most TNT-induced GST genes, GSTU24 and GSTU25, conjugate glutathione to HADNT via the methyl group, and GSTU25 additionally conjugates glutathione directly to the aromatic ring of TNT, replacing a nitro group (Gunning et al., 2014). These conjugates are shown in Figure 6. Arabidopsis seedlings overexpressing *GSTU24* or *GSTU25* have greater biomass than WT in the presence of TNT (Gunning et al., 2014).

Phase III (Sequestration) TNT-detoxification reactions

Conjugation of TNT derivatives to glucose and glutathione presumably promotes sequestration to cell vacuoles. In a *Phaseolus vulgaris* L. (bushbean) cell fractionation study by Sens et al. (1998), approximately 50 % of [^{14}C]-TNT was detected in cell wall fractions (mostly in lignin and hemicellulose fractions), with thin layer chromatography Rf values indicating covalent binding to cell wall components. It therefore appears that TNT derivatives may be exported to the apoplast. Schoenmuth and Pestemer (2004) assessed the uptake of [^{14}C]-TNT by four-year old hybrid willow (*Salix spec* clone EW-20) and Norway spruce (*Picea abies*), and found after two months that 80 % of ^{14}C was non-extractably bound in root, stem, leaf and needle tissue, with the majority remaining in root tissue.

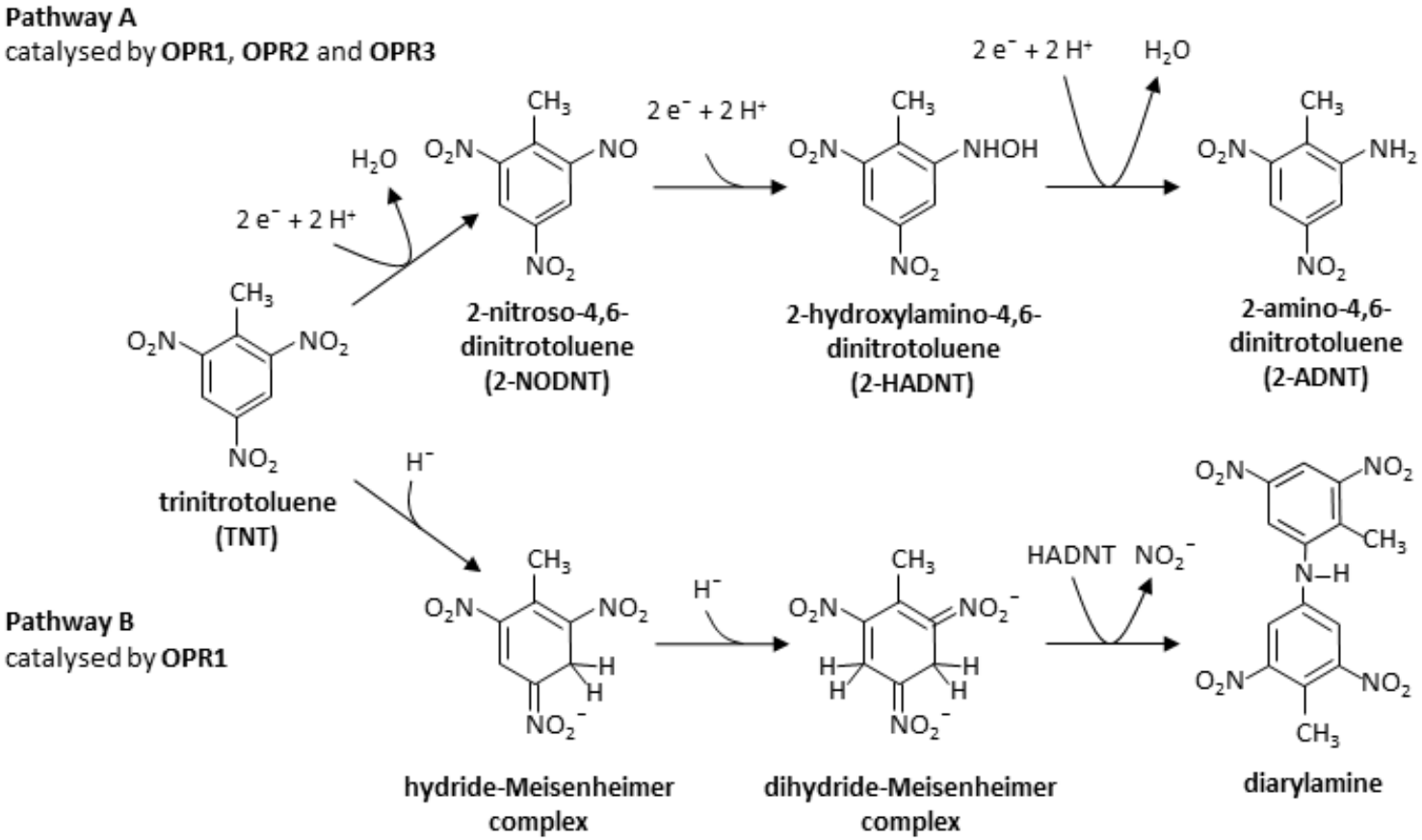

Figure 4: Reduction of TNT in Arabidopsis by oxophytodienoate reductase enzymes

Adapted from Beynon et al. (2009). Reduction of the nitro group in position 2 shown. The nitro group at position 4 can alternatively be reduced. The OPR1 and OPR2 enzymes are cytosolic, while the OPR3 enzyme is peroxisomal (TAIR, 2015).

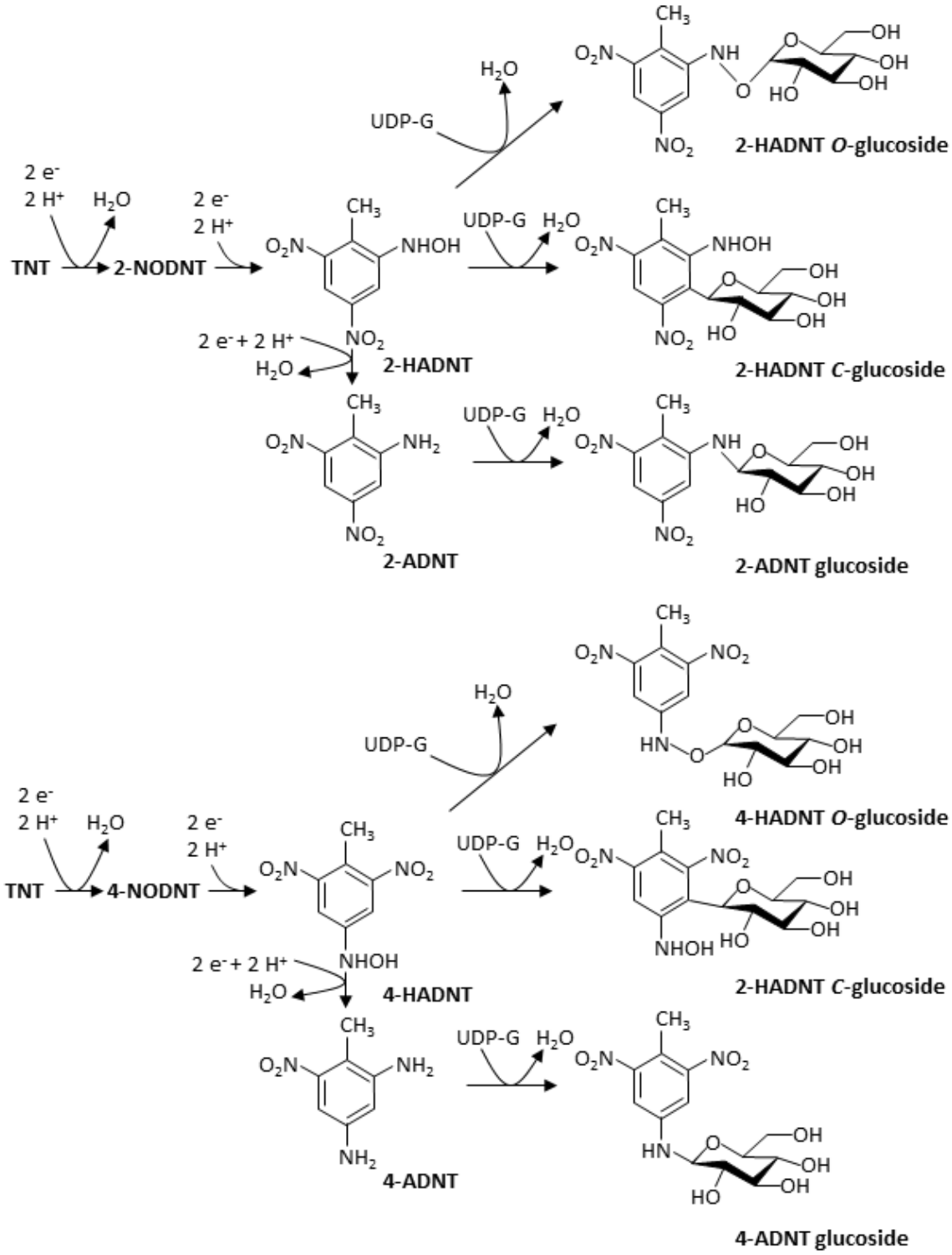

Figure 5: Glycosylation of TNT derivatives in Arabidopsis

Adapted from Gandia-Herrero et al. (2008). UDP-G; uridine diphosphate-glucose. Of the six UGTs which conjugate glucose to TNT, three are of unknown subcellular location, UGT73B4 is cytosolic, UGT73C1 is plastidial, and UGT73B5 is associated with endomembranes (TAIR, 2015).

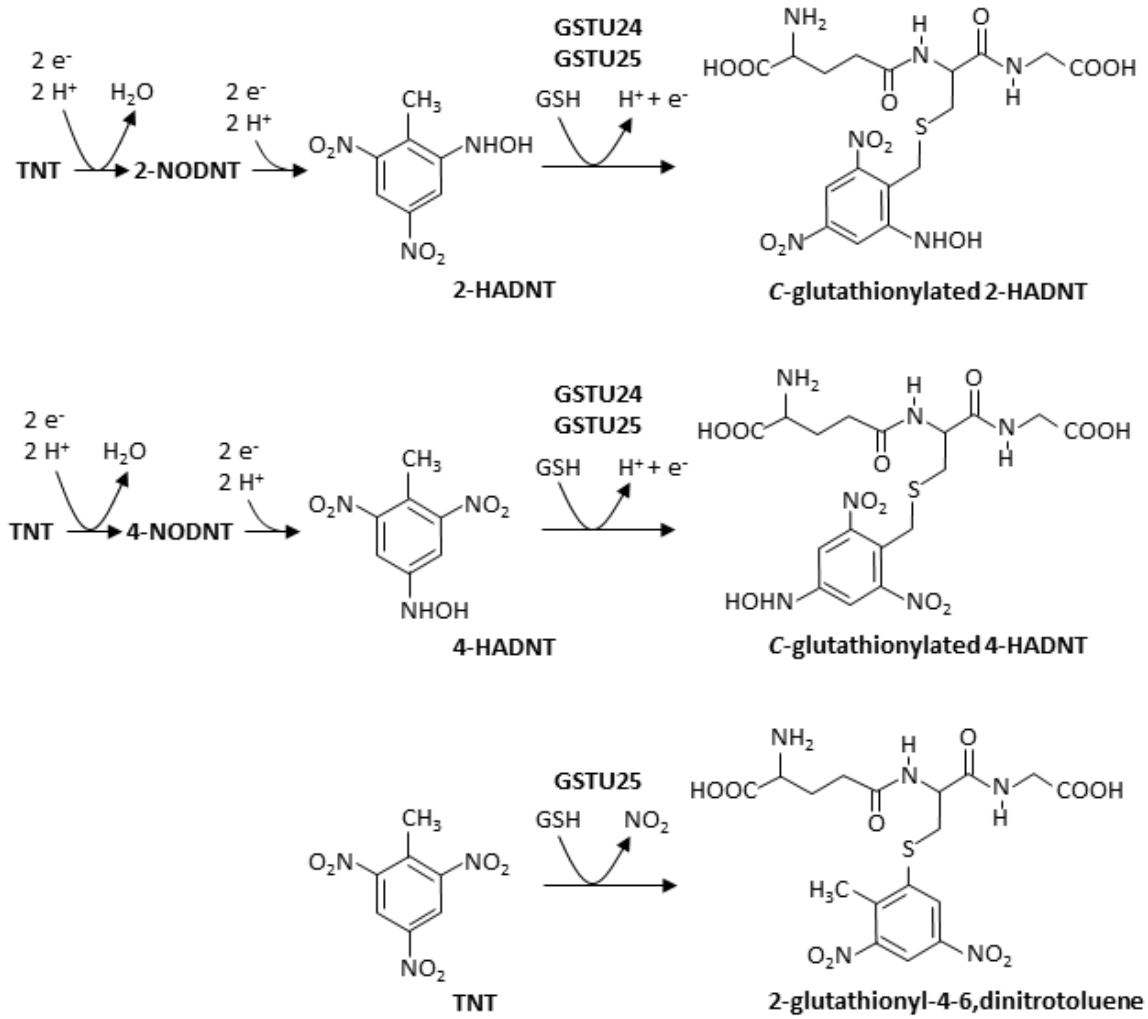

Figure 6: Glutathionylation of TNT and TNT derivatives in Arabidopsis

These conjugates were identified by Gunning et al. (2014). GSH; reduced glutathione. The GSTU24 and GSTU25 enzymes are cytosolic (TAIR, 2015).

1.5 REGULATION OF DETOXIFICATION GENES IN PLANTS

1.5.1 Xenobiotic-response signalling in animal biology

In animal biology, a number of Xenobiotic-Activated Receptors have been described, which interact directly with xenobiotics including drugs, and upon such interaction, are activated to directly induce detoxification gene expression (Ma, 2008; Pascussi et al., 2008; Tolson and Wang, 2010). No homologues of these receptors have been identified in plants (Baker, 2005; Ramel et al., 2012).

It is debated whether some synthetic compounds are sensed directly *in planta*, or whether plant responses synthetic compounds are ubiquitously secondary responses, to cellular perturbations induced by the xenobiotic. Ramel et al. (2012) highlights that responses differ between xenobiotics (although these compounds could induce different cellular perturbations), and argues that the large-scale transcriptome changes following safener[1] treatment indicate a direct regulatory role. It is likely to be of greater evolutionary advantage to respond to environmental stimuli before deleterious cellular perturbations are caused. In support of this theory, plants have evolved receptors to detect Pathogen-Associated Molecular Patterns (PAMPs), and bacterial effector proteins which otherwise suppress plant immune responses (Zipfel, 2014; Cui et al., 2015). These receptors are critical for early induction of defence responses, minimising the damage caused by infection.

Little is known of the signalling involved in responses to synthetic compounds in plants.

[1] Safeners are agrochemicals used to induce detoxification genes in crops, for protection against subsequent herbicide application.

1.5.2 Defence signalling in plants

Detoxification genes are induced following a range of stress treatments, to detoxify both endogenous and foreign compounds. Activation pathways involve both stress-specific and shared components. As will be discussed in 5.1.2, there is correlation between the detoxification genes induced by TNT treatment, and those induced by treatment with phytoprostanes, salicylic acid (SA) or jasmonate (JA). This section therefore presents an overview of biotic stress and wound responses, of which SA, JA and possibly phytoprostanes are involved, with a focus on the role of redox changes in mediating stress responses, and class II TGACG-binding (TGA) factors. The structures of the defence hormones discussed are included in Figure 7.

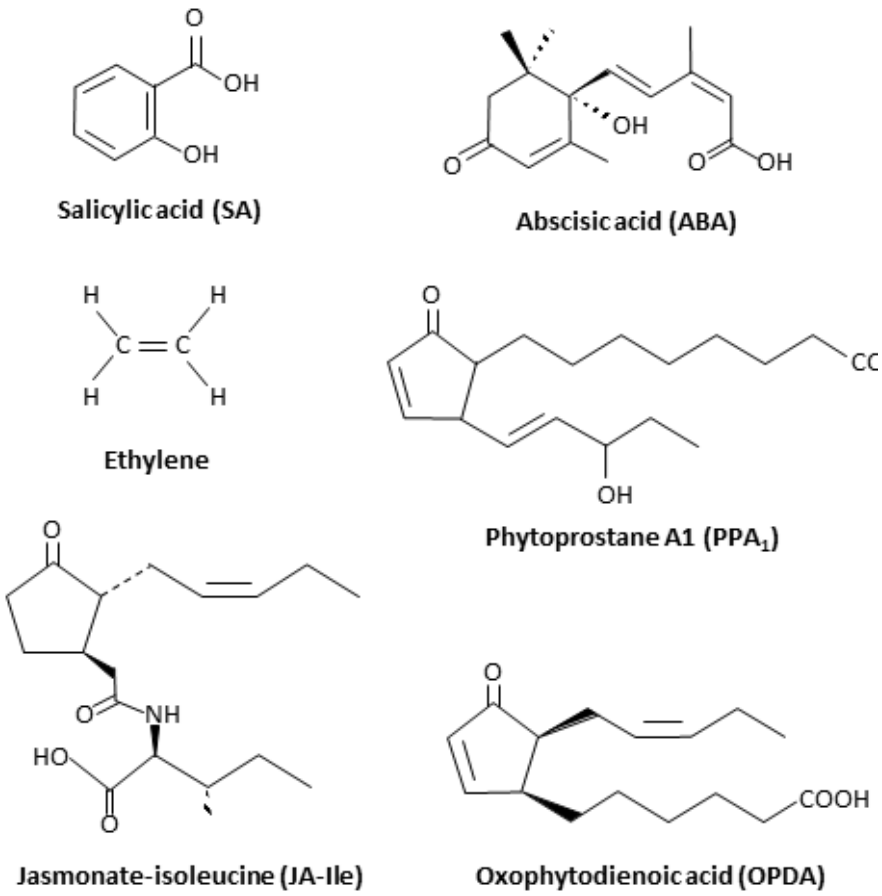

Figure 7: Structure of defence signalling hormones

The (-)-JA-$_L$-Ile isoform of JA-Ile is shown.

Basal (or "non-host") disease resistance

Basal disease resistance is the induction of defences upon recognition of PAMPs (such as outer membrane lipopolysaccharide of Gram negative bacteria), or endogenous Damage-Associated Molecular Patterns (DAMPs, such as plant cell wall fragments released by microbial enzymes; Senthil-Kumar and Mysore, 2013).

The response includes restriction of pathogen entry, for example through increased wax, callose and lignin deposition, and an increase in the production of antimicrobial compounds (Senthil-Kumar and Mysore, 2013).

A small number of PAMP receptors have been identified; for example, *FLAGELLIN SENSING 2* (*FLS2*) detects the Flg22 protein of flagellin, inducing defence responses at nM concentrations of Flg22 (Gómez-Gómez and Boller, 2000). The FLS2 protein is a receptor-like kinase (RLK), with an extracellular leucine-rich repeat (LRR) recognition domain, and an internal serine/threonine kinase domain (Gómez-Gómez and Boller, 2000). Ethylene also has a role in basal disease resistance (Clay et al., 2009).

Effector-mediated disease resistance (also known as "*Resistance/R* gene-mediated" or "gene-for-gene" resistance)

Many strains of pathogen have evolved effector proteins, which enable the pathogen to evade or suppress basal disease resistance. In response, some plant lines have evolved so-called *R*-genes, the products of which recognise specific effectors or their activity, and trigger strong defence mechanisms (Dangl and Jones, 2001). If recognised, effector proteins are termed "avirulence proteins".

Recognition is followed by calcium influx, alkalinisation of the extracellular space, kinase activation, production of Reactive Oxygen Species (ROS) and nitric oxide (NO), and transcriptome changes (Dangl and Jones, 2001).

The oxidative burst and Hypersensitive Response (HR)

Following pathogen recognition (basal or effector-mediated), rapid, transient, biphasic ROS accumulation occurs at the site of infection. The first phase of ROS increase (and subsequent decrease) is a non-specific stress response, however the second, more pronounced and long-lasting increase in ROS, correlates with the establishment of disease resistance (Stael et al., 2015). The increase in hydrogen peroxide level could have a role in disease resistance by (i) having a toxic effect on microbial membranes, (ii) catalysing bonds between expansins, strengthening cell walls, and/or (iii) through a signalling role; hydrogen peroxide is implicated

in increasing SA biosynthesis rate (Leon et al., 1995) and inducing kinase signalling via serine/threonine kinase OXI1 (Rentel et al., 2004). Hydrogen peroxide is debated to be a threshold trigger for the Hypersensitive Response (HR)- programmed cell death, which limits the spread of biotrophic pathogen infection (Levine et al., 1994; Mur et al., 2005).

There are upstream signalling components to this oxidative burst; the burst is abolished in double mutants of the NADPH oxidase homologues *respiratory burst oxidaseD* and *F* (Torres et al., 2002), and in ethylene-insensitive mutants (Mersmann et al., 2010), in response to pathogen infection and Flg22 treatment, respectively.

Systemic Acquired Resistance (SAR) following biotic pathogen recognition

Following pathogen recognition, a state of potentiated defences against a broad range of infection types is established, which decreases the severity of subsequent infections; this is termed Systemic Acquired Resistance (SAR; Ross, 1961), and is associated with activation of *PATHOGENSIS-RELATED* (*PR*) genes (van Loon et al., 2006). Of the *PR* genes, regulation of *PR-1* (encoding an antifungal agent) has been most studied. Salicylic acid (SA) induces and is required for SAR (White, 1979; Gaffney et al., 1993).

The ankirin repeat protein NON-EXPRESSOR OF PR1 (NPR1) is a requirement for SAR, downstream of SA accumulation (Cao et al., 1994). *S*-nitrosylation oligomerises NPR1 in the cytosol, however following SA treatment, thioredoxins catalyse the monomerisation of NPR1, which then accumulates in the nucleus and activates *PR-1* (Tada et al., 2008). Interaction of NPR1 with class II TGA factors appears to be important for inducing SAR; these basic/leucine zipper (bZIP) transcription factors (TFs) interact with NPR1 in yeast one hybrid assays (Lam and Lam, 1995; Zhang et al., 1999; Fan and Dong, 2002), and triple *tga2 tga5 tga6* mutants do not exhibit SAR (Zhang et al., 2003). The TGA factors of Arabidopsis are discussed further in 0.

To investigate whether increased oxidative state is involved in SA signalling, Garretón et al. (2002) treated tobacco leaves with antioxidants dimethylthiourea (DMTU) or butylated hydroxyanisole (BHA) before SA treatment, and found protein binding to *as-1* and expression from *as-1* to be reduced following these antioxidant treatments.

In the *npr1* background, a suppressor of the *npr1* phenotype has also been identified, in which INA[2]-mediated *PR-1* induction is re-established (*sni1*; Li et al., 1999), indicating that NPR1-mediated regulation of *PR-1* functions via SNI1 inactivation.

[2] INA (2,6-dichloroisonicotinic acid) is a homologue of SA, which is often used in SA-response studies, as SA can be toxic to some mutants.

Blanco et al. (2005, 2009) analysed early transcriptome responses to SA more broadly, and found that while SA-responsive signal transduction genes (e.g. protein kinases and transcription factors) are induced NPR1-dependently, induction of detoxification genes (*UGT*s and *GST*s) in response to SA, is generally NPR1-independent. As discussed in 1.4.2, detoxification genes such as *UGT*s and *GST*s are highly induced by TNT treatment.

Jasmonates and responses to herbivory and necrotrophic pathogens

Jasmonic acid (JA) is derived enzymatically from the lipid linolenic acid (Wasternack and Hause, 2013). In addition to roles in plant growth and development (Wasternack and Hause, 2013), the JA-isoleucine conjugate (JA-Ile) is an important mediator of responses to herbivorous insects (e.g. induction of the anti-insect acid phosphatase *VEGETATIVE STORAGE PROTEIN 2*; Liu et al., 2005), and nectrotrophic pathogens (e.g. induction of *PLANT DEFENSIN1.2*; *PDF1.*2), which involves cross-talk with abscisic acid (ABA) and ethylene (Wasternack and Hause, 2013).

The JA-Ile receptor CORONATINE INSENSITIVE1 (COI1) is an F-box protein, which functions as part of an E3 ubiquitin ligase. Binding of JA-Ile to COI1 promotes ubiquitination of jasmonate ZIM domain (JAZ) proteins, which are repressors of jasmonate-response genes. Ubiquitination and degradation of JAZ proteins enables MYC basic Helix Loop Helix (bHLH) TFs to promote transcription of JA-response genes (Wasternack and Hause, 2013).

The ethylene-activated APETALA2 (AP2)/ETHYLENE RESPONSE FACTOR (ERF) transcription factor OCTADECANOID-RESPONSIVE ARABIDOPSIS AP2/ERF protein domain59 (ORA59) is an activator of *PDF1.2*, and is also repressed by JAZ proteins (Wasternack and Hause, 2013).

Antagonism between SA and JA

While activation of the JA pathway suppresses SA biosynthesis (Zheng et al., 2012), induction of *VSP2* and *PDF1.2* following JA treatment is suppressed by SA (Koornneef et al., 2008), downstream of COI1 (Does et al., 2013). Zander et al. (2014), report that the SA-mediated suppression is abolished in class II TGA factor mutants, which usually have a role in *ORA59* induction (as discussed earlier, ORA59 is an activator of *PDF1.2*; Wasternack and Hause; 2013). The glutaredoxin GRX480 is also required for SA-mediated suppression of *PDF1.2*, and interacts with TGA2 and TGA6 in yeast two hybrid assays (Ndamukong et al., 2007). It is therefore proposed that following SA treatment, GRX480 interacts with TGA factors at the *ORA59* promoter, to repress transcription.

Oxophytodienoic acid and phytoprostanes in stress responses

Recently, there has been focus on whether other linolenic acid-derived compounds could have a signalling role, independent of JA-Ile (Farmer and Mueller, 2013). Namely, 12-oxophytodienoic acid (OPDA), which is an enzymatically-generated precursor to JA, and phytoprostanes, a group of cyclopentenone isoprostanes, generated sequentially from the non-enzymatic oxidation of linolenic acid.

Taki et al. (2005) compared Arabidopsis transcriptome responses to JA, MeJA[3] and OPDA, and identified 214 genes which are induced or repressed >3-fold by OPDA, but neither induced or repressed >2-fold by MeJA. Approximately half of these genes are also responsive to wounding. Park et al. (2013) identified that OPDA binds cyclophilin 20-3 with strong affinity, promoting complex formation with serine acetyltransferase 1, and stabilisation of the hetero-oligomeric cysteine synthase complex which regulates sulphur uptake and reduction. This results in increased cysteine and glutathione biosynthesis.

Application of phytoprostane AI (PPA_1), BI and BII have also been shown to induce detoxification and defence responses, with a response profile similar to that of OPDA (Loeffler et al., 2005; Mueller et al., 2008). Levels of phytoprostane have been found to increase in California poppy (*Eschscholzia californica*) and peppermint (*Mentha piperita*) cell cultures following oxidative stress and wounding (Imbusch and Mueller, 2000), in tobacco (*Nicotiana tabacum* cv. Xanthi) cells following butyl hydroperoxide treatment (Thoma et al., 2003), and in Arabidopsis following infection with virulent or avirulent *Pseudomonas syringae* (Grun et al., 2007). It is therefore hypothesised that phytoprostanes could also have a signalling role (Farmer and Mueller, 2013). Due to the structural similarity of phytoprostanes with OPDA, signalling could potentially also be via activation of cyclophilin 20-3, and elevation of glutathione synthesis.

In the study by Mueller et al. (2008), induction of 60 % of the PPA_1-response genes, and 30 % of the OPDA-response genes, were class II TGA factor-dependent.

[3] Methyl jasmonate (MeJA) is converted to the COI1 ligand JA-Ile *in vivo* (Wasternack and Hause, 2013).

Role of redox change in defence signalling

It is now well-established that ROS and Reactive Nitrogen Species (RNS) have important signalling roles, although the exact mechanisms of signal transduction remain controversial (Mullineaux and Baker, 2010). A schematic showing the transition between molecular oxygen and ROS is included in Figure 8. Superoxide and hydrogen peroxide are highly selective in their reactions with biological molecules, while singlet oxygen, the hydroperoxyl radical and hydroxyl radical, are highly reactive, and can directly oxidise protein, DNA and lipids, initiating self-perpetuating lipid peroxidation reactions (Halliwell, 2006). Peroxynitrite rapidly protonates to peroxynitrous acid (ONOOH), which is also a powerful oxidising agent (Halliwell, 2006). Hydrogen peroxide is non-polar, and has a longer half-life than the other ROS (Halliwell, 2006), which are useful properties for a direct signalling role.

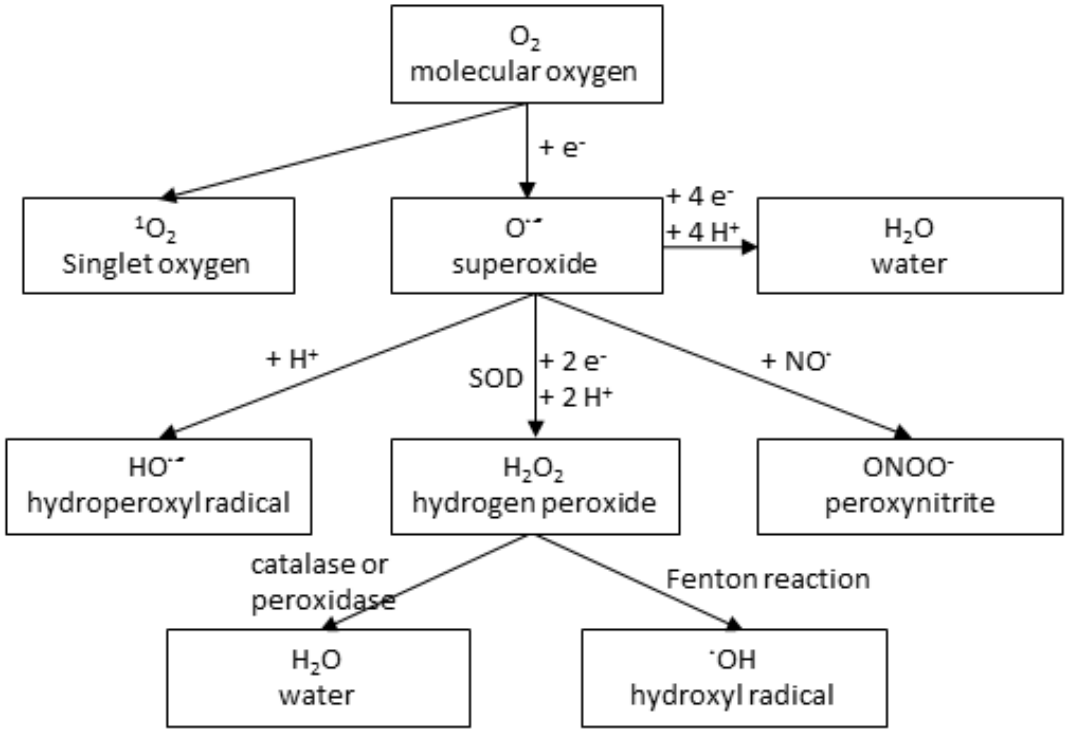

Figure 8: Schematic of transitions between molecular oxygen and ROS

SOD; superoxide dismutase.

As discussed earlier, a well-defined oxidative burst correlates with pathogen recognition and defence responses (Stael et al., 2015), while it is also postulated that phytoprostanes, generated non-enzymatically following wounding, may have a signalling role (Farmer and Mueller, 2013), perhaps (as with OPDA signalling; Park et al., 2013) through direct activation of CYP20-3, resulting in increased glutathione synthesis.

Generally, while SA-treatment increases glutathione content, JA-treatment reduces glutathione concentration, and elevates the percentage glutathione oxidation (Spoel and Loake, 2011). Glutathione is synthesised in two steps, each catalysed by the product of a single gene in Arabidopsis (Figure 9); γ-glutamylcysteine synthetase (γ-ECS; *GSH1*, At4g23100) and glutathione synthetase (*GSH2*, At5g27380). As reviewed by Noctor et al. (2012), a number of reports indicate that elevated H_2O_2 levels lead to an increase in reduced glutathione (GSH) content, without an increase in *GSH1* or *GSH2* transcription. Cysteine, glycine and ATP availability may affect GSH content (and as referenced previously, OPDA induces cysteine biosynthesis in the wound response; Park et al., 2013), while there is also evidence for post-translational regulation of γ-ECS; structural analysis of the γ-ECS of *Brassica juncea* revealed that the γ-ECS homodimer has two intramolecular redox-sensitive disulphide bonds. When one of these is reduced, the active site is shielded, and when both are reduced, the resulting γ-ECS monomers are inactive (Hothorn et al., 2006).

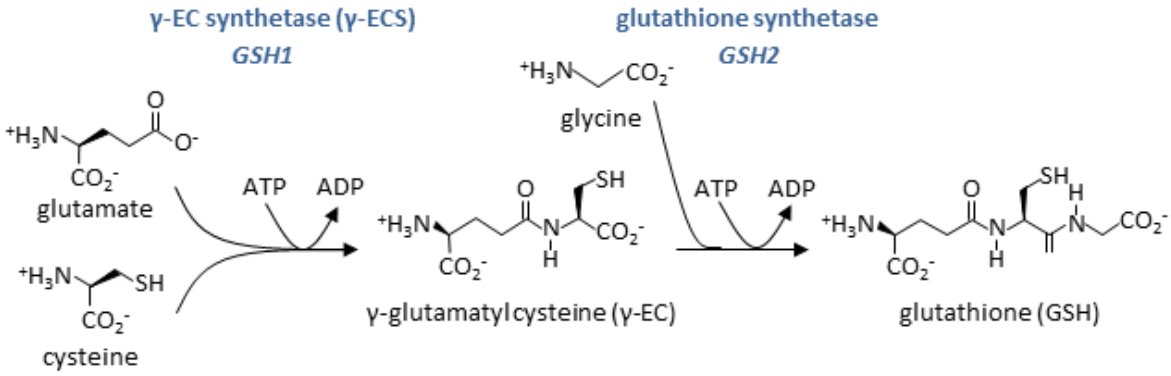

Figure 9: Glutathione biosynthesis in Arabidopsis

Adapted from Galant et al. (2011). The enzymes catalysing these two final reaction steps are shown in blue, with corresponding gene acronyms used in this thesis in italics. Immunogold labelling has identified γ-ECS in chloroplasts, and glutathione synthetase in both chloroplasts and in the cytosol (Galant et al., 2011).

A number of studies report disrupted gene expression in mutants with altered glutathione levels. The *rax1-1* (*regulator of APX2 1-1*) allele of *GSH1* results in >50 % lower foliar glutathione content in Arabidopsis, corresponding with reduced expression of 20 genes, which are implicated in stress defence (Ball et al., 2004). Arabidopsis *lesions simulating disease* (*lsd*) mutants develop HR in the absence of pathogens (Dietrich et al., 1997). Senda and Ogawa (2004) report suppression of this phenotype upon treatment with buthionine sulfoximine (BSO, an inhibitor of γ-ECS; Griffith and Meister, 1979). Both Senda and Ogawa (2004) and Gomez et al. (2004) report induction of *PR-1* upon exogenous application of glutathione, in Arabidopsis and *Nicotiana tabacum* cv. Samsung (tobacco), respectively. Gomez et al. (2004) additionally report an increase in free calcium in tobacco leaf discs treated with reduced or oxidised glutathione.

Interestingly, Li et al. (2013) report that activation of 19 GSH-response genes (72 % of those induced) is dependent on *GLUTAMATE RECEPTOR-LIKE CHANNEL 3.3* (*GLR3.3*). This corresponds with an increase in cytosolic Ca^{2+}, however other GLR3.3 ligands (glutamate, glutathione disulphide, alanine, asparagine, cysteine, glycine and serine) activated the transient increase in Ca^{2+}, but not the transcriptome response. Meanwhile Cheng et al. (2015) report exogenous GSH application to increase ribosome-loading, with overrepresentation of transcripts for JA and ABA biosynthesis genes.

Flohé (2013) cautions that the glutathione redox potential should be interpreted in the first instance as a consequence of the redox environment, rather than a factor which can regulate biological processes; the author comments that enzyme use of glutathione depends on the glutathione concentration, rather than $[GSH]^2$ as predicted by the Nernst equation, and that enzyme use of GSH is not typically affected by the concentration of glutathione disulphide (oxidised glutathione; GSSG).

Oxidation of protein cysteine (Cys) residues can modify the protein activity, or rate of degradation (Sevilla et al., 2015). The effect of the redox environment on Cys residues is summarised in

Figure 10. The *S*-nitrosylation can be reversed by reduction via GSH and thioredoxins, while oxidation to sulfinic (SO_2H) and sulfonic (SO_3H) species, is less readily reversible (Sevilla et al., 2015).

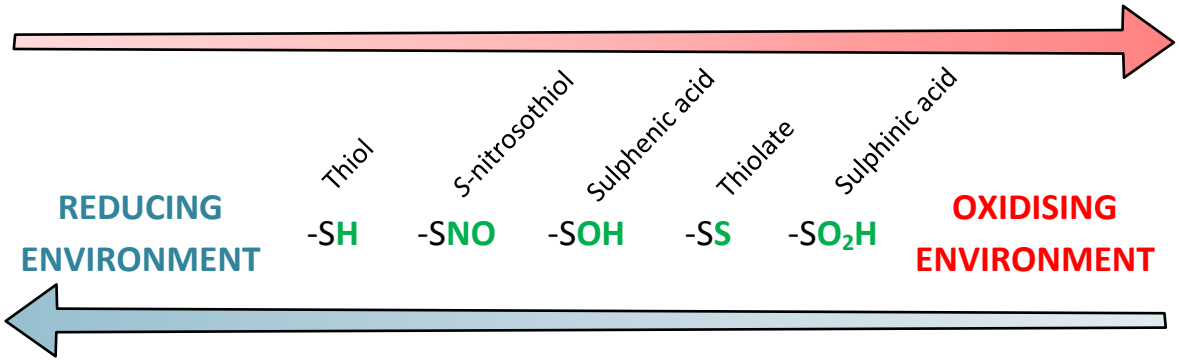

Figure 10: Modifications of cysteine with redox environment

Cysteine thiols (SH) are *S*-nitrosylated (SNO), *S*-sulphenated (SOH), *S*-thiolated (SS) and *S*-sulphinated (SO_2H) at increasingly oxidising environments (Spoel and Loake, 2011).

In addition to ascorbate and glutathione, thioredoxins (Trx; aprroximately 12 kDa) and peroxiredoxins (Prx; 17 – 24 kDa) together buffer against redox change (Prxs have peroxidase activity, and are subsequently themselves reduced by Trxs; Dietz, 2011; Sevilla et al., 2015). The Prx and Trx proteins also have chaperone activity, and Trxs can act as disulphide oxidoreductases, reducing disulphides to thiols, at faster rates than dithiothreitol or GSH (Sevilla et al., 2015). Trxs and Prxs themselves contain highly reactive Cys residues (while free Cys has a pKa of ~8.3, Cys residues of Trxs range from ~3 to 7, and of Prx range from 5.4 to 6; Dietz, 2011; Sevilla et al., 2015), and Cys oxidation modifies their activity (Chi et al., 2013); for example, Trx-h3 polymerises upon oxidation, and the polymerised form loses disulphide oxidoreductase activity, but retains chaperone activity (Park et al., 2009). It has been proposed that this loss of activity could have a signalling role, acting as a "floodgate", facilitating oxidation of other redox proteins, when H_2O_2 reaches a threshold level (Wood et al., 2003). The redox changes to Trx and Prx are summarised in Figure 11.

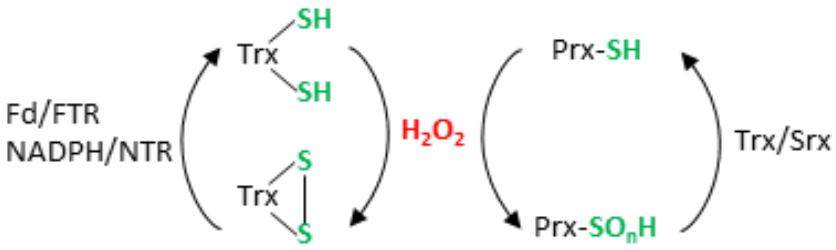

Figure 11: Redox-mediated modification of Trx and Prx proteins

Adapted from Sevilla et al. (2015). GSNO; S-nitrosoglutathione. Fd; ferredoxin. FTR; ferredoxin-dependent Trx reductase. NADPH; nicotinamide adenine dinucleotide phosphate. NTR; NADH-dependent Trx reductase.

A number of redox-regulated plant TFs have now been described. The RAP2.4a TF (AP2/DREB-type) has been identified as a redox sensor and activator of chloroplast antioxidant protein *2-Cys peroxiredoxin (Prx)-A* (*2CPA*); RAP2.4a dimerises upon oxidation, which enables DNA-binding at the CGCG core of *CE3*-like promoter elements (Shaikhali et al., 2008).

Promoters repressed by excess light, such as that of *LIGHT-HARVESTING CHLOROPHYLL A/B-BINDING PROTEIN2.4* (*LHCB2.4*), are enriched in G-boxes. Shaikhali et al. (2012) demonstrated that binding of bZIP TF ZIP16 (which is a transcriptional repressor) requires Cys^{330} for repressive activity. Although bZIP TFs dimerise at promoter elements, DNA binding was increased by dithiothreitol (DTT) treatment, which might improve DNA binding through a pathway in which a bZIP monomer first associates with the DNA, followed by dimerization (Shaikhali et al., 2012).

As referred to earlier, SAR involves the redox-mediated monomerisation of NPR1, which then migrates to the nucleus and interacts with class II TGA factors, to induce *PR-1* expression (Spoel and Loake, 2011). *S*-nitrosylation of NPR1 at Cys^{156} facilitates oligomerisation, while the reduction is catalysed by Trx-h5; Arabidopsis mutants in NPR Cys^{156}, Trx-h5 and *S*-nitrosoglutathione reductase are compromised in disease resistance (Feechan et al., 2005; Tada et al., 2008). While SAR is abolished in class II TGA factor triple mutants (Zhang et al., 2003), class I TGA factor double mutant plants, also have reduced tolerance to pathogen infection (Kesarwani et al., 2007; Shearer et al., 2012), although SAR is not effected (Shearer et al., 2012), and detoxification genes are still induced following JA, OPDA or PPA_1 treatment (Stotz et al., 2013). It has been demonstrated that a disulphide bridge within TGA1 precludes interaction with NPR1, and that when this is reduced, followed by *S*-nitrosylation and *S*-glutathionylation, TGA1 is able to interact with NPR1 (Després et al., 2003; Lindermayr et al., 2010).

1.5.3 Focus on TGA factors

Class II TGA factors are involved in responses to defence hormones SA and JA, and in response to phytoprostane treatment. As discussed in 5.1.1, there is a particularly high level of correlation between the detoxification genes induced following phytoprostane treatment, and those induced following TNT treatment. The class II TGA factors could therefore potentially also have a role in responses to TNT treatment, and are discussed below.

Discovery of TGA factors

Study of TGA factors began with the dissection of *Agrobacterium tumefaciens* (Agrobacterium) and viral T-DNA promoters; Bouchez et al. (1989) described a 16-bp sequence necessary for expression from the Agrobacterium *octopine synthase* (*ocs*) promoter in tobacco and maize, while Lam et al. (1989) described binding of tobacco proteins to a 21-bp element of the *Cauliflower mosaic virus* (*CaMV*) *35S* promoter, termed *activation sequence-1* (*as-1*). Both *ocs* and *as-1* contained the sequence TGACG, as a palindrome and in tandem respectively. Tobacco TGACG-binding (TGA) factors were cloned by Katagiri et al. (1989), and identified as bZIP transcription factors- a TF family which form hetero- and homodimers at (typically) palindromic sequences (Jakoby et al., 2002).

Ellis et al. (1993) first questioned whether the *ocs*-element could have a functional role in plant gene regulation, and the *as-1* element was subsequently found to be activated by auxin, SA and MeJA treatment (Liu and Lam, 1994; Qin et al., 1994; Xiang et al., 1996).

Ten Arabidopsis TGA factors have now been identified, which fall into five classes (Gatz, 2013); an overview of the roles of these proteins is included in Table 7, with mutant studies summarised in Table 8. While class IV and V TGA factors are involved in development, class I and II TGA factors are required for basal regulation and induction of defence genes. Class III TGA factors have not been highly studied.

Table 7: The five classes of Arabidopsis TGA factors

Class	Genes	Overview
I	*TGA1* (At5g65210) *TGA4* (At5g10030)	TGA1 interacts with NPR1 following SA treatment (Després et al., 2003), and double *tga1 tga4* mutants are more susceptible to infection (Shearer et al., 2012). The mutants are not compromised in SAR however (Shearer et al., 2012), or in transcriptome responses to JA, OPDA or PPA_1 (Stotz et al., 2013).
II	*TGA2* (At5g06950) *TGA5* (At5g06960) *TGA6* (At3g12250)	Triple mutants are compromised in SAR (Zhang et al., 2003) and transcriptome responses to JA, OPDA and PPA_1 (Stotz et al., 2013). All interact with NPR1, TGA2 with highest affinity (Zhou et al., 2000). Basal *PR-1* expression is higher in *tga2* mutants, indicating that this TF also has a repressive role (Kesarwani et al., 2007).
III	*TGA3* (At1g22070) *TGA7* (At1g77920)	TGA3 partially interacts with NPR1 (Zhou et al., 2000), and is considered to have a role in the basal regulation of defence genes (Kesarwani et al., 2007). TGA3 was found to recruit cytokinin-activated transcription factor ARR2 to *PR-1* in response to SA by Choi et al. (2010). TGA7 is highly expressed in xylem, and has not been highly studied.
IV	*TGA9* (At1g08320) *TGA10* (At5g06839)	TGA9 and TGA10 interact with glutaredoxins ROXY1 and ROXY2 to regulate anther development (Murmu et al., 2010).
V	*TGA8*/*PERIANTHIA* (At1g68640)	TGA8 is a repressor of petal development (Chuang et al., 1999).

Table 8: Defence responses in class I – III TGA factor mutants

ACC; 1-aminocyclopropane-1-carboxylic acid (ethylene precursor). *GUS*; *BETA-GLUCURONIDASE* reporter gene.

Experiment	Mutant	Phenotype compared with WT	Reference
Induction of *GSTF8::LUC* by SA or H_2O_2 treatment	Knockdown of *TGA4* expression to 40 % of WT, knockdown of *TGA1* expression to 64 % of WT	Increased induction	Foley and Singh (2004)
	Knockdown of *TGA5* expression to 23 % of WT	Reduced induction	
Induction of *PR-1* following INA treatment	*tga6-1*	As WT	Zhang et al. (2003)
	tga2-1 tga5-1	As WT	
	tga2-1 tga5-1 tga6-1	Abolished	
Sensitivity to the toxicity of SA	*tga6-1*	WT	
	tga2-1 tga5-1	As WT	
	tga2-1 tga5-1 tga6-1	As *npr1*	
SAR following INA treatment	*tga6-1*	As WT	
	tga2-1 tga5-1	As WT	
	tga2-1 tga5-1 tga6-1	Abolished	
PR-1 expression on INA-supplemented plates	*tga2-2*	Higher than WT	Kesarwani et al. (2007)
	$TGA6_{ACT}$	Higher than WT	
	tga3-1	Lower than WT	
	tga7-1	Higher than WT	
	tga1-1	A little lower than WT	
	tga4-1	As WT	
	tga1-1 tga4-1	As WT	
Infection with nectrotrophic *Pseudomonas syringae* pv *maculicola* ES4326; test for basal disease resistance	*tga1-1*	Greater infection	
	tga4-1	As WT	
	tga1-1 tga4-1	Greater infection than WT and *tga1-1*. Similar to *npr1-1*.	
	tga2-1 tga3-1 tga5-1 tga6-1	Greater infection than WT or *tga2-1 tga5-1 tga6-1*. Similar to *npr1*.	
Basal *PR-1* expression	*tga2-1 tga5-1 tga6-1*	Higher than WT	
	tga2-1 tga3-1 tga5-1 tga6-1	As WT	
	$TGA6_{ACT}$	Higher than WT	
	tga2-2	Higher than WT	
	$TGA6_{ACT}$ *tga2-2*	Much higher than WT	
Cell culture PPA_1 treatment	*tga2-1 tga5-1 tga6-1*	60% of PPA1-responsive genes not induced	Mueller et al. (2008)
Expression of five NPR1-dependent and two NPR1-independent SA-responsive genes to SA	*tga2-5 tga5-1 tga6-1*	Induction decreased	Blanco et al. (2009)

Cell culture OPDA treatment	*tga2-1 tga5-1 tga6-1*	30% of OPDA-responsive genes not induced	Matthes et al. (2010)
Lesion size after biotrophic *Botrytis cinerea* infection	*tga2-5 tga5-1 tga6-1*	Larger than WT	Zander et al. (2010)
PDF1.2 expression after biotrophic *Botrytis cinerea* infection	*tga2-5 tga5-1 tga6-1*	Induction almost abolished	
PDF1.2 expression after nectrotrophic *Pseudomonas syringae* infection	*tga2-5 tga5-1 tga6-1*	Lower transcript level than WT but basal level also lower	
PDF1.2 expression when treated with ACC and JA	*tga2-5 tga5-1 tga6-1*	Induction almost abolished	
	tga6	As WT	
	tga2-5 tga5-1 tga6-1 jin1 (*jin1* is MYC2 mutant)	Induced higher than WT but not as high as *jin1*	
	tga2-5 tga5-1 tga6-1 with *35S:TGA2, 5* or *6*	Induction greater than WT, especially for *35S:TGA5*	
Safener treatment (5 mM mefenpyr and 7.2 mM isoxadifen) of Arabidopsis transformed with a maize safener-responsive *GST* promoter: *GUS* construct	*tga2-1 tga3-1 tga5-1 tga6-1*	Activation of the promoter abolished in the *tga* quadruple mutant. The response also required SA (through study with *sid2-2* mutant) but not NPR1 (studies with *npr1*).	Behringer et al. (2011)
Pseudomonas syringae or *Hyaloperonospora arabidopsidis* infection	*tga1-1 tga4-1*	Ten-fold more bacterial growth *PR-1* still induced	Shearer et al. (2012)
	tga1-1 tga4-1 npr1	More *P. syringae* growth than in *tga1 tga4*	
SAR following treatment with avirulent strain	*tga1-1 tga4-1*	Pre-inoculation with avirulent strain still effective at inducing SAR	
Detoxification gene induction following PPA_1 treatment	*tga1-1 tga4-1*	Increased or as WT	Stotz et al. (2013)
	tga2-5 tga5-1 tga6-1	Decreased	
Detoxification gene induction following OPDA treatment	*tga1-1 tga4-1*	As WT	
	tga2-5 tga5-1 tga6-1	Decreased	
Detoxification gene induction following JA treatment	*tga1-1 tga4-1*	Increased or as WT	
	tga2-5 tga5-1 tga6-1	Decreased	

Binding and recruitment of TGA factors to promoter elements

Promoter studies have focused on induction of *PR-1* in response to SA or INA. Lebel et al. (1998) implemented linker scanning mutagenesis, and found reduced *PR-1* induction in response to INA when *LS7* is mutated[4], and higher basal expression when *LS4* or *LS5* are mutated. Elements *LS7* and *LS5* contain TGACG motifs, while *LS4* contains a WRKY transcription factor binding motif[5]. It is proposed that TGA factor binding to the *LS7* element induces *PR-1* expression, while binding to *LS5* represses basal *PR-1* levels (Kesarwani et al., 2007). Pape et al. (2010) further identified that when both *LS7* and *LS5* are mutated, response to INA is restored, but not when *LS4* is mutated, or in the *npr1* mutant background. These studies highlight the interplay between various regulatory factors at the *PR-1* promoter.

Zander et al. (2010) found induction of *PDF1.2* following ACC and JA treatment to be abolished in *tga2 tga5 tga6*, however induction from this promoter was unaffected when the TGACG motif was mutated to TTTTT. The reduction in response is therefore indirect, presumably via reduced *ORA59* transcription, of which class II TGA factors are activators (Zander et al., 2014).

Chromatin immunoprecipitation (ChIP) experiments investigating TGA factor recruitment have yielded some conflicting results; Johnson et al. (2003) used antiserum against the N-termini of TGA2 and TGA3, and reported SA- and NPR1-mediated recruitment of TGA2 and 3 to the *PR-1* promoter. Rochon et al. (2006) meanwhile overexpressed HIS-tagged TGA2 in *tga2 tga5 tga6*, and reported comparable promoter recovery from SA-treated and untreated plants. The ChIP result of Johnson et al. (2003) was further supported however by a gel-shift binding assay between leaf nuclear extracts and labelled promoter probes. It is possible that in the experiment of Rochon et al. (2006), the HIS-tag interfered with TGA factor recruitment, or was out-competed by endogenous TGA factors, or alternatively, that when *TGA2-HIS* is overexpressed, there is a greater incidence of non-recruited promoter binding.

Post-translational regulation of TGA factor activity, including protein-protein interaction

A number of studies have identified interaction between NPR1 and TGA factors in yeast two hybrid screens (Zhang et al., 1999; Després et al., 2000; Zhou et al., 2000; Fan and Dong, 2002); Zhou et al. (2000) conclude that TGA2 and TGA3 have strong binding affinity towards NPR1, while TGA5 and TGA6 have weaker affinity, and TGA1 and TGA4 little affinity. Using a plant two hybrid assay, Després et al. (2003) identified interaction between TGA1 and NPR1 in

[4] The promoter segments replaced with heterologous sequence (of same length) were denoted *LS1* to *LS13*.

[5] WRKY transcription factors are zinc finger TFs of the WRKY-GCM1 superfamily. The name derives from a conserved WRKYGQK sequence at the protein N-terminus (Chen et al., 2012).

Arabidopsis leaves following SA treatment. Site mutagenesis of TGA1 Cys^{260} and Cys^{266} enabled interaction of TGA1 with NPR1; these residues are predicted to form intramolecular disulphide bridge, which inhibits binding to NPR1. When this disulphide bridge is reduced, interaction with NPR1 is enabled (Després et al., 2003).

Electrophoretic mobility shift assays by Després et al. (2000) indicate that *in vitro*, binding of TGA2 to the *as-1* promoter, and *LS5* and *LS7* elements of the *PR-1* promoter, is increased by the presence of NPR1.

Interestingly, binding to the *as-1* element in tobacco cells of a TF immunologically-similar to tobacco TGA factor TGA1a, was reduced following phosphatase treatment in a study by Jupin and Chua (1996); phosphorylation may have a role in the regulation of TGA factor DNA binding. Kang and Klessig (2005) have since identified that TGA2 is phosphorylated by Arabidopsis crude extract, and that this phosphorylation is increased in extract from plants which have been treated with SA for 10 min.

It was prior hypothesised that class II TGA factors also interact with the NPR1 paralogues NPR3 and NPR4, to form repressive units, however NPR3 and NPR4 have since been found to have a role in mediating NPR1 degradation (Fu et al., 2012).

In a yeast two hybrid screen, Fode et al. (2008) also identified interaction between TGA2 and the GRAS protein[6] SCARECROW-LIKE 14 (SCL14). In comparison between a *scl14* mutant and a *SCL14*-overexpressor, 14 genes were identified as expressed >five-fold (log2) more in the overexpressor line, eleven of which are also induced by TNT treatment (Gandia-Herrero et al., 2008).

In another yeast two hybrid screen, Ndamukong et al. (2007) identified that TGA2 and TGA6 interact with glutaredoxin GRX480. When GRX480 was constitutively expressed in Arabidopsis, if was found to negatively regulate *as-1*. This glutaredoxin is also required for SA-mediated suppression of *PDF1.2* (Ndamukong et al., 2007).

[6] This group of proteins is named after the first three members to be described: GIBBERELLIC-ACID-INSENSITIVE (GAI), REPRESSOR OF GAI (RGA) and SCARECROW (SCR). Numerous GRAS domain proteins have been found to have important roles in plant growth and development (Hirsch and Oldroyd, 2009).

1.5.4 Studies specifically on plant detoxification gene regulation

Although detoxification genes are induced by SA and JA, study of these signalling pathways has focused on the regulation of *PR-1* and *PDF1.2*, respectively. More recently, the regulation of specific detoxification gene promoters in response to various stimuli, including xenobiotics, has been studied in more detail.

Köster et al. (2012) sought to identify components involved in *CYP81D11* induction in response to JA, 2,3,5-triiodobenzoic acid (TIBA; an auxin transport inhibitor) and benzoxazolin-2(3H)-one (BOA; an allelochemical). The *CYP81D11* gene is induced by a broad range of stimuli, including TNT treatment (25-fold induction; Gandia-Herrero et al., 2008). Their findings are summarised in Table 9; induction of *CYP81D11* following JA treatment required class II TGA factors and MYC2, and the *as-1* and *G-box* binding sites (for TGA factors and MYC2, respectively). Meanwhile JA-mediated induction of *VSP2* and *GRX480* was increased in the *tga2 tga5 tga6* triple mutant. Induction of *CYP81D11* following TIBA treatment was abolished when *as-1* was mutated, but only halved when the *G-box* motif was mutated. Induction in *coi1* was reduced 10-fold, but reduced only 3-fold in the *dde2-2* mutant which does not accumulate OPDA or JA, and in contrast to following wounding, no change in JA-Ile or JAZ levels was detected following TIBA treatment. These findings indicate a role for COI1 in response to TIBA, partially independent of JA and MYC2.

Stotz et al. (2013) also studied the *CYP81D11* promoter, along with the promoters of *GSTF8*, *GSTU7*, *OPR1*, *TolB-like* and *VSP1*[7], investigating components required for induction following treatment with PPA_1, OPDA or JA. The authors' findings are summarised in Table 10; while induction in response to all three treatments was abolished or reduced in *tga2 tga5 tga6*, the response in *tga1 tga4* mutants was unchanged, or increased relative to wild type. Notably, loss of COI1 differentially affects the induction of different genes.

The studies detailed above highlight differences in signalling pathways in response to different stimuli, and the varying roles of shared components, such as COI1, in these pathways.

Previous studies investigating responses to synthetic compounds in plants are summarised in Table 11. In this thesis, Arabidopsis response to TNT treatment is investigated, as an exemplar aromatic pollutant in the environment.

[7] These genes are induced in response to TNT as follows: *CYP81D11* 25-fold, *GSTF8* 3-fold, *GSTU7* 8-fold, *OPR1* 14-fold (primers also target *OPR2* transcript) and *TolB-like* 30-fold. The *VSP1* gene is not induced by TNT treatment (Gandia-Herrero et al., 2008).

Table 9: Requirements for *CYP81D11* induction in response to JA, TIBA or BOA treatment

Summary of findings reported by (Köster et al., 2012). The *jasmonate-insenstive1* mutant allele encodes MYC2.

Experiment condition	**Induction of *CYP81D11* promoter in response to treatment**		
	JA	**TIBA**	**BOA**
tga2 tga5 tga6 mutant	abolished		
coi1 mutant (JA-Ile receptor mutant)		almost abolished	almost abolished
jin1-1 mutant (MYC2 mutant)	abolished	reduced	almost abolished
dde2-2 mutant (doesn't accumulate OPDA or JA)		reduced	reduced
as-1-like motif (TGA factor binding site) mutated	abolished	almost abolished	
G-box motif (MYC2 binding site) mutated	abolished	reduced	

Table 10: Requirements for detoxification gene induction in response to PPA_1, OPDA or JA

Summary of findings reported by Stotz et al. (2013). The *jasmonate-insenstive1* mutant allele encodes MYC2.

	coi1			***jin1***		
	PPA_1	OPDA	JA	PPA_1	OPDA	JA
CYP81D11	reduced	as WT	reduced	as WT	as WT	reduced
GSTF8	as WT	as WT	as WT	as WT	as WT	as WT
GSTU7	as WT	as WT	as WT	as WT	as WT	as WT
OPR1	increased	increased	increased	as WT	increased	as WT
TolB-like	as WT	increased	increased	as WT	as WT	as WT
VSP1		abolished	abolished		as WT	reduced
	tga2 tga5 tga6			***tga1 tga4***		
	PPA_1	OPDA	JA	PPA_1	OPDA	JA
CYP81D11	abolished	abolished	abolished	as WT	as WT	increased
GSTF8	reduced	reduced	abolished	increased	as WT	as WT
GSTU7	abolished	abolished	abolished	increased	as WT	as WT
OPR1	abolished	abolished	abolished	increased	as WT	as WT
TolB-like	abolished	abolished	abolished	as WT	as WT	as WT

Table 11: Studies investigating responses to synthetic compounds

The *CYP81D11* gene is induced 25-fold by TNT treatment, *GSTU24* 37-fold, and *GSTU19* is not induced (Gandia-Herrero et al., 2008).

Chemical structure	Study
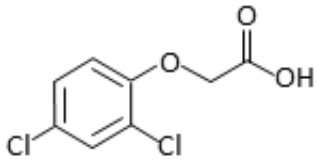 2,4-dichlorophenoxyacetic acid (2,4-D)	2,4-D is a synthetic auxin, which is used as a herbicide. Fode et al. (2008) reported increased expression from *as-1:GUS* when treated with 2,4-D, and when SCL14 was overexpressed.
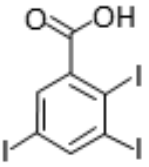 2,3,5-triiodobenzoic acid (TIBA)	TIBA is an auxin transport inhibitor. Köster et al. (2012) report that *CYP81D11* induction following TIBA treatment requires class II TGA factors, and is partially dependent on COI1, MYC2, and lipids in the jasmonic acid pathway.
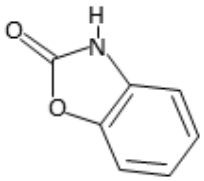 Benzoxazolin-2(3H)-one (BOA)	BOA is an allelochemical. Köster et al. (2012) report that *CYP81D11* induction following BOA treatment requires COI1 and MYC2.
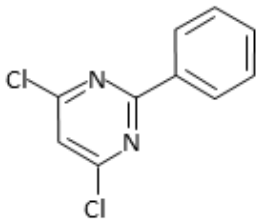 Fenclorim	Fenclorim is a herbicide safener. Skipsey et al. (2011) report higher transcript abundance of *GSTU19* and *GSTU24* in *fad3-2 fad7-2 fad8* compared with wild type in control (acetone) treatment, but reduced transcript abundance relative to wild type following fenclorim treatment.
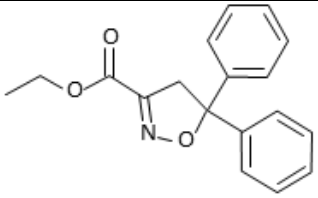 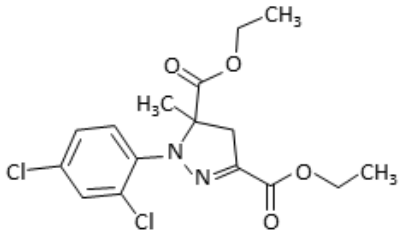 Isoxadifen-ethyl with mefenpyr-diethyl	Isoxadifen-ethyl with mefenpyr-diethyl are used in herbicide safeners. Behringer et al. (2011) report that induction from a maize GST promoter was abolished in Arabidopsis *tga2-1 tga3-1 tga5-1 tga6-1*.
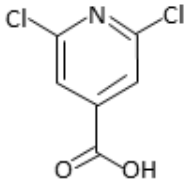 2,6-dichloroisonicotinic acid (INA)	INA is a salicylic acid homolog, often used in the study of SA signalling, as SA can have toxic effects on some mutants.

1.6 THESIS OBJECTIVES

As discussed in 1.3, phytoremediation may be the most cost-effective and environmentally-friendly means of tackling explosives pollution at large sites, however there is a need to develop plants which are able to both tolerate and degrade energetic residues. Previous work in Neil Bruce's group identified that Arabidopsis plants deficient in MONODEHYDROASCORBATE REDUCTASE 6 (MDHAR6) have greatly enhanced TNT tolerance (Johnston et al., 2015). The aims of this study are:

(i) to explore the means behind the enhanced TNT tolerance of *mdhar6* mutants (Chapter 3),

(ii) to further elucidate the endogenous role of MDHAR6, by investigating the subcellular location of this protein (Chapter 4), and

(iii) to explore the regulation of detoxification genes in response to TNT treatment (Chapter 5).

2 Materials and methods

2.1 MATERIALS AND METHODS

2.1.1 Plant material

monodehydroascorbate reductase (mdhar)6-1

This mutant, in the Columbia7 (Col7) background, was identified in a screen of Weigel T-DNA activation lines (Weigel et al., 2000) obtained from the Nottingham Arabidopsis Stock Centre.

mdhar6-2

This mutant, in the Nossen (Nos) background, was obtained from the RIKEN Arabidopsis transposon-tagged mutant (RATM) lines (Ito et al., 2005).

mdhar6-3

This mutant, in the Columbia0 (Col0) background, is line 258H07 of the GABI-Kat T-DNA mutagenised lines (Kleinboelting et al., 2012).

tgacg motif binding factor* (*tga*)*2 tga5 tga6

This mutant, in the Col0 background, was constructed by Zhang et al. (2003), and kindly provided by Prof. Christiane Gatz (Georg-August-Universität Göttingen).

fatty acid desaturase* (*fad*)*3-2 fad7-2 fad8

This mutant, in the Col0 background, was isolated by McConn and Browse (1996), and kindly provided by Prof. Robert Edwards (Newcastle University).

***allene oxide synthase* (*aos*)**

This mutant, in the Columbia6 (Col6) background, was isolated by Park et al. (2002), and kindly provided by Prof. Ian Graham (University of York).

2.1.2 Plant growth conditions

Agar plates

Half strength Murashige and Skoog basal medium (Sigma M5524) with 0.8 % w/v agar (Sigma A1296), indicated by acronym ½ MS(A) or ½ MS(A)(S), where (A) denotes addition of agar, and (S) denotes addition of 20 mM sucrose.

Growth in liquid media and treatment with TNT

Liquid culture experiments in this thesis are replications of the TNT-response experiment described by Gandia-Herrero et al. (2008). Stratified seedlings were germinated on ½ MS(A)(S) for 24 h, then ten seedlings were transferred to 500 ml conical flasks containing 100 ml of ½

MS(S) with 1 x Gamborg's Vitamin Solution (Sigma G1019), and grown for 13 d with 130 rpm shaking and low light conditions (20 µmol.m^{-2}.s^{-1}, 16 h light, 8 h dark cycle). The 14-d old seedlings were then dosed with 60 µM TNT in DMF (end 0.06% v/v DMF) or DMF alone, and harvested after 6 h.

Hydroponic growth

In this thesis, "hydroponic" is used to refer to the growth of seedlings on a raft, so that roots, but not leaves, are submerged in the liquid growth medium (Figure 12). The 5 mm diameter holes of Foamex rafts (dimensions: 5 mm thickness, 8 cm diameter, 2 cm diameter hole for raft removal, 84 x 5 mm diameter holes for germinating seedlings- produced by the University of York, Department of Biology Workshop) were plugged with ½ MS(S)(A), and transferred to 100 ml ½ MS(S), within 560 ml jars. Ten seeds, which had already been stratified in sterilised water, were then transferred per Foamex raft, and the jars were sealed with micropore tape and metal clamps. Before setup, the jars were sterilised in a 150 °C oven for 2 h, while the rafts, agar and liquid media were autoclaved.

Figure 12: Hydroponic growth of Arabidopsis seedlings

Seeds are germinated upon ½ MS agar-plugged holes in the raft.

Soil

Levington's F2 compost.

Soil treated with TNT

The TNT concentration of soil is reported as mg TNT per kg of soil, which consists of 55 % dry mass (70 % Levington's F2 compost, 30 % fine silica sand) and 45 % water. To prepare this soil, TNT dissolved in acetone was first added to the sand within a tub. After the acetone had evaporated overnight, a large (2.5 cm diameter) glass marble was added, and the sand and TNT mixed by mechanical rotations for 20 min. The compost was then also added, and the soil mixed overnight by mechanical rotations with the marble.

Seed sterilisation

Within a box containing the seeds, 3 ml concentrated hydrochloric acid was added to 100 ml sodium hypochlorite, to generate chlorine gas. The box was then immediately sealed, and the seeds were incubated with the gas for 4 h.

Seed stratification

Seeds were applied to ½ MS(A) or damp soil, and stratified in the dark at 6 °C for 3 d.

Growth room conditions

The growth room used in non-soil experiments had low lighting (20 $\mu mol.m^{-2}.s^{-1}$), with a 16 h light, 8 h dark cycle.

Growth cabinet conditions

Growth cabinets (SANYO Electric Co. Ltd., MLR-350) were used in experiments where plants were grown on TNT-treated soil. The cabinets had a light level of 180 $\mu mol.m^{-2}.s^{-1}$, with a 12-h photoperiod, and 18 and 21 °C dark and light temperatures respectively.

2.1.3 Source of TNT

The TNT was kindly provided by the Defence Science and Technology Laboratory (DSTL; Fort Halstead, Kent, UK).

2.1.4 Growth of plants on TNT-treated soil

Compost was treated with TNT as outlined in 2.1.2, and 20 g (consisting of 55 % dry weight) was transferred to individual pots. Five 5-day old seedlings (germinated on non TNT-treated compost) were transferred to each test pot, and grown in a Sanyo growth cabinet. Plant tissue and soil was harvested when plants were six-weeks of age.

2.1.5 Recovery of TNT from soil

Soil was dried at 50 °C for 72 h, with vortexing at 48 h, then ground to a fine powder by mechanical rotations with two steel ball bearings (of 1 cm diameter) overnight. Aliquots of 2 g

dried soil were weighed into glass vials, and sonicated with 10 ml acetonitrile for 18 h (Sonorex Digital 10P, 100% power, chilled with ice). Samples were centrifuged (20,000 rpm, 40 min), and the supernatant concentrated 10-fold by evaporating acetonitrile at 60 °C, then resuspending with 50:50 water:acetonitrile for High Performance Liquid Chromatography analysis.

2.1.6 High Performance Liquid Chromatography (HPLC)

A Waters HPLC system (Waters 2695 separator with Waters Photodiode array detector and Waters X-Bridge C18 column; 300 x 4.5 mm, 5 µM) was used to measure TNT or CDNB concentration of samples. Running solvent was isocratic 50:50 acetonitrile:water. To measure TNT concentration, A_{230} peak area at 9.4 min retention time was compared against a standard curve. To measure CDNB concentration, A_{250} peak area at 10.5 min retention time was compared against a standard curve.

2.1.7 Root length analysis

Root length was measured from photographs using ImageJ (Schneider et al., 2012).

2.1.8 Ascorbate measurement

Two different methods were used to measure ascorbate.

In Figure 24, where ascorbate is quantified in roots and leaves, the protocol outlined by Kampfenkel et al. (1995) was used; 100 mg tissue crash-frozen in liquid nitrogen was ground in a bead mill with 500 µl 6 % trichloroacetic acid (TCA; 30 1/s, 3 min), then incubated on ice for 15 min before centrifugation (13,000 rpm, 5 min, 6 °C). Ascorbate measurement is based on detecting reduction of Fe^{3+} to Fe^{2+} by reduced ascorbate. To measure reduced ascorbate, the assay contained 50 µl sample or standard, 150 µl 0.2 M sodium phosphate (pH 7.4), 50 µl water, 250 µl 10 % TCA (v/v), 200 µl 42 % H_3PO_4 (v/v), 200 µl 4 % 2,2'-dipyridyl (v/v) in 70% ethanol and 100 µl 3 % $FeCl_3$ (v/v). Reactions were incubated at 42 °C for 40 min before reading A_{525}. To measure total ascorbate, after addition of the buffer, 50 µl of 10 mM DTT in 0.2 M sodium phosphate (pH 7.4) was added and the samples were incubated at 42 °C for 15 min. Instead of water, 50 µl of 0.5 % *N*-ethylmaleimide was then added to remove excess DTT, and after 1 min incubation at room temperature (RT), the remaining assay components were added.

In Figure 25, where ascorbate is quantified in control and TNT-treated seedlings, the protocol outlined by Queval and Noctor (2007) was used; seedlings were ground in liquid nitrogen and 1 ml 0.2 N HCl added per 100 mg FW. Following centrifugation (13,000 rpm, 10 min, 6 ^{o}C),

supernatant pH was adjusted to between 5 and 6 by the addition of 100 µl 0.2 M NaH_2PO_4 (pH 5.6) and 830 µl 0.2 M NaOH, per 1 ml supernatant. Ascorbate measurement is based on the difference in A_{265} between reduced and oxidised ascorbate. To measure reduced ascorbate, 60 µl sample or standard was added to 300 µl 0.2 M NaH_2PO_4 (pH 5.6) and 225 µl water. A_{265} was measured before and after addition of 15 µl 40 $U.ml^{-1}$ ascorbate oxidase (Sigma A0157) in 0.2 M NaH_2PO_4 (pH 5.6). To reduce all ascorbate for total ascorbate measurement, 300 µl of neutralized extract was incubated with 420 µl 0.12 M NaH_2PO_4 (pH 7.5) and 30 µl 25 mM DTT at RT for 30 min.

2.1.9 Glutathione measurement

Glutathione was measured as described by Queval and Noctor (2007); samples were extracted and neutralised as described in 2.1.8. The glutathione measurement is based on glutathione-mediated reduction of 5,5'-dithiobis(2-nitrobenzoic acid) (DTNB) to thionitrobenzoic acid, which corresponds with an increase in A_{412}. The complete assay consisted of 500 µl 0.2 M NaH_2PO_4 10 mM EDTA (pH 7.5), 50 µl 10 mM NADH, 50 µl 12 mM DTNB, 300 µl water, 50 µl neutralised sample or glutathione standard and 50 µl 20 U/ml glutathione reductase (Sigma G3664) in 0.2 M NaH_2PO_4 10 mM EDTA (pH 7.5). The rate of A_{412} increase before and after glutathione reductase addition was recorded. To measure the concentration of oxidised glutathione in samples, reduced glutathione was first complexed with 2-vinylpyridine (VPD); 400 µl of neutralised supernatant was incubated at room temperature with 2 µl VPD for 30 min, and then centrifuged at 14,000 rpm for 5 min to remove the VPD-glutathione complex. For oxidised glutathione measurement, the complete assay contained 10 % (v/v) sample or standard.

2.1.10 Plant protein extraction and analysis of extract activity

Plant protein extraction and analysis of MDHAR activity was as reported in Colville and Smirnoff (2008).

For protein extraction, 1 ml ice-cold extraction buffer (100 mM Tricine, 1 mM Na_2EDTA, 5% polyvinylpyrrolidine-40 (v/v), 20% glycerol (v/v) and 2 mM DTT added fresh before use) was added per 100 mg of fresh tissue, and the tissue was homogenised using a pestle connected to an electric drill. Samples were centrifuged at 13,000 rpm for 2 min at 4°C, and the supernatant kept on ice before assayed.

To measure MDHAR activity, assays contained 362.5 µl 50 mM Tris (pH7.6) 1 mM EDTA buffer, 12.5 µl 4.29 mM NADH (end 107 µM), 25 µl 2.5 mM sodium ascorbate (end 125 µM) and 50 µl extract. The oxidation rate of NADH was measured before and after the addition of 50 µl 5.6

U/ml ascorbate oxidase (Sigma A0157; end 0.56 U/ml) in 4 mM sodium phosphate buffer 0.05% BSA (pH 5.6). The rate of NADH reduction was calculated assuming an extinction coefficient of NADH at 340 nm of 6.22 $mM^{-1}.cm^{-1}$.

To assay activity towards TNT, the same reaction buffer and NADH concentration was used, and A_{340} was followed before and after addition of 50 µl 10 mM TNT in DMSO (end 1 mM).

2.1.11 Production of MDHAR6 in *Escherichia coli*

The *MDHAR6* gene, lacking organelle-targeting sequences, was codon-optimised for *E. coli* by GeneART® Gene Synthesis (ThermoFisher Scientific), and cloned into the vector pET52b by Liz Rylott and Maria Budarina. This introduced an N-terminal Strep-tag and C-terminal polyHistidine (HIS)-tag to the expressed protein (Figure 13).

MASWSHPQFEKGADDDDKVPDPSLVTASFANENREFVIVGGGNAAGYAARTFVENGMADGRLCI
VTKEAYAPYERPALTKAYLFPPEKKPARLPGFHTCVGGGGERQTPDWYKEKGIEVIYEDPVAGA
DFEKQTLTTDAGKQLKYGSLIIATGCTASRFPDKIGGHLPGVHYIREVADADSLIASLGKAKKI
VIVGGGYIGMEVAAAAVAWNLDTTIVFPEDQLLQRLFTPSLAQKYEELYRQNGVKFVKGASINN
LEAGSDGRVSAVKLADGSTIEADTVVIGIGAKPAIGPFETLAMNKSIGGIQVDGLFRTSTPGIF
AIGDVAAFPLKIYDRMTRVEHVDHARRSAQHCVKSLLTAHTDTYDYLPYFYSRVFEYEGSPRKV
WWQFFGDNVGETVEVGNFDPKIATFWIESGRLKGVLVESGSPEEFQLLPKLARSQPLVDKAKLA
SASSVEEALEIAQAALQSAAAGAPGFSSISAHHHHHHHHHH

Figure 13: Sequence of the epitope-tagged MDHAR6 expressed in *E. coli*

The N-terminal organelle-targeting sequences (first 48 residues of m-MDHAR6) are omitted, i.e. the sequence starts after the RIAS motif for protein cleavage after import into mitochondria. N-terminal Strep-tag and C-terminal HIS-tag highlighted.

The vector *pET52b MDHAR6* was transformed into *E. coli* strain Arctic Express (Agilent Technologies) following the manufacturer's instructions, and transformed colonies were selected on 50 µg/ml carbenicillin Luria Broth (LB) agar plates.

A single transformed colony was used to inoculate 50 ml of LB, which was cultured at 37 °C with 250 rpm for 15 h. Ten ml of this starter culture was then used to inoculate 500 ml LB (50 µg/ml carbenicillin) within a 2 L conical flask, and incubated at 37 °C 250 rpm until the OD_{600} approximated 0.6. At this point 300 µl 1 M isopropyl β-D-1-thiogalactopyranoside (IPTG, end concentration 0.6 mM) was added to induce *MDHAR6* expression, and the culture was

incubated at 15°C with 180 rpm for 24 h. The cultures were centrifuged (4,000 rpm, 5 min, 4°C), pellets transferred to Falcon tubes, crash-frozen in liquid nitrogen and stored at -80°C.

2.1.12 Purification of Strep-tagged MDHAR6

Two pellets, each from 500 ml of induced culture, were defrosted slowly on ice, each with the addition of 30 ml binding buffer (50 mM sodium phosphate, pH 8, 300 mM NaCl) with 0.1 % Tween20 (v/v) , 70 µl 0.1 M phenylmethanesulfonylfluoride in isopropanol, and 55 µg avidin. These were sonicated on ice at amplification 70 for 4 min (3 sec on, 7 sec off), centrifuged (15,000 rpm, 15 min, 4°C), and the supernatant syringed through a 22 µm-filter to obtain soluble protein. Strep-tagged MDHAR6 was then purified on a 5 ml StrepTrap column (GE HealthCare 28-9075-48), which was equilibrated with 7 ml water then 25 ml binding buffer before the sample was applied. The column was then washed with a further 15 ml binding buffer, before the addition of elution buffer (binding buffer with 2.5 mM desthiobiotin) over a gradient of 0 - 100 % in 20 min. Purified MDHAR6 was dialysed (using cassette ThermoScientific #88251) against 2.5 L of dialysis buffer (50 mM potassium phosphate, pH 7) at 6 °C for 2 h, and then 2.5 L fresh dialysis buffer for a further 18 h.

2.1.13 SDS-PAGE electrophoresis

Protein samples were denatured at 95 °C for 10 min with a four-fold dilution of stock sample buffer (25 % 1 M Tris-HCl pH 6.8, 20 % mercaptoethanol, 40 % glycerol, 10 % SDS, 15 % water, 0.1 % bromophenol blue, all v/v), and loaded into pre-cast 10 % polyacrylamide gels (Bio-Rad 456-8033). The ladder used in Figure 28 is Fermentas S26619.

2.1.14 Western blot against HIS-tag

The proteins separated on an SDS-PAGE gel were transferred to 0.45 µm nitrocellulose membrane (Bio-Rad #162-0115) using a Bio-Rad Trans-Blot® with three layers of filter paper (Whatman 4) on either side of the gel and nitrocellulose, all soaked in transfer buffer (24.5 mM Tris, 191.8 mM glycine, 20 % methanol (v/v)). Voltage 25 for 20 min (100 mA) was used to transfer the protein.

Protein transfer was checked by staining protein on the membrane with Ponceau S (0.1 % Ponceau S (v/v), 5 % acetic acid (v/v)). This was reversed by rinsing with water.

For western blot, the membrane was first washed in PBS (137 mM NaCl, 2.5 mM KCl, 10 mM Na_2HPO_4, 1.5 mM KH_2PO_4, pH 7.4), then blocked by incubation in PBS with 3 % milk powder (v/v), for 1 h. After three 5-minute washes in PBS with 0.05 % Tween20 (v/v), the membrane was incubated for 3 h in PBS with 0.05 % Tween20 (v/v), 1 % bovine serum albumin (BSA;

(w/v), and a 1:2,000 dilution of Anti-polyHistidine Peroxidase Conjugate (Sigma-Aldrich A7058). The membrane was washed another three times in PBS with 0.05 % Tween20 (v/v), then developed; for the development buffer, one tablet of 4-chloro-1-napthtol (Sigma C6788) was dissolved in 10 ml methanol, then 2 ml of this was added to 10 ml triethanolamine buffer saline (137 mM NaCl, 27 mM KCl, 12 mM triethanolamine, pH 7.5) with 5 µl 30 % H_2O_2.

2.1.15 Protein identification following Strep-MDHAR6 purification

Identification of eluted protein was carried out by the University of York Bioscience Technology Facility, using trypsin digestion of samples extracted from an SDS-PAGE gel, and mass spectrometry (identification code for samples B696).

2.1.16 Michaelis-Menten plots for MDHAR6 activity towards MDA, TNT and CDNB

Activity was determined by measuring rate of A_{340} decrease, assuming an extinction coefficient of the cofactor NADH at 340 nm of 6.22 $mM^{-1}.cm^{-1}$. Assay conditions are detailed in the figure legends. The concentration of MDA generated was estimated by measuring the increase in A_{360} upon ascorbate oxidase addition, in the absence of NADH (which absorbs at 360 nm) or extract, and assuming an absorbance coefficient for MDA at 360 nm of 3.3 $mM^{-1}.cm^{-1}$ (Bielski et al., 1971; Hossain et al., 1984). Kinetic analysis was carried out using Sigma Plot v12.0.

2.1.17 Electron Paramagnetic Resonance spectrometry

Spectra were recorded on Bruker EMX Micro spectrometer at X band (9.86 GHz), with modulation amplitude 1 G, microwave power 5 mW, scan time 80 s and time constant 80 ms. The activity assays contained 1.5 mg/ml MDHAR6 in 50 mM KH_2PO_4 (pH 7), 80 mM DMPO or DEPMPO, 300 µM NADH and 500 µM TNT in DMF (end DMF concentration 1 % v/v). For assays containing superoxide dismutase (SOD; Sigma S8409), 2,500 U/ml SOD in 100 mM KH_2PO_4 pH 7.5 was added to the assay to an end concentration of 50 U/ml, before addition of TNT and NADH. For the control with denatured MDHAR6, the protein was boiled for 5 min. Simulations of anticipated EPR spectra were constructed using WinSim freeware, available from the National Institute of Environmental Health Sciences (http://www.niehs.nih.gov/research/resources/software/tox-pharm/tools/). The line widths and hyperfine constants used in the simulations were optimized to fit the experimental spectra. Simulation parameters for DMPO-superoxide adduct: a_N = 14.09 G, $a_{\beta\text{-}H}$ = 11.33 G, $a_{\gamma\text{-}H}$ = 1.23 G, DMPO-OH a_N = 14.97 G, $a_{\beta\text{-}H}$ = 14.68 G, DEPMPO-superoxide adduct, isomer 1 (42%): a_N = 13.03 G, $a_{\beta\text{-}H}$ = 11.85 G, $a_{\gamma\text{-}H}$ = 0.68 G, a_P = 50.76 G, and DEPMPO-superoxide adduct, isomer 2 (58%): a_N = 13.15 G, $a_{\beta\text{-}H}$ = 10.29 G, $a_{\gamma\text{-}H}$ = 0.61 G, a_P 49.63 G.

2.1.18 Staining with 3,3'diaminobenzene

Seedlings were vacuum infiltrated in 1 mg/ml 3,3'diaminobenzene (DAB) in 50 mM Tris-acetate (pH 5) for 30 min. The vacuum was then released, and seedlings were incubated for a further 2.5 h. The DAB staining was carried out in the dark and at room temperature (RT). Images were taken using a Nikon SMZ800 dissection microscope with AxioVision Rel. 4.5 software.

2.1.19 Genomic DNA (gDNA) extraction

Plant tissue was ground with a pestle within a 1.5 ml Eppendorf tube with 500 µl CTAB buffer (2 % cetyl trimethylamin bromide, 1.4 M NaCl, 100 mM Tris-HCl pH 8, 20 mM Na_2EDTA), then incubated at 65 °C for 1 h. This was vortexed with 300 µl of 24:1 chloroform:iso-amyl-alcohol, centrifuged (13,000 rpm, 10 min) and 300 µl of aqueous layer transferred to a new 1.5 ml Eppendorf tube containing 960 µl ethanol and 40 µl 3 M NaAc. Genomic DNA was precipitated at RT over 40 min, then pelleted with centrifugation (13,000 rpm, 15 min, 6 °C). The pellet was rinsed in 70 % ethanol, dried (Savant DNA Speed-Vac, high temperature setting, 10 min) then resuspended in 100 µl sterile water.

2.1.20 Polymerase chain reaction (PCR)

Phusion High-Fidelity DNA Polymerase (New England Biolabs M0530) was used, following the manufacturer's instructions.

Primers used in PCR and qPCR experiments are detailed in section 1.1.

2.1.21 DNA sequencing

The qPCR amplicons were sequenced by GATC Biotech, and analysed using SeqScanner2.0 (Applied Biosystems) and ClustalW2 (Larkin et al., 2007).

2.1.22 RNA extraction and cDNA preparation

RNeasy (QIAGEN 74104) with DNase I (QIAGEN 79254; in *MDHAR6* TSS preference study only) was used for RNA extraction, and SuperScript II Reverse Transcriptase (Invitrogen 18064-022) for cDNA synthesis.

2.1.23 Quantitative PCR

The qPCR experiments used Fast SYBR Green Master Mix (Applied Biosystems 4385612), StepOne Plus Real Time PCR System (Applied Biosystems) and StepOne Software v2.2.2.

For primer efficiency testing, an end concentration of 8,000, 800, 80 or 8 pg/µl cDNA was added per well, with 200 nM of each primer, and three technical replicates.

The qPCR experiments typically used an end cDNA concentration of 80 pg/ul, with 200 nM of each primer.

2.1.24 Treatment of root and leaf tissue with antimycin A, TNT or methyl viologen for *MDHAR6* transcription start site study

Col7 seedlings were grown hydroponically, as described in 2.1.2, for 3 weeks. Test treatments were carried out within a sterile Category 3 fume hood.

For the root treatments, rafts were transferred to petri dishes containing 50 ml of ½ MS(S) with control treatment (0.1 % DMSO v/v), 25 µM antimycin A (Sigma A8674) or 50 µM TNT. The leaves were also sprayed with 1.8 ml water (the leaf control treatment).

For leaf treatment, rafts were transferred to petri dishes containing 50 ml of ½ MS(S) 0.1 % DMSO (root control treatment), and sprayed with 1.8 ml of either control treatment (water) or 50 µM methyl viologen (Aldrich Cat. 85,617-7).

The petri dishes were then moved to a growth room for 2 h, before the tissue was harvested.

2.1.25 Antibody raised against MDHAR6

Antibody against purified Strep-MDHAR6 was produced in rabbit by Covalab UK, Ltd.

2.1.26 Western blot using antibody raised against MDHAR6

Protein was extracted from two-week old Col7, Nossen, *mdhar6-1* and *mdhar6-2* seedlings, which were grown vertically on ½ MS(A). Root tissue was homogenised in extraction buffer (100 mM Tricine, 1 mM Na_2EDTA, 5% (v/v) polyvinylpyrrolidine-40, 20% (v/v) glycerol, 2 mM DTT) using a bead mill, then samples were centrifuged (13,000 rpm, 4 min), and denatured supernatant ran on an SDS-PAGE gel (10 µg protein per lane).

Protein was transferred to nitrocellulose, and stained with Ponceau S, as described in 2.1.14.

For western blot analysis against MDHAR6, the secondary antibody, goat anti-rabbit alkaline phosphatase (Sigma A3687), was used. The membrane was washed in TBST buffer (50 mM Tris pH 7.5, 20 mM NaCl, 0.1% Tween-20 v/v) for 5 min, blocked in TBST with 5 % BSA (w/v) for 1 hour, then incubated with a 1:1,000 dilution of primary antibody (rabbit 1344025, or pre-immune serum) in TBST with 3 % BSA, for 2 h. The membrane was washed another three times in TBST, then incubated with a 1:20,000 dilution of the secondary antibody in TBST with 3 % BSA for 1 h. The membrane was washed in TBST another three times, then developed using SigmaFAST (Sigma B5655) for 10 min, then washed in TBST again for 3 x 5 min.

2.1.27 Cloning of *promoter:GUS* contructs

Promoter regions were amplified using Phusion High-Fidelity DNA Polymerase (New England Biolabs M0530) and the primers listed in Table 14. The promoters were first cloned into pCR™-Blunt II-TOPO® plasmid and transformed into TOP10 competent cells using Zero Blunt® TOPO® PCR Cloning Kit (Invitrogen K2800), following the manufacturer's instructions. After the sequence of the cloned promoter region was confirmed, BamHI (New England Biolabs R0136) was used to excise the promoter region, for ligation into BI101.1 (for *CYP81F2* promoter regions; Arabidopsis Biological Resource Center i.e. ABRC stock number CD3-385) or BI101.2 (for *UGT73C1* and *GSTU25* promoter regions; ABRC stock number CD3-386) (Jefferson, 1987). Antarctic phosphatase (New England Bioloabs M02895) was used to prevent religation of the vectors before ligation of insert. The ligation reactions used vector:insert ratios of 1:3, 1:1, 3:1 and 6:1, with 100 ng vector, and T4 DNA Ligase (New England Biolabs M02025), and were incubated for 1h30 before transformation of ligated constructs (in a 2 µl ligation reaction volume) into *E. coli* strain DH5α. The transformation reactions were the same as for the *E. coli* strain Arctic Express cells, except a longer (45 sec) heat shock at 42 °C was used.

QIAprep Spin Miniprep Kit (QIAGEN 27104) was used to extract plasmid DNA from 5 ml cultures (in LB) of transformed bacteria, and Wizard® SV Gel and PCR Clean-Up (Promega A9281) was used to purify PCR product, and promoter regions from 1 % agarose gels after digestion from pCR™-Blunt II-TOPO®, and electrophoresis.

To select for cells transformed with pCR™-Blunt II-TOPO®, BI101 or BI121 plasmids, 50 µg/ml kanamycin was used. Colony PCR with GoTaq® Flexi DNA Polymerase (Promega M829; with end 5 mM $MgCl_2$) and primers listed in Table 14 were used to confirm presence of promoter insert, and orientation.

The BI121 plasmid, in which *GUS* is constitutively expressed via the *Cauliflower Mosaic Virus 35S* promoter (ABRC stock number CD3-388; Jefferson, 1987), was also amplified for transformation into Arabidopsis.

2.1.28 Stable transformation of Arabidopsis with *promoter:GUS* constructs

The *promoter:GUS* contructs were stably transformed into Arabidopsis Col0 ecotype using floral dip with *Agrobacterium tumefaciens* (Agrobacterium) strain GV3101 carrying the Ti (pMP90RK) plasmid.

The Agrobacterium was transformed by electroporation; 100 µl aliquots of competent cells were incubated with 1 µl purified plasmid on ice for 1 min, then pulsed with 2.5 kV voltage in a MicroPulser™ (Bio-Rad 165-2100; setting Ec2) within a 2 mm electroporation cuvette (EQUIBIO

ECU102). The Agrobacterium was then added to 750 µl SOC medium (20g/L tryptone, 5 g/L yeast extract, 0.5 g/L NaCl, autoclaved, then to 1 L additional 10 ml 1 M $MgCl_2$, 10 ml 1 M $MgSO_4$ and 10 ml 2 M glucose, all filter-sterilised before addition) and incubated at 30 °C with 180 rpm for 3 h, before plating on 50 µl/ml kanamycin and 50 µl/ml gentamycin LB plates, for incubation at 30 °C for two days.

Ten ml starter cultures (inoculated with a single Agrobacterium colony) were cultured for 18 h with 180 rpm and 50 µl/ml kanamycin and 50 µl/ml gentamycin, then 1 µl of starter culture was added to PCR reactions (using GoTaq® Flexi DNA Polymerase; Promega M829) to confirm for the presence of *promoter:GUS* constructs in the Agrobacterium. The starter culture was then used to inoculate 500 ml LB in a 500 ml conical flask, which was incubated in the dark at 30 °C with 180 rpm for 2-3 days.

Arabidopsis was transformed by floral dip with Agrobacterium, based on the method described by Clough and Bent (1998); Agrobacterium from a 500 ml culture was pelleted by centrifugation (10 min, 5,000 rpm), then resuspended in 600 ml 5 % (w/v) sucrose, 0.05 % TritonX-100. The influorescence of Arabidopsis, with developing buds, was dipped in this solution at two time points, approximately one week apart. Dipped plants were closed within autoclave bags for 24 h after dipping, to increase humidity. Transformed seedlings were selected on ½ MS(A) containing 50 µl/ml kanamycin.

2.1.29 Statistical analysis

Statistical analyses were carried out using IBM SPSS Statistics 22 software, with the exception of kinetic analysis, which was carried out using Sigma Plot v12.0.

2.2 PRIMER SEQUENCES

Primers were obtained from Sigma Aldrich.

The primers in Table 12 were used to amplify the *MDHAR6* TSS region, and for amplicon sequencing.

Primers used in qPCR experiments are shown in Table 13. In all qPCR, *ACTIN2* was used as the endogenous control.

Primers used to clone promoter regions are shown in Table 14.

Table 12: Primers used to amplify and sequence the *MDHAR6* transcription start site region

Primer label	Primer sequence (5' to 3')
TSS seq F	CCGCGACGAATTGTTTTCCA
TSS seq R	CGTTAGCGAACGAAGCAGTG

Table 13: Quantitative PCR primers

Target gene/ primer pair	Primer label	Primer sequence (5' to 3')
ACTIN2	qActinF	TACAGTGTCTGGATCGGTGGTT
	qActinR	CGGCCTTGGAGATCCACAT
mA	q mA F	CAGAGAGACTCACACACTTGTTTCAA
	q mA R	TAATGTCTGCAGTTCGTAGAGTCATG
mB	q mB F	GCTCTTCTTATAAACTAATGTCTGCAGTTC
	q mB R	AACCACGTTGCCGACGAA
mC	q mC F	GCTCTTCTTATAAACTAATGTCTGCAGTTC
	q mC R	GAAGTCCGGATTATCTCTTTGGTG
mD	q mD F	ATCTGAATTTGGCTCTTCTTATAAAC
	q mD R	CAACGTGGTTGATGCTAACG
mE	q mE F	CACTACAGAGAGACTCACACACTTGTTTC
	q mE R	CATGACTCTACGAACTGCAGACATTAG
pA	q pA F	CGATTGTCAAAACCCTAGATCGA
	q pA R	TTCGTAGAGTCATGGCGTTAGC
pB	q pB F	CATCTTCTTCCTCGATTGTCAAAA
	q pB R	AATCTGTTGTTACAGTTCGTAGAGTCATG
pC	q pC F	TCTTCTTCCTCGATTGTCAAAACC
	q pC R	TTACAGTTCGTAGAGTCATGGCGT
pD	q pD F	TCTCTCACTCACCACCATCTTC
	q pD R	CAGATTAGAGAGATAAGATTTCGATCT
pE	q pE F	CTCTCTAATCTGTTGTTACAGTTCGT
	q pE R	CGTCGGCAACGTGGTT

mpA	q mpA F	CCACGTTGCCGACGAAGT
	q mpA R	TCTCTCGCTCGCCGATTT
mpB	q mpB F	TGGTCGGCTATGCATTGTGA
	q mpB R	TGAGAGACCGGCTTTGACAA
mpC	q mpC F	TGGAAAATGGAATGGCTGATG
	q mpC R	CCAAAGAGGCTTACGCACCT
mpD	q mpD F	TTCGTAGAGTCATGGCGTTAGC
	q mpD R	CACCAAAGAGATAATCCGGACTTC
mpE	q mpE F	CATGGCGTTAGCATCAACCA
	q mpE R	GGAGAAGACGGACACCAAAGAG
mpF	q mpF F	CCGACGAAGTCCGGATTATC
	q mpF R	AAAAACGAGCGGGAAATCG
AOX1a	q AOX1 F	GACGATTGGAGGTATGAGATTCG
	q AOX1 R	TCGCGTCCTCCTCCTTCA
APX2	v2 q APX2 F	TGGGTCGGTGCCACAAG
	v2 q APX2 R	GAGCGGGTTTGGTGTCCAT
CYP71A12	CYP71A12 qF	GCCAACCGCCCGAGAT
	CYP71A12 qR	TCACGCCCCCCATTCATA
CYP81D11	qCYP81D11F	AGATTGTATAGTTGATGGCTATGACGTT
	qCYP81D11R	TCTATGGATGGCCCATGCA
CYP81D8	CYP81D8 qF	TTTTGCGGTTGGTTTCAGATT
	CYP81D8 qR	CGAGCCTACCCGCCAACT
CYP81F2	qCYP81F2F	TCTCCCACCAGGACCAACTC
	qCYP81F2R	CGGTGGACCGGTGGTTT
GSTU24	GSTU24 qF	GTGTACGAGAAGTTTGGAAATGTCA
	GSTU24 qR	GGCCCACGCAACCAATT
GSTU25	qGSTU25F	TGTCAAATTCGATTACAGAGAACAAG
	qGSTU25R	GGTATTTTCTTATGAACCGGATTCA
GSTU4	GSTU4 qF	GGTCCAATGGCGGAGAAA
	GSTU4 qR	AGGGCTTGCCCAAAAACC
OPR1	OPR1 qF	ATCCAGGAGCATTAGGGC
	OPR1 qR	CGCTTTCCTCATCGGCAT
OPR2	OPR2 qF	CCAGAAGCATTAGGGCTG
	OPR2 qR	GGCTTCCCTCATTGGCAT
OPR3	OPR3 qF	AAAGCTCGCTTACCTTCACGTT
	OPR3 qR	CATCACTCCCTTGCCTTCCA
UGT73B4	UGT74E2 qF	GGACTGATCAGCCCACGAAT
	UGT74E2 qR	CCCTTACCCCAACCTTCCA
UGT73C1	qUGT73C1F	AGGTTAAAGCGGGTAAGATATGGA
	qUGT73C1R	CCTCTCAGCTTGGTCTTCTCCTAA
UGT74E2	UGT74E2 qF	GGACTGATCAGCCCACGAAT
	UGT74E2 qR	CCCTTACCCCAACCTTCCA

Table 14: Primers used to clone promoter regions

Promoter region	Primer label	Sequence
UGT73C1 -1,088 to + 50 bp from start ATG	UGT F BamHI NW	CAGGGATCCATGAAAGGGAAGAGAACA
	UGT R BamHI	CTTGGATCCATATCATATTTTTGCTAC
UGT73C1 -244 to + 50 bp from start ATG	UGT R BamHI -244	TCGGGATCCATGAATACAAAAGAACAT
	UGT R BamHI	CTTGGATCCATATCATATTTTTGCTAC
GSTU25 -1,563 to +83 bp from start ATG	GST F BamHI	TGTGGATCCTCATTACATTCATTTCCG
	GST R BamHI	TGGGGATCCACATTTTTCTCTTCTAAAG
GSTU25 -220 to +83 bp from start ATG	GST F BamHI -220	TGCGGATCCTATTCCCTTCATATTAAA
	GST R BamHI	TGGGGATCCACATTTTTCTCTTCTAAAG
CYP81F2 -997 to +48 bp from start ATG	CYP F BamHI -997	TGAGGATCCAAAACAAGGTGGGTACAT
	CYP R BamHI	TCTGGATCCAGCTATGAGAAACAATGC
CYP81F2 -270 to +48 bp of start ATG	CYP F BamHI -270	TGAGGATCCGAAATGGTCAAGGAGAAT
	CYP R BamHI	TCTGGATCCAGCTATGAGAAACAATGC
Primer within *GUS* gene, used in PCR to check orientation of promoter insert	GUS +69 R	TCCACAGTTTTCGCGATCC

3 MDHAR6 mediates TNT toxicity in Arabidopsis

3.1 INTRODUCTION

3.1.1 Screen identifying *mdhar6* mutants as having enhanced TNT tolerance

The Arabidopsis mutant *enhanced TNT tolerance* (*ett*) was originally isolated by Lorenz (2007), in screen of Weigel T-DNA activation tagged lines (Weigel et al., 2000), for mutants with longer primary roots on agar containing 7 µM TNT. In a screen of 72,000 seeds, 59 putative mutants were isolated. From the following selfed generation (T5), the enhanced TNT tolerance was only confirmed for one line, N23093.

The mutation was subsequently mapped by Beynon (2008). It had been anticipated that the tolerance would be due to overexpression of a TNT-detoxifying enzyme, however the *ett* phenotype mapped to a loss-of function deletion in *MONODEHYDROASCORBATE REDUCTASE 6* (*MDHAR6*; At1g63940); a thymine deletion 2,181 bp from the start codon (in exon 11) resulted in an early stop codon, truncating over a third of the protein (Figure 14). This mutant (in the Col7 background) is subsequently referred to as *mdhar6-1.*

The enhanced TNT tolerance phenotype, on both TNT-supplemented agar and soil, was confirmed for two further *mdhar6* mutants by Liz Rylott and Maria Budarina (CNAP, University of York; Figure 14); *mdhar6-2* (Nossen background) contains a transposon 538 bp downstream of the start codon, while *mdhar6-3* (Col0 background) contains a T-DNA insert 76 bp upstream of the start codon, which decreases transcript abundance.

Complementation studies confirmed that functional MDHAR6 decreases TNT tolerance; Emily Beynon, Liz Rylott and Maria Budarina (CNAP, University of York) transformed both *p-MDHAR6* (transcript variant *MDHAR6.1*, encoding plastid-targeted MDHAR6) and *m-MDHAR6* (transcript variant *MDHAR6.2*, encoding mitochondria-targeted MDHAR6) into Col7 and *mdhar6-1* mutants; the *m-MDHAR6* gene fully complemented the phenotype, while *p-MDHAR6* complemented the phenotype by approximately 66 % (Figure 15).

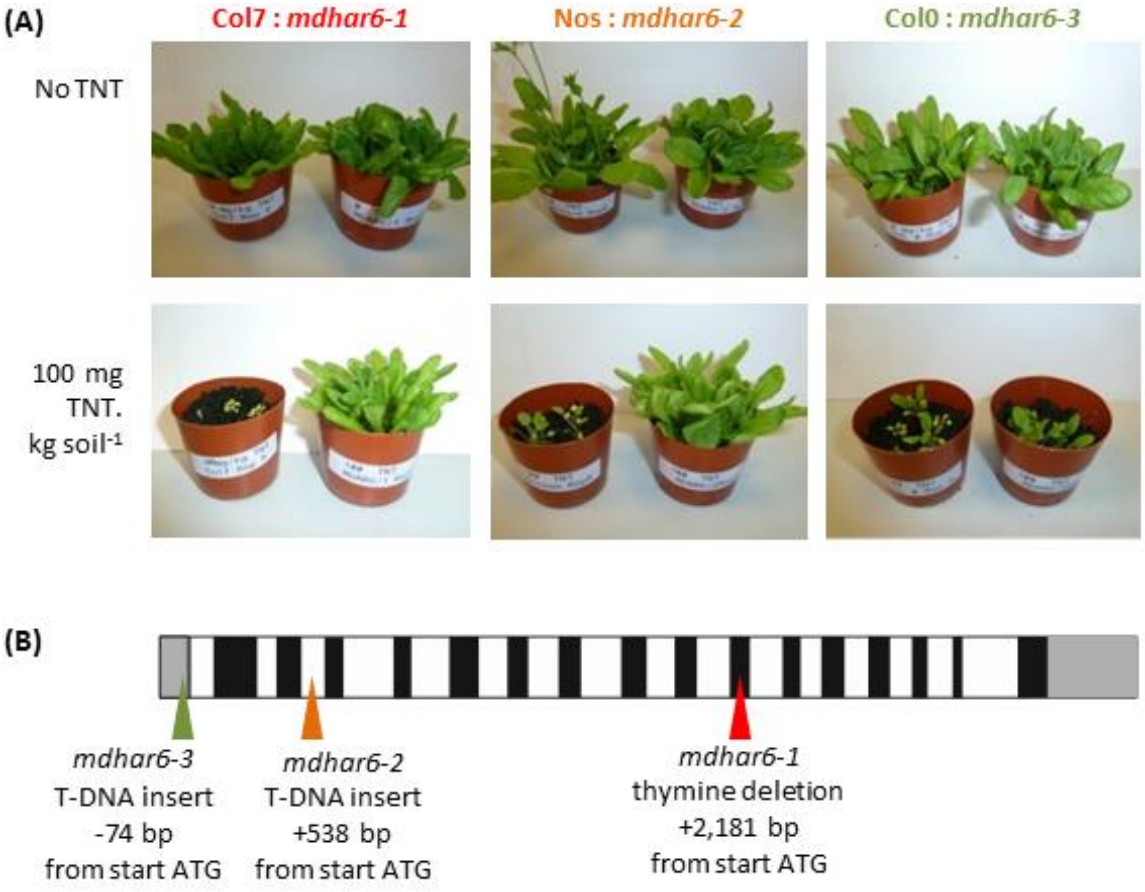

Figure 14: Three *mdhar6* mutants with enhanced TNT tolerance

(A) Six-week old *mdhar6* plants (right) adjacent to wild type backgrounds (left), which were transferred to TNT-treated or control-treated soil at 5 d of age. There are five plants per pot. Experiment by Liz Rylott and Maria Budarina. **(B)** Scale representation of *m-MDHAR6* showing mutation locations. Black boxes; exons. White boxes; introns. Grey boxes; untranslated regions.

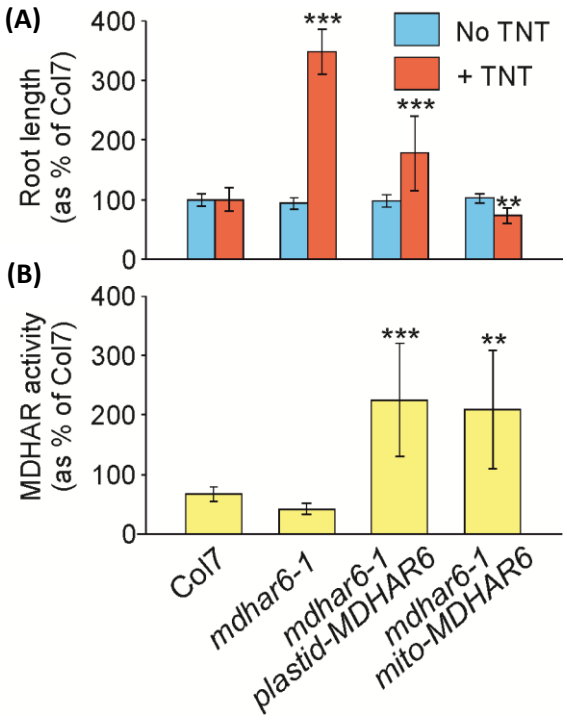

Figure 15: Complementation of TNT tolerance phenotype in *mdhar6-1*

Summary of complementation experiments carried out by Liz Rylott and Maria Budarina. Three independent lines of Col7 and *mdhar6-1* were transformed with *m-MDHAR6* or *p-MDHAR6,* constitutively expressed using the *Cauliflower Mosaic Virus 35S* promoter. These summary charts display the average root length and MDHAR activity for the median of three complementation lines, compared with Col7. **(A)** Root lengths of 7-day old seedlings germinated on 0 or 7 µM TNT-treated ½ MS(A). Six biological replicates per line ± SD. **(B)** Rosette leaf MDHAR activity as percentage of activity from Col7 leaf tissue. Five biological replicates ± SD. Student's t test comparing with values for Col7, * P<0.05, ** P<0.01, *** P<0.001. Figure reproduced from Johnston et al. (2015).

3.1.2 Monodehydroascorbate reductases

Activity

The finding that a deficiency in MDHAR6 increases TNT tolerance was surprising, as MDHARs are usually considered to protect plants from oxidative stress, by recycling the antioxidant ascorbic acid; MDHARs are flavin adenine dinucleotide (FAD)-dependent oxidoreductases, which reduce monodehydroascorbate (MDA), the free radical primary oxidation product of ascorbate (Figure 16; Yamazaki and Piette, 1961; Hossain et al., 1984).

Monodehydroascorbate reductase activity was first described by Arrigoni et al. (1981), and MDHAR enzymes from cucumber (Hossain and Asada, 1985; Sano et al., 1995), potato (Borraccino et al., 1986; De Leonardis et al., 1995), soybean root nodules (Dalton et al., 1992) and spinach (Miyake et al., 1998; Sano et al., 2005), have since been purified either directly from tissue, or recombinantly. These studies have demonstrated reductase activity towards MDA, and a double replacement mechanism has been proposed (Scheme 2).

$$E\text{-FAD} + \text{NADH} \rightarrow E\text{-FADH}_2\text{-NAD}^+$$

$$E\text{-FADH}_2\text{-NAD}^+ + \text{MDA} \rightarrow E\text{-FADH}^{\bullet}\text{-NAD}^+ + \text{ascorbate}$$

$$E\text{-FADH}^{\bullet}\text{-NAD}^+ + \text{MDA} \rightarrow E\text{-FAD} + \text{NAD}^+ + \text{ascorbate}$$

Scheme 2: Double replacement mechanism for MDA reduction by MDHAR
Mechanism proposed by Hossain and Asada (1985); NADH is used to reduce FAD to the charge transfer complex E-$FADH_2$-NAD^+, which then sequentially donates two electrons to MDA.

In this way, MDHAR regenerates the antioxidant ascorbate. There is also evidence that MDHARs further replenish the antioxidant pool, by reducing radicals of flavonoid and lignin precursors, which can also act as antioxidants; Sakihama et al. (2000) detected cucumber MDHAR activity towards radicals of quercetin, chlorogenic acid, ferulic acid and coniferyl alcohol. Hossain and Asada (1985) also report MDHAR activity against ferricyanide and 2,6-dichloroindophenol (DPIP). Ferricyanide complexes form in soil where cyanide has been applied for metal extraction (Yu et al., 2008), while DPIP is an oxidant commonly used as a colorimetric redox dye. The structures of these diverse putative substrates are shown in Figure 17.

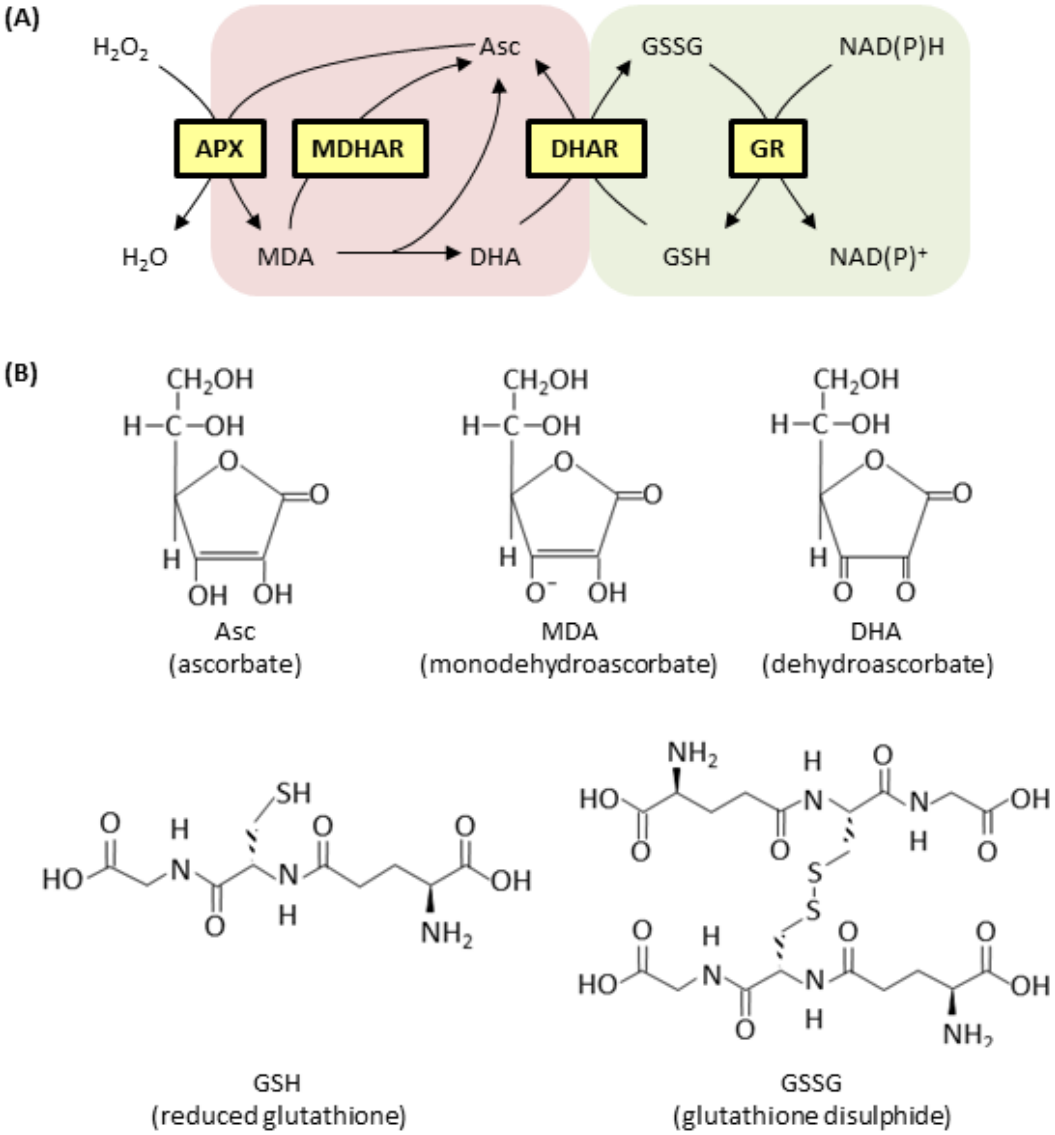

Figure 16: The ascorbate-glutathione cycle

(A) Schematic; ascorbate (Asc) is oxidised by ascorbate peroxidase (APX), superoxide or hydroxyl radicals, to monodehydroascorbate (MDA). The MDA radical can be reduced back to Asc by monodehydroascorbate reductase (MDHAR), or will spontaneously disproportionate to Asc and dehydroascorbate (DHA). The DHA may catabolise to 2,3-diketogulonic acid or L-threarate, or can be reduced back to Asc by dehydroascorbate reductase (DHAR), with the concurrent oxidation of reduced glutathione (GSH) to glutathione disulphide (GSSG). The GSSG can be subsequently reduced by glutathione reductase (GR). **(B)** Structures of reduced and oxidised ascorbate and glutathione.

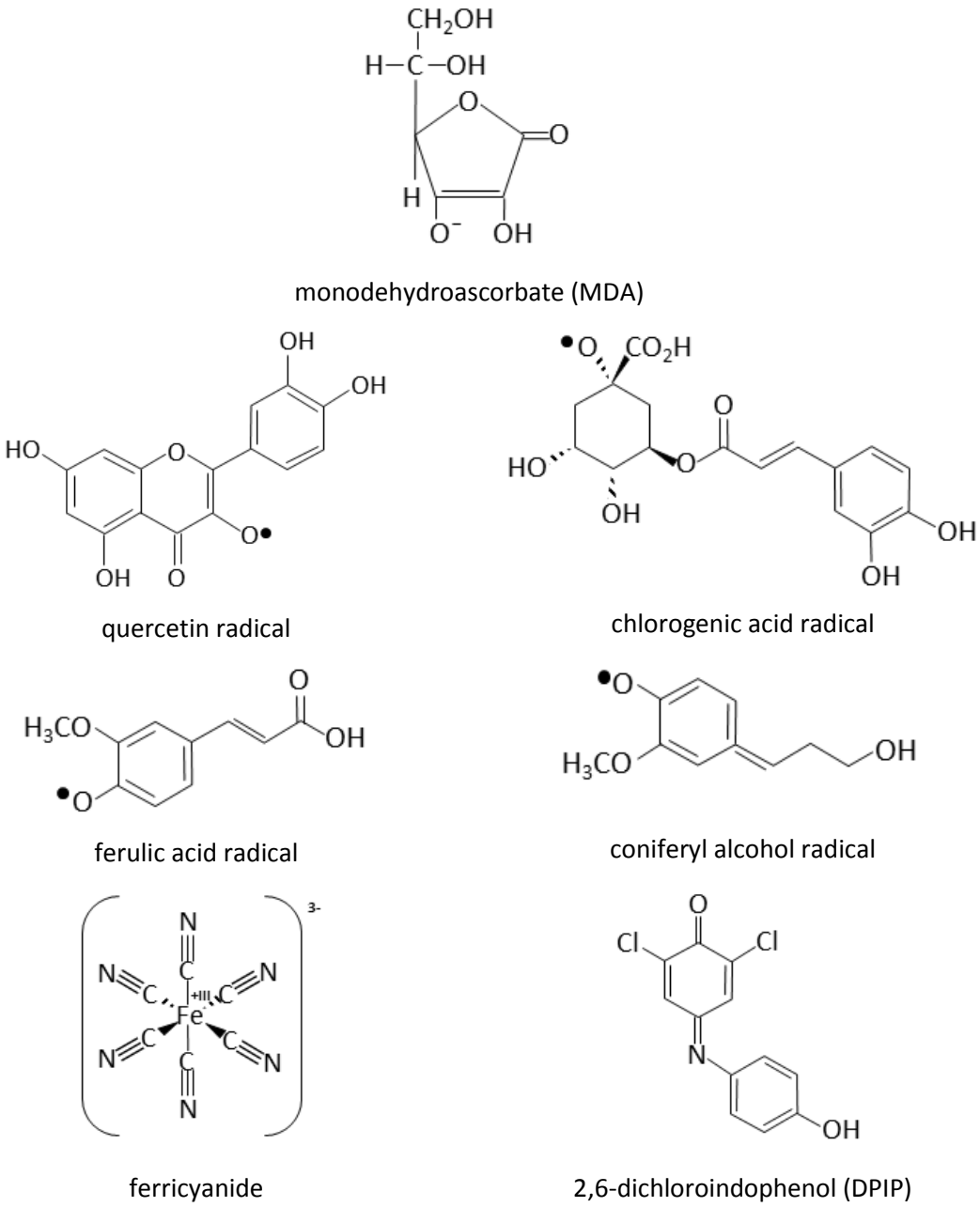

Figure 17: Structures of reported MDHAR substrates

Activity towards these compounds reported by Hossain and Asada (1985), Sano et al. (1995) and Sakihama et al. (2000).

Overexpression studies

Due to the proposed antioxidant recycling role of MDHARs, a number of studies have investigated whether *MDHAR* overexpression could be used to increase stress tolerance in plants (Table 15); in most published studies, increased MDHAR activity enhances stress tolerance (Eltayeb et al., 2006; Kavitha et al., 2010; Li et al., 2010). Eltayeb et al. (2006) report a 2.2-fold increase in reduced ascorbate levels in *MDHAR*-overexpressing tobacco leaves. Overexpression studies in tomato however, conversely report decreases in reduced ascorbate content when *MDHAR* is overexpressed (Haroldsen et al., 2011; Gest et al., 2013). This could be due to differences between test species, or the location of the overexpressed MDHAR protein.

Table 15: *MDHAR* overexpression studies

Study	Plant system	Overexpressed *MDHAR*	Results (relative to untransformed plants)
Eltayeb et al. (2006)	Tobacco	Arabidopsis *MDHAR1* (cytosolic)	2.2-fold increase in reduced ascorbate. Higher net photosynthetic rates following ozone, salt and polyethylene stress treatments.
Kavitha et al. (2010)	Tobacco	Mangrove *MDHAR* (chloroplastic)	Delayed wilting following NaCl treatment.
Li et al. (2010)	Tomato	Tomato *MDHAR*	Lower H_2O_2 levels and higher net photosynthetic rate and maximal photochemical efficiency under high or low temperature stress, or methyl viologen treatment.
Yin et al. (2010)	Tobacco	Arabidopsis *MDHAR1* (cytosolic)	No increased tolerance to aluminium (overexpression of *DHAR* however increased aluminium tolerance).
Haroldsen et al. (2011)	Tomato	Tomato *MDHAR3* (cytosolic and peroxisomal)	No difference in leaf ascorbate content, however a 0.7-fold decrease in reduced ascorbate in fruit.
Gest et al. (2013)	Tomato	Tomato *MDHAR3* (cytosolic and peroxisomal)	Decrease in leaf reduced ascorbate content. Knock-down of *MDHAR3* increased levels of reduced ascorbate.

Arabidopsis MDHARs

There are five *MDHAR* genes in Arabidopsis (Table 16), of which only the product of *MDHAR6* is plastid- or mitochondria-targeted; MDHAR2 and MDHAR3 are cytosolic, while MDHAR1 and MDHAR4 are peroxisomal. Microarray data available through Genevestigator (Hruz et al., 2008) indicate that all but *MDHAR3* are highly expressed throughout all tissues and developmental stages (Figure 18), however *MDHAR3* is induced by biotic attack or treatment with MeJA, SA, cold or hypoxia. Expression of the other cytosolic MDHAR, *MDHAR2*, is also induced in some biotic attack and high light studies, while *MDHAR6* is downregulated in some ABA treatment studies, and expression is higher in the presence of sucrose.

Microarray data available through DIURNAL indicate that unlike the other *MDHAR*s, *MDHAR6* expression is highly induced at night, while expression of *MDHAR4* and possibly *MDHAR1* (the peroxisomal MDHARs), is higher during the day (Mockler et al., 2007; Figure 19). The nocturnal induction of *MDHAR6* appears to be dependent on cold night temperature (Figure 20).

Arabidopsis mutants in *mdhar4* are seedling-lethal in the absence of supplemented sugar (Eastmond, 2007); the mutants are defective in lipase activity, required for breakdown of stored triacylglycerol in early seedling growth. Eastmond (2007) postulates that in the absence of MDHAR4, oxidative damage occurs to the lipase SUGAR-DEPENDENT 1 at oil bodies close to peroxisomes. Mutants in the other MDHAR enzymes have not yet been characterised.

Table 16: Arabidopsis *MDHAR* genes

Arabidopsis Genome Initiative (AGI) code and protein size data from TAIR (Huala et al., 2001), protein location from papers cited.

AGI	Gene	Protein size	Protein location
At3g52880	*MDHAR1*	50 kDa	peroxisome matrices (Lisenbee et al., 2005)
At5g03630	*MDHAR2*	47 kDa	cytosol (Lisenbee et al., 2005)
At3g09940	*MDHAR3*	48 kDa	cytosol (Lisenbee et al., 2005)
At3g27820	*MDHAR4*	54 kDa	peroxisome membranes (Lisenbee et al., 2005)
At1g63940	*MDHAR6*	53 kDa	plastid stroma or mitochondria matrices, depending on transcription start site used (Obara et al., 2002)

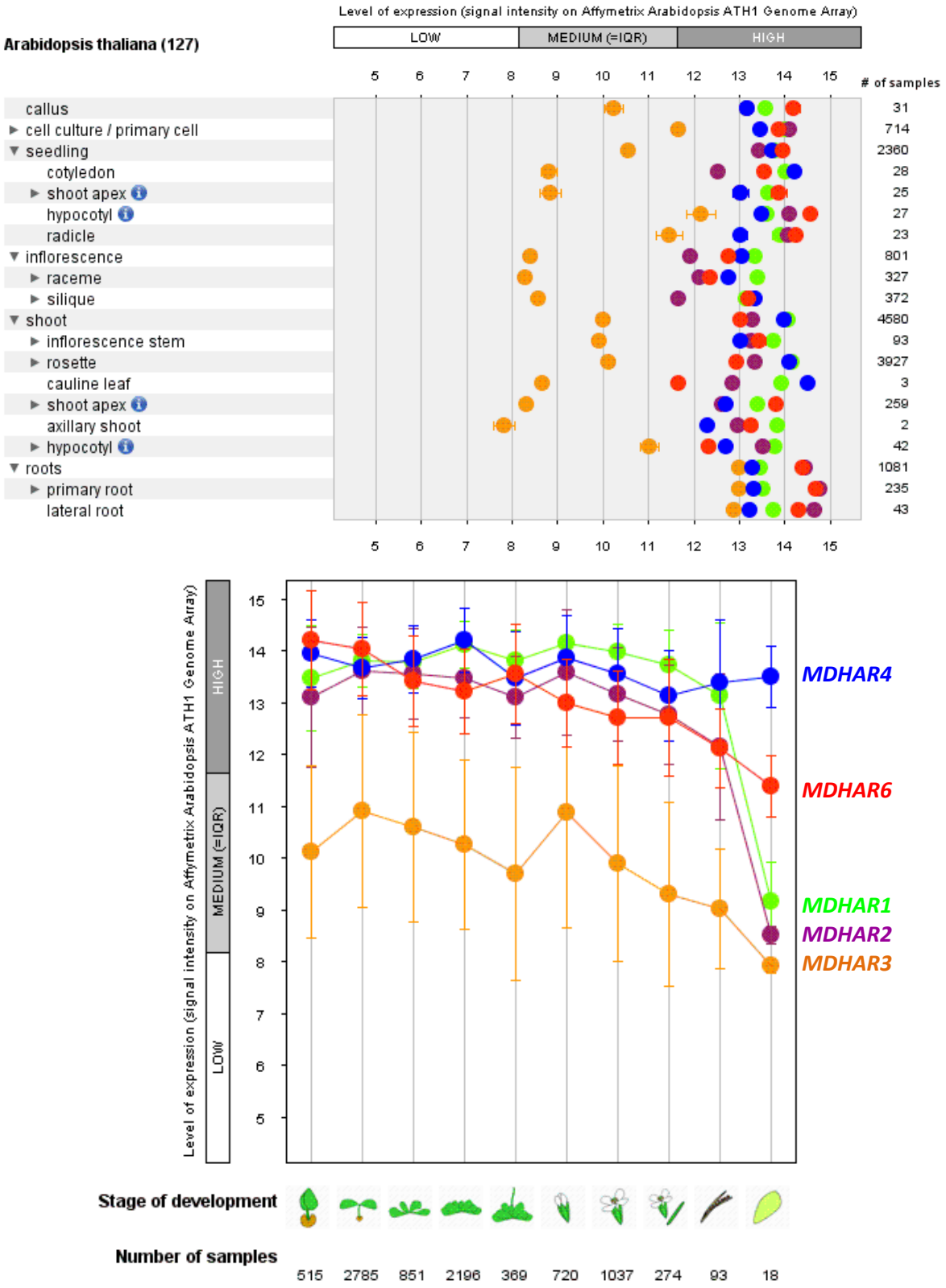

Figure 18: Expression of Arabidopsis *MDHAR* genes anatomically and throughout development

Level of expression in log2 scale. *MDHAR1*; green. *MDHAR2*; purple. *MDHAR3*; orange. *MDHAR4*; blue. *MDHAR6*; red. Source Genevestigator (Hruz et al., 2008), accessed 4th June 2015.

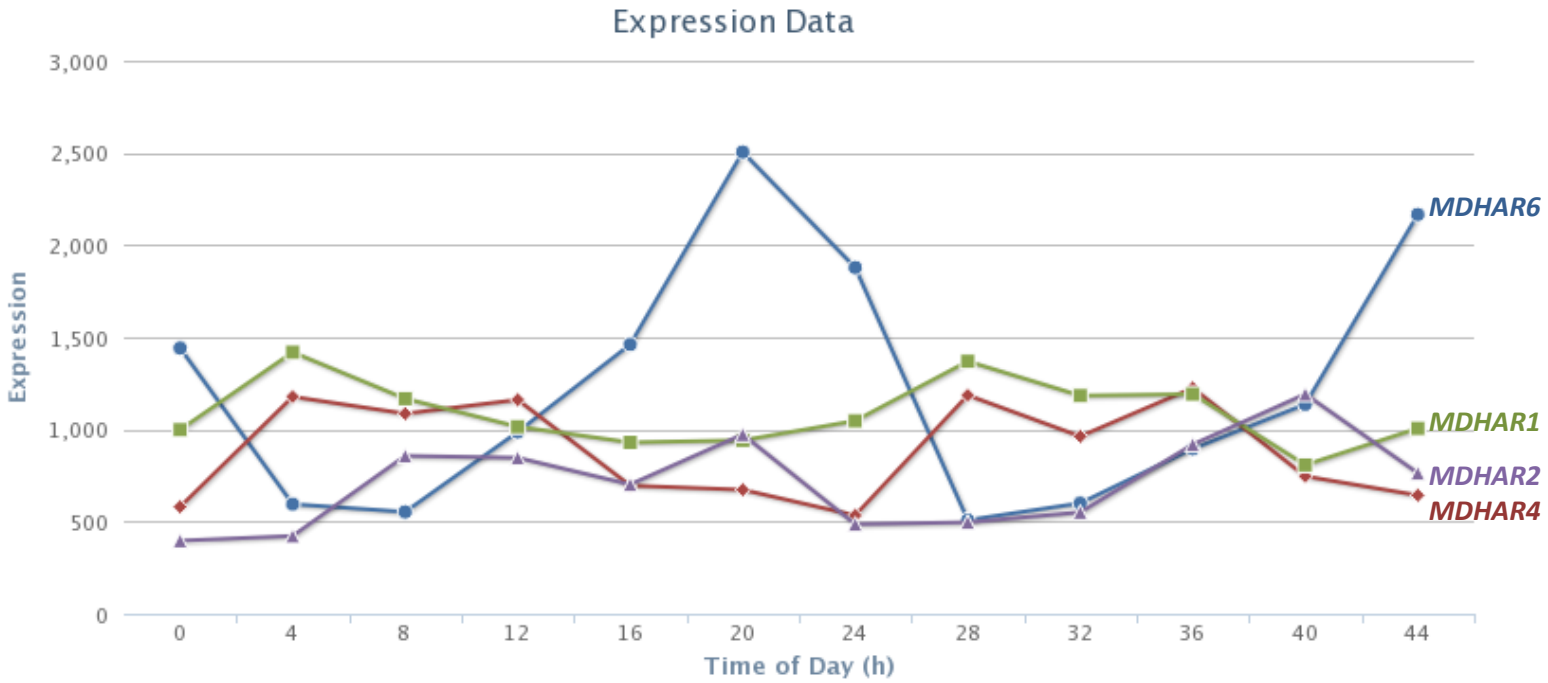

Figure 19: Temporal expression of Arabidopsis *MDHAR* genes

Data from DIURNAL (Mockler et al., 2007), accessed 14th September 2015. Temporal expression under cycle of 12 h light, 22°C/12 h dark, 12°C. Temporal expression results for *MDHAR3* not returned in search. Gene expression for whole seedlings, grown on agar without sucrose. The Robust Multi-array Average expression values are exponentiated using base 2.

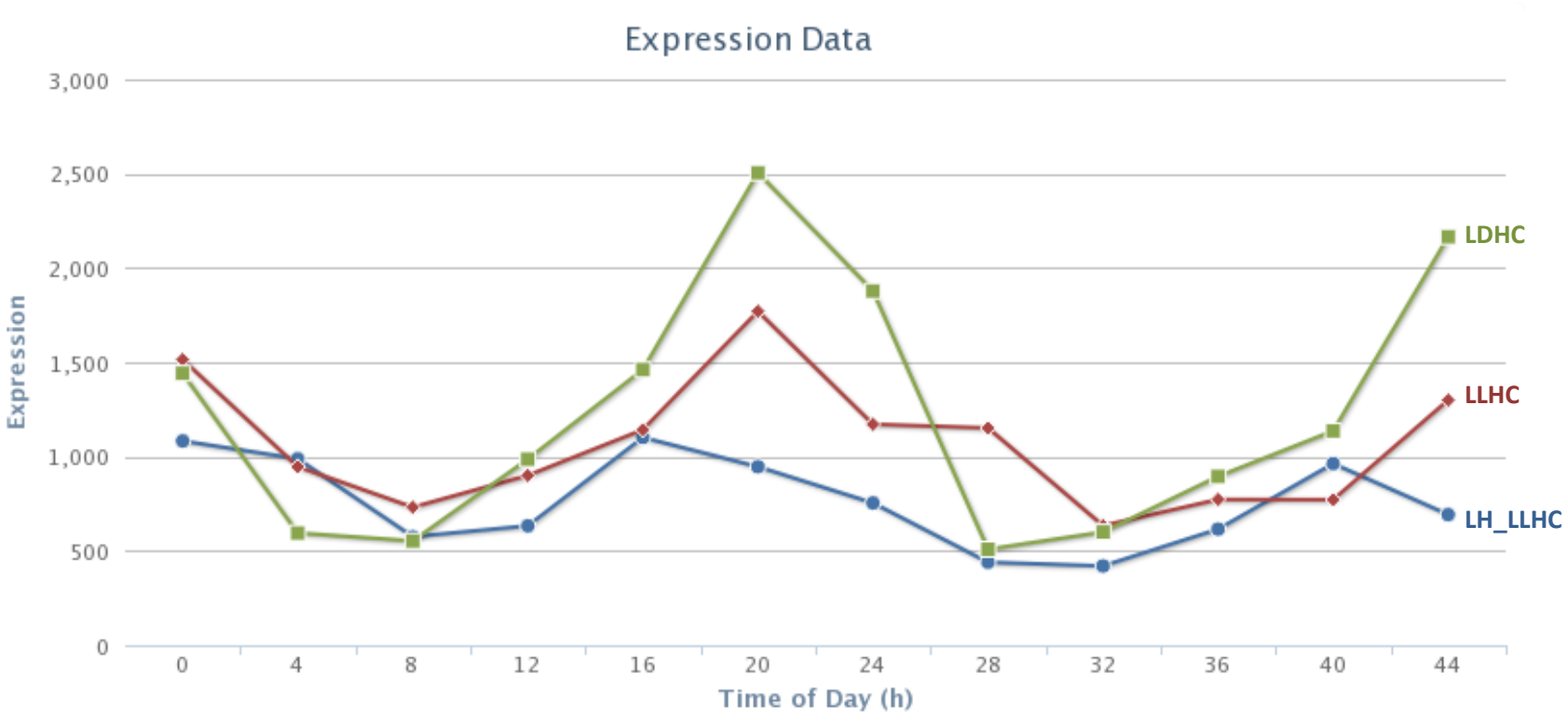

Figure 20: Diurnal expression of *AtMDHAR6* in different experiments

Data from DIURNAL (Mockler et al., 2007), accessed 14th September 2015. LDHC; temporal expression under cycle of 12 h light, 22°C/12 h dark, 12°C. LLHC; temporal expression under cycle of 12 h light, 22°C/12 h light, 12°C. LH_LLHC; entrained to cycle of 12 h light, 22°C/12 h light, 12°C, then subjected to 24 h light, 22°C. Gene expression for whole seedlings, grown on agar without sucrose. The Robust Multi-array Average expression values are exponentiated using base 2.

3.1.3 The ascorbate-glutathione cycle

The ascorbate-glutathione cycle (as depicted in Figure 16) has been referred to as a "redox hub" (Foyer and Noctor, 2011) of interconnecting redox reactions, which function as a buffering mechanism against oxidative stress. Although it is established that ROS have important biological roles in defence and abiotic stress signalling (Mullineaux and Baker, 2010), it is still generally considered that there is the potential in plants for uncontrolled and self-perpetuating oxidative reactions, which can damage lipids, proteins and nucleic acids- this is referred to "oxidative stress" (Halliwell, 2006).

Numerous studies have isolated cell fractions to measure ascorbate and glutathione content, with the caveats that fractions could be contaminated during isolation, and that the isolation process may affect metabolite levels and oxidation states. More recently, using a different approach, antibodies have been raised against ascorbate- or glutathione-BSA (Bovine Serum Albumin) conjugates, and Transmission Electron Microscopy (TEM) with immuno-gold labelling used to examine the relative distribution of ascorbate and glutathione between cellular compartments (Zechmann and Müller, 2010; Zechmann et al., 2011). These studies reveal a difference in the relative distribution of ascorbate and glutathione (Table 17); while ascorbate is proposed to be most concentrated in peroxisomes and the cytoplasm, glutathione is proposed to be most concentrated in mitochondria and nuclei. Notably, in these studies ascorbate was not detected at the apoplast, where ascorbate has been previously identified in a number of other studies (Luwe et al., 1993; Takahama, 1993; Vanacker et al., 1998), and is considered to have an important role in redox buffering and defence signalling (Pignocchi and Foyer, 2003). Metabolite distribution could also differ greatly between tissues, and developmental stages; for example, Vivancos et al. (2010) used confocal microscopy with 5-chloromethylfluorescein to probe for glutathione, and identified recruitment of glutathione to the nucleus during phase G1 of interphase in the cell cycle, corresponding with severe depletion of glutathione in the cytosol.

Table 17: Distribution of ascorbate and glutathione within Arabidopsis mesophyll cells

Ratio of distribution between cellular compartments as determined by immunogold-labelling (Zechmann and Müller, 2010; Zechmann et al., 2011).

Compartment	Relative level of ascorbate	Relative level of glutathione
Peroxisomes	27.1	16.6
Cytoplasm	25.8	12.3
Nuclei	19.4	24.2
Chloroplast stroma	12.8	6
Mitochondria matrices	12.2	40.9
Vacuoles	2.7	below detection
Endoplasmic reticulum	below detection	observed but not quantified
Apoplast	below detection	below detection

The redox cycle depicted in Figure 16 is simplified; ascorbate can also be regenerated through reduction by ferredoxin (Miyake and Asada, 1994), while glutathione peroxidases oxidise GSH to GSSG in reducing H_2O_2 to H_2O (Bela et al., 2015).

Ascorbate and glutathione are sacrificial antioxidants; they scavenge ROS, protecting more biologically-important compounds, and the radicals they form are of relative low reactivity (Halliwell, 2006). The oxidised products are then rapidly recycled (Foyer and Nocter, 2011). Tocopherols, carotenoids and flavonoids are also abundant sacrificial antioxidants in plants, however are not recycled after oxidation (Falk and Munné-Bosch, 2010; Han et al., 2012). Regarding protein-mediated control of ROS, superoxide dismutases actively reduce ROS by catalysing the dismutation of superoxide to H_2O_2 and O_2 (Alscher et al., 2002), and in addition to peroxidases, catalases catalyse the decomposition of H_2O_2 to H_2O and O_2 (Mhamdi et al., 2012). Prxs are possibly the most important proteins involved in H_2O_2 removal in plants (Halliwell, 2006); a Cys thiol group in peroxiredoxin is oxidised to sulfenic acid by H_2O_2, with high affinity (<20 μM). In 2-cys Prxs (the most abundant), the sulphenic acid group forms a disulphide bridge within the protein, which is subsequently reduced by thioredoxins (Halliwell, 2006; Dietz, 2011).

Proteins involved in the ascorbate-glutathione cycle and ROS control are listed in Table 18.

Table 18: Location of Arabidopsis proteins involved in the ascorbate-glutathione cycle and redox homeostasis

Putative locations as stated on TAIR (Huala et al., 2001), accessed July 2015. Thioredoxins as listed by Meyer et al. (2005). MDHAR locations as determined by Obara et al. (2002) and Lisenbee et al. (2005). There are 73 peroxidases in the *Arabidopsis thaliana* genome (Valério et al., 2004); only ascorbate and glutathione peroxidases are included in this table.

Type	AGI	Gene	Location
Ascorbate peroxidases; detoxify peroxides using ascorbate as a substrate	At1g07890	*ASCORBATE PEROXIDASE 1*	cytosol
	At3g09640	*ASCORBATE PEROXIDASE 2*	cytosol
	At4g32320	*ASCORBATE PEROXIDASE 6*	cytosol
	At4g08390	*STROMAL ASCORBATE PEROXIDASE*	chloroplast stroma
	At1g77490	*THYLAKOIDAL ASCORBATE PEROXIDASE*	chloroplast thylakoid
	At4g35000	*ASCORBATE PEROXIDASE 3*	cytosol
	At4g09010	*ASCORBATE PEROXIDASE 4*	cytosol
	At4g35970	*ASCORBATE PEROXIDASE 5*	cytosol
Monodehydroascorbate reductases; reduce monodehydroascorbate, regenerating ascorbate	At3g52880	*MONODEHYDROASCORBATE REDUCTASE 1*	peroxisome matrices
	At5g03630	*MONODEHYDROASCORBATE REDUCTASE 2*	cytosol
	At3g09940	*MONODEHYDROASCORBATE REDUCTASE 3*	cytosol
	At3g27820	*MONODEHYDROASCORBATE REDUCTASE 4*	peroxisome membranes
	At1g63940	*MONODEHYDROASCORBATE REDUCTASE 6*	chloroplast stroma, mitochondria matrices
Dehydroascorbate reductase/glutathione dehydrogenases; oxidise glutathione and reduce dehydroascorbate concurrently	At1g19570	*DEHYDROASCORBATE REDUCTASE 1*	apoplast, chloroplast stroma, cytoplasm, cytosol, mitochondrion, peroxisome, plasma membrane, vacuole
	At1g75270	*DEHYDROASCORBATE REDUCTASE 2*	cytosol, plasma membrane
	At5g16710	*DEHYDROASCORBATE REDUCTASE 3*	chloroplast envelope, chloroplast stroma
Glutathione peroxidases; catalyse reduction of peroxides using glutathione as a hydrogen donor	At2g25080	*GLUTATHIONE PEROXIDASE 1*	chloroplast envelope, chloroplast stroma, chloroplast thylakoid membrane
	At2g31570	*GLUTATHIONE PEROXIDASE 2*	cytosol, mitochondrion, nucleus, plasma membrane
	At2g43350	*GLUTATHIONE PEROXIDASE 3*	Golgi apparatus, cytosol, endosome, mitochondrion, trans-

			Golgi network
	At2g48150	*GLUTATHIONE PEROXIDASE 4*	cytosol, mitochondrion
	At3g63080	*GLUTATHIONE PEROXIDASE 5*	endoplasmic reticulum, plasma membrane
	At4g11600	*GLUTATHIONE PEROXIDASE 6*	apoplast, chloroplast, cytosol, mitochondrion, plasma membrane
	At4g31870	*GLUTATHIONE PEROXIDASE 7*	chloroplast
	At1g63460	*GLUTATHIONE PEROXIDASE 8*	cytosol, nucleus
Glutathione reductases; reduce glutathione disulphide to reduced glutathione	At3g24170	*GLUTATHIONE REDUCTASE 1*	cytosol
	At3g54660	*GLUTATHIONE REDUCTASE 2*	chloroplast stroma, mitochondrion
Ferredoxins; iron sulphur proteins which mediate electron transfer in a variety of processes	At 1g10960	*FERREDOXIN 1*	chloroplast stroma
	At1g60950	*FERREDOXIN 2*	chloroplast stroma
	At2g27510	*FERREDOXIN 3*	chloroplast, plastid
	At5g10000	*FERREDOXIN 4*	chloroplast
Catalases; catalyse decomposition of peroxide to water and oxygen	At1g20630	*CATALASE 1*	cell wall, chloroplast envelope, cytosolic ribosome, mitochondrion, nucleus, peroxisome
	At4g35090	*CATALASE 2*	chloroplast, cytosolic ribosome, glyoxysome, mitochondrion, nucleus, peroxisome
	At1g20620	*CATALASE 3*	apoplast, cell wall, chloroplast envelope, chloroplast stroma, cytosolic ribosome, membrane, mitochondrion, nucleus, peroxisome, plasma membrane, plasmodesmata, vacuole
Superoxide dismutases; catalyse dismutation of superoxide to hydrogen peroxide and molecular	At1g08830	*COPPER/ZINC SUPEROXIDE DISMUTASE 1*	apoplast, cytosol, nucleus
	At2g28190	*COPPER/ZINC SUPEROXIDE DISMUTASE 2*	apoplast, chloroplast stroma, chloroplast thylakoid, cytoplasm

oxygen	At5g18100	*COPPER/ZINC SUPEROXIDE DISMUTASE 3*	chloroplast, cytoplasm, apoplast, peroxisome, vacuole
	At3g10920	*MANGANESE SUPEROXIDE DISMUTASE 1*	mitochondria matrix
	At4g25100	*IRON SUPEROXIDE DISMUTASE 1*	chloroplast envelope, chloroplast membrane, chloroplast stroma, chloroplast thylakoid, cytoplasm, mitochondria, plasma membrane
	At5g23310	*IRON SUPEROXIDE DISMUTASE 3*	chloroplast nucleoid, chloroplast thylakoid
	At5g51100	*IRON SUPEROXIDE DISMUTASE 2*	chloroplast nucleoid, chloroplast thylakoid
	At3g56350	*Iron/manganese superoxide dismutase family protein*	mitochondria matrix
Peroxiredoxins; small antioxidant proteins with peroxidase activity	At1g48130	*1-CYSTEINE PEROXIREDOXIN 1*	cytoplasm, nucleus
	At3g11630	*2-CYSTEINE PEROXIREDOXIN*	apoplast, chloroplast envelope, chloroplast stroma, thylakoid
	At5g06290	*2-CYSTEINE PEROXIREDOXIN B*	apoplast, chloroplast stroma, mitochondrion
	At1g65990	*TYPE II PEROXIREDOXIN A*	cytoplasm, nucleus
	At1g65980	*TYPE II PEROXIREDOXIN B*	chloroplast, cytosol, plasma membrane
	At1g65970	*TYPE II PEROXIREDOXIN C*	cytosol
	At1g60740	*TYPE II PEROXIREDOXIN D*	cytosol, plasma membrane
	At3g52960	*TYPE II PEROXIREDOXIN E*	chloroplast envelope, chloroplast stroma, cell wall, thylakoid
	At3g06050	*TYPE II PEROXIREDOXIN F*	mitochondrial matrix
	At3g26060	*PEROXIREDOXIN Q*	chloroplast envelope, chloroplast thylakoid, plastoglobule
Thioredoxins; small antioxidant proteins	AT4G04610	*ADENOSINE-5'-PHOSPHOSULFATE REDUCTASE REDUCTASE 1*	chloroplast thylakoid
	AT1G62180	*ADENOSINE-5'-PHOSPHOSULFATE REDUCTASE REDUCTASE 2*	chloroplast thylakoid
	AT4G21990	*ADENOSINE-5'-PHOSPHOSULFATE REDUCTASE REDUCTASE 3*	chloroplast
	AT1G52990	thioredoxin family protein	Secretion

	AT1G03680	*ARABIDOPSIS THIOREDOXIN M-TYPE 1*	apoplast, chloroplast envelope, chloroplas stroma, cytosol, thylakoid
	AT4G03520	*THIOREDOXIN M2*	plastid
	AT2G15570	*ARABIDOPSIS THIOREDOXIN M-TYPE 3*	plastid
	AT3G15360	*ARABIDOPSIS THIOREDOXIN M-TYPE 4*	plastid
	AT1G76760	*THIOREDOXIN Y1*	plastid
	AT1G43560	*THIOREDOXIN Y2*	plastid
	AT1G50320	*THIOREDOXIN X*	plastid
	AT4G04950	*Picot1*	cytosol
	AT4G32580	*Picot2*	cytosol
	AT2G40790	*CxxS1 (h6)*	cytosol
	AT3G08710	*THIOREDOXIN h9*	plasma membrane
	AT1G11530	*CxxS2*	cytosol
	AT3G56420	*THIOREDOXIN h10*	cytosol
	AT3G51030	*THIOREDOXIN h1*	cytosol
	AT5G42980	*THIOREDOXIN h3*	cytosol
	AT1G19730	*THIOREDOXIN h4*	cytosol
	AT1G45145	*THIOREDOXIN h5*	cytosol
	AT3G17880	*TDX*	cytosol/nucleus
	AT1G60420	*Nucleoredoxin1*	nucleus
	AT4G31240	*Nucleoredoxin2*	nucleus
	AT2G35010	*THIOREDOXIN o1*	mitochondria
	AT1G31020	*THIOREDOXIN o2*	cytosol, mitochondria
	AT5G39950	*THIOREDOXIN h2*	cytosol
	AT1G59730	*THIOREDOXIN h7*	cytosol
	AT1G69880	*THIOREDOXIN h8*	cytosol
	AT1G08570	*Lilium1*	cytosol
	AT4G29670	*Lilium2*	plastid
	AT5G61440	*Lilium3*	plastid
	AT2G33270	*Lilium4*	plastid
	AT4G26160	*Lilium5*	plastid
	AT3G02730	*THIOREDOXIN f1*	plastid
	AT5G16400	*THIOREDOXIN f2*	plastid
	AT1G76080	*CDSP32*	plastid
	AT5G42850	*Clot TRP14*	cytosol
	AT5G06690	*THIOREDOXIN 1*	chloroplast stroma
	AT5G04260	*WCRKC2*	plastid
	AT4G37200	*HCF164*	plastid
	AT3G53220	*WCGVC*	cytosol

Ascorbate and glutathione are not functionally redundant, and each has roles besides redox regulation. This is demonstrated by the low viability of mutants with decreased ascorbate or glutathione content; mutants in ascorbate biosynthesis via the GDP-mannose pathway arrest growth at germination (Dowdle et al., 2007), and knockout mutants in *GSH1*, are embryo-lethal (Cairns et al., 2006).

Roles of ascorbate

Ascorbate is not ubiquitous; it is not produced by bacteria (with the possible exception of cyanobacteria), fungi, and certain animals such as humans and apes. In fungi, D-erythroascorbic acid is believed to function as an analogue of ascorbic acid (Loewus, 1999), while apes and humans rely on dietary intake of ascorbate for sufficient collagen, carnitine and neurotransmitter biosynthesis (Naidu, 2003). The use of ascorbate by cyanobacteria has been debated (Gest et al., 2012). A recent report from Wheeler et al., (2015), concluded early evolutionary origins of ascorbate biosynthesis in eukaryotes, with subsequent divergence of synthesis pathways, and loss in some groups.

In plants, bryophytes contain low levels of ascorbate (typically 0.5 µmol.gFW^{-1}), while the ascorbate content of higher plants varies greatly, from 5 to 138 µmol.gFW^{-1}, with the higher concentrations detected in alpine plants (Gest et al., 2012). It has been hypothesised that ascorbate, as a low cost antioxidant, acts as a first line of defense in redox regulation, buffering short term oxidising changes in the environment, enabling finer control of glutathione-mediated redox signalling and other functions (Gest et al., 2012).

As previously mentioned, ascorbate scavenges ROS directly and indirectly, however ascorbate is also used as an electron donor in numerous biochemical reactions; for example, it is used by violaxanthin de-epoxidase as a cofactor in the biosynthesis of the carotenoid zeaxanthin (Hager and Holocher, 1994). Ascorbate is also believed to have an important role in reducing Fe^{3+} to Fe^{2+}, which is used by oxygenases in the synthesis of hormones, flavonoids, alkaloids and in cell wall modification (Prescott and John, 1996).

Roles of glutathione

In contrast to ascorbate, glutathione (a thiol-containing tripeptide; Glu-Cys-Gly) is utilised throughout all Kingdoms (Margis et al., 2008), although substitute low-molecular-weight thiols have been identified in some species of halobacteria and parasitic protozoa (Fairlamb et al., 1985; Newton and Javor, 1985). Glutathione is a highly effective antioxidant, oxidised via the activity of DHAR or other glutathione transferases (GSTs), glutaredoxins (GRXs), peroxiredoxins

or methionine sulfoxide reductases, with reduced glutathione rapidly regenerated by action of glutathione reductases (Foyer and Noctor, 2011).

Arabidopsis plants with lower glutathione content (due to a mutant *GSH1* allele) are more susceptible to pathogen and herbivore attack, which corresponds with lower levels of camalexin and glucosinolate deterrents (Ferrari et al., 2003; Parisy et al., 2007; Schlaeppi et al., 2008).

Glutathione conjugation has an important role in detoxification (Cummins et al., 2011), as conjugates are more readily sequestered to the vacuole by ATP-binding cassette proteins (Verrier et al., 2008). As the precursor of phytochelatins, glutathione also has an important role in heavy metal detoxification (Rea et al., 2004); heavy metals such as cadmium can displace endogenous metal cofactors, and are thought to elicit oxidative stress. Phytochelatins form complexes with heavy metals, promoting their sequestration to the vacuole.

There are 55 GSTs in Arabidopsis (Dixon and Edwards, 2010), and the function of most remains largely unclear. As *GST* gene expression is induced in response to infection, cell division and environmental stress, a key role in the detoxification of endogenous compounds as well as foreign compounds is assumed (Dixon et al., 2010). It is also considered that GSTs may have an important role in the transport and compartmentation of endogenous metabolites including reactive oxylipins, phenolics and flavonoids (Dixon and Edwards, 2009).

Plant glutaredoxins reduce protein disulphide bonds with the oxidation of glutathione, and some catalyse *S*-glutathionylation or de-glutathionylation reactions (Rouhier, 2010). Such reactions can affect the activity of targets, and GRXs have been implicated in stress responses and developmental regulation. For example, GRX40 interacts with TGA2 to regulate salicylic and jasmonic acid responses (Ndamukong et al., 2007), while GRXs ROXY1 and ROXY2 interact with TGA9 and TGA10 to regulate anther development (Murmu et al., 2010).

3.1.4 Phylogenetic analysis of MDHAR6

Protein sequence similarity results for m-MDHAR6 are shown in Table 19. There are homologues with very high similarly to m-MDHAR6 across monocot and dicot species, including *Amborella trichopoda*, which is placed phylogenetically at the base of the Angiosperm lineage. Homologues with less similarity were identified in Gymnosperms, lower plants and algae. Low sequence similarity was found against the proteomes of animals including *Homo sapiens.*

In mammalian biology, MDHAR activity has been attributed to NADH-cytochrome b_5 (Iyanagi and Yamazaki, 1969; Ito et al., 1981), and thioredoxin reductase (May et al., 1998) activities. Theoredoxin reductase 1 of *H. sapiens* shares only 30 % similarity with MDHAR6, over 38 % coverage (Table 19). This highlights that enzymes in other Kingdoms may have the same activity, but with low protein sequence similarity.

Within cyanobacteria, MDHAR activity has been detected in *Nostoc* (Miyake et al., 1991), however the enzymes responsible have not been identified. It is notable that from genomic analysis, plastidial and mitochondrial use of MDHAR appears to be a feature of higher plants (Pitsch et al., 2010; Gest et al., 2012). The three MDHAR genes of the moss *Physcomitrella patens* are predicted to be cytosol or peroxisome-targeted (Lunde et al., 2006; Drew et al., 2007).

Table 19: Protein sequence similarity between Arabidopsis m-MDHAR6, and the closest homologues in other species

Examples of BLASTx (Altschul et al., 1990) search results using the National Center for Biotechnology Information (NCBI) database (http://www.ncbi.nlm.nih.gov/). Protein sequences are compared with m-MDHAR6 (TAIR AASequence 1009107687). Results shown are highest scoring hits for the species listed, expect for *Homo sapiens* thioredoxin reductase.

Species	Relevance	Accession and annotation of closest hit	Total score	% coverage	% identity	E value
Populus trichocarpa	Remediation relevant genus	XP 002299509.2 hypothetical protein	795	100	78	0.0
Elaeis guineensis	Monocot	XP-010941082.1 predicted chloroplastic MDHAR	729	99	72	0.0
Amborella trichopoda	Placed at base of Angiosperm lineage	XP 011628912.1 predicted MDHAR	734	99	72	0.0
Picea sitchensis	Gymnosperm	ABK24288.1 unknown	360	81	46	1e-119
Ginkgo biloba	Gymnosperm	AGG40646.1 isoflavone reductase-like protein	29.6	13	31	0.067
Physcomitrella patens	Lower plant (moss)	XP 001776830.1 predicted protein	374	84	48	1e-124
Ostreococcus tauri	Alga	XP 003079182.1 MDHAR	361	83	46	3e-119
Synechococcus sp. PCC 7335	Cyanobacteria, of interest considering possible evolutionary origin	WP 006457515.1 NAD(FAD)-dependent dehydrogenase	177	89	28	2e-48
Homo sapiens	Mammal	BAH14413.1 unnamed protein product	137	72	27	4e-34
Homo sapiens	Thioredoxin reductase has been reported to have MDHAR activity	EAW97745.1 thioredoxin reductase 1	58.9	38	30	4e-08

3.2 RESULTS

3.2.1 The *mdhar6-1* mutants remove TNT from soil

One hypothesis for the increased TNT tolerance of *mdhar6* mutants, is that they do not take up as much TNT as wild type. Emily Beynon and Liz Rylott previously demonstrated that when transferred to liquid media, *mdhar6-1*, *mdhar6-2* and *mdhar6-3* remove TNT from the liquid at the same rate as their wild type backgrounds (Johnston et al., 2015). To investigate whether *mdhar6-1* seedlings also remove TNT from soil, where TNT binds strongly to the humic fractions, five-day old seedlings were transferred to 0 and 100 mg TNT/kg soil, and grown to six weeks of age. At six weeks, aerial biomass was removed and weighed, and the pots of soil were halved vertically; root biomass was extracted and weighed from one half of the soil, and TNT was extracted and quantified from the other half, including the roots.

The aerial and root fresh biomass of *mdhar6-1* were 2.4 and 3.3-fold greater than Col7 on 100 mg TNT/kg soil (Figure 21), a smaller difference than seen in previous experiments. Percentage TNT recovery from soil is usually low, and in the No Plant Control (NPC) soil of this experiment, was 4.3 %. Extractable TNT from *mdhar6-1*-treated soil was significantly lower than NPC, with $P < 0.001$, while the significance of the difference in TNT content between Col7 and *mdhar6-1* treated soil was lower ($P = 0.108$; Table 20). Untransformed TNT within the roots of *mdhar6-1* was included in the extraction, which may account for the lower significance in difference between Col7- and *mdhar6-1*-treated soil.

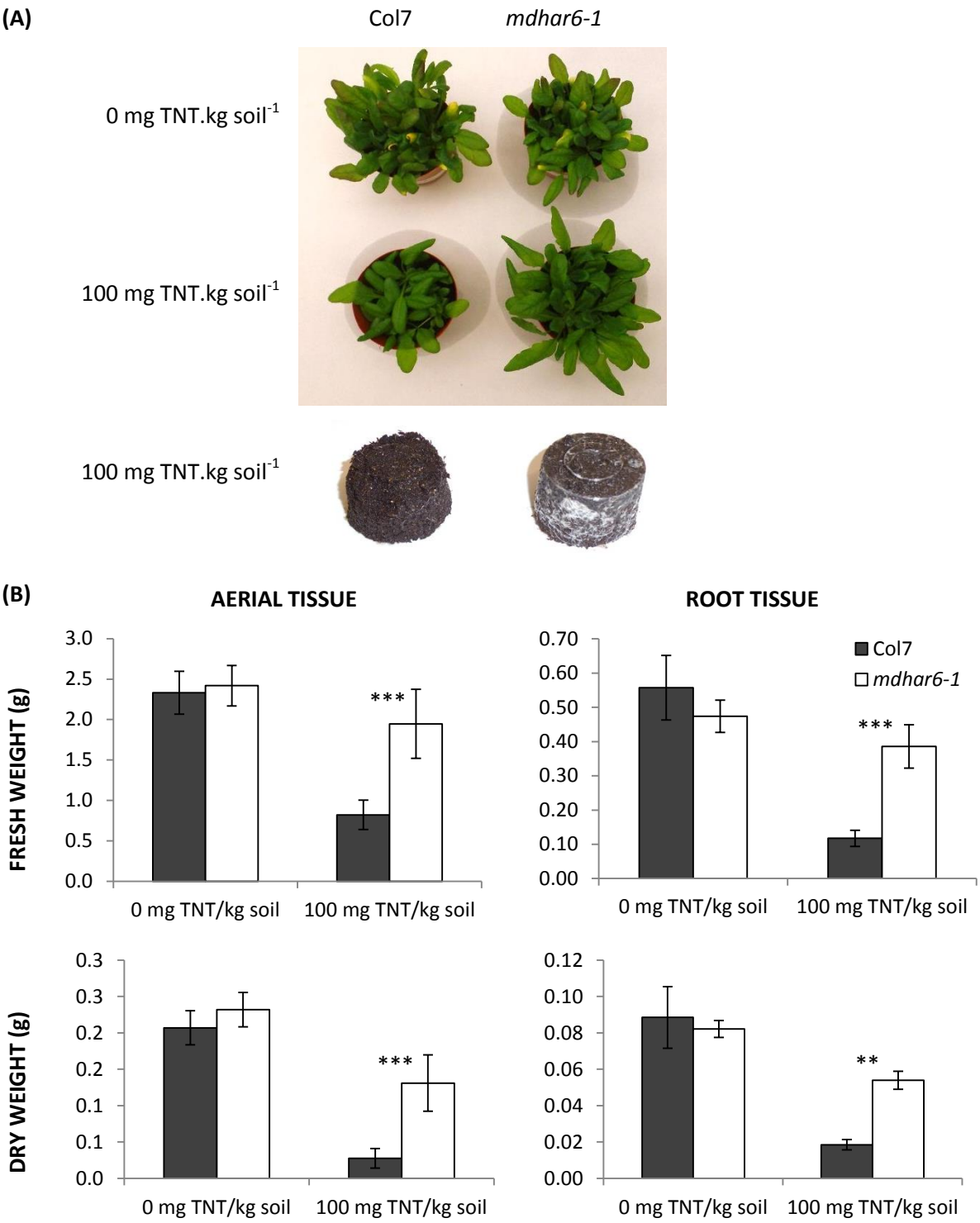

Figure 21: Biomass of Col7 and *mdhar6-1* grown in TNT-treated soil

Five-day old seedlings were transferred to pots of 0 or 100 mg TNT.kg soil^{-1} (five seedlings per pot), and grown to six weeks of age. (A) Representative seedlings from this experiment at six weeks of age, photographs courtesy of Liz Rylott. (B) Fresh and dry weights of the five seedlings at six weeks of age. Roots were extracted and measured from half of each pot, then doubled to give the values shown here. Mean of eight biological replicates ± SD shown. Student's t test * P<0.05, ** P<0.01, *** P<0.001.

Table 20: Extractable TNT from 100 mg TNT.kg soil^{-1} after 5 week treatment with no plants, Col7 or *mdhar6-1*

Mean of eight biological replicates ± SEM shown. NPC; No Plant Control. Roots were included in the soil processed for TNT extraction. One-way ANOVA with Bonferroni correction, * P<0.05, ** P<0.01, *** P<0.001.

Sample	Extractable TNT (nmol/g dry soil)	P value against		
		NPC	Col7	*mdhar6-1*
NPC	31 ± 2.7			
Col7	21 ± 1.6	0.004 *		
mdhar6-1	15 ± 0.9	0.000 ***	0.108	

3.2.2 Mutants in *mdhar6* are no more tolerant than wild type to a range of stresses, including hydrogen peroxide and methyl viologen treatment

Another theory for the enhanced TNT tolerance of *mdhar6* is that due to the mutation, general defences are elevated which increase resistance to a variety of stress treatments, including TNT. To investigate this, Liz Rylott and Maria Budarina measured the root lengths of seven-day old Col7 and *mdhar6-1* seedlings, germinated on agar containing inhibitory levels of the solute sorbitol, salt NaCl or superoxide-inducing methyl viologen (the active component of the herbicide Paraquat, which transfers electrons from photosystem I to molecular oxygen); no significant differences between the wild type and mutant were found. To supplement this prior research, root growth on agar treated with hydrogen peroxide was measured (Figure 22), and two-week old seedlings leaves were sprayed with methyl viologen (Figure 23); no significant difference in tolerance between Col7 and *mdhar6-1* were found.

The *mdhar6-1* seedlings were however, slightly less tolerant to growth in the hypoxic conditions of growth in liquid media; when one-day old seedlings were transferred to ½ MS(S) 1 x Gamborg's vitamin solution, *mdhar6-1* seedlings were 76 % the fresh weight of Col7 seedlings at two-weeks of age (10 biological replicates, Student's t test P = 0.052).

The lack of increased tolerance to other stress treatments demonstrates the specificity of the tolerance to TNT in *mdhar6* mutants, and indicates that the higher tolerance of *mdhar6* to TNT cannot be explained by enhanced general defences.

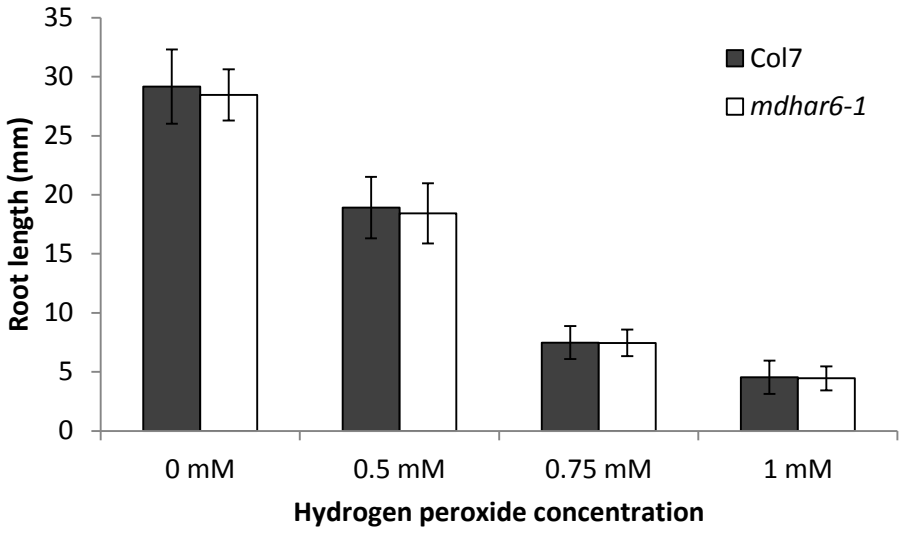

Figure 22: Root lengths of Col7 and *mdhar6-1* seedlings germinated on hydrogen peroxide-supplemented ½ MS(S)(A)

Root lengths of seven-day old seedlings. Mean of 30 biological replicates ± SD shown.

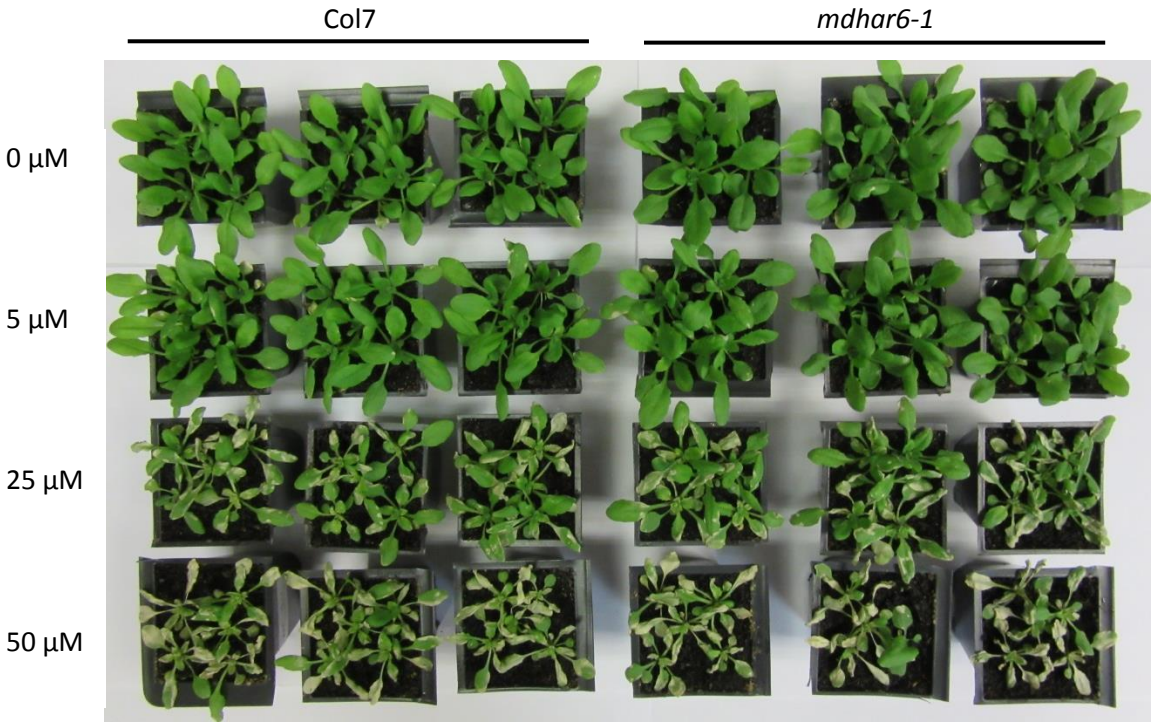

Figure 23: Appearance of Col7 and *mdhar6-1* seedlings two days after being sprayed with 0 - 50 µM methyl viologen

Punnets of five two-week old seedlings, which were sprayed with 1.8 ml 0, 5, 25 or 50 µM methyl viologen two days previously. Three representative punnets per treatment pictured.

3.2.3 When grown on ½ MS(S)(A), *mdhar6-1* roots have higher glutathione levels than Col7

Glutathione conjugation has a direct role in detoxifying TNT (Gunning et al., 2014). To investigate whether ascorbate-glutathione pools are affected in a manner which may enhance TNT tolerance, leaf and root extracts from two-week old seedlings grown vertically on agar plates, were assayed for ascorbate and glutathione content (Figure 24). The only significant difference between Col7 and *mdhar6-1* was a 1.3-fold increase in the total glutathione content of *mdhar6-1* roots.

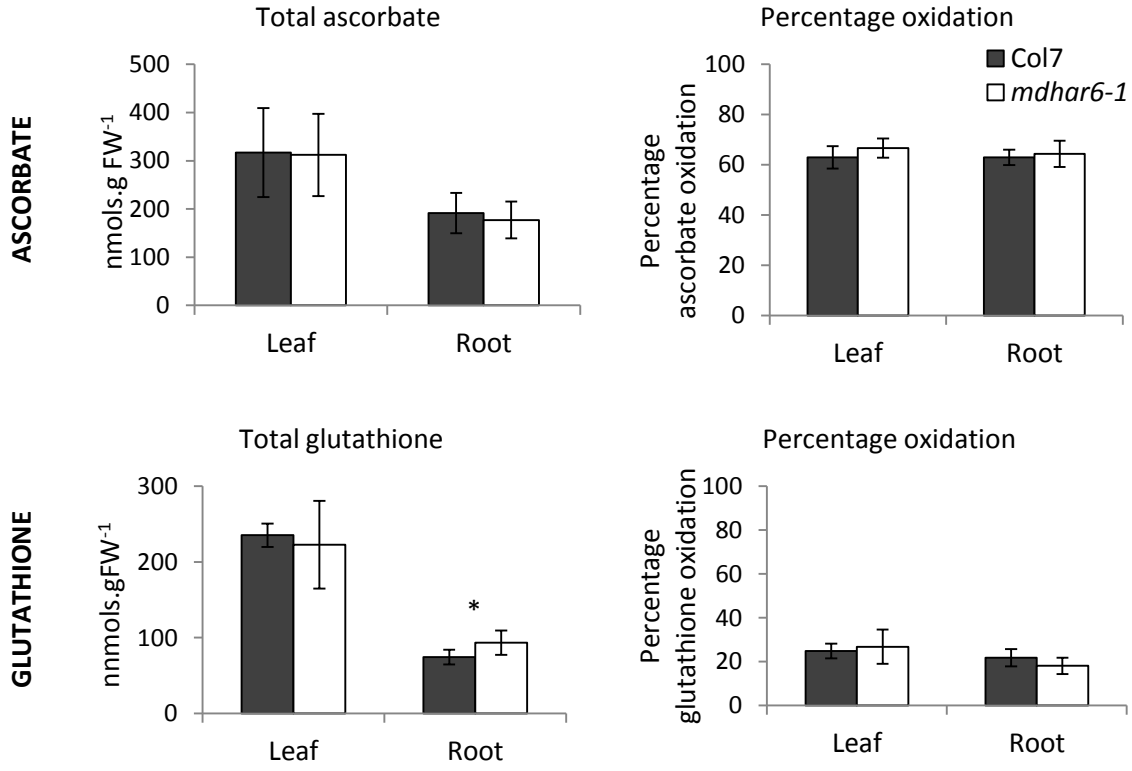

Figure 24: Ascorbate and glutathione levels of 15-d old Col7 and *mdhar6-1* seedlings

Seedlings were grown vertically on ½ MS(S)(A) for 15 d. Mean values for eight biological replicates ± SD shown. Student's t test * P<0.05, ** P<0.01, *** P<0.001.

3.2.4 When grown in liquid media and treated with TNT or a control treatment, there are no significant differences in ascorbate and glutathione between Col7 and *mdhar6-1*

To investigate the effect of TNT treatment on Col7 and *mdhar6-1* ascorbate and glutathione levels, two-week old seedlings were treated with 60 µM TNT or a control treatment for 6 h, as described in Gandia-Herrero et al. (2008). Ascorbate and glutathione levels were higher than when grown on ½ MS(S)(A), perhaps due to the more hypoxic conditions of liquid culture. There were no significant differences in ascorbate or glutathione between Col7 and *mdhar6-1* (Figure 25).

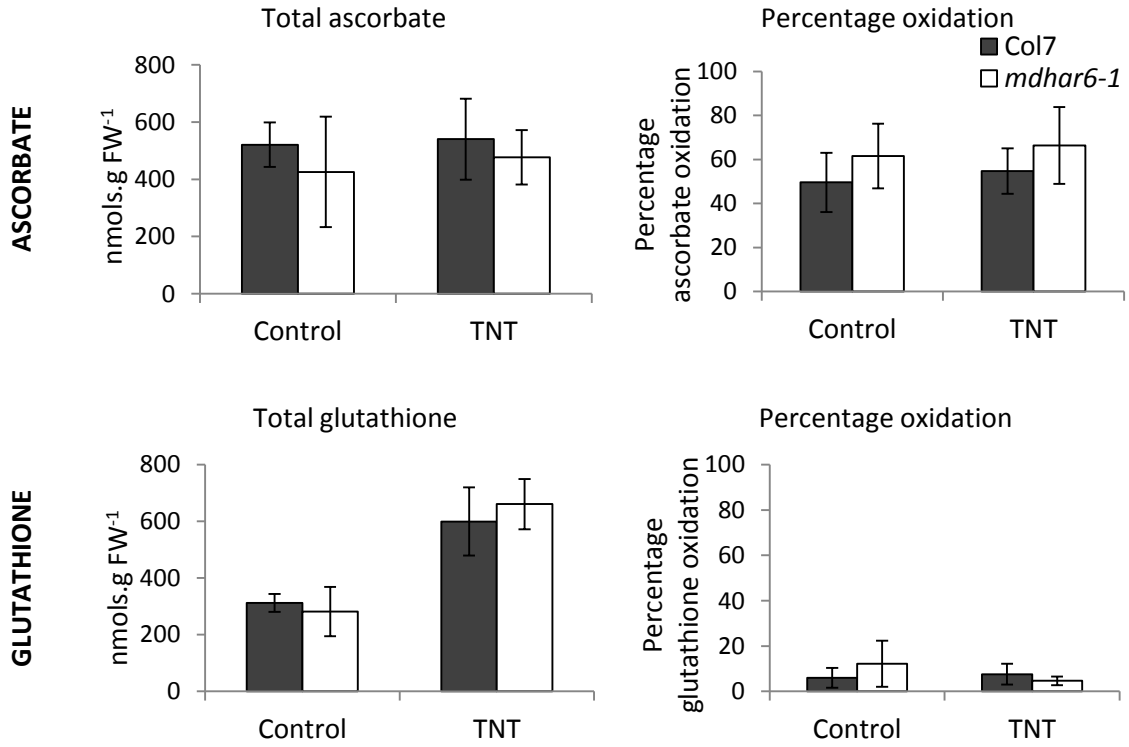

Figure 25: Ascorbate and glutathione levels of two-week old TNT- or control-treated Col7 and *mdhar6-1* seedlings

Two-week old seedlings grown in ½ MS(S) 1 x Gamborg's vitamin solution, were treated with 60 µM TNT in DMF (end 0.06% v/v DMF) or DMF alone for 6 h. Mean of six biological replicates ± SD shown. Student's t test * P<0.05, ** P<0.01, *** P<0.001.

3.2.5 The *mdhar6-1* mutant has enhanced TNT tolerance in the presence of a glutathione synthesis inhibitor

To investigate the importance of the higher glutathione levels previously measured in *mdhar6-1* roots (Figure 24), TNT tolerance in the presence of the γ-ECS inhibitor buthionine sulfoximine (BSO; Griffith and Meister, 1979), was explored in a preliminary experiment. If glutathione levels are reduced to the same extent in Col7 and *mdhar6-1*, yet *mdhar6-1* maintains enhanced TNT tolerance, this would suggest that increased glutathione conjugation to TNT does not account for the enhanced TNT tolerance in *mdhar6-1*.

Col7 and *mdhar6-1* root lengths were measured seven days after germination on ½ MS(A) treated with various concentrations of TNT and BSO (Figure 26). The *mdhar6-1* mutant was more tolerant to BSO, which complicates interpretation of this experiment. In the presence of 250 µM BSO, roots of *mdhar6-1* were longer than Col7 both in the presence and absence of TNT. In the presence of 500 µM BSO, roots of *mdhar6-1* were not significantly longer than Col7 in the presence or absence of TNT (one-way ANOVA $P < 0.05$), but root growth was greatly inhibited in both genotypes at concentration. Without measurement of glutathione concentration in the roots, and without measurement of root lengths in the presence of BSO concentrations between 250 µM and 500 µM, the results of this experiment are difficult to interpret.

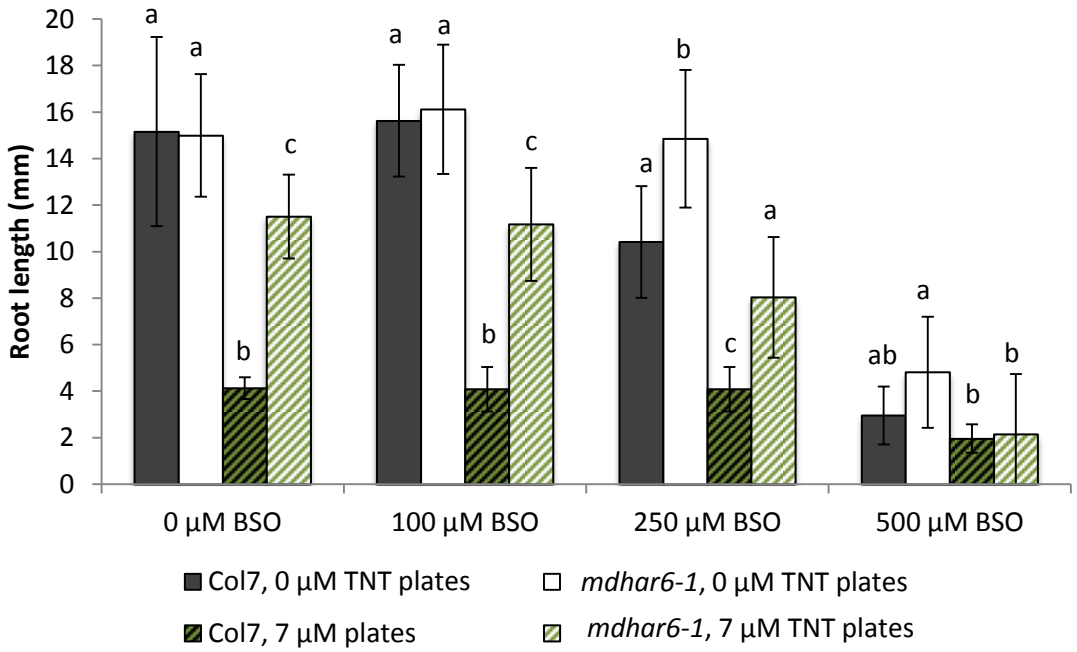

Figure 26: The effect of glutathione synthesis inhibitor BSO on the enhanced TNT tolerance of *mdhar6-1*

Root lengths of seven-day old seedlings. Mean of 25 biological replicates ± SD. One-way ANOVA with *post hoc* Tukey HSD test used for each BSO treatment. Different letters indicate significant differences at $P < 0.05$.

3.2.6 The activity of crude protein extract towards both MDA and TNT is reduced in *mdhar6* mutants

To determine the effect of the three different *mdhar6* mutations on total MDHAR activity, crude protein extract from seedling leaves and roots were assayed for activity against the putative endogenous substrate MDA. These extracts were also assayed for activity towards TNT. There was an overall decrease in activity towards both MDA and TNT in the three *mdhar6* mutants (Figure 27), suggesting that MDHAR6 may have activity towards TNT.

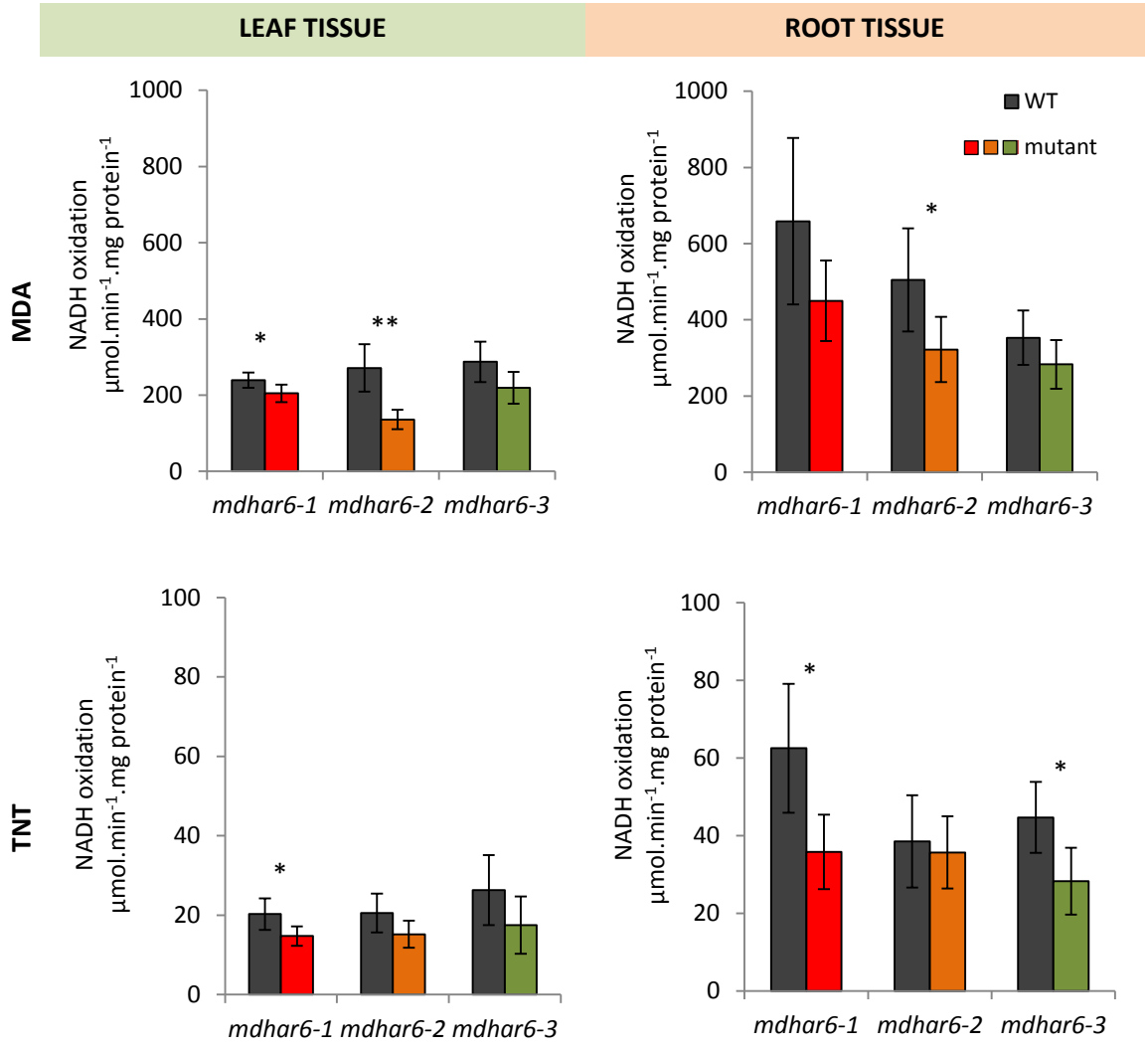

Figure 27: Activity of WT and *mdhar6* crude protein extract towards MDA and TNT

Seedlings were grown vertically on ½ MS(S)(A) for 14 days. Activity was determined by following rates of A_{340} decrease, corresponding with NADH oxidation. Mean of five biological replicates ± SD shown. Student's t test * P<0.05, ** P<0.01, *** P<0.001.

3.2.7 Purification of MDHAR6 for enzymatic analysis

Direct activity of MDHAR6 with TNT would not be unsurprising, as flavin enzymes with broad specificity are known to reduce nitroaromatics as substrates (Williams and Bruce, 2002). To investigate the activity of MDHAR6 further, codon-optimised *MDHAR6* with a C-terminal HIS-tag and N-terminal STREP-tag (cloned by Liz Rylott and Maria Budarina), was expressed in *E. coli*, and purified to near homogeneity in a 1:1 molar ratio with cofactor FAD (Figure 28). The identity of the purified protein was confirmed by mass spectrometry.

The purified MDHAR6 enzyme had high affinity towards MDA, with an estimated K_m of 4.1 µM (Figure 29). To generate MDA, ascorbate oxidase was added to assays containing increasing concentrations of sodium ascorbate. As dehydroascorbate is also generated in this reaction, activity towards DHA alone was also tested. No activity towards DHA was found.

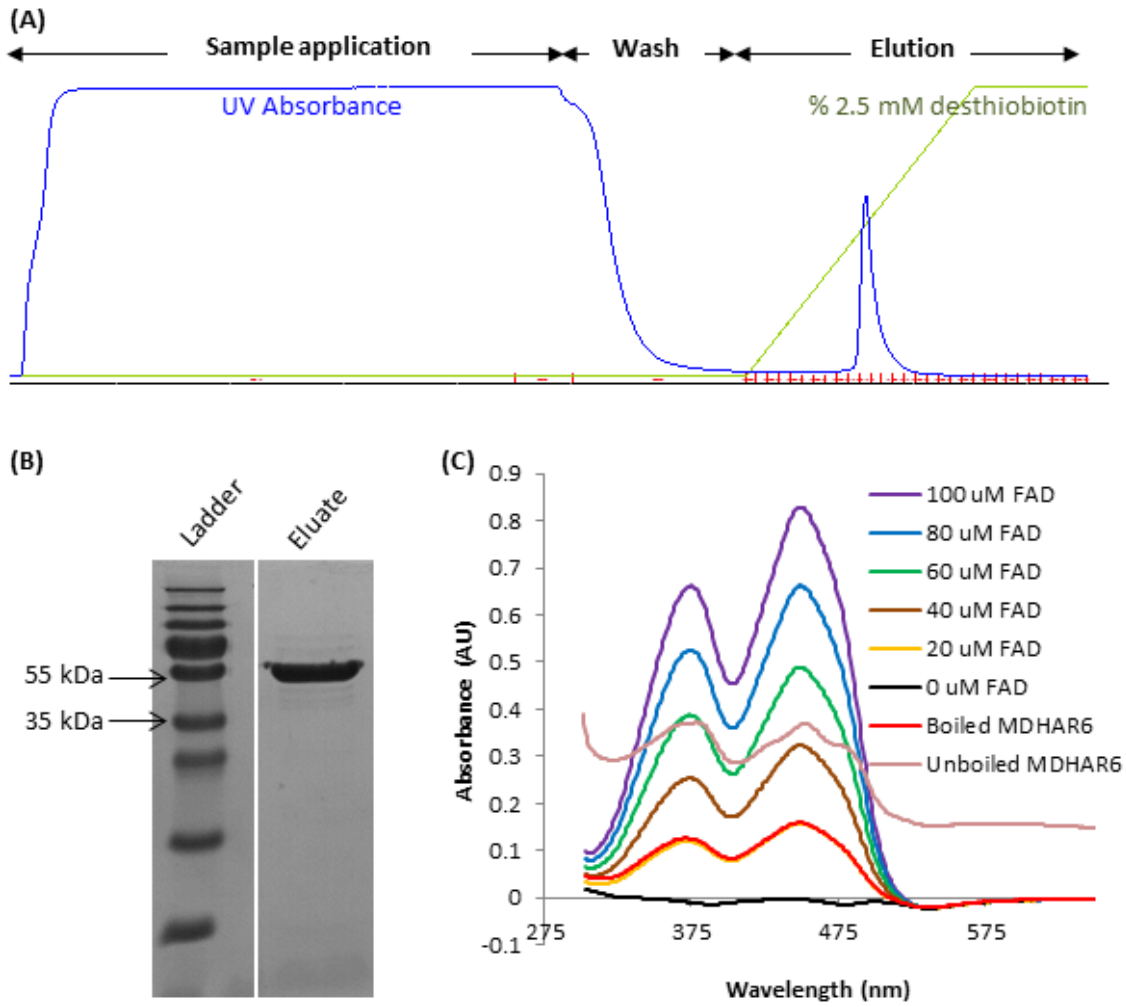

Figure 28: Purification of MDHAR6

(A) Purification profile; UV absorbance of column flow-through (corresponding with protein concentration), and percentage of 2.5 mM desthiobiotin in the column wash buffer. A peak in protein elution corresponding with approximately 1.25 mM desthiobiotin was observed. **(B)** Coomassie stain of eluted protein on an SDS-PAGE gel. The expressed MDHAR6 protein is 53 kDa. **(C)** Absorbance spectra of boiled and unboiled MDHAR6 eluate and of FAD standards (average of three replicates).

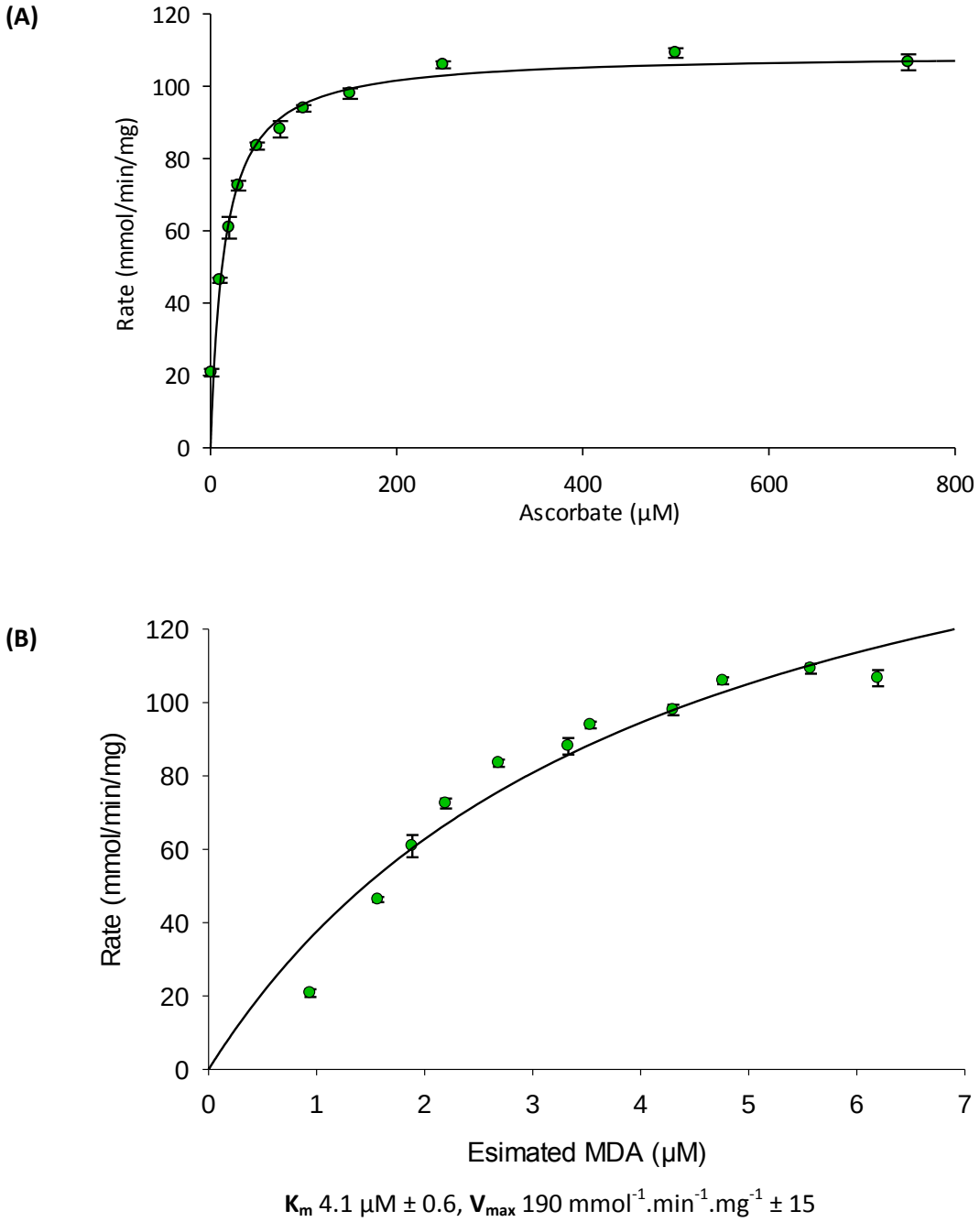

K_m 4.1 µM ± 0.6, V_{max} 190 $mmol^{-1}.min^{-1}.mg^{-1}$ ± 15

Figure 29: Michaelis-Menten for MDHAR6 activity with MDA substrate

Activity was determined by following decrease in A_{340} corresponding with NADH oxidation. Assay conditions: 50 mM Tris 1 mM EDTA (pH 7.6), 100 µM NADH, 509 ng/ml MDHAR6 and increasing concentrations of sodium ascorbate. Absorbance at 340 nm was measured before and after addition of 1.12 U ascorbate oxidase, to generate MDA. **(A)** Michaelis-Menten plot showing original sodium ascorbate concentration in assay on x axis. **(B)** Michaelis-Mentan plot showing estimated MDA concentration, generated by ascorbate oxidase addition, on x axis. Three technical replicates ± SEM.

3.2.8 Enzymatic analysis indicates that MDHAR6 reduces TNT to a TNT nitro radical, which autoxidises generating superoxide

Purified MDHAR6 was also found to have activity towards TNT, although with much lower affinity (K_m 522 µM; Figure 30) than towards MDA (K_m 4.1 µM; Figure 29). To investigate the reduction products, assays containing 200 µM TNT and 200 µM NADH were incubated at room temperature for 90 min, by which time all NADH was depleted. The end concentration of TNT was then determined using High Performance Liquid Chromatography (HPLC), however no decrease in TNT concentration was observed (Figure 30).

The activity of MDHAR6 towards TNT, with no decrease in TNT concentration, could be explained by a one electron reduction of TNT, to a TNT nitro radical (Figure 31). This radical would then most likely autoxidise, transferring the electron to molecular oxygen, generating highly reactive superoxide, in a cyclic reaction. In addition to generating potentially harmful levels of ROS, this cyclic reaction involves the futile use of NADH, which could otherwise be used in productive reactions.

To investigate whether radicals are generated in the reaction of MDHAR6 with TNT, Electron Paramagnetic Resonance (EPR) spectrometry was used in collaboration with Dr. Victor Chechik (Department of Chemistry, University of York). The commonly-used spin traps 5,5-dimethyl-pyrroline N-oxide (DMPO) and 5-diethoxyphosphoryl-5-methyl-1-pyrroline-N-oxide (DEPMPO) were incorporated into the assays; these spin traps form relatively stable adducts with otherwise short-lived radicals. When DMPO was incorporated into the assay, a spectrum correlating with DMPO-superoxide was observed (Figure 32). At the end of the reaction, when NADH was depleted, a spectrum corresponding with the decomposition product of DMPO-superoxide, DMPO-hydroxyl, was observed. The DMPO-superoxide adduct was not observed if superoxide dismutase (SOD) was included in the assay, if TNT was omitted, or if heat-denatured MDHAR6 was used. When DEPMPO was applied in the assay, a spectrum corresponding with DEPMPO-superoxide was also observed (Figure 32).

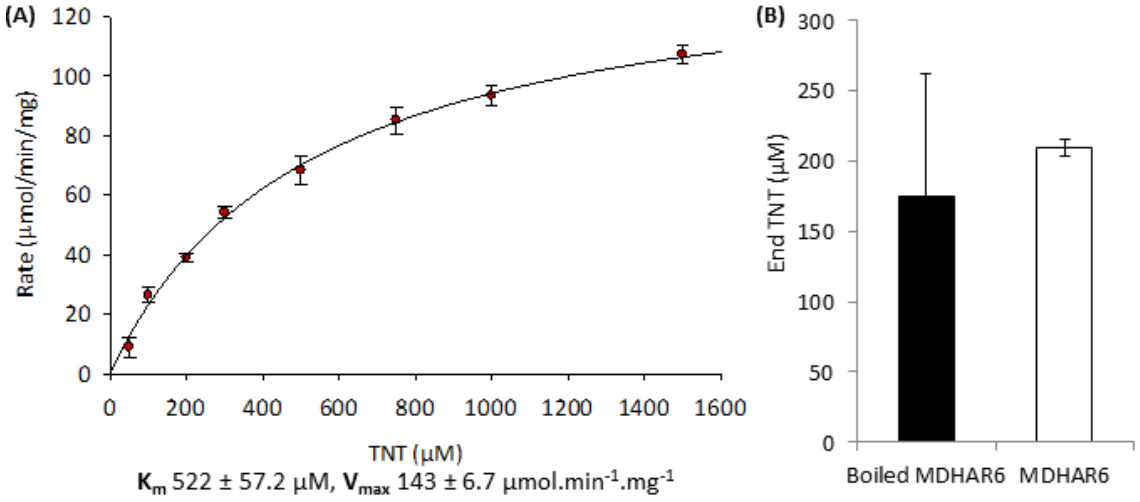

Figure 30: Michaelis-Menten for MDHAR6 activity with TNT substrate, and TNT concentration following activity

(A) Michaelis-Menten plot. Three technical replicates ± SEM. Activity was determined by following decrease in A_{340} corresponding with NADH oxidation. Assay conditions: 50 mM Tris 1 mM EDTA (pH 7.6), 10.3 µg/ml MDHAR6, 15 % DMSO, 100 µM NADH, 25°C. **(B)** Concentration of TNT at end of assay. Five technical replicates ± SD. Assays consisted of 50 mM Tris (pH 7.6), 1 mM Na_2EDTA, 200 µM NADH, 200 µM TNT, 15% DMSO and 52 µg/ml MDHAR6. The TNT concentration after 90 min incubation at room temperature, when NADH was depleted, was determined using HPLC.

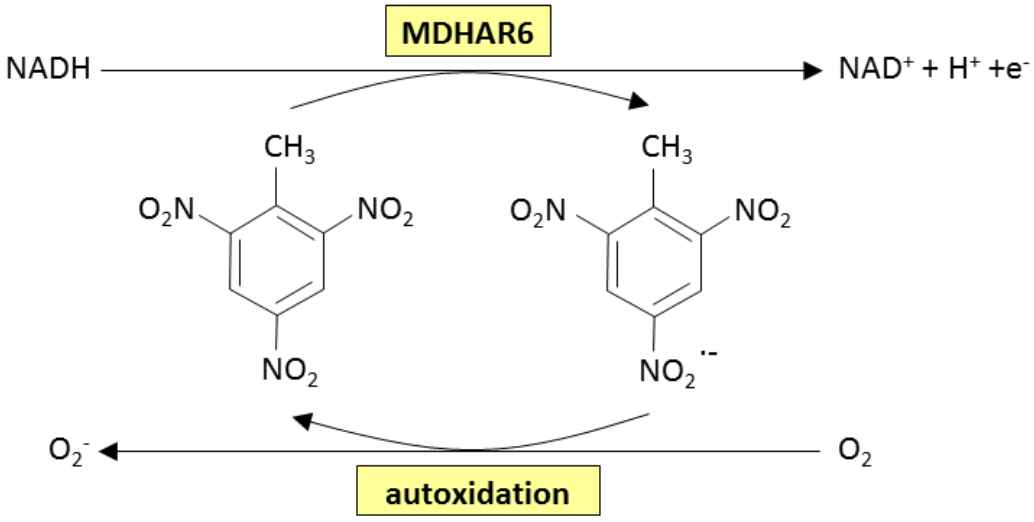

Figure 31: Hypothesised reaction of MDHAR6 with TNT

Schematic for the hypothesised reaction of MDHAR6 with TNT; MDHAR6 uses cofactor NADH to reduce TNT by one electron, forming a TNT nitro radical, which is then able to autoxidise, transferring the electron to molecular oxygen, generating superoxide.

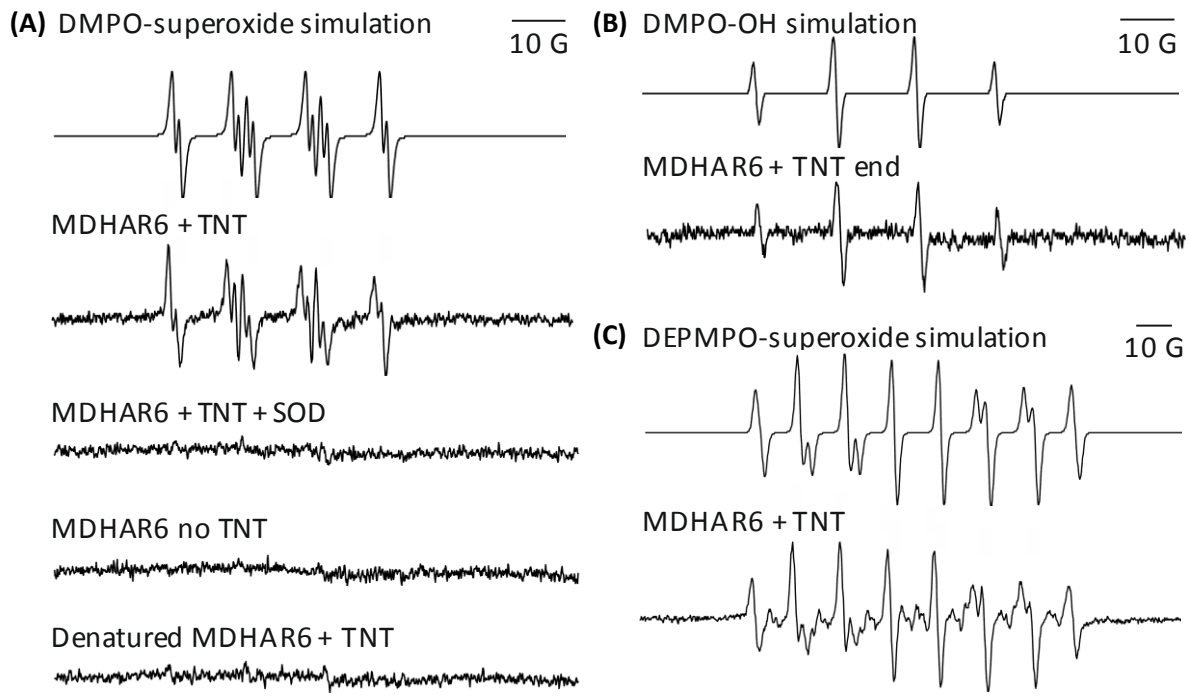

Figure 32: Electron paramagnetic resonance spectra from MDHAR6 activity with TNT

(A) Spectrum of DMPO-superoxide, followed by the observed spectrum when MDHAR6 reacts with TNT in the presence of DMPO (assay conditions; 1.5 mg/ml MDHAR6 in 50 mM KH_2PO_4 (pH 7), 80 mM DMPO, 300 µM NADH and 500 µM TNT in DMF, end DMF 1 % v/v), then when 50 U/ml SOD was incorporated in the assay, TNT was omitted or heat-denatured MDHAR6 used. **(B)** Spectrum of the DMPO-superoxide degradation product, DMPO-OH, followed by the spectrum observed at the end of MDHAR6 reaction with TNT, when NADH has been depleted. **(C)** Spectrum of DEPMPO-superoxide, followed by the spectrum observed when MDHAR6 reacted with TNT in the presence of 80 mM DEPMPO (same assay conditions as with DMPO).

If this reaction occurs *in vivo*, higher levels of cellular H_2O_2 when exposed to TNT might be expected, as SOD catalyses the dismutation of superoxide to O_2 and H_2O_2 (Alscher et al., 2002). To assess the level of H_2O_2 in whole seedlings, 3,3'-diaminobenzidine (DAB) staining was used; DAB monomer is oxidised by H_2O_2 in the presence of peroxidase, to form an insoluble brown polymer. Seedlings were germinated on ½ MS(A) containing 0 or 15 µM TNT, and DAB-stained after 7 days. Col7 seedlings grown in the presence of TNT stained much darker than those grown in the absence of TNT, and *mdhar6-1* seedlings were stained to comparable levels as Col7 in the absence of TNT. Images at different magnifications from two technical replicate experiments are shown in Figure 33 and Figure 34.

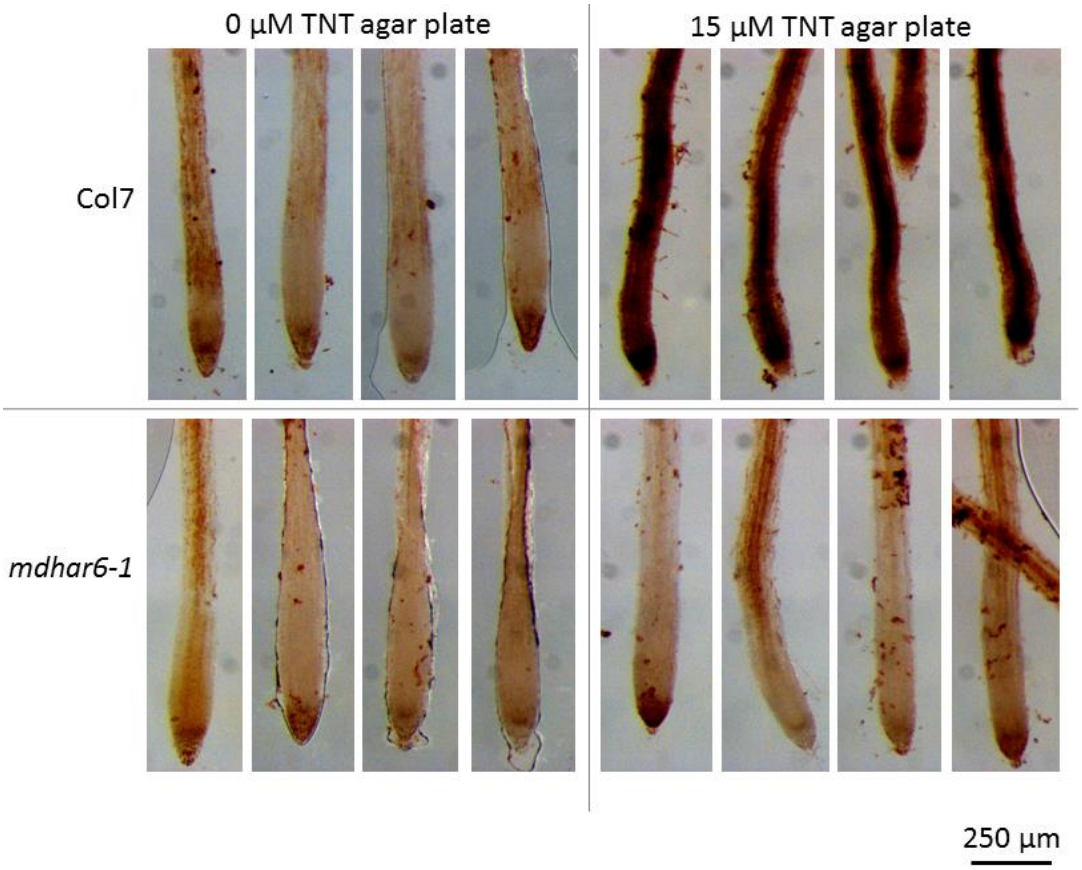

Figure 33: DAB stain of Col7 and *mdhar6-1* seedlings germinated in the presence or absence of TNT; high magnification

Seedlings were germinated and grown vertically on ½ MS(A) plates containing 0 or 15 µM TNT (0.05 % v/v DMSO), then DAB-stained for 3 h.

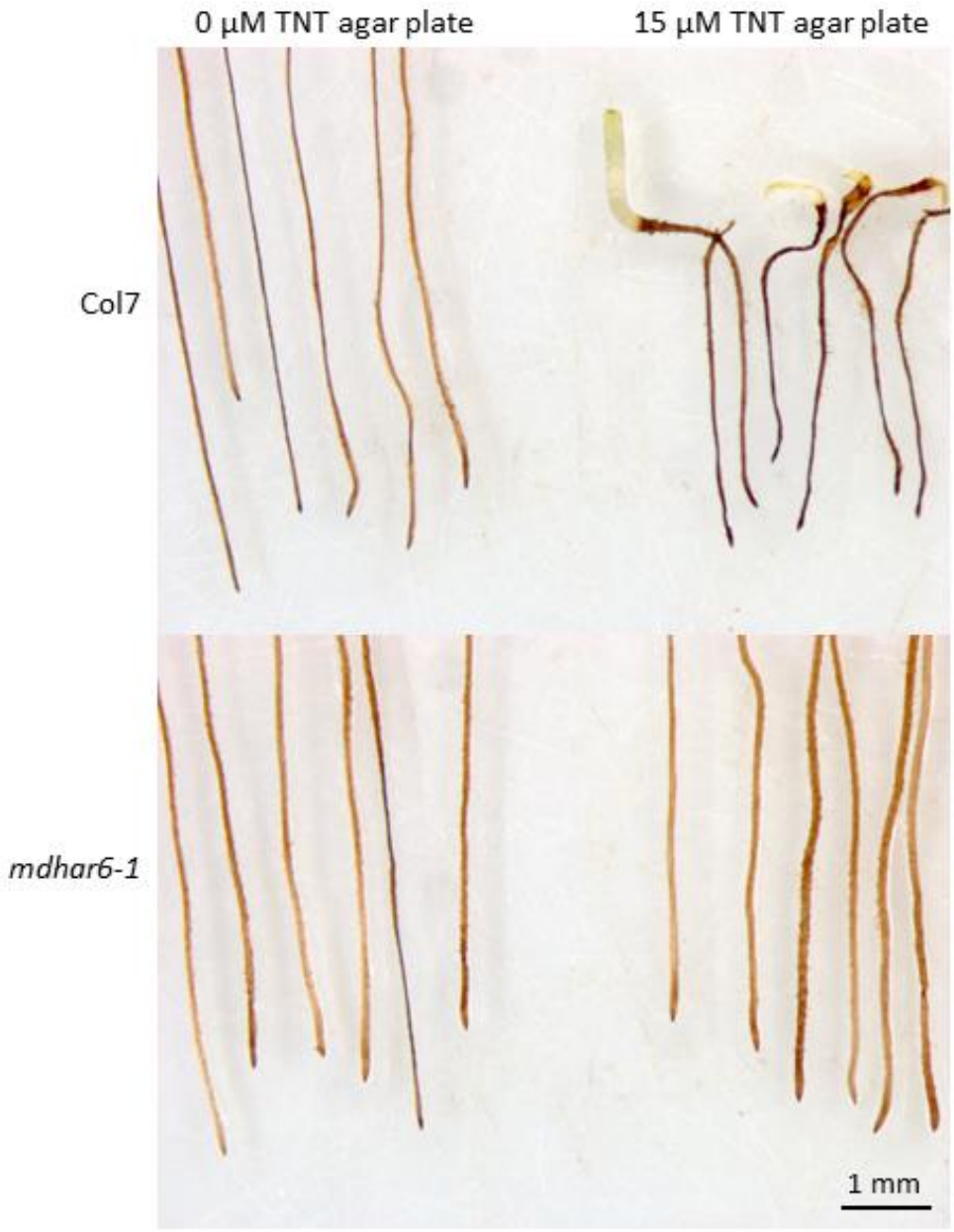

Figure 34: DAB stain of Col7 and *mdhar6-1* seedlings germinated in the presence or absence of TNT; low magnification

Seedlings were germinated and grown vertically on ½ MS(A) plates containing 0 or 15 µM TNT (0.05 % v/v DMSO), then DAB-stained for 3 h. Leaves were removed to facilitate alignment of roots on slide.

3.2.9 Investigating the potential of using MDHAR6 as a herbicide target

Herbicides are grouped into 25 classes, according to the herbicide mode of action (MOA), i.e. the protein or process inhibited by the chemical (HRAC, 2010; Heap, 2014). Since the 1970s, there has been a steady increase in herbicide tolerance in weed species, including the "stacking" of tolerance to a number of herbicide MOA (Heap, 2015). This highlights the necessity of careful farming practise, with alternation in the class of herbicide used. At the same time however, no herbicide with a new MOA has been commercialised since the 1980s (Duke, 2012). Reflecting on this, and the apparent toxic effect of MDHAR6 upon reaction with TNT, it was considered whether an agrochemical could be designed, which MDHAR6 would similarly reduce by one electron, with toxic effect.

To investigate the specificity of the reaction further, nitro group-containing chemicals 1-chloro-2,4-dinitrobenzene(CDNB) and 1-chloro-4-nitrobenzene (CNB) were also tested as MDHAR6 substrates. The enzyme was found only to have activity towards CDNB, which correlated with enhanced CDNB tolerance in *mdhar6-1* (Figure 35; Figure 36).

A summary of the chemical structures tested as MDHAR6 substrates in this study, with kinetic values, is included in Figure 37.

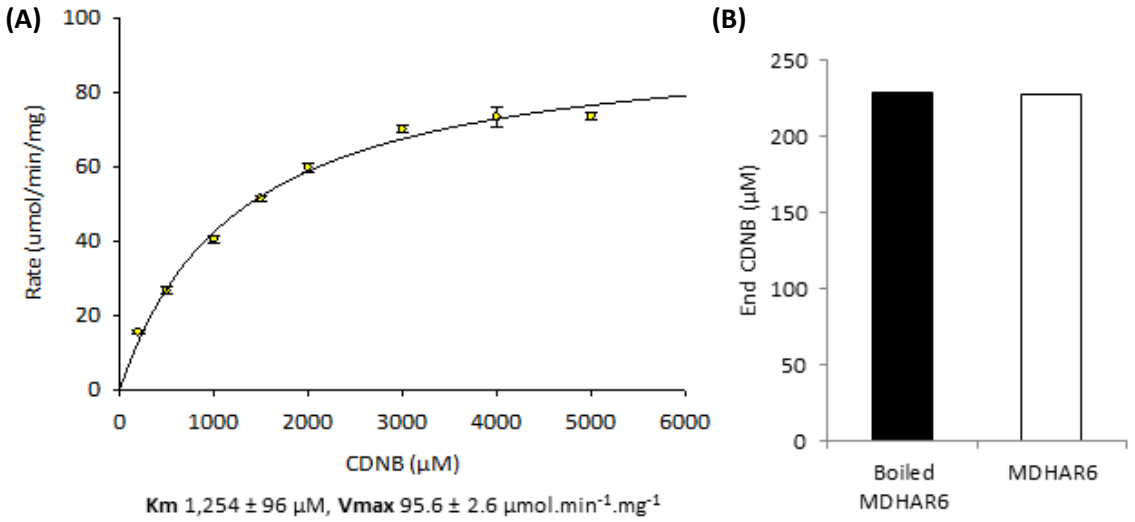

Figure 35: Michaelis-Menten for activity of MDHAR6 with CDNB, and CDNB concentration following reaction

(A) Michaelis-Menten plot and kinetics for MDHAR6 activity with CDNB. Three technical replicates ± SEM. Activity was determined by following decrease in A_{340} corresponding with oxidation of cofactor NADH. Assay conditions: 50 mM Tris 1 mM EDTA pH 7.6, 128 µg/ml MDHAR6, 15 % DMSO, 100 µM NADH, 25°C. **(B)** Concentration of CDNB following reaction with MDHAR6. Five technical replicates ± SD. Assays consisted of 50 mM Tris (pH 7.6), 1 mM Na_2EDTA, 200 µM NADH, 200 µM CDNB, 15% DMSO and 52 ug/ml MDHAR6. Concentration of CDNB after 90 min incubation at room temperature was determined using HPLC.

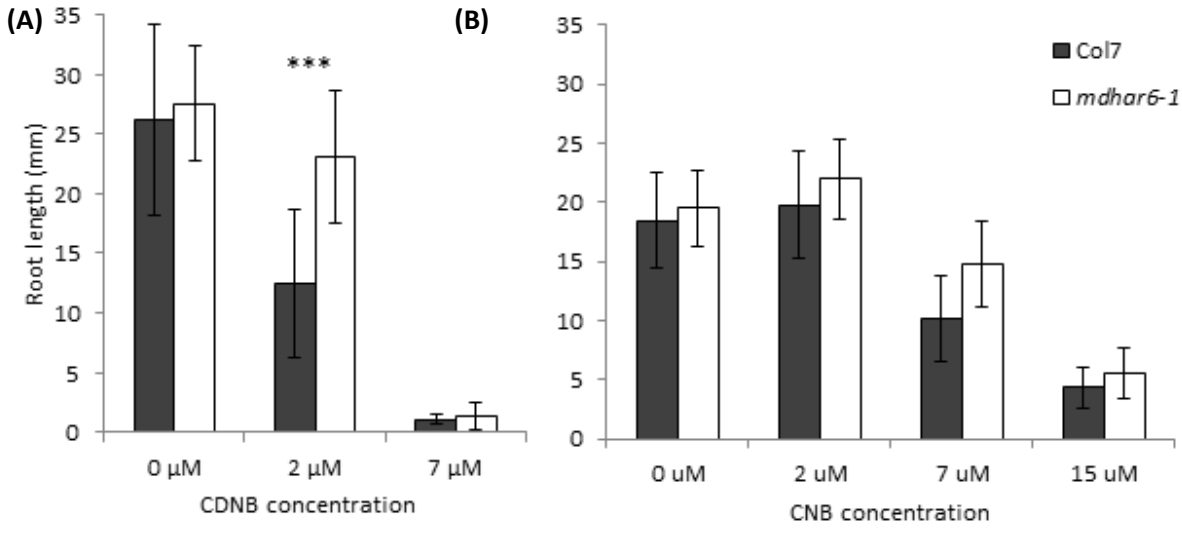

Figure 36: Col7 and *mdhar6-1* root growth in presence of CDNB or CNB

Root lengths of seven-day old seedlings germinated on ½ MS(A) containing increasing concentrations of **(A)** CDNB or **(B)** CNB. Mean of 30 biological replicates ± SD shown. Student's t test * P<0.05, ** P<0.01, *** P<0.001.

(A)

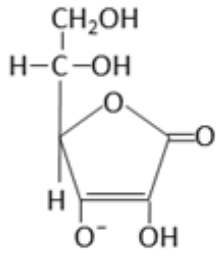

monodehydroascorbate (MDA)

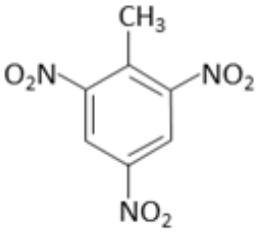

2,4,6-trinitrotoluene (TNT)

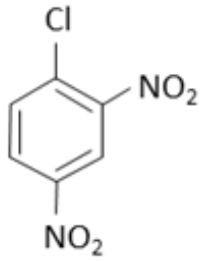

1-chloro-2,4-dinitrobenzene (CDNB)

(B)

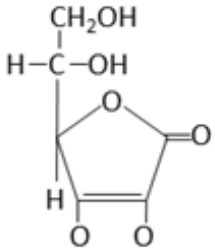

dehydroascorbate (DHA)

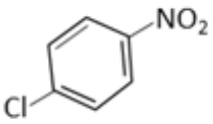

α-chloro-4-nitrobenzene (CNB)

(C)

Substrate	Km (μM)	Vmax ($mmol^{-1}.min^{-1}.mg^{-1}$)
MDA	4.1 ± 0.6	109 ± 1.7
TNT	522 ± 57	0.143 ± 0.0067
CDNB	1,254 ± 96	0.960 ± 0.0026
DHA	ND	ND
CNB	ND	ND

Figure 37: Structures of chemicals tested for MDHAR6 substrates in this study, and kinetic values

(A) Chemicals identified as MDHAR6 substrates in this study. **(B)** Chemicals identified not to be MDHAR6 substrates in this study. **(C)** Michaelis-Menten kinetic activity values ± SEM. ND; activity not detected.

Some herbicides such as atrazines are applied to soil, while others including glyphosates are sprayed onto foliage. The phytotoxic effects of TNT in soil have previously been demonstrated. To establish the effect of foliage treatment with TNT, 16-d old Col7 and *mdhar6-1* seedlings were sprayed with 0, 5, 50, 200 or 400 µM TNT (maximum solubility in water without added organic solvent) for 7 d. Chlorosis and stunted growth was visible from 48 h after treatment with 400 µM TNT, and to a lesser extent 200 µM TNT. Following 7 d of treatment, there were still no visible difference between Col7 and *mdhar6-1* (Figure 38).

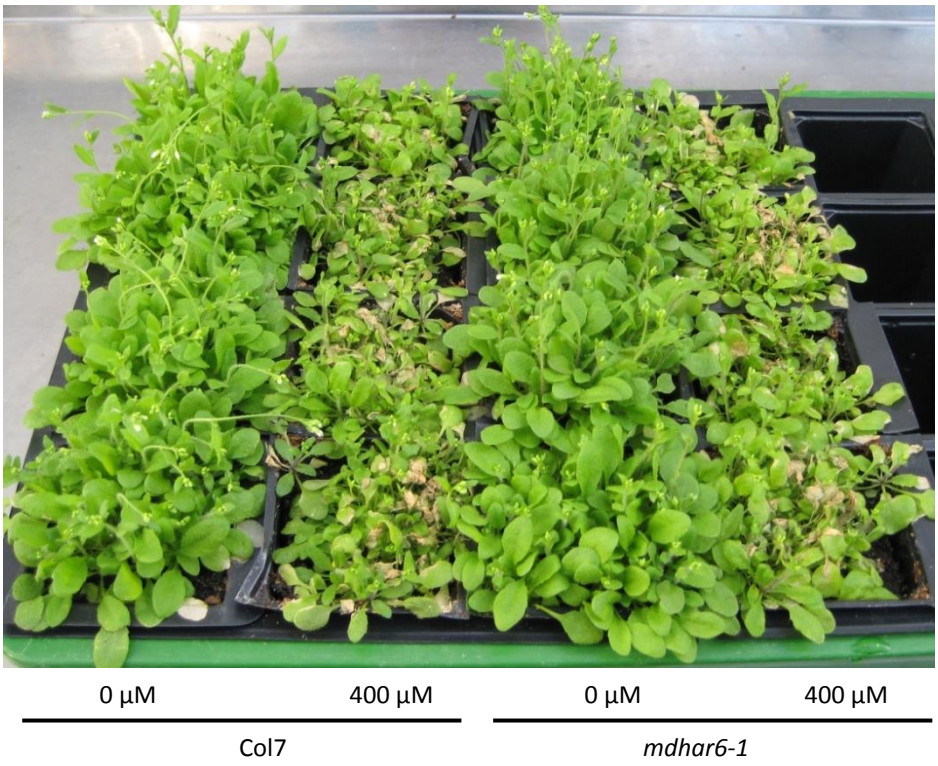

Figure 38: Aerial treatment of two-week old seedlings with TNT

Three-week old Col7 and *mdar6-1* seedlings which have been sprayed daily with 2.6 ml (per punnet) 0 or 400 µM TNT in water for 7 d.

3.3 DISCUSSION

3.3.1 The endogenous role of MDHAR6

This study has included the first purification of an Arabidopsis MDHAR for enzymatic analysis, and has confirmed that AtMDHAR6 has reductase activity against MDA, but not DHA. The estimated K_m for activity with MDA (4.1 μM) is within the range of previously reported K_m values for MDHAR enzymes; 0.9 μM (Borraccino *et al.* 1986) to 7 μM (Dalton *et al.* 1992).

A surprising outcome, is the finding that *mdhar6-1* mutants are little compromised in high solute, salt or oxidative stress tolerance (Johnston et al., 2015), although biomass is lower than wild type when seedlings are grown in the hypoxic conditions of liquid culture (3.2.2). As MDHAR6 is the only plastid and mitochondria-targeted MDHAR in Arabidopsis, and chloroplasts and mitochondria are such redox-active compartments, this may be surprising, however plastid and mitochondria-targeting of MDHAR appears to be a feature of higher plants (Gest et al., 2012); genetic analysis indicates that lower plants have only cytosolic and peroxisomal MDHARs (Lunde et al., 2006; Drew et al., 2007). As ascorbate oxidation was found to be unchanged in *mdhar6-1* in this study (Figure 24, Figure 25), it could be the case that ferredoxin is sufficient to reduce MDA (Miyake and Asada, 1994) in the mutants.

3.3.2 Rejected hypotheses for the enhanced TNT tolerance of *mdhar6* mutants

That there is no difference in root growth between Col7 and *mdhar6-1* in the presence of high solute, salt or oxidative stress, suggests that the enhanced TNT tolerance of *mdhar6-1* is not due to enhanced general defences.

Another hypothesis has been that the *mdhar6* mutation results in increased DHA levels, which have been proposed to promote cell wall loosening and cell expansion (Lin and Varner, 1991; Green and Fry, 2005). Contradictory to this theory however, in this study no enhanced DHA levels were measured in *mdhar6-1* mutants (Figure 24, Figure 25), and roots are no longer than wild type in the absence of TNT (Figure 22; Student's t test, $P < 0.05$).

3.3.3 The significance of increased glutathione in *mdhar6* roots in explaining *mdhar6* enhanced TNT tolerance

Glutathione conjugation and subsequent sequestration of conjugates is known to have a role in agrochemical detoxification (Cummins et al., 2011), and in Arabidopsis, overexpression of *GSTU24* or *GSTU25* enhances TNT tolerance (Gunning et al., 2014); these enzymes have been found to conjugate glutathione to HADNT via the methyl group, with GSTU25 additionally

conjugating glutathione directly to the aromatic ring of TNT, replacing a nitro group at position 2 or 5 (Gunning et al., 2014).

On ½ MS(A), *mdhar6-1* roots had 1.3-fold more glutathione than Col7 (Figure 24). Under the more stressful conditions of liquid culture, there were higher glutathione levels in both Col7 and *mdhar6-1*, which increased in the presence of TNT, however the content was not significantly different between Col7 and *mdhar6-1* under both TNT and control treatments (to $P < 0.05$ with Student's t test; Figure 25).

To explore whether reducing glutathione content affects TNT tolerance and the enhanced TNT tolerance of the *mdhar6-1* mutant, Col7 and *mdhar6-1* were germinated on ½ MS(A) containing various concentrations of BSO, which inhibits γ-ECS (Griffith and Meister, 1979), and 0 or 7 µM TNT (Figure 26). Glutathione concentration was not measured in this preliminary experiment however, and if repeated, a lower TNT concentration would be better, as the combined effect of BSO and TNT is highly inhibitory to root development. As 250 µM BSO resulted in a small degree of root growth inhibition (perhaps indicating reduced glutathione content), while with 500 µM, BSO roots were only 4 mm in length (making significant differences between genotypes and treatments difficult to measure), measuring root growth and glutathione content in the presence of BSO concentrations between 250 and 450 µM may be optimal. As it stands, conclusions cannot be made from this preliminary experiment without glutathione measurement, however considering that (i) under the stressful conditions of liquid culture, and in the presence of TNT, glutathione levels between Col7 and *mdhar6-1* are comparable (Figure 25), and (ii) that if *mdhar6-1* seedlings contained higher levels of glutathione than Col7 under stressful conditions, enhanced tolerance to other stresses may be expected (Chen et al., 2012; Cheng et al., 2015), which was not observed (Johnston et al., 2015), it is likely that glutathione levels are not having a huge contribution towards the enhanced TNT tolerance of *mdhar6-1*.

3.3.4 The significance of MDHAR6 activity towards TNT in explaining *mdhar6* enhanced TNT tolerance

Although Genevestigator microarray data indicate high levels of *MDHAR6* expression throughout all tissues, my quantitative Polymerase Chain Reaction (qPCR) data (discussed in Chapter 4) indicate higher *MDHAR6* expression in roots compared with leaves. This corresponds with the greater toxicity of TNT when taken up by roots, as opposed to sprayed onto leaves, and also the location of TNT in plants when removed from soil; >95 % of TNT remains in plant roots following uptake (studies with poplar and switchgrass; Brentner et al., 2010).

The hypothesis of one electron reduction of TNT by MDHAR6 is supported by measurement of cofactor oxidation in the presence of TNT, HPLC analysis of reaction products, EPR spectrometry and *in vivo* probing of oxidative state. The one electron reduction of TNT would have a detrimental effect through superoxide generation, and via the futile use of NADH. The rate of MDHAR6 activity towards TNT compared with MDA is relatively low, however as the TNT substrate is regenerated, only catalytic concentrations of TNT are needed for cyclic activity towards TNT, with superoxide generation.

Superoxide reacts readily with nitric oxide ($NO^{\cdot}$) to form peroxynitrite ($ONOO^{-}$), which rapidly protonates to peroxynitrous acid (ONOOH). Peroxynitrous acid is a powerful oxidising and nitrating agent, which can damage protein, lipids and DNA, or split to reactive nitrogen dioxide and hydroxyl radicals (Halliwell, 2006). Hydroxyl radicals react quickly with low specificity, and can initiate self-perpetuating cascades of lipid peroxidation (Halliwell, 2006). Nitrogen dioxide is also a powerful oxidising agent (Halliwell, 2006). Superoxide and peroxynitrite also release iron from enzymes with iron-sulphur clusters; this can result in Fenton chemistry, catalysing the disproportionation of hydrogen peroxide, forming hydroperoxyl and hydroxyl radicals, perpetuating cellular ROS content (Halliwell, 2006).

3.3.5 The importance of MDHAR6 location in conferring toxicity upon reaction with TNT

The importance of MDHAR location in relaying TNT phytotoxicity is implied through two findings; (i) that *mdhar6* mutations confer such high TNT tolerance, when there are four further MDHAR enzymes in Arabidopsis, and (ii) that overexpression of mitochondria-targeted MDHAR6 (*m-MDHAR6*) complements the mutant phenotype more than the plastid-targeted variant (*p-MDHAR6*).

The *mdhar6-1* mutants are not entirely TNT tolerant; for example in Figure 21, the FW of six-week old *mdhar6-1* seedlings growing on 100 mg TNT.kg $soil^{-1}$ are 81 % of those growing in the absence of TNT. It is possible that activity of the other MDHAR enzymes could account for the remaining toxic effect. Mutants in peroxisome membrane-targeted MDHAR *mdhar4* are no more tolerant to TNT (unpublished data- Liz Rylott). Mutants in *mdhar1*, *mdhar2* and *mdhar3* have not been characterised.

Regarding the more complete mutant complementation by *m-MDHAR6*, there are no reliable studies localising TNT at the subcellular level, which would determine whether TNT diffuses into mitochondria more easily than plastids. Chloroplasts accumulate flavonoids, the radicals of which could be additional MDHAR substrates in competition with TNT (Sakihama et al.,

2000). In roots however, flavonoids primarily accumulate at nuclei and the endomembrane systems (Peer et al., 2001). It is highly plausible that there is greater potential for oxidative stress at mitochondria, compared with the amyloplasts and elaioplasts of roots, and/or that the diversion of NADH from respiration has a greater inhibitory effect than from processes in amyloplast and elaioplast organelles.

3.3.6 Application of this finding in the development of phytoremediation technologies

As discussed in Chapter 1, with regards to explosives remediation, removal and degradation of RDX is of higher immediate priority than TNT. Plants developed to degrade RDX however, need tolerance to the co-pollutant TNT. Phytoremediation-appropriate species include grasses, which are fast-spreading, tolerant to physical perturbation, and have extensive root networks, and poplar, which has previously been used to remediate groundwater pollution at US EPA Superfund sites (US EPA, 2015). Recent explosives remediation studies have focused on transforming RDX-degrading activity into switchgrass, a species native to North America, following successful experiments in transgenic Arabidopsis (Rylott et al., 2006, 2011). Knocking out *MDHAR6* in these lines, for example through use of CRISPR-Cas genome editing technology (Sander and Joung, 2014), may increase TNT tolerance and the efficacy of explosives phytoremediation.

3.3.7 Consideration of MDHAR6 as a potential herbicide target

If the increase in stacking of target site-based resistance traits in weeds continues, the demand for new herbicide target sites will greatly increase. As mentioned earlier, no herbicide with a new target site has been commercialised since the 1980s (Duke, 2012). An MDHAR6 substrate would need to be developed which is much more environmentally-friendly and biodegradable than TNT however, and as our preliminary experiments indicate high specificity in the targets for one electron reduction, this could be a challenging task. Use of such a herbicide would also require identification of MDHAR6 orthologue(s) for environmental risk assessment, and development of crops with engineered loss of MDHAR6 activity.

4 The dual targeting of MDHAR6

4.1 INTRODUCTION

4.1.1 The dual targeting of MDHAR6

Two *MDHAR6* transcription start sites (TSSs) were identified and studied by Obara et al. (2002; Figure 39); when the first is used, the transcript encodes seven additional residues at the N-terminus. These form an amphiphilic alpha helix, which is predicted to promote targeting to the mitochondria (Dudek et al., 2013). A mitochondrial peptide cleavage motif (RIAS) is present at residues 45 to 48. There is an intron within the sequence of the amphiphilic helix, and a second TSS within this intron sequence is also used. The uncharged N-terminus of this transcript, with methionine followed by alanine, is frequently found in plastid-targeted proteins, and additionally the central domain enriched in hydroxylated residues, and C-terminus enriched in alanine, are common of plastid-targeted proteins (Bruce, 2000, 2001).

To avoid confusion with the mutant alleles discussed in Chapter 3, in this thesis, *MDHAR6.2* (the transcript variant for mitochondria-targeting) is referred to as *m-MDHAR6*, and *MDHAR6.1* (the transcript variant for plastid targeting) is referred to as *p-MDHAR6*.

Figure 39: Transcription start sites of *MDHAR6*

Adapted from Obara et al. (2002). N-terminus of Col0 *MDHAR6* showing the two TSSs, and amino acids encoded following translation start sites. Grey highlight; intron. Blue highlight; transcript specific to *m-MDHAR6*. Green highlight; beginning of p-MDHAR6 translation. Black double-underline; reverse primer used by Obara et al. (2002) to identify the *p-MDHAR6* TSS.

Obara et al. (2002) analysed cDNA databases, and identified two MDHAR transcripts (*m-MDHAR6* and *p-MDHAR6*) which could arise from At1g63940. To identify the TSSs shown in Figure 39, Obara et al. (2002) used cap site hunting. In cap site hunting, the 5' cap of mRNA is replaced with an artificially synthesised oligoribonucleotide, before reverse transcription. Primers can then be designed against the 5' oligoribonucleotide for PCR, cloning and sequencing. The first cap site hunting experiment by the authors used a nested reverse primer against the *MDHAR6* 3'-terminus. Only the *m-MDHAR6* transcript was amplified, indicating that this is the dominant transcript. To identify the *p-MDHAR6* TSS, the authors needed to use a nested reverse primer, within the intron which should be absent from *m-MDHAR6* (indicated in Figure 39).

To study protein targeting, Obara et al. (2002) fused the 5' sequences of *MDHAR6* (first 50 bases of *m-MDHAR6*, and separately, the first 43 bases of *p-MDHAR6*) to *Green Fluorescent Protein* (*GFP*), and expressed the constructs in Arabidopsis using the constitutive *CaMV 35S* promoter. The N-terminus of m-MDHAR6 targeted GFP to small moving compartments, characteristic of mitochondria when probed separately by the authors with MitoTracker Orange. The N-terminus of p-MDHAR6 targeted GFP to chloroplasts, co-localising with chloroplast autofluorescence. In these experiments, the termini resulted in exclusive targeting to mitochondria or plastids.

Chew et al. (2003) also explored the targeting of MDHAR6, along with other enzymes of the ascorbate-glutathione cycle. The authors used a system in which purified mitochondria and chloroplasts are mixed, incubated with [^{35}S]methionine-labelled protein-of-interest, and then separated again. The import of the labelled protein into mitochondria and/or chloroplasts is then assessed. The authors concluded that m-MDHAR6 is imported to both mitochondria and chloroplasts, however the *in vitro* import protocol is subject to a degree of contamination (the authors estimate 1.5 % contamination of mitochondria with chloroplasts in each separation). In the same study, Chew et al. (2003) also fused full length *m-MDHAR6* to *GFP*, and found exclusive targeting of GFP to mitochondria. The report of exclusive targeting of m-MDHAR6 and p-MDHAR6, to mitochondria or plastids respectively, is more reliable in this respect.

As discussed further below, MDHAR6 appears to be unusual in that dual targeting to plastids or mitochondria is determined by TSS. Considering (i) the research interest in retrograde signalling (discussed further in 4.1.3 and 4.1.4), which could be competitive between organelles at *MDHAR6*, and (ii) the questions raised in this thesis regarding the endogenous role of MDHAR6, it was considered of interest to further investigate *MDHAR6* TSS preference, and protein location, in different tissues, and in response to different stress treatments.

4.1.2 Regulation of dual targeting to mitochondria and plastids

Mitochondria and plastids are derived from the endosymbiosis of α-proteobacterium and cyanobacterium-like ancestors respectively, >1.5 and 1.2 to 1.5 billion years ago (Dyall et al., 2004). During endosymbiosis, approximately 95 % of mitochondria and plastid genes have been transferred to the cell nuclear genome (Carrie and Small, 2013), and consequentially, the encoded proteins are imported, as unfolded precursor proteins. Carrie and Small (2013) list over 100 of these which have been identified as dual targeting to plastids and mitochondria, most of which are involved in DNA replication, protein translation, or protein folding. Of these, *MDHAR6* is the only for which targeting is dependent on the TSS used (Obara et al., 2002).

Dual targeting raises interesting questions regarding mechanism and regulation. In mitochondria, unfolded protein precursors are recognised by the outer membrane TRANSPORTER OUTER MEMBRANE (TOM) complex, which transfers outer membrane proteins to the outer membrane SORTING AND ASSEMBLY MACHINERY (SAM) complex, inner membrane proteins to the inner membrane TRANSPORTER INNER MEMBRANE (TIM) 22 complex, and soluble matrix proteins to the inner membrane TIM23 complex, for translocation (Dudek et al., 2013). The N-terminal signal/transit peptide (usually an amphiphilic alpha helix) is recognised by a receptor in TOM, and cleaved (at sequence RIAS) within the matrix following import (Dudek et al., 2013). The receptor components of TOM in plants are considered to be non-orthologous to those in animals (Perry et al., 2006).

In plastids, unfolded protein precursors are translocated through TOC and TIC complexes (*T*ranslocon at the *O*uter/Inner envelope membrane of *C*hloroplasts) at the outer and inner membrane respectively (Jarvis, 2008). Transit peptides appear to be highly variable and unstructured, ranging from 20 to >100 residues, but are generally positively charged (Jarvis, 2008). The transit peptides are also cleaved, within the stroma (Jarvis, 2008). Intriguingly, there are multiple genes encoding receptor components of TOC, regulation of which could mediate plastid differentiation (Jarvis et al., 1998; Yan et al., 2006; Jarvis, 2008). A transportation pathway via endoplasmic reticulum (ER) and Golgi apparatus has also been proposed (Radhamony and Theg, 2006).

Dual targeting of an identical precursor protein may be mediated by (i) an ambiguous signal peptide, recognised by receptors at TOM and TOC which also associate with single organelle-targeted protein, (ii) recognition of the same signal by receptors specific for dual targeted proteins at TOM and TOC, or (iii) recognition of different signals on the same protein by TOM and TOC. Experiments involving fusion of protein domains to reporters such as GFP have

provided evidence for both shared and multiple signal peptides. For example, Berglund et al. (2009) identified that for the amino acyl-tRNA synthetases (aaRSs) TyrRS, ValRS and ThrRS, 27, 22 and 23 residues, respectively, were required for targeting to both plastids and mitochondria. These sequences had a high percentage of hydroxylated residues (26 – 51 %). Meanwhile removal of 20 residues from the N-terminus of ProRS inhibited translocation to plastids only, and removal of 16 residues from N-terminus of AspRS inhibited translocation to mitochondria only.

Regulation of destination in dual targeting could involve (i) regulation of import machinery (for example, TOM translocase is activated by phosphorylation; Schmidt et al., 2011), (ii) regulation of guidance complexes (cytosolic chaperones have an important role in maintaining the unfolded structure of precursor proteins in the cytosol, and are considered to promote organelle targeting; Lee et al., 2013) and/or (iii) post-translational modifications of the signal peptide (for example, by phosphorylation; May and Soll, 2000).

The MDHAR6 protein differs from the models above, in that targeting to mitochondria or plastids depends on the TSS used, resulting in the presence or absence of seven additional residues at the N-terminus. Although there are examples of TSS preference determining transport to mitochondria or retention in the cytosol (histidine tRNA synthetase 1 and valyl-tRNA synthetase in yeast; Yogev and Pines, 2011), or to mitochondria or the ER (renin in rat; Yogev and Pines, 2011), MDHAR6 is the only known example where TSS determines targeting to plastids or mitochondria, and TSS preference could potentially be regulated by organelle retrograde signalling. For example, Baier et al. (2000) report induction of *MDHAR6* in mutants with decreased levels of 2-cysteine peroxiredoxin (2CPA; a chloroplast-targeted antioxidant protein); it would be interesting to further elucidate whether such induction is specifically of the transcript for plastid-targeting.

4.1.3 Retrograde signalling from chloroplasts

Following the migration of genes from plastid and mitochondria genomes to the nucleus, tight coordination between organelle and nuclear genomes is required for efficient and appropriate responses to changing environmental conditions and organelle requirements. Retrograde signalling pathways originate from stimuli at organelles, and culminate in changing nuclear gene expression. Retrograde pathways from plastids and mitochondria could potentially be competitive at the *MDHAR6* gene.

Chloroplast retrograde signalling (reviewed; Barajas-López et al., 2013) is considered to include (i) repression of nuclear-encoded components of the photosynthetic electron transport chain

(e.g. *LIGHT HARVESTING CHLOROPHYLL A/B BINDING PROTEIN B1*; *LHCB1*) in response to accumulating levels of chlorophyll precursor Mg-protoporphyrin IX (Mg-proto), (ii) cell death in response to singlet oxygen, and (iii) activation of antioxidant genes (such as *ASCORBATE PEROXIDASE 2*; *APX2*) in response to hydrogen peroxide and/or 3'phosphoadenosine 5'-phosphate (PAP).

Chloroplast Mg-proto signalling

Repression of *LHCB1* in response to norflurazon treatment (a carotenoid biosynthesis inhibitor, which increases Mg-proto levels) requires pentatricopeptide repeat protein GENOMES UNCOUPLED 1, and has been linked with AP2-type transcription factor ABSCISIC ACID INSENSITIVE 4 (ABI4; Koussevitzky et al., 2007), GOLDEN-LIKE (GLK) transcription factors GLK1 and GLK2 (Waters et al., 2009), and LONG HYPOCOTYL 5 (HY5; Kindgren et al., 2012). It should be noted however that this pathway is highly debated; correlation between Mg-proto levels and *LHCB1* expression has been contested (Mochizuki et al., 2008; Moulin et al., 2008), and norflurazon treatment is arguably a severe stress, unrepresentative of changing environmental conditions.

Chloroplast singlet oxygen signalling

The Arabidopsis *fluorescent* mutant accumulates photosensitizer protochlorophyllide in the dark, and upon shift to light, exhibits a burst of $^1O_2$ in chloroplasts, followed by necrotic lesion development (Camp et al., 2003). The cell death response is reduced when treated with Vitamin B6, which quenches $^1O_2$, and when salicylate hydroxylase is expressed, indicating a role for salicylic acid (Danon et al., 2005). Plastid proteins EXECUTER 1 and 2 attenuate the cell death response in dark-light treated *flu* (Lee et al., 2007; Wagner et al., 2004).

Chloroplast hydrogen peroxide and 3'phosphoadenosine 5'-phosphate (PAP) signalling

The transcriptome of catalase-deficient mutants under high light (HL) indicate that H_2O_2 could have a role in inducing 88 genes and repressing 349 genes in response to HL (Vanderauwera et al., 2005). Hydrogen peroxide-mediated induction of *APX2* has been a focus in studying the H_2O_2 response. Mutant screens have identified constitutive *APX2* expression in lines with mutant alleles of *GSH1*, which have lower glutathione levels (Ball et al., 2004).

A role for PAP in retrograde signalling was identified in a screen for mutants that did not induce *APX2* under HL or drought conditions. The phosphatase mutant, *sal1*, was found to have reduced *APX2* expression under HL, corresponding with reduced PAP levels (Estavillo et al., 2011). It is proposed that under HL/drought, SAL1 is inhibited, and PAP levels increase, which could have a signalling role through inhibition of miRNA-targeting exoribonucleases (Estavillo et al., 2011).

4.1.4 Retrograde signalling from mitochondria

Mitochondrial retrograde signalling is best understood in the budding yeast *Saccharomyces cerevisiae*; these cells can use fermentation to derive ATP in the absence of respiration, and so it is possible to study *S. cerevisiae* cell lines with severe mitochondria defects (Woodson and Chory, 2008). In what is referred to as the RTG (Retrograde) pathway, loss in mitochondrial membrane potential results in the induction of genes for α-ketoglutarate biosynthesis (the precursor for glutamate, and part of the citric acid cycle; review, Liu and Butow, 2006). Mutants in this pathway are glutamate auxotrophs (Liu and Butow, 2006). Upon mitochondria dysfunction, the bHLH/Zip transcription factor Rtg3p becomes partially dephosphorylated, and migrates from the cytosol to the nucleus with Rtg1p (Sekito et al., 2000). A number of upstream positive and negative regulators have been characterised (Liu and Butow, 2006). Glutamate is a negative regulator of the signalling pathway, introducing a negative feedback loop (Liu and Butow, 2006).

Haem biosynthesis is oxygen-dependent, and in *S. cerevisiae*, haem levels appear to function as an oxygen sensor; haem binds to HEME ACTIVATOR PROTEIN 1 (HAP1; a zinc finger protein) to promote HAP1-mediated activation of genes for aerobic respiration and restriction of oxidative damage, and *ROX1*, the product of which represses hypoxic-response genes (Hickman and Winston, 2007; Woodson and Chory, 2008). Under hypoxic conditions, HAP1 no longer activates genes for aerobic respiration, and directly represses ergosterol biosynthesis genes (Hickman and Winston, 2007; Woodson and Chory, 2008).

In response to plant mitochondrial electron transport chain (mtETC) disruption, a number of nuclear genes are activated, including *ALTERNATIVE OXIDASE 1A* (*AOX1a*), which is commonly used as a marker for mitochondria dysfunction. The ABI4 transcription factor (implicated in gene repression in Mg-proto plastid retrograde signalling; Koussevitzky et al., 2007) is also required for *AOX1a* repression (Giraud et al., 2009). Clercq et al. (2013) identified 34 genes which are induced >two-fold in five or more (out of 22) conditions which induce mitochondria dysfunction. A common motif was identified in 24 of these genes, which the authors then termed "Mitochondria Dysfunction Stimulon" (MDS) genes, and chromatin immunoprecipitation experiments demonstrated recruitment of NAC[8] transcription factor ANAC013 to the motif in MDS gene promoters following mitochondria dysfunction.

[8] The NAC family is named after the first members to be described; NO APICAL MERISTEM/ARABIDOPSIS TRANSCRIPTION ACTIVATION FACTOR/CUP-SHAPED COTYLEDON (Olsen et al., 2005).

4.2 RESULTS

4.2.1 Designing qPCR primers for investigating *MDHAR6* TSS preference

The N-terminus sequence in Figure 39 was determined by Obara et al. (2002) in Col0 ecotype. This study uses Col7, so that qPCR data can be compared with immuno-gold labelling of MDHAR6 localisation, using *mdhar6-1* as a negative control. To confirm the sequence of this region in Col7, genomic DNA was extracted from three Col7 plants, and the TSS region amplified by PCR and sequenced. The TSS region in Col7 was found to be the same sequence as in Col0 (Figure 40).

As shown in Figure 39, there are untranslated mRNA regions specific to the transcripts *m-MDHAR6* or *p-MDHAR6*. Quantitative PCR primers were designed against these transcript-specific regions, and also against the N-terminal region present in both *m-MDHAR6* and *p-MDHAR6*, referred to in this thesis as *mp-MDHAR6* (Figure 41). Primer pairs specific to *m-MDHAR6* are referred to as "mA" to "mD", specific to *p-MDHAR6* as "pA" to "pD", and targeting both *m-MDHAR6* and *p-MDHAR6* as "mpA" to "mpF". The primer efficiency results are summarised in Table 21.

The most appropriate primers for each region, with efficiencies closest to that of the endogenous control (*ACTIN2*), and a single amplicon indicated by melt curve analysis, were mE, pB and mpA. For confirmation of the qPCR targets, fresh qPCR product was purified and sequenced using the qPCR primers. The sequencing results support that the primers are targeting *MDHAR6* (Figure 44).

Figure 40: ClustalW comparison of Col7 and Col0 *MDHAR6* N-terminal sequence

Genomic DNA was extracted from three separate Col7 plants for TSS region amplification (amplicons A-C). The sequence quality of amplicon B decreases greatly at nucleotide 330. Alignment by ClustalW2 (Larkin et al., 2007).

Primer pair mA

AACACTACAGAGAGACTCACACACTTGTTTCAATAATTAAATCTGAATTTGGCTCTTCTTATAA
ACTAATGTCTGCAGTTCGTAGAGTCATGGCGTTAGCATCAACCACGTTGCCGACGAAGTCCGGA
TTATCTCTTTGGTGTCCGT…

Primer pair mB

AACACTACAGAGAGACTCACACACTTGTTTCAATAATTAAATCTGAATTTGGCTCTTCTTATAA
ACTAATGTCTGCAGTTCGTAGAGTCATGGCGTTAGCATCAACCACGTTGCCGACGAAGTCCGGA
TTATCTCTTTGGTGTCCGT…

Primer pair mC

AACACTACAGAGAGACTCACACACTTGTTTCAATAATTAAATCTGAATTTGGCTCTTCTTATAA
ACTAATGTCTGCAGTTCGTAGAGTCATGGCGTTAGCATCAACCACGTTGCCGACGAAGTCCGGA
TTATCTCTTTGGTGTCCGT…

Primer pair mD

AACACTACAGAGAGACTCACACACTTGTTTCAATAATTAAATCTGAATTTGGCTCTTCTTATAA
ACTAATGTCTGCAGTTCGTAGAGTCATGGCGTTAGCATCAACCACGTTGCCGACGAAGTCCGGA
TTATCTCTTTGGTGTCCGT…

Primer pair mE

AACACTACAGAGAGACTCACACACTTGTTTCAATAATTAAATCTGAATTTGGCTCTTCTTATAA
ACTAATGTCTGCAGTTCGTAGAGTCATGGCGTTAGCATCAACCACGTTGCCGACGAAGTCCGGA
TTATCTCTTTGGTGTCCGT…

Figure 41: Quantitative PCR primers tested for study of *m-MDHAR6* transcript abundance

The 5' terminus of *m-MDHAR6* cDNA is shown, with primers highlighted in blue. The underlined region is specific to the *m-MDHAR6* transcript variant.

Primer pair pA

ATCTCTCTCACTCACCACCATCTTCTTCCTCGATTGTCAAAACCCTAGATCGAAATCTTATCTC
TCTAATCTGTTGTTACAGTTCGTAGAGTCATGGCGTTAGCATCAACCACGTTGCCGACGAAGTC
CGGATTATCTCTTTGGTGTCCGT…

Primer pair pB

ATCTCTCTCACTCACCACCATCTTCTTCCTCGATTGTCAAAACCCTAGATCGAAATCTTATCTC
TCTAATCTGTTGTTACAGTTCGTAGAGTCATGGCGTTAGCATCAACCACGTTGCCGACGAAGTC
CGGATTATCTCTTTGGTGTCCGT…

Primer pair pC

ATCTCTCTCACTCACCACCATCTTCTTCCTCGATTGTCAAAACCCTAGATCGAAATCTTATCTC
TCTAATCTGTTGTTACAGTTCGTAGAGTCATGGCGTTAGCATCAACCACGTTGCCGACGAAGTC
CGGATTATCTCTTTGGTGTCCGT…

Primer pair pD

ATCTCTCTCACTCACCACCATCTTCTTCCTCGATTGTCAAAACCCTAGATCGAAATCTTATCTC
TCTAATCTGTTGTTACAGTTCGTAGAGTCATGGCGTTAGCATCAACCACGTTGCCGACGAAGTC
CGGATTATCTCTTTGGTGTCCGT…

Primer pair pE

ATCTCTCTCACTCACCACCATCTTCTTCCTCGATTGTCAAAACCCTAGATCGAAATCTTATCTC
TCTAATCTGTTGTTACAGTTCGTAGAGTCATGGCGTTAGCATCAACCACGTTGCCGACGAAGTC
CGGATTATCTCTTTGGTGTCCGT…

Figure 42: Quantitative PCR primers tested for study of *p-MDHAR6* transcript abundance

The 5' terminus of *p-MDHAR6* cDNA is shown, with primers highlighted in green. The underlined region is specific to the *p-MDHAR6* transcript variant.

Primer pair mpA

…TTCGTAGAGTCATGGCGTTAGCATCAACCACGTTGCCGACGAAGTCCGGATTATCTCTTTGGTGTCCG
TCTTCTCCGTCTCTCGCTCGCCGATTTCCCGCTCGTTTTTCTCCGATCGGTTCTAGAATCGCTTCCAGAAG
CCTCGTCACTGCTTCGTTCGCTAACGAGAATCGCGAGTTTGTGATTGTTGGTGGAGGAAATGCTGCTGG
TTATGCTGCTAGAACTTTTGTGGAAAATGGAATGGCTGATGGTCGGCTATGCATTGTGACCAAAGAGG
CTTACGCACCTTATGAGAGACCGGCTTTGACAAA…

Primer pair mpB

…TTCGTAGAGTCATGGCGTTAGCATCAACCACGTTGCCGACGAAGTCCGGATTATCTCTTTGGTGTCCG
TCTTCTCCGTCTCTCGCTCGCCGATTTCCCGCTCGTTTTTCTCCGATCGGTTCTAGAATCGCTTCCAGAAG
CCTCGTCACTGCTTCGTTCGCTAACGAGAATCGCGAGTTTGTGATTGTTGGTGGAGGAAATGCTGCTGG
TTATGCTGCTAGAACTTTTGTGGAAAATGGAATGGCTGATGGTCGGCTATGCATTGTGACCAAAGAGG
CTTACGCACCTTATGAGAGACCGGCTTTGACAAA…

Primer pair mpC

…TTCGTAGAGTCATGGCGTTAGCATCAACCACGTTGCCGACGAAGTCCGGATTATCTCTTTGGTGTCCG
TCTTCTCCGTCTCTCGCTCGCCGATTTCCCGCTCGTTTTTCTCCGATCGGTTCTAGAATCGCTTCCAGAAG
CCTCGTCACTGCTTCGTTCGCTAACGAGAATCGCGAGTTTGTGATTGTTGGTGGAGGAAATGCTGCTGG
TTATGCTGCTAGAACTTTTGTGGAAAATGGAATGGCTGATGGTCGGCTATGCATTGTGACCAAAGAGG
CTTACGCACCTTATGAGAGACCGGCTTTGACAAA…

Primer pair mpD

…TTCGTAGAGTCATGGCGTTAGCATCAACCACGTTGCCGACGAAGTCCGGATTATCTCTTTGGTGTCCG
TCTTCTCCGTCTCTCGCTCGCCGATTTCCCGCTCGTTTTTCTCCGATCGGTTCTAGAATCGCTTCCAGAAG
CCTCGTCACTGCTTCGTTCGCTAACGAGAATCGCGAGTTTGTGATTGTTGGTGGAGGAAATGCTGCTGG
TTATGCTGCTAGAACTTTTGTGGAAAATGGAATGGCTGATGGTCGGCTATGCATTGTGACCAAAGAGG
CTTACGCACCTTATGAGAGACCGGCTTTGACAAA…

Primer pair mpE

…TTCGTAGAGTCATGGCGTTAGCATCAACCACGTTGCCGACGAAGTCCGGATTATCTCTTTGGTGTCCG
TCTTCTCCGTCTCTCGCTCGCCGATTTCCCGCTCGTTTTTCTCCGATCGGTTCTAGAATCGCTTCCAGAAG
CCTCGTCACTGCTTCGTTCGCTAACGAGAATCGCGAGTTTGTGATTGTTGGTGGAGGAAATGCTGCTGG
TTATGCTGCTAGAACTTTTGTGGAAAATGGAATGGCTGATGGTCGGCTATGCATTGTGACCAAAGAGG
CTTACGCACCTTATGAGAGACCGGCTTTGACAAA…

Figure 43: Quantitative PCR primers tested for study of *MDHAR6* total transcript abundance

The 5' terminus region of *MDHAR6* which is present in both *m-MDHAR6* and *p-MDHAR6* cDNA is shown, with primers highlighted in grey.

Table 21: Summary of primer efficiency results for *MDHAR6* TSS study

The PCR efficiency ($10^{(-1/slope)}$-1) of the primer pairs was determined using cDNA from 2-week old Col7 seedlings, grown in liquid culture. A PCR efficiency between 90 and 105 % is acceptable for qPCR. Melt curve analysis of qPCR product was also used to determine the number of different amplicons resulting from the qPCR; multiple Tm peaks indicate more than one amplicon product. Large peaks at 65° also indicate a high degree of primer dimerization.

Primer pair	Rank	PCR efficiency	Melt curve
ACTIN2	1	92.8 % (Acceptable)	Good
mA	-	64.7 % (Too low)	Good
mB	-	91.3 % (Acceptable)	Peak asymmetrical
mC	-	90.1 % (Acceptable)	Multiple Tm peaks
mD	-	102.5 % (Acceptable)	Possible second Tm peak
mE	1	91.3 % (Acceptable)	Good
pA	2	96.2 % (Acceptable)	Good
pB	1	92.0 % (Acceptable)	Good
pC	3	92.7 % (Acceptable)	Good
pD	4	102.7 % (Acceptable)	Good
pE	5	94.2 % (Acceptable)	Large 65° peak
mpA	1	93.1 % (Acceptable)	Large 65° peak
mpB	-	118.5 % (Too high)	Multiple Tm peaks
mpC	-	94.5 % (Acceptable)	Large 65° peak
mpD	2	96.3 % (Acceptable)	Large 65° peak
mpE	3	97.6 % (Acceptable)	Large 65° peak

Primer pair mE

Anticipated amplicon sequence

CACTACAGAGAGACTCACACACTTGTTTCAATAATTAAATCTGAATTTGGCTCTTCTTA
TAAACTAATGTCTGCAGTTCGTAGAGTCATG

Forward primer sequence read

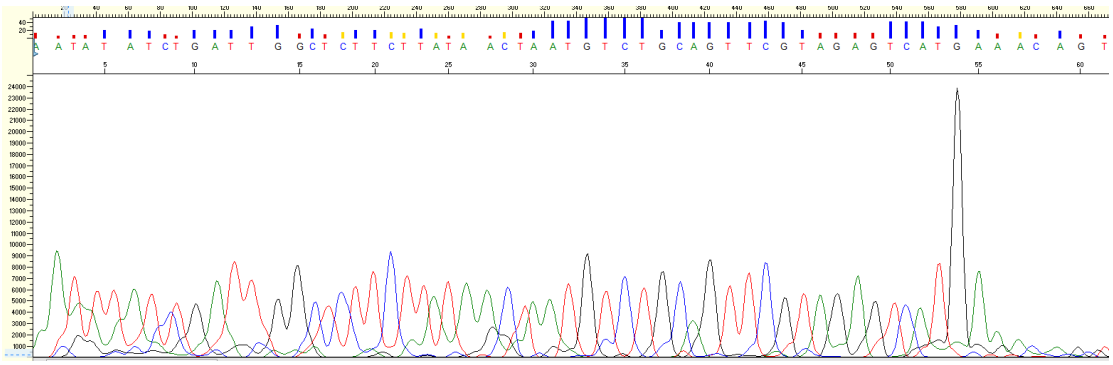

```
mE       CACTACAGAGAGACTCACACACTTGTTTCAATAATTAAATCTGAATTTGGCTCTTCTTAT 60
seqF     ---------------------------------AATATATCTGA--TTGGCTCTTCTTAT 25
                                           *:**:******  **************

mE       AAACTAATGTCTGCAGTTCGTAGAGTCATG- 90
seqF     -AACTAATGTCTGCAGTTCGTAGAGTCATGA 55
          ******************************
```

Reverse primer sequence read

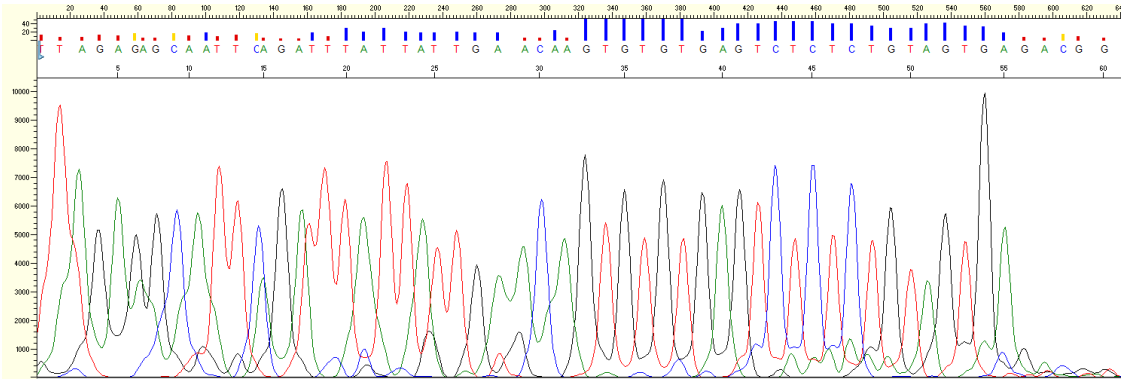

```
mErev    CATGACTCTACGAACTGCAGACATTAGTTTATAAGAAGAGCCAAATTCAGATTTAATTAT 60
seqR     ----------------------TTAG---------AGAGC--AATTCAGATTT-ATTAT 25
                                ****         *****  *********** *****

mErev    TGAAACAAGTGTGTGAGTCTCTCTGTAGTG--- 90
seqR     TG-AACAAGTGTGTGAGTCTCTCTGTAGTGAGA 57
         ** ***************************
```

Primer pair pB

Anticipated amplicon sequence

CATCTTCTTCCTCGATTGTCAAAACCCTAGATCGAAATCTTATCTCTCTAATCTGTTGT TACAGTTCGTAGAGTCATG

Forward primer sequence read

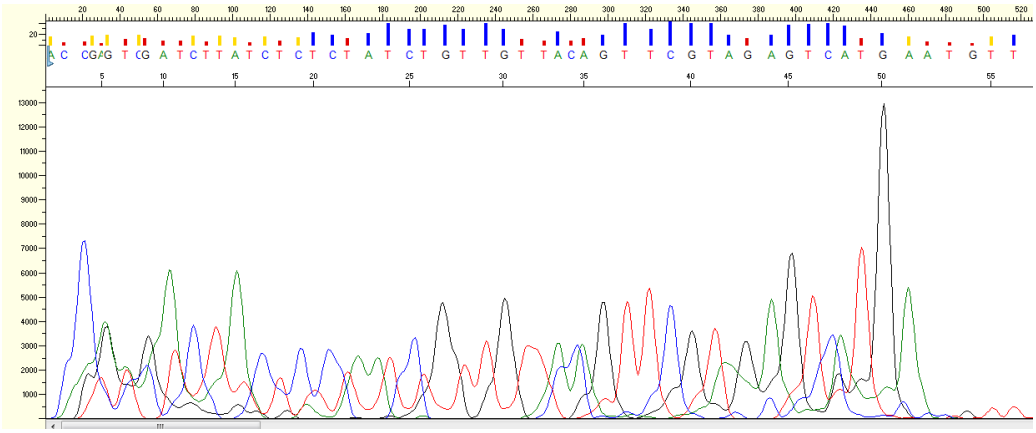

```
pB      CATCTTCTTCCTCGATTGTCAAAACCCTAGATCGAAATCTTATCTCTCTAATCTGTTGTT 60
seqF    -------------------------ACCGAG-TCG--ATCTTATCTCTCT-ATCTGTTGTT 32
                                  .** ** ***  ************* **********

pB      ACAGTTCGTAGAGTCATG- 78
seqF    ACAGTTCGTAGAGTCATGA 51
        ******************
```

Reverse primer sequence read

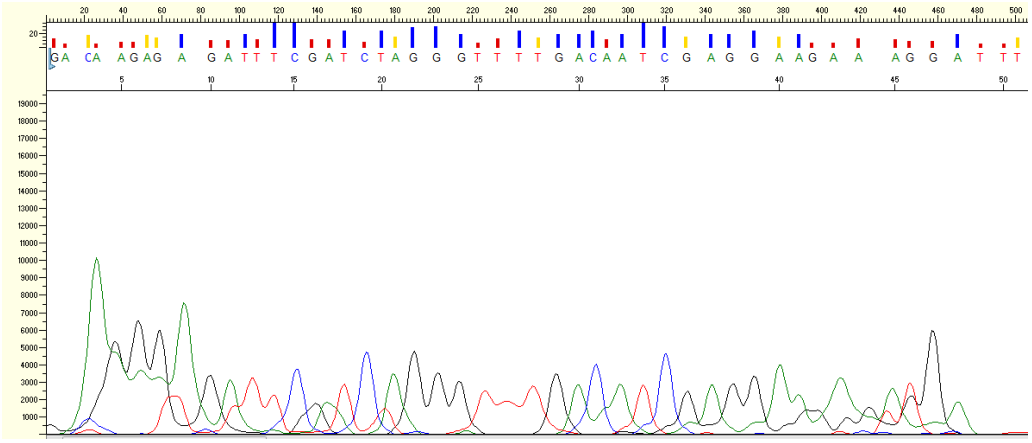

```
pBrev   CATGACTCTACGAACTGTAACAACAGATTAGAGAGATAAGATTTCGATCTAGGGTTTTGA 60
seqR    -------------------------GACAAGAGA-----GATTTCGATCTAGGGTTTTGA 30
                                 ** :*****     ********************

pBrev   CAATCGAGGAAGAAG--ATG 78
seqR    CAATCGAGGAAGAAAGGAT- 49
        **************.  **
```

Primer pair mpA

Anticipated amplicon sequence

CCACGTTGCCGACGAAGTCCGGATTATCTCTTTGGTGTCCGTCTTCTCCGTCTCTCGCT
CGCCGATTT

Forward primer sequence read

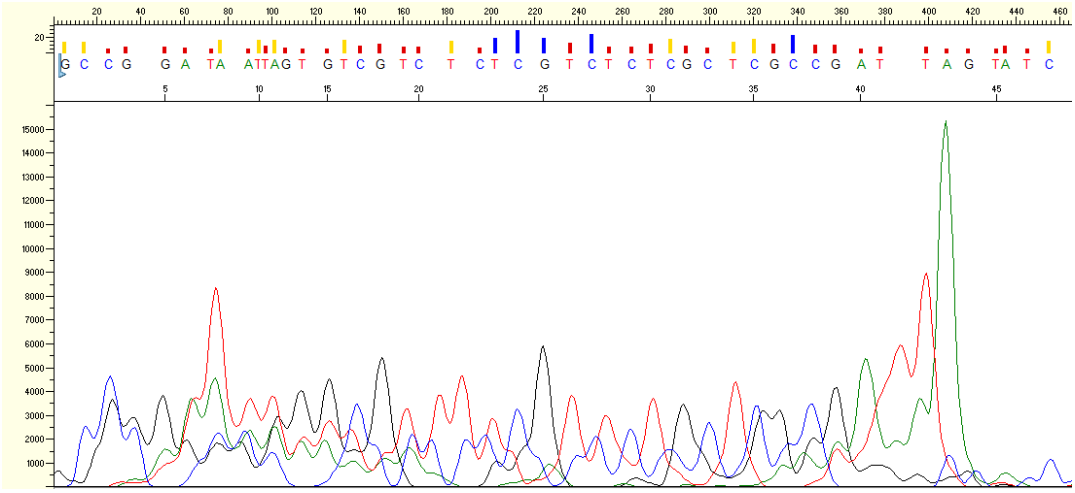

```
mpA      CCACGTTGCCGACGAAGTCCGGATTATCTCTTTGGTGTCCGTCTTCTCCGTCTCTCGCTC 60
seqF     ----------------G-CCGGATAAT-----TAGTGT-CGTCT-CT-CGTCTCTCGCTC 35
                         * ******:**     *.**** ***** ** ************

mpA      GCCGATTT- 68
seqF     GCCGATTAG 44
         *******:
```

Reverse primer sequence read

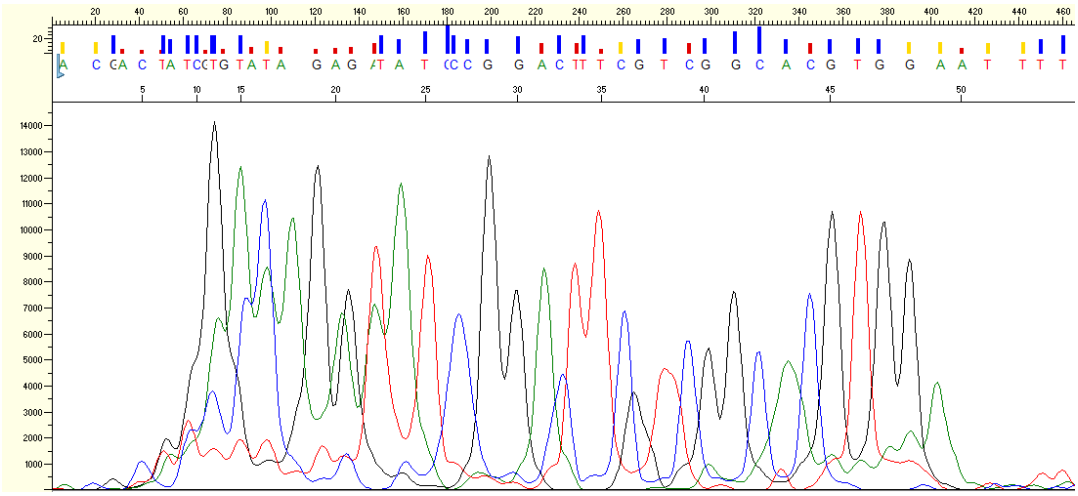

```
mpArev   AAATCGGCGAGCGAGAGACGGAGAAGACGGACACCAAAGAGATAATCCGGACTT-CGTCG 59
seqR     ---ACG-----------ACG----TATCG--CTGTATAGAGATATCCCGGACTTTCGTCG 40
            :**           ***    :.:**  *:  *:********: ******** *****

mpArev   GCAACGTGG- 68
seqR     GCA-CGTGGA 49
         *** *****
```

Figure 44: Sequencing of qPCR amplicons in *MDHAR6* TSS study

Anticipated qPCR amplicon sequences shown with regions specific to *m-MDHAR6* or *p-MDHAR6* underlined, and primer sequences highlighted. Amplicons were sequenced using both forward and reverse primers. Sequence data as analysed by SeqScanner2.0 (Applied Biosystems) displayed, with alignment against anticipated sequence calculated by ClustalW2 (Larkin et al., 2007).

4.2.2 The qPCR primers indicate that a third, previously undescribed TSS could be dominant

In order to investigate TSS preference in different tissues, and in response to different treatments, Col7 seedlings were grown hydroponically (on rafts with roots submerged in ½ MS(S)). This was chosen so that roots could be easily and uniformly treated in subsequent experiments.

In a preliminary experiment, root and leaf tissue from 3-week old seedlings were harvested for RNA extraction, cDNA synthesis and qPCR. All qPCR primers with appropriate efficiencies (Table 21) were used to estimate *m-MDHAR6* and *p-MDHAR6* transcript abundance, relative to the endogenous control *ACTIN2*. This was done to verify the qPCR primers; if the amount of unspliced *m-MDHAR6* is negligible, it was considered that the relative abundance of *m-MDHAR6* and *p-MDHAR6* should equal that of *mp-MDHAR6*.

Surprisingly, the abundance of *m-MDHAR6* and *p-MDHAR6* indicated by primers pairs mE and pA-pE, were approximately two orders of magnitude lower than the combined transcript abundance, indicated by the primers against *mp-MDHAR6* (Figure 45). The abundance of *p-MDHAR6* indicated by primer pair pE however, was in line with that of the *mp-MDHAR6* primers. It is very possible, that by using the reverse primer within the *m-MDHAR6* intron in cap site hunting (Figure 39), Obara et al. (2002) were unable to identify a third TSS, located between the pE and pA forward primers (Figure 41). The Arabidopsis Information Resource (TAIR; Huala et al., 2001) does predict two further *MDHAR6* transcripts (with lower confidence than for *m-MDHAR6* and *p-MDHAR6*), which use a TSS approximately 55 bases upstream of the *p-MDHAR6* TSS in Figure 39. This would be within the reverse primer sequence used in cap site hunting to identify *p-MDHAR6* TSS, and so would not have been identified in the Obara et al. (2002) study.

To differentiate between the different results indicated by primer pairs pB and pE, abundance of transcript indicated by primer pair pB (i.e. from the *p-MDHAR6* TSS indicated in Figure 39) is subsequently referred to as *pB-MDHAR6*, and the abundance indicated by primer pair pE

(indicating use of a third TSS), is subsequently referred to as *pE-MDHAR6*. These transcripts would both encode plastid-targeted MDHAR6.

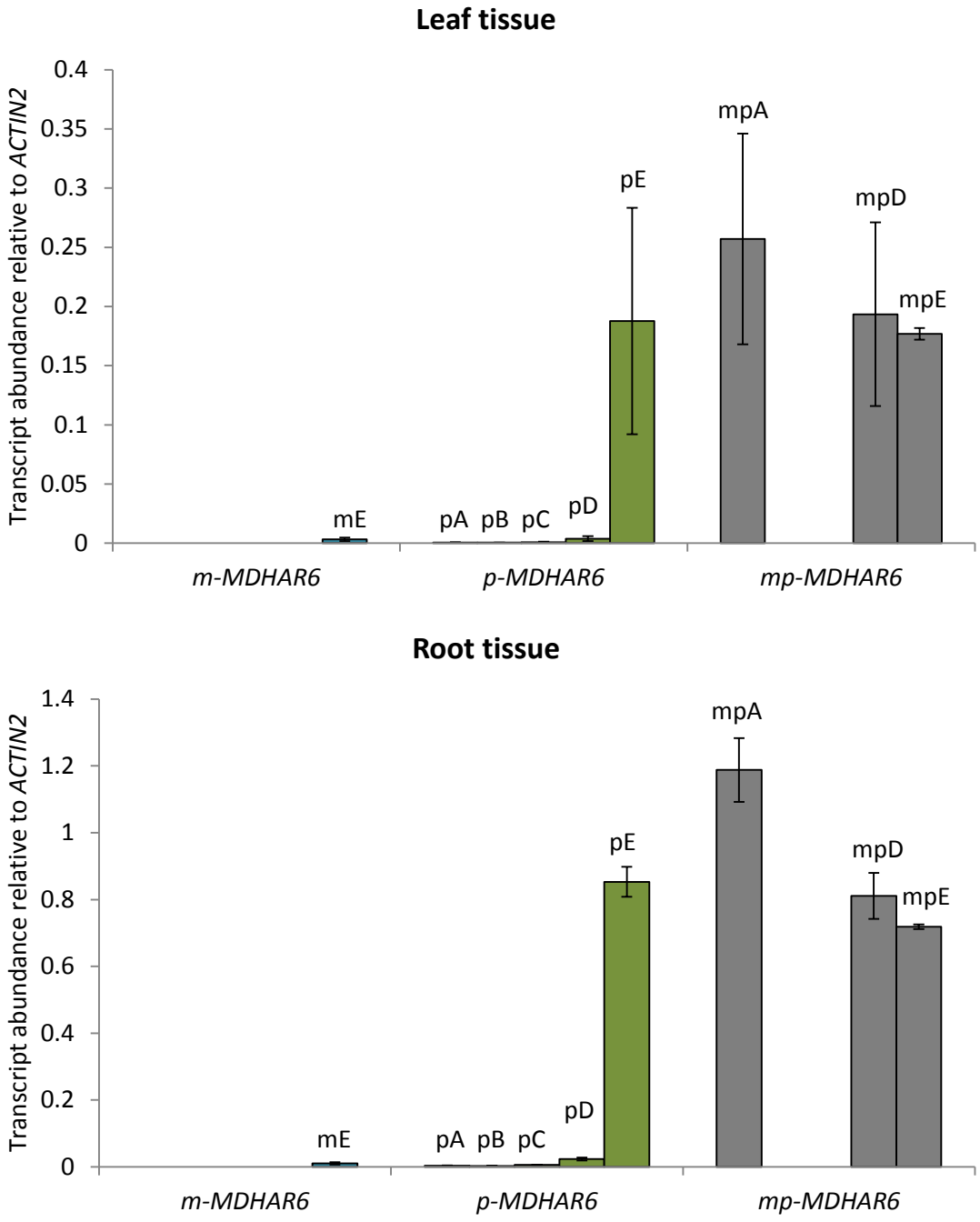

Figure 45: *MDHAR6* transcript abundance in leaf and root, relative to *ACTIN2*, indicated by different qPCR primer pairs

Mean of five biological replicates ± SD. Primer pair code (see Figure 41 - Figure **43**) indicated above bars. Only primers with PCR efficiencies between 90 and 105 %, which amplify a single amplicon (as indicated by melt curve analysis) are included in this study.

As the reverse transcription in cDNA synthesis is in the 3' to 5' direction from the polyA tail, another possible explanation for the discrepancy in transcript abundance is that the reverse transcriptase dissociates from the RNA before reaching the 5' terminus. However, the forward primer of pair mE is 28 bases closer to the 5' terminus than pA, with three-fold greater transcript abundance, suggesting that proximity to the 5' terminus is insufficient to explain the difference in transcript level.

To investigate whether RNA secondary structure at the 5' termini could impede complete reverse transcription, the predicted secondary structure of the 150 bases most proximal to the 5' termini of the three putative *MDHAR6* transcripts was investigated, using ViennaRNA Package 2.0 (Lorenz et al., 2011). The free energy of the predicted structures for the terminus of *pE-MDHAR6* is more negative than for *m-MDHAR6* or *pB-MDHAR6* (Table 22), indicating that the difference in transcript abundance cannot be explained by inhibitory secondary structures.

From the data presented in Figure 45, it would appear that the putative third TSS, which would encode plastid-targeted MDHAR6, is the dominant of the three.

Table 22: Secondary structure of *MDHAR6* RNA 5' termini

Secondary structure of RNA predicted by RNAfold via ViennaRNA Package 2.0 (Lorenz et al., 2011). Optimal secondary structure colour-coded by base pairing probabilities, from 0 (blue) to 1 (red). MFE; Minimum Free Energy.

Sequence input	***m-MDHAR6*** i.e. 150 bp from *m-MDHAR6* TSS indicated in Figure 39	***pB-MDHAR6*** i.e. 150 bp from *p-MDHAR6* TSS indicated in Figure 39	***pE-MDHAR6*** i.e. 150 bp from possible third TSS within *m-MDHAR6* intron
Optimal secondary structure	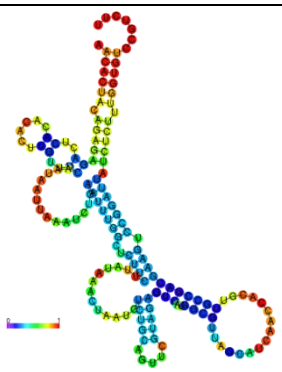	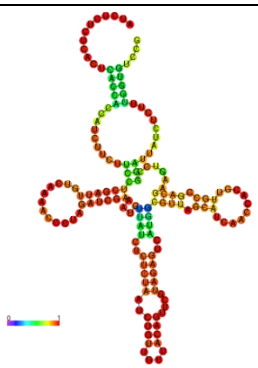	
MFE of optimal secondary structure	-27.7 kcal/mol	-27.2 kcal/mol	-34.3 kcal/mol
Frequency of MFE structure in thermodynamic ensemble	0.4 %	6.08 %	2.5 %
Free energy of thermodynamic ensemble	-31.1 kcal/mol	-28.93 kcal/mol	-36.57 kcal/mol

4.2.3 Transcript Start Site preference changes between tissues

Comparing transcript abundance in root relative to leaf tissue, *m-MDHAR6*, *pB-MDHAR6* and *pE-MDHAR6* are more highly expressed in roots, however the increase in abundance in root tissue is 1.9 and 1.6-fold greater than *m-MDHAR6* for *pB-MDHAR6* and *pE-MDHAR6* respectively (Figure 46).

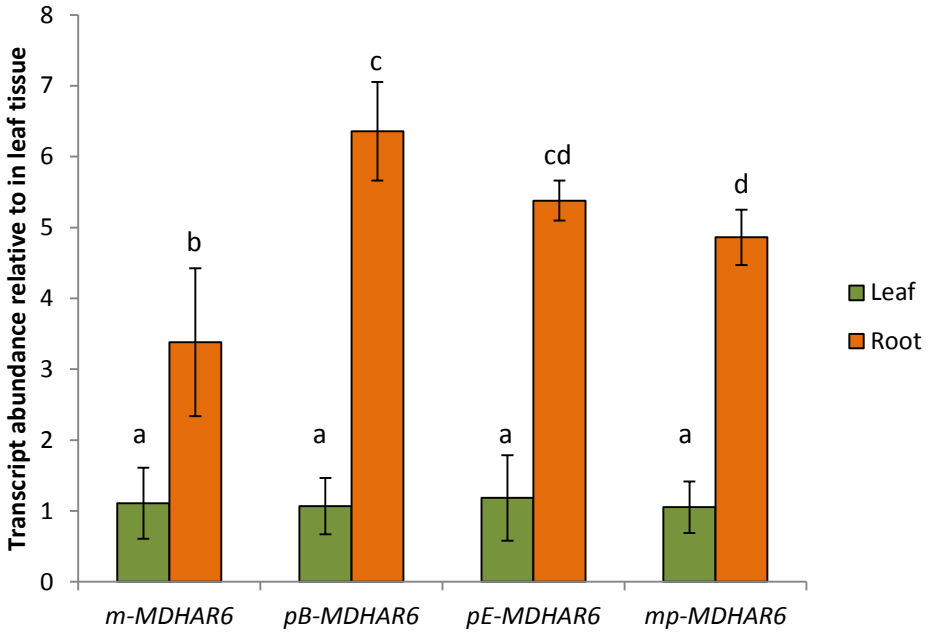

Figure 46: Expression of *m-MDHAR6* and *p-MDHAR6* in root and leaf tissue

Three-week old seedlings grown hydroponically. Mean of five biological replicates ± SD. One-way ANOVA with post hoc Tukey, P <0.05.

4.2.4 Preliminary investigation of TSS preference in response to organelle stress treatments

To investigate whether TSS preference changes with organelle demand, the effect of stress treatments which primarily target plastids or mitochondria were explored.

Finding a mitochondria- or plastid-specific stress condition is challenging, as chemicals which disrupt the function of one (usually by targeting the electron transport chain), generally also affect the function of the other. Based on the literature outlined below, the treatment of roots with 25 µM antimycin A or 50 µM TNT for 2 h, and treatment of leaves with 50 µM methyl viologen for 2 h was decided upon.

Antimycin A binds to mitochondria cytochrome c reductase, inhibiting the oxidation of ubiquinol and disrupting the proton gradient, resulting in superoxide formation (Xia et al., 1997). Schwarzländer et al. (2009) found oxygen consumption to decrease by 75 % following 2 h 20 µM antimycin A treatment, and subsequently used this treatment in a study of transcriptome responses to mitochondria dysfunction (Schwarzländer et al., 2012). Chew et al. (2003) reported *MDHAR6* induction 1 and 6 h after painting 17-day old seedling leaves with 25 µM antimycin A, supporting that transcriptional changes should be observed after 2 h 25 µM treatment. However, antimycin A-like compounds have also been found to inhibit electron transport in chloroplasts (Taira et al., 2013), and so to avoid this, roots were treated rather than leaves.

The effect of root treatment with TNT was of interest, as *mdhar6-1* complementation experiments discussed, in 3.1.1, indicate that MDHAR6 reaction with TNT could cause greater disruption within mitochondria than plastids.

Methyl viologen accepts electrons from ferredoxin of photosystem I, and transfers them to oxygen. Dalal et al. (2014) sprayed 15-day old seedlings with 50 µM methyl viologen, and measured a doubling in H_2O_2 and malondialdehyde, 2 h after treatment. Chew et al. (2003) reported induction of *MDHAR6* at 1 h but not 6 h following leaf treatment with 437.5 mg/L Paraquat with 225 mg/L Diquat (50 µM methyl viologen is 13 mg/L).

Transcript abundance of commonly used mitochondria stress marker *AOX1a* (Schwarzländer et al., 2012) and plastid stress marker *APX2* (Chang et al., 2004; Jarvis and López-Juez, 2013) following these treatments was also assessed, in order to gauge whether the treatments were having measurably stressful effects on mitochondria and/or plastids.

In this preliminary experiment, there was a high degree of variation between biological replicates, possibly due to differences in wounding during sample collection, and the low PCR

efficiency of the *APX2* primers. The only significant difference in stress marker transcript abundance (one-way ANOVA, $P < 0.05$), was an increase in *APX2* expression following leaf treatment with methyl viologen (Figure 47A). Interestingly this corresponds with a significant increase in *m-MDHAR6*, *pB-MDHAR6* and *mp-MDHAR6* (two-way ANOVA with post hoc Tukey, $P < 0.05$; Figure 47B), however overall few significant changes in transcript abundance were identified in this experiment. Transcript abundance of *pE-MDHAR6* in these samples has not yet been tested.

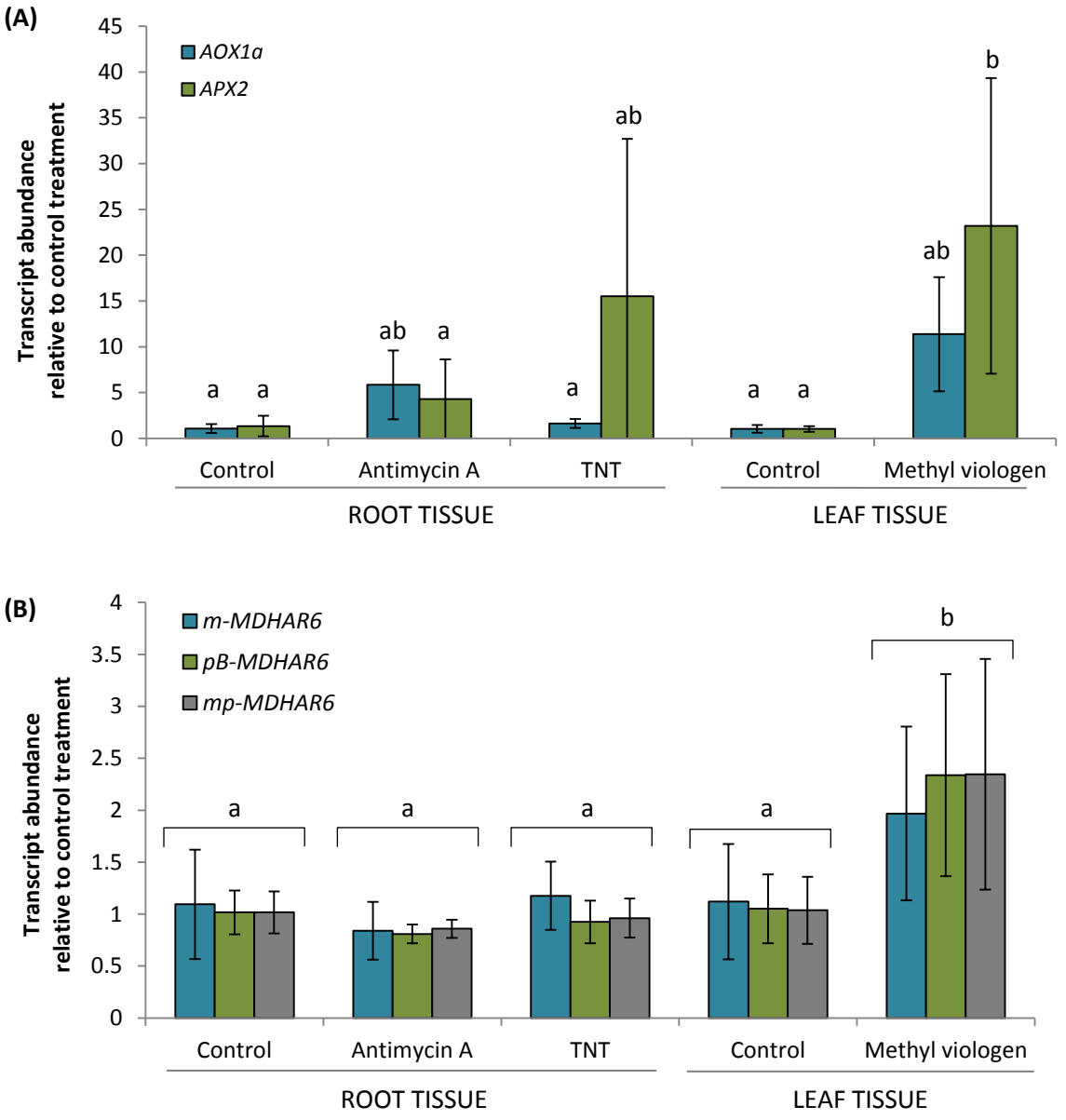

Figure 47: Preliminary organelle stress treatment experiment: induction of organelle stress markers and *MDHAR6* transcript variants following treatment with antimycin A, TNT or methyl viologen

Mean of six biological replicates ± SD. Three-week old seedlings were grown hydroponically. Roots were treated with 25 µM antimycin A, 50 µM TNT or a control treatment (0.03 % ethanol) for 2 h. Leafs were sprayed with 50 µM methyl viologen or control (water), and harvested after 2 h. (A) Induction of mitochondria stress marker *AOX1a* and chloroplast stress marker *APX2*. One-way ANOVA with post hoc Tukey, $P < 0.05$. Note, primer efficiency for *APX2* only 87.3 %. (B) Induction of *MDHAR6* transcript variants. Two-way ANOVA with post hoc Tukey, $P < 0.05$. Due to outlier removal, in (A) there are only 4 and 3 replicates of the root and leaf controls included in analysis respectively, and in (B) only 5 replicates of leaf control.

4.2.5 Anti-MDHAR6 antibody is specific to MDHAR6

An antibody was raised against purified MDHAR6, so that the location of MDHAR6 could be determined using Transmission Electron Microscopy with immuno-gold labelling. The specificity of the antibody was tested in a preliminary western blot against root extracts of Col7, Nossen, *mdhar6-1* and *mdhar6-2* (Figure 48). Labelled bands were only observed against the extracts of wild type roots, indicating that the antibody is specific to MDHAR6.

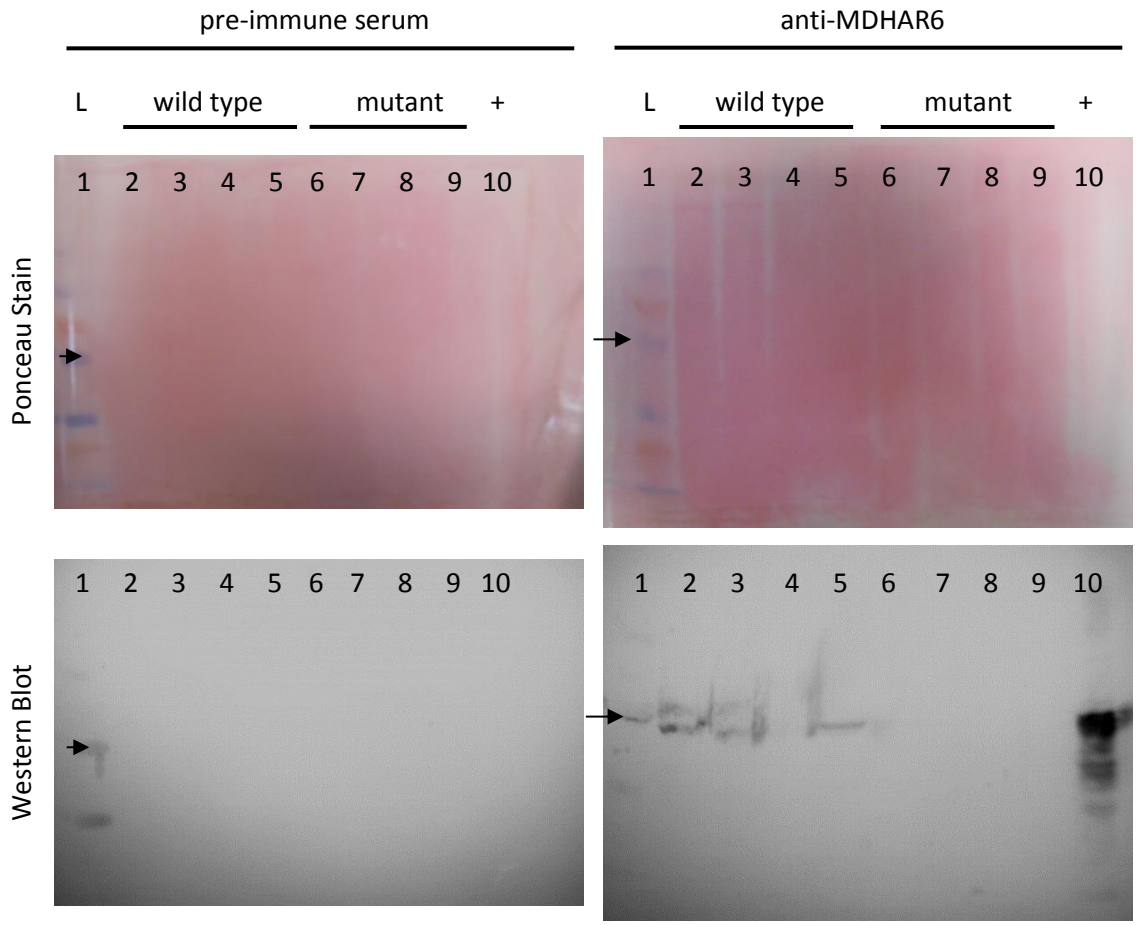

Figure 48: Western Blot of root extracts against anti-MDHAR6

Ponceau stain and western blots against MDHAR6, where pre-immune serum (control) or anti-MDHAR6 has been used as primary antibody. Lane 1, ladder (Fermentas PageRuler S26619). Lane 2, Col7 root biological replicate 1. Lane 3, Col7 root biological replicate 2. Lane 4, Nossen root biological replicate 1. Lane 5, Nossen root biological replicate 2. Lane 6, *mdhar6-1* root biological replicate 1. Lane 7, *mdhar6-1* root biological replicate 2. Lane 8, *mdhar6-2* root biological replicate 1. Lane 9, *mdhar6-2* root biological replicate 2. Lane 10, purified MDHAR6. Ten µg protein loaded per lane. Arrows indicate 55 kDa protein marker in ladder. The expressed MDHAR6 protein is 53 kDa.

4.3 DISCUSSION

4.3.1 Comparison of *MDHAR6* transcript abundance

Comparing transcript abundance relative to the endogenous control is a valid method of comparing the abundance of different transcripts, although differences in primer efficiency can affect results. The small differences between primer pair PCR efficiencies in this experiment however (Table 21), cannot account for the large (~100-fold) differences in transcript abundance presented in Figure 45. For example, compared with primer pair pB (PCR efficiency 92.0 %), pD has a higher PCR efficiency (102.7 %) than pE (94.2 %), however reports an 8-fold higher transcript abundance, while pE reports a 409-fold higher transcript abundance. The difference in transcript abundance reported by the different primers also cannot be explained by proximity to the 5' terminus, or differences in RNA secondary structure at cDNA synthesis.

The data presented in this Chapter strongly suggest that in contrast to the results presented by Obara et al. (2002), a third TSS, within the first intron of *m-MDHAR6*, is the most dominant TSS. Such a site is predicted by TAIR (Huala et al., 2001), however opposes the cap site hunting experiment result of Obara et al (2002), which indicated *m-MDHAR6* to be the dominant transcript. It is possible that the dominant MDHAR6 transcript is shorter at the 3' terminus, lacking the sequence used in nested PCR by Obara et al. (2002).

The data indicate that (i) the majority of *MDHAR6* transcripts encode the plastid-targeted variant, (ii) both plastid and mitochondria-targeted *MDHAR6* are more highly expressed in root than leaf tissue, and (iii) there is greater relative increase in abundance of transcript for plastid-targeted than mitochondria-targeted MDHAR6 in roots compared with leaves.

4.3.2 Evidence for change in TSS preference

The greater relative increase in *pB*- and *pE-MDHAR6* than *m-MDHAR6* in root tissue (compared with leaf tissue) is indicative that the TSSs or transcript stabilities are differentially regulated. Whether this is influenced by environmental conditions cannot be determined by the preliminary stress treatment experiment presented here. The stress marker qPCR results, although unreliable (due to the high variability between results, and need for testing additional stress markers), indicate that the methyl viologen treatment is inducing a stress response, corresponding with increased *MDHAR6* transcript levels, with no difference between transcript variants.

4.3.3 The role of MDHAR6 in root plastids and mitochondria

It is interesting that *MDHAR6* is more highly expressed in roots than leaves, and that transcript data implies that the majority of MDHAR6 is plastid-targeted, as it may be considered that there is greater demand for redox regulation at redox-active chloroplasts and mitochondria, than the non-photosynthetic plastids of plant roots.

In roots, proplastids develop into amyloplasts, which store starch, and elaioplasts, which store lipids (Jarvis and López-Juez, 2013). In the root cap, amyloplasts have an important role in gravitropism (Leitz et al., 2009).

As discussed in Chapter 3, *MDHAR6* is most highly expressed at night (DIURNAL; Mockler et al., 2007), when growth rates increase (Dowson-Day and Millar, 1999), and starch is broken down in leaf amyloplasts (Graf et al., 2010). The MDHAR6 enzyme could have an important role in protecting amyloplasts and elaioplasts during these processes at night.

4.3.4 Future direction of this research

Transmission Electron Microscopy with immuno-gold labelling of MDHAR6 is required to explore whether transcript abundance correlates with protein localisation; relative distribution could also be regulated by control of ribosome loading, precursor protein stability, or regulation of the protein import machinery for example. The preliminary western blot against wild type and *mdhar6* mutant plant protein extract indicates that the anti-MDHAR6 antibody is specific to MDHAR6, and can be used to determine MDHAR6 location using immuno-gold labelling.

Although MDHAR6 activity towards MDA has been demonstrated (3.2.7), the role of MDHAR6 remains elusive, as mutants are little compromised in stress tolerance (3.2.2), with unaffected ascorbate pools (3.2.3 and 3.2.4). If MDHAR6 has a pivotal role in protecting elaioplasts from lipid peroxidation, decreased stress tolerance, especially to growth on H_2O_2-supplemented agar, would be expected. This has been tested, and increased H_2O_2 sensitivity has not been observed (3.2.2). The effect of the *mdhar6* mutation on amyloplasts could be investigated further, by growing seedlings under low and high light conditions, and comparing starch granule formation. Effectiveness of gravitropism could be investigated, by rotating seedlings growing on agar plates.

The effect of organelle demand on TSS preference could also be explored further, for example by treatment of roots with a greater concentration of antimycin A, menadione or rotenone to disrupt the electron transport chain in root mitochondria, or comparing *MDHAR6* expression in tissues with different demands.

5 Exploring detoxification gene regulation in response to TNT treatment

5.1 INTRODUCTION

5.1.1 Regulation of detoxification genes in plants

As reviewed in detail in 1.5, although detoxification genes are induced to varying extents in response to numerous stimuli, the regulation of these genes, particularly in response to foreign compounds, has not been studied in great detail. A couple of prior studies have focused on regulation of the *CYP81D11* gene, and these studies have highlighted the different signalling pathways involved in responses to different stimuli; for example, Stotz et al. (2013) studied *CYP81D11* induction in response to PPA_1, OPDA and JA, and found induction in response to PPA_1 and JA, but not OPDA, to be reduced in the JA-receptor *coi1* mutant. Only induction in response to JA was reduced in the MYC2 TF mutant *jin1* however.

In this chapter, the regulation of detoxification genes in response to TNT, as an example aromatic xenobiotic and environmental pollutant, is explored. A prior study by Gandia-Herrero et al. (2008; discussed in 1.4.2) identified early TNT response detoxification genes, deemed to be most specific to the perturbation of TNT treatment. For the microarray, two-week old Arabidopsis seedlings growing in liquid culture were dosed with 60 µM TNT or a control treatment (0.06 % DMF) for 6 h. Arabidopsis OPRs, 12 P450, 15 UGT, 15 GST, 1 MT and 11 ABC transporter genes were induced over two-fold in the TNT treatment (Figure 3). The induction of these genes following 6 h 60 µM TNT treatment is the focus of this study.

5.1.2 The TNT response is very similar to that from phytoprostane treatment

The Genevestigator "Signature" tool was used to identify Arabidopsis treatments with the most similar expression profiles to TNT treatment (Hruz et al., 2008), as these might involve overlapping signalling pathways. The heatmap display of results is shown in Figure 49, with further detail and correlation values listed in Table 23.

Genes classically used in SA- and JA-signalling studies (i.e. *PR-1* and *PDF1.2*, respectively) are not induced in response to TNT (Gandia-Herrero et al., 2008), however the Signature tool indicates that there is some correlation in detoxification gene responses to SA, MeJA and TNT.

The TNT response most closely correlates with safener, antimycin A, and phytoprostane treatment. There is also correlation with ozone and hypoxia treatments.

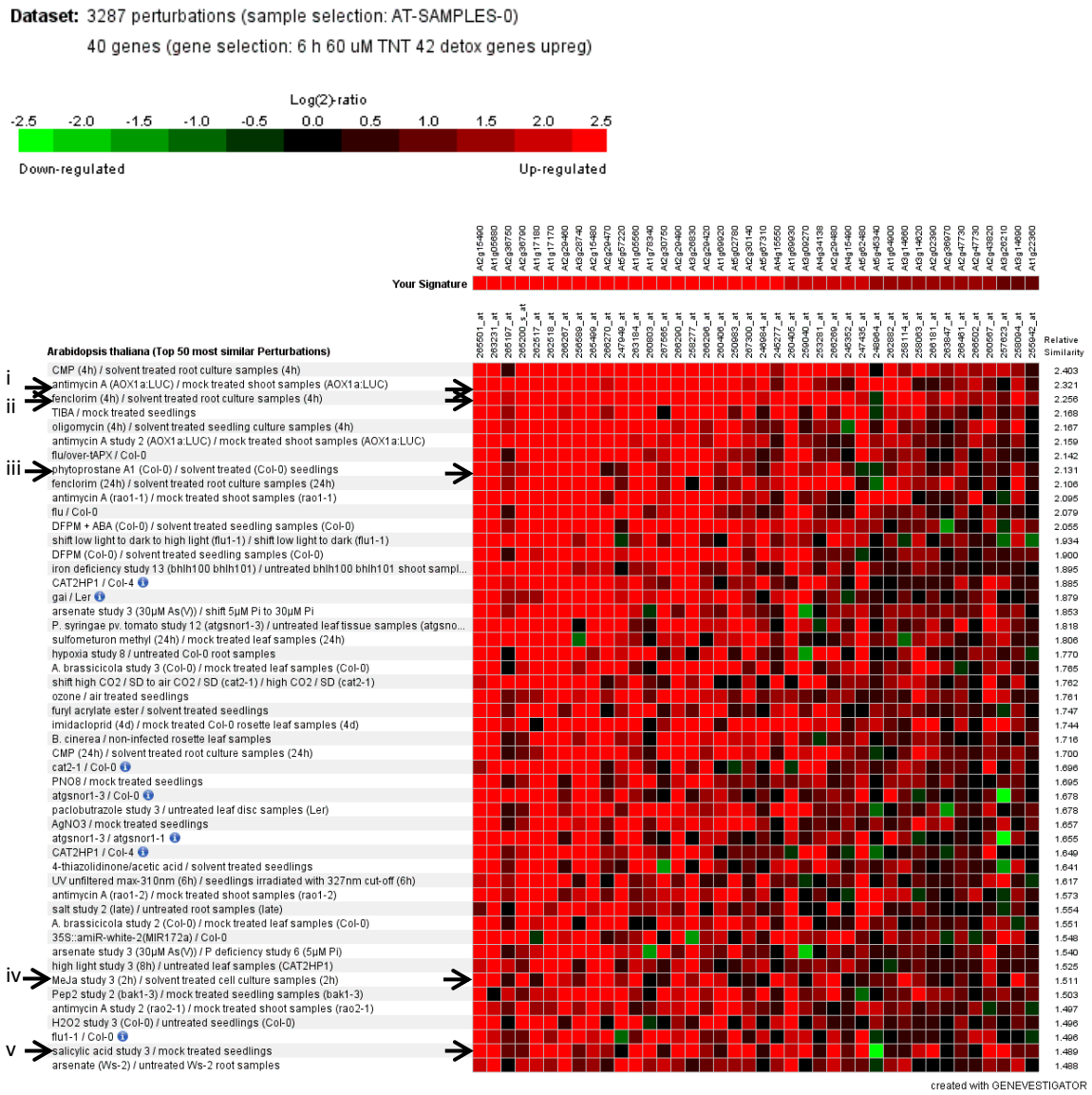

Figure 49: Detoxification gene induction profiles most closely correlating with the TNT response; heatmap of results

Genevestigator (Hruz et al., 2008) "Signature" search against the TNT-induced detoxification genes shown Figure 3 (displayed as "Your Signature" in this Figure). Search results from 7th August 2014. Perturbations highlighted with arrows; (i) antimycin A treatment of shoots, (ii) fenclorim treatment of roots, (iii) PPA_1 treatment of seedlings, (iv) MeJa treatment of cell culture and (v) SA treatment of seedlings. Further perturbation detail in Table 23.

Table 23: Detoxification gene induction profiles most closely correlating with response to TNT; experiment details

Genevestigator (Hruz et al., 2008) "Signature" search against the TNT-induced detoxification genes shown in Figure 3. Search results from 7th August 2014. A heatmap display of results is included as Figure 49.

Perturbation summary	Further information	Relative similarity score
CMP	Col0 root cell culture treated with 100 µM 4-chloro-6-methyl-2-phenylpyrimidine (CMP) in acetone for 4 h. CMP is a close derivative of the safener fenclorim.	2.403
Antimycin A	*AOX1a:LUC* shoot samples sprayed with 50 µM antimycin A and incubated for 3 h. Antimycin A inhibits complex III of the mitochondrial electron transport chain.	2.321
Fenclorim	Col0 root cell culture treated with 100 µM of the safener 4,6-dichloro-2-phenylpyrimidine (Fenclorim) in acetone for 4 h. Herbicide safeners are used to induce detoxification genes and prime crops for herbicide treatment.	2.256
TIBA	Col0 rosette leaves treated with 10 µM of the auxin inhibitor 2,3,5-triiodobenzoic acid (TIBA) for 3 h.	2.168
Oligomycin	Col0 seedlings in liquid culture dosed at 9 d with 10 µM oligomycin in ethanol for 4 h in darkness. Oligomycin is an inhibitor of ATP synthase.	2.167
Antimycin A	*AOX1a:LUC* shoot samples sprayed with 50 µM antimycin A and incubated for 3 h.	2.159
Flu OEx ascorbate peroxidase vs. Col0	Rosette leaves of *flu* mutant overexpressing ascorbate peroxidase compared with Col0. *FLU e*ncodes a chloroplast-membrane coiled-coil protein involved in chlorophyll biosynthesis. Mutants accumulate the chlorophyll intermediate protochlorophyllide in the dark, and release singlet oxygen within plastids upon dark-to-light shift.	2.142
PPA_1	Col0 samples treated with 75 µM phytoprostane A1 in 0.5% methanol for 4 h.	2.131
Fenclorim	Col0 root culture treated with 100 µM 4-chloro-6-methyl-2-phenylpyrimidine in 0.1% acetone for 24 h.	2.106
Antimycin A	*rao1-1* seedlings sprayed with 50 µM antimycin A and incubated for 3 h. The *rao1-1* mutant was derived from a screen of ethyl methanesulfonate-generated *AOX1a:LUC* mutants for mutants in *AOX1a* transcription.	2.095
Flu	Mutant rosette leaves compared with Col0.	2.079
DFPM + ABA	Col0 seedlings treated with 30 µM 5-(3,4-Dichlorophenyl)Furan-2-yl]-Piperidin-1-ylMethanethione for 30 min then 10 µM	2.055

	abscisic acid for 5.5 h. Control treated with 1:5000 v/v DMSO for 6 h. DFPM inhibits expression of ABA-induced genes.	
flu1-1 shift from low, to dark, to high light	Control not shifted to high light.	1.934
DFPM	Col0 seedlings treated with 30 µM 5-(3,4-Dichlorophenyl)Furan-2-yl]-Piperidin-1-ylMethanethione for 6 h. Control treated with 1:5,000 v/v DMSO.	1.9
Iron deficiency	*bhlh100 bhlh101* double mutant grown for 10 days on agar plates without FeEDTA. Control supplemented with 100 µM FeEDTA. The mutations are in iron-regulated transcription factors which are hypersensitive to iron deficiency, accumulating less iron and chlorophyll than wild type.	1.895
Catalase deficient + high light	Leaves of six-week old catalase-deficient *cat2* mutant plants exposed to 8 h high light irradiation compared with leaves from Col4 plants exposed to 8 h high light irradiation.	1.885
Gibberellic acid insensitive	Leaf samples from five-week old gibberellic acid-insensitive *gai* mutants compared with Ler.	1.879
Arsenate	Col0 seedlings transferred to liquid medium containing 30 µM arsenate for 8 h.	1.853
atgsnor1-3 P. syringae pv. tomato	Leaf samples from *atgsnor1-3* mutants treated with *Pseudomonas syringae pv. tomato* avirulent strain DC3000 avrB for 6h, compared with non-treated. The mutant has a T-DNA insertion within the *S-nitrosoglutathione reductase* gene; involved in *R* gene-mediated defence, basal and non-host disease resistance. Mutant shows 21% of the S-nitrosoglutathione reductase activity compared to Col-0 wild type.	1.818
Sulfometuron methyl	Col0 sprayed with the herbicide Oust™ (active ingredient sulfometuron methyl) with 0.25% surfactant Preference™. Control sprayed with 0.25% Preference™.	1.806
Hypoxia	Col0 plants moved to anaerobic cannisters, flushed with 0.1% O_2 and sealed for 5 h, compared with unsealed cannisters.	1.77
A. brassicocola	Droplets of *Alternaria brassicicola* spore suspension placed on Col0 leaf for 24 h. Control treated with droplets of water.	1.765
Shift high CO_2/SD to air CO_2/SD	Leaves from *cat2-1* mutant grown in high CO_2 concentration moved to ambient CO_2 concentration for 2 days, compared with not moved. *CAT2* is a catalase which metabolises H_2O_2 produced during photorespiration.	1.762
Ozone	Fumigation with 500 ppb ozone for 6 h, compared with fumigation with scrubbed air.	1.761

Furyl acrylate ester	10 uM furyl acrylate ester treatment for 1 h. Furyl acrylate ester is an auxin signalling inhibitor.	1.747
Imidacloprid	Col0 treated with soil application of 4 mM imidacloprid and sampled after 4 d. Imidacloprid is a neonicotinoid insecticide.	1.744
B. cinerea	Exposed to germinated *Botrytis cinerea* spores for 3 h.	1.716
CMP	Col0 root culture samples treated with 100 uM 4-chloro-6-methyl-2-phenylpyrimidine (CMP) in acetone for 24 h.	1.7
cat2-1 vs. Col0 high to low CO_2	Leaf samples from *cat2-1* mutants grown in high CO_2 concentration then moved to ambient CO_2 concentration for 2 days, compared with Col0 given the same treatment.	1.696
PNO8	N-octyl-3-nitro-2,4,6-trihydroxybenzamide (PNO8) treatment for 3 h. PNO8 is a photosystem II inhibitor.	1.695
atgsnor1-3 vs. Col0 *P. syringae* treatment	Leaf tissue from 4 week old *atgsnor1-3* treated with *Pseudomonas syringae* strain DC3000 avrB for 6 h compared with Col0 treated the same.	1.678
Paclobutrazole	Ler leaf discs treated with paclobutrazol compared with non-treated. Paclobutrazol is an antagonist of gibberellin.	1.678
$AgNO_3$	10 µM $AgNO_3$ treatment for 3 h. $AgNO_3$ is an ethylene inhibitor.	1.657
atgsnor1-3 vs. *atgsnor1-* *P. syringae* treatment	Leaf tissue from *atgsnor1-3* treated with *P. syringae* strain DC3000 avrB for 6 h, compared with *atgsnor1-1* treated with *P. syringae* strain DC3000 avrB for 6 h.	1.655
CAT2HP1 vs. Col4 high light	Leaf samples from CAT2HP1 vs. Col4 plants exposed to high light irradiation for 3 h.	1.649
4-thiazolidinone	10 µM 4-thiazolidinone for 1 h. 4-thiazolidinone is an auxin signalling inhibitor.	1.641
UV	Ws seedling samples taken 6 h after the seedlings were treated with UV-B irradiation for 15 min.	1.617
Antimycin A	*rao1-2* shoots treated with 50 µM Antimycin A for 3 h.	1.573
Salt study	Col0 seedlings grown hydroponically. Media treated with 150 mM NaCl.	1.554
A. brassicola	Col0 leaves incoculated with *A. brassicicola* spores for 9 h.	1.551
35S::amiR-white-2 (MIR172a)	Constitutive overexpressor of *amiR-white-2* compared with Col0.	1.548
Arsenate	Seedlings in liquid culture treated with 30 µM arsenate for 8 h.	1.54
High light	Leaf samples from CAT2HP1 plants exposed to HL irradiation for 8 h.	1.525
MeJa	Cell suspension treated with 50 µM MeJA for 2 h.	1.511
Pep2 treatment in	*Bak1-3* seedlings in liquid culture treated with 1 µM Pep2 for 10 h. Control *bak1-3* not treated with Pep2.	1.503

bak1-3	Pep2 is an Arabidopsis DAMP. BAK1 is a Leucine-Rich Repeat Receptor Like Kinase.	
Antimycin A	*Rao1-2* shoots treated with 50 µM antimycin A for 3 h. Control treated with water.	1.497
H_2O_2	Col0 seedlings treated with 20 mM H_2O_2 for 1 h.	1.496
Flu	Shoot samples of 12 d old *flu1-1* compared with Col0.	1.496
Salicylic acid	Col0 treated with 2 mM SA for one day.	1.489
Arsenate	Root samples of Ws-2 seedlings treated with 100 µM arsenate for 1.5 and 3 h.	1.488

5.1.3 Hypothesis for phytoprostane and class II TGA factor involvement in TNT-response detoxification gene induction

Considering that (i) results discussed in Chapter 3 indicate that TNT phytotoxicity is caused by MDHAR6-mediated superoxide generation (Johnston et al., 2015), (ii) phytoprostanes are induced following oxidative treatment (Imbusch and Mueller, 2000; Thoma et al., 2003; Grun et al., 2007), (iii) phytoprostane application has been found to induce detoxification gene expression, class II TGA factor-dependently (Mueller et al., 2008), and (iv) the induction profile following TNT treatment closely matches that of phytoprostane treatment, it was hypothesised that in response to TNT, phytoprostanes accumulate, and induce detoxification genes, class II TGA factor-dependently.

To test this hypothesis, the following mutants were sourced; (i) the class II TGA factor triple mutant *tga2 tga5 tga6*, (Zhang et al., 2003), (ii) the triple mutant *fatty acid desaturase (fad)3-2 fad7-2 fad8* (McConn and Browse, 1996), and (iii) *allene oxide synthase* (*aos*) (Park et al., 2002). The *fad3-2 fad7-2 fad8* mutant has negligible levels of linolenic acid (McConn and Browse, 1996), so should not accumulate phytoprostanes, OPDA or JA. The AOS enzyme catalyses the conversion of 13(*s*)-hydroperoxy-octadecatrienoic acid to (13*S*)-12,13-epoxy-octadecatrienoic acid in the JA biosynthesis pathway (Wasternack and Hause, 2013), and so the *aos* mutant can accumulate phytoprostanes, but not OPDA or JA. The hypothesis above would be supported if the response is abolished in *mdhar6-1*, *fad3-2 fad7-2 fad8* and *tga2 tga5 tga6* mutants, but maintained in *aos* mutant seedlings.

5.2 RESULTS

5.2.1 The TNT response requires class II TGA factors

Repeating the TNT treatment conditions used by Gandia-Herrero et al. (2008; see 2.1.2), two-week old Col0 and *tga2 tga5 tga6* seedlings, grown in liquid culture, were treated with 60 µM TNT or a control treatment for 6 h. Abundance of detoxification gene transcripts, and fold induction in response to TNT, are shown in Figure 50.

In the control treatment, abundance of transcript for two genes is significantly higher in *tga2 tga5 tga6* (Students t test $P < 0.05$; *CYP81D8*, *OPR3*), while abundance of transcript for three genes is significantly lower (*GSTU25, GSTU24, OPR2*).

In response to TNT treatment, fold induction of all transcripts is lower in *tga2 tga5 tga6* than in Col0. The frequency of TGACG, the TGA factor binding motif, in the promoters of the genes studied is shown in Figure 51.

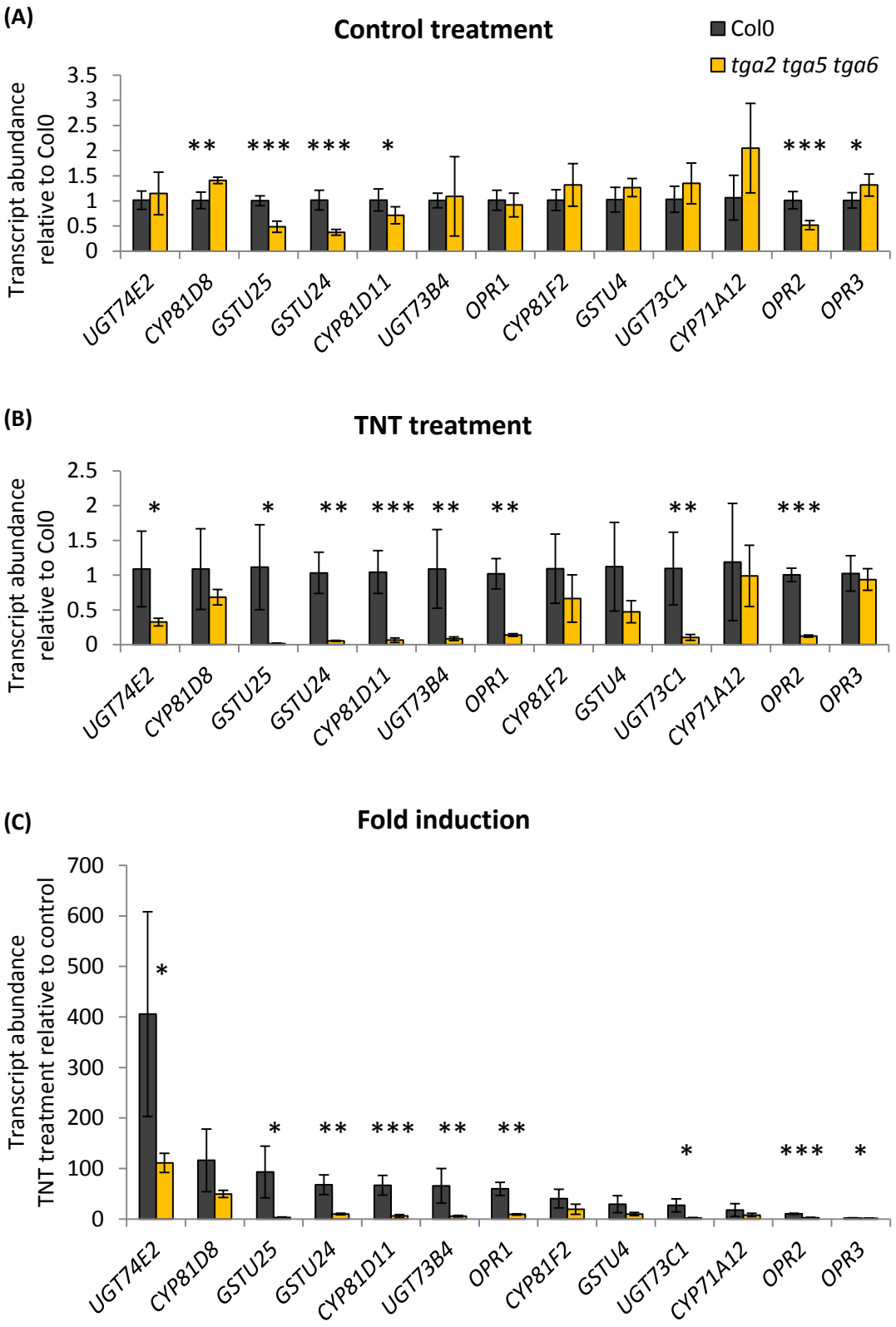

Figure 50: Col0 vs. *tga2 tga5 tga6* TNT response detoxification gene induction

Transcript abundance in (A) control and (B) TNT treatment (6 h 60 µM TNT) compared with transcript abundance in Col0. (C) Fold increase in transcript abundance in TNT treatment compared with control treatment. Mean of five biological replicates ± SD. Student's t test; * P<0.05, ** P<0.01, *** P<0.001.

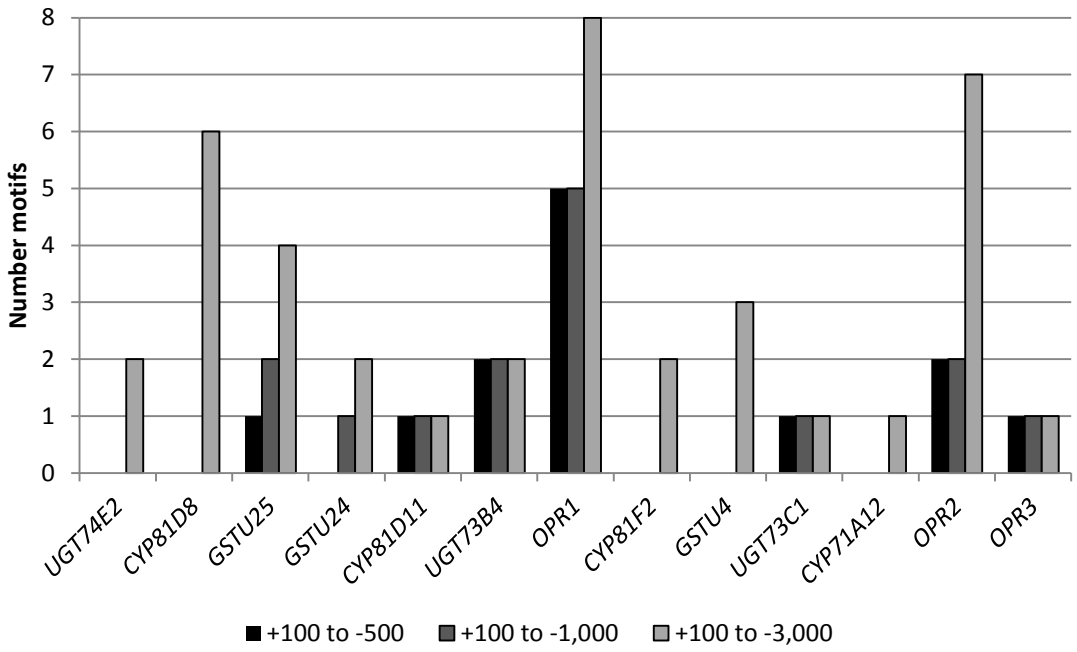

Figure 51: Frequency of the TGACG motif in TNT-response detoxification genes

Frequency of TGACG motifs in forward or reverse orientation. Promoter range indicated in legend; bp following (+) or prior (-) to the gene start ATG.

5.2.2 Mutants in class II TGA factors are compromised in TNT tolerance to a small extent

As there is interest in engineering plants for the remediation of explosives, the effect of the *tga2 tga5 tga6* mutation, and lower transcript abundance for enzymes with putative involvement in TNT detoxification, was assessed.

Seven-day old *tga2 tga5 tga6* seedlings had shorter roots than Col0 when germinated on 2 and 7 µM TNT ½ MS(A), but not on 15 µM TNT (Figure 52). In soil, no significant difference in seedling FW in the presence of TNT was observed (Student's t test, P <0.05; Figure 53).

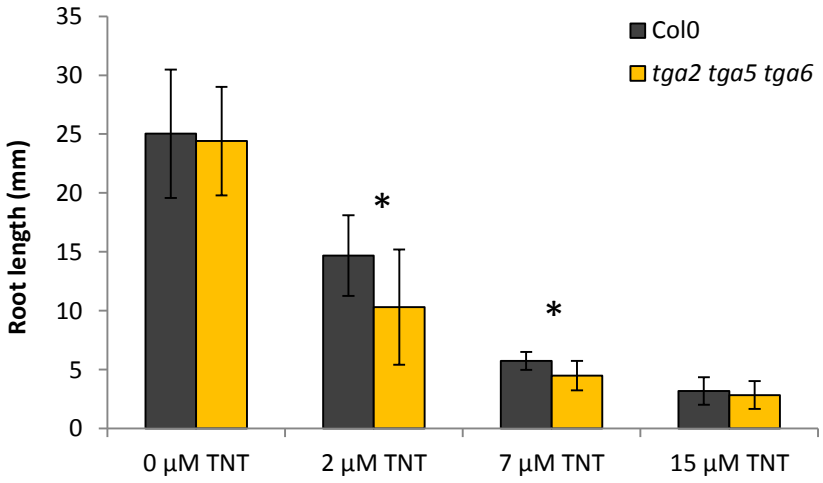

Figure 52: Root lengths of 7-d old Col0 and *tga2 tga5 tga6* seedlings on TNT-treated agar
Mean of 10 replicates ± SD. Student's t test * P<0.05, ** P<0.01, *** P<0.001.

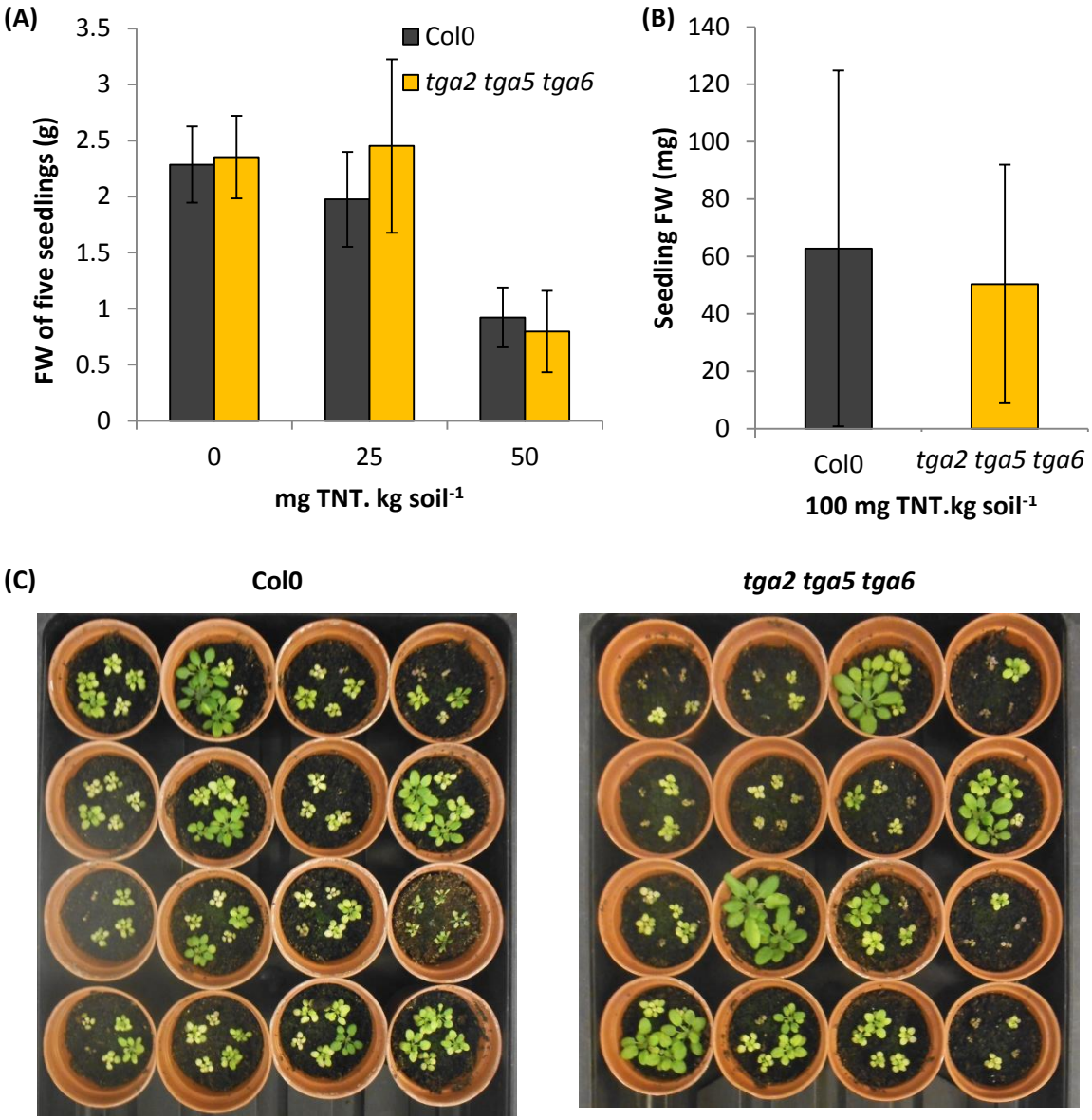

Figure 53: Biomass of Col0 and *tga2 tga5 tga6* seedlings grown on TNT-treated soil for five weeks

Five-day old seedlings were transferred to pots of 0 or 100 mg TNT.kg soil^{-1} (five seedlings per pot), and grown to six weeks of age. Mean fresh weights of six-week old seedlings. (A) Fresh weight of all five seedlings in pot (eight biological replicates ± SD). (B) Fresh weight of individual seedlings (40 biological replicates ± SD). (C) Six-week old Col0 and *tga2 tga5 tga6* seedlings on 100 mg TNT.kg soil^{-1}.

5.2.3 The TNT response does not require oxylipins

The qPCR results for the *fad3-2 fad7-2 fad8* mutant are shown in Figure 54, and for the *aos* mutant in Figure 55.

Following TNT treatment, transcript abundance of four genes (*CYP81D11, UGT73B4, CYP81F2* and *GSTU4*) is significantly lower in *fad3-2 fad7-2 fad8* (Students t test, $P < 0.05$), however when fold induction is compared between Col0 and *fad3-2 fad7-2 fad8*, only the fold induction of *CYP81F2* is significantly lower in *fad3-2 fad7-2 fad8*.

The qPCR results involving the *aos* mutant were highly variable. An increase in the fold induction of *CYP81F2*, *GSTU4* and *CYP71A12* in *aos* is indicated, however due to the variability in results between biological replicates, this is not a reliable result.

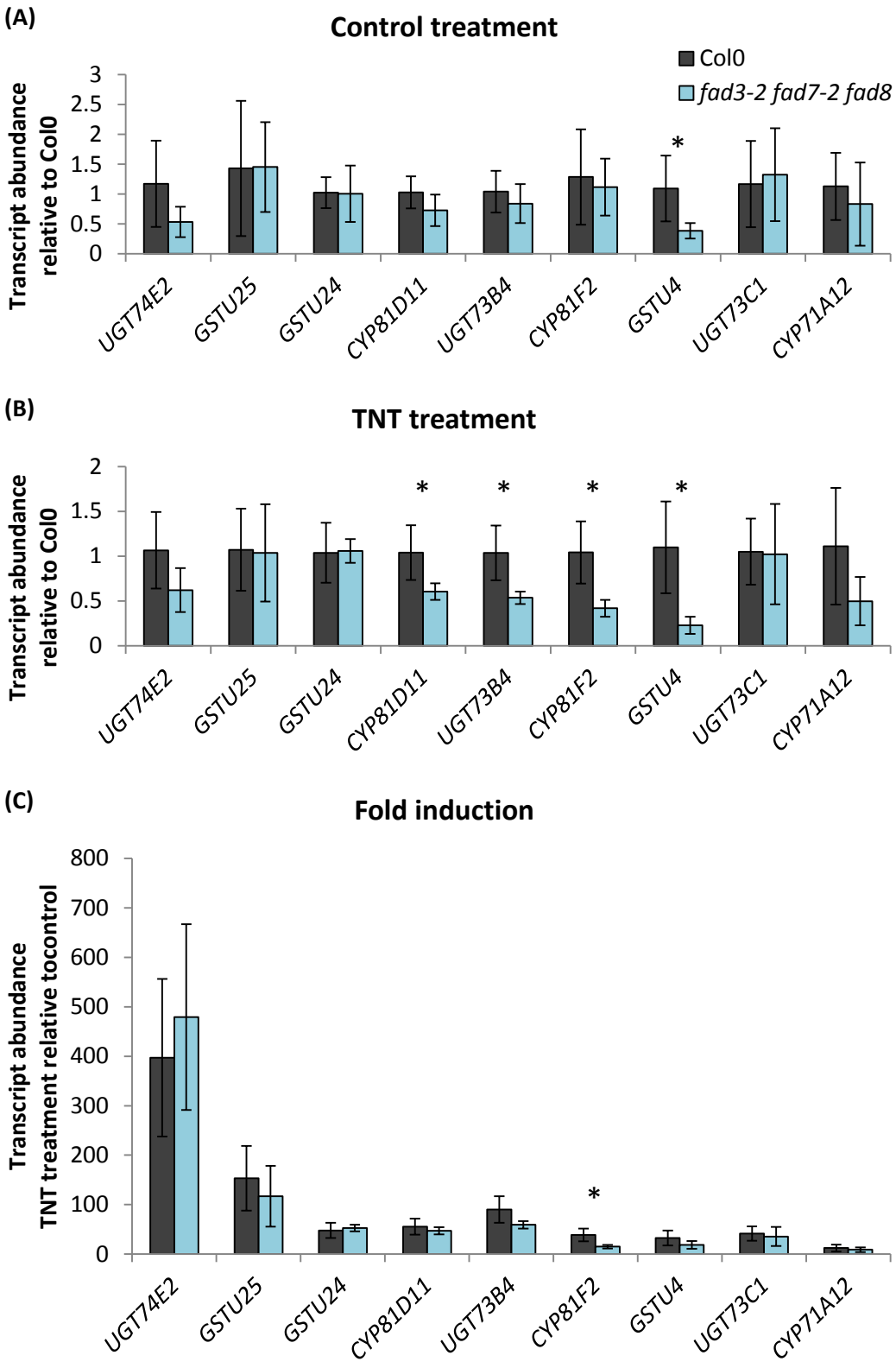

Figure 54: Col0 vs. *fad3-2 fad7-2 fad8* TNT response detoxification gene induction

Transcript abundance in (A) control and (B) TNT treatment (6 h 60 µM TNT) compared with transcript abundance in Col0. (C) Fold increase in transcript abundance in TNT treatment compared with control treatment. Mean of five biological replicates (two technical replicates of each) ± SD. Student's t test; * P<0.05, ** P<0.01, *** P<0.001.

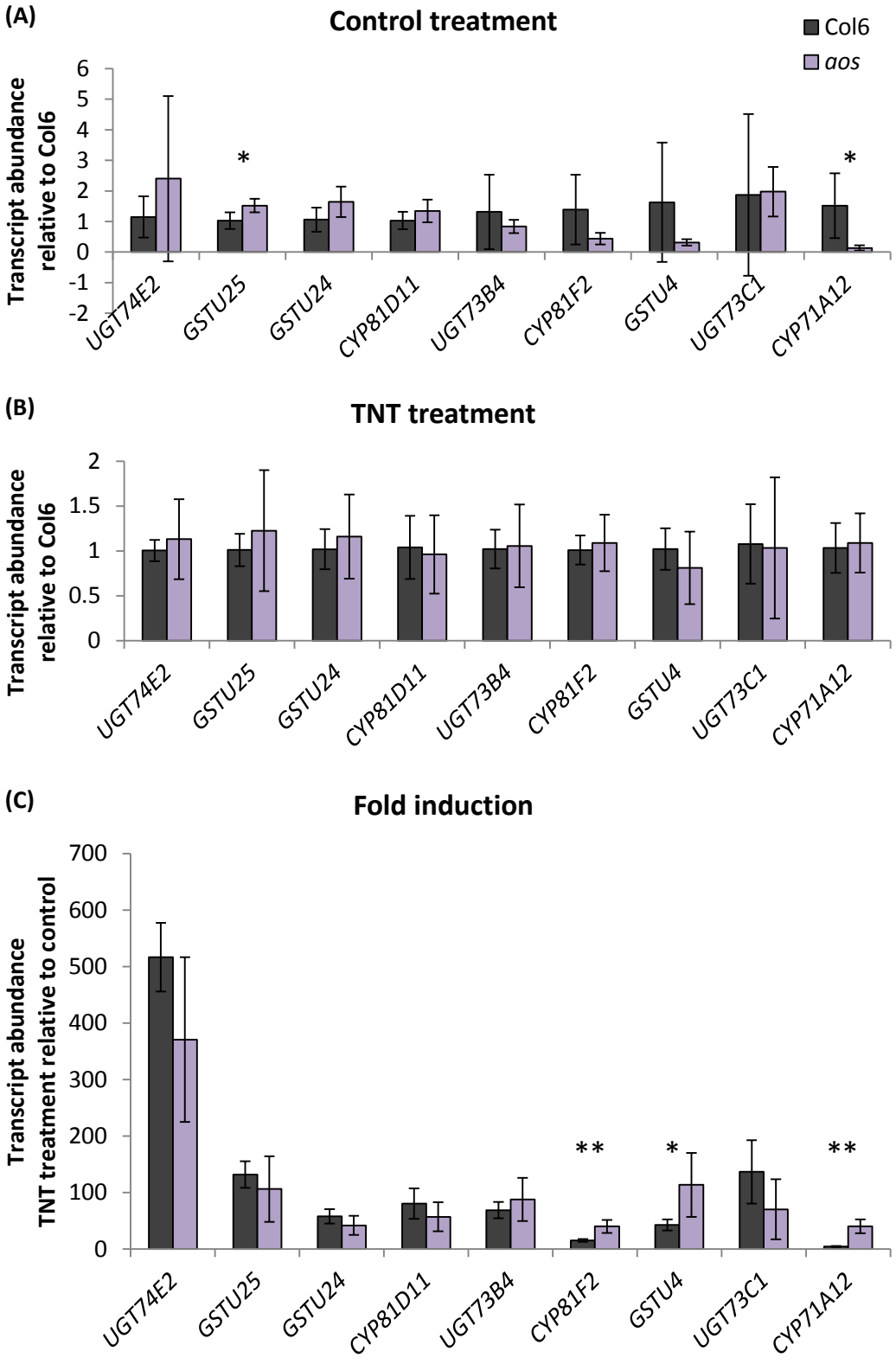

Figure 55: Col6 vs. *aos* TNT response detoxification gene induction

Transcript abundance in (A) control and (B) TNT treatment (6 h 60 µM TNT) compared with transcript abundance in Col0. (C) Fold increase in transcript abundance in TNT treatment compared with control treatment. Mean of five biological replicates ± SD. Student's t test; * P<0.05, ** P<0.01, *** P<0.001.

5.2.4 The TNT response does not require MDHAR6

Considering that MDHAR6 appears to be the main cause of increased oxidative state in the presence of TNT (Chapter 3), the effect of the *mdhar6-1* mutation on TNT-response detoxification gene induction was investigated (Figure 56). The abundance of the *GSTU25* transcript was significantly higher in *mdhar6-1* compared with Col7, in the presence of TNT (Student's t test, $P<0.05$), however there were no further significant differences.

5.2.5 Summary of TNT response in different mutants

A summary of the qPCR results discussed in this Chapter is included in Table 24. These indicate that while class II TGA factors are required for the induction of the majority of TNT-response detoxification genes tested, the induction does not appear to require oxylipins, or MDHAR6.

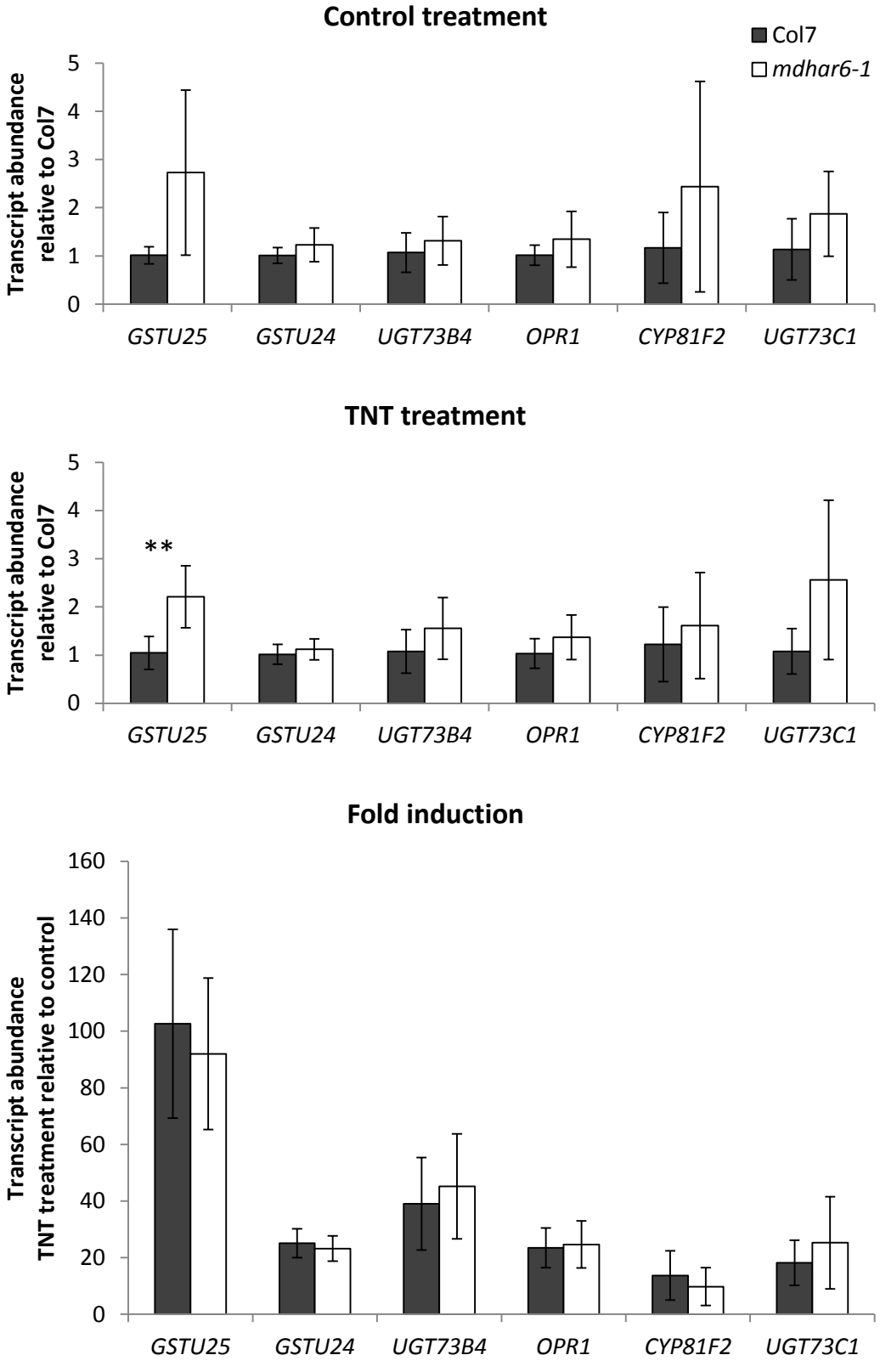

Figure 56: Col7 vs. *mdhar6-1* TNT response detoxification gene induction

Transcript abundance in (A) control and (B) TNT treatment (6 h 60 µM TNT) compared with transcript abundance in Col0. (C) Fold increase in transcript abundance in TNT treatment compared with control treatment. Mean of five biological replicates ± SD. Student's t test; * P<0.05, ** P<0.01, *** P<0.001.

Table 24: Comparison of detoxification gene transcript level and fold induction in mutants relative to wild type, in TNT-response experiments

Transcript abundance or fold induction following TNT treatment for the four mutants tested, relative to their wild type backgrounds. Results are colour-coded: red; reduction in transcript abundance/induction. Green; increase in transcript abundance/induction. Blank; not tested. Emboldened numbers; significant difference between mutant and wild type (Student's t test, P <0.05).

	Transcript abundance in control treatment				**Transcript abundance in TNT treatment**				**Fold induction**			
	tga2 tga5 tga6	*fad3-2 fad7-2 fad8*	*aos*	*mdhar 6-1*	*tga2 tga5 tga6*	*fad3-2 fad7-2 fad8*	*aos*	*mdhar 6-1*	*tga2 tga5 tga6*	*fad3-2 fad7-2 fad8*	*aos*	*mdhar 6-1*
UGT74E2	1.15	0.53	2.40		**0.32**	0.62	1.13		**0.27**	1.21	0.72	
CYP81D8	**1.41**				0.68				0.43			
GSTU25	**0.49**	1.45	**1.52**	2.73	**0.02**	1.04	1.23	**2.21**	**0.03**	0.76	0.80	0.90
GSTU24	**0.37**	1.01	1.65	1.23	**0.05**	1.06	1.16	1.12	**0.14**	1.10	0.72	0.92
CYP81D11	**0.71**	0.73	1.35		**0.06**	**0.61**	0.96		**0.09**	0.85	0.71	
UGT73B4	1.09	0.84	0.83	1.32	**0.08**	**0.54**	1.06	1.55	**0.08**	0.66	1.28	1.16
OPR1	0.92			1.35	**0.14**			1.37	**0.15**			1.05
CYP81F2	1.32	1.12	0.44	2.44	0.66	**0.42**	1.09	1.61	0.48	**0.39**	**2.66**	0.71
GSTU4	1.27	**0.38**	0.31	1.87	0.47	**0.23**	0.81	2.56	0.34	0.57	**2.66**	1.39
UGT73C1	1.35	1.32	1.97		**0.10**	1.02	1.03		**0.07**	0.86	0.51	
CYP71A12	2.05	0.83	**0.13**		0.99	0.50	1.09		0.44	0.73	**9.23**	
OPR2	**0.52**				**0.12**				**0.24**			
OPR3	**1.32**				0.94				**0.70**			

5.2.6 Generation of promoter-reporter Arabidopsis lines

At the beginning of this investigation, three TNT-response detoxification gene promoters were cloned and constructed adjacent to the *β-GLUCURONIDASE* (*GUS*) reporter gene. The aim was to verify the TNT-responsiveness of the promoter regions, before use in yeast one hybrid assays, to identify interacting proteins. The promoter-reporter constructs in Figure 57 have been stably transformed into Arabidopsis, but have not yet been tested for TNT-responsiveness.

The *UGT73C1* promoter was chosen as it is induced by a smaller number of perturbations than other detoxification genes induced by TNT (Figure 49, third column from left), suggesting that it could be regulated by a signalling pathway more specific to the stress of TNT treatment.

The two most TNT-responsive *GST*s, *GSTU24* and *GSTU25*, have similar expression profiles, however *GSTU25* is not induced by biotic stress treatment, and so was chosen for this study.

The most TNT-responsive *P450*s have similar expression profiles, however regulation of the second most TNT-responsive *P450*, *CYP81F2*, was chosen as regulation of this gene may be of wider interest; *CYP81F2* is involved in the biosynthesis of 4-methoxy-indole-3-ylmethyl-glucosinolate (4MI3G), which induces callose deposition in response to the inducer of basal defense Flg22. While the induction of other 4MI3G-biosynthesis genes in response to Flg22 is dependent on ethylene signalling and the TF MYB51, Flg22-mediated induction of *CYP81F2* is ethylene and MYB51-independent (Bednarek et al., 2009; Clay et al., 2009).

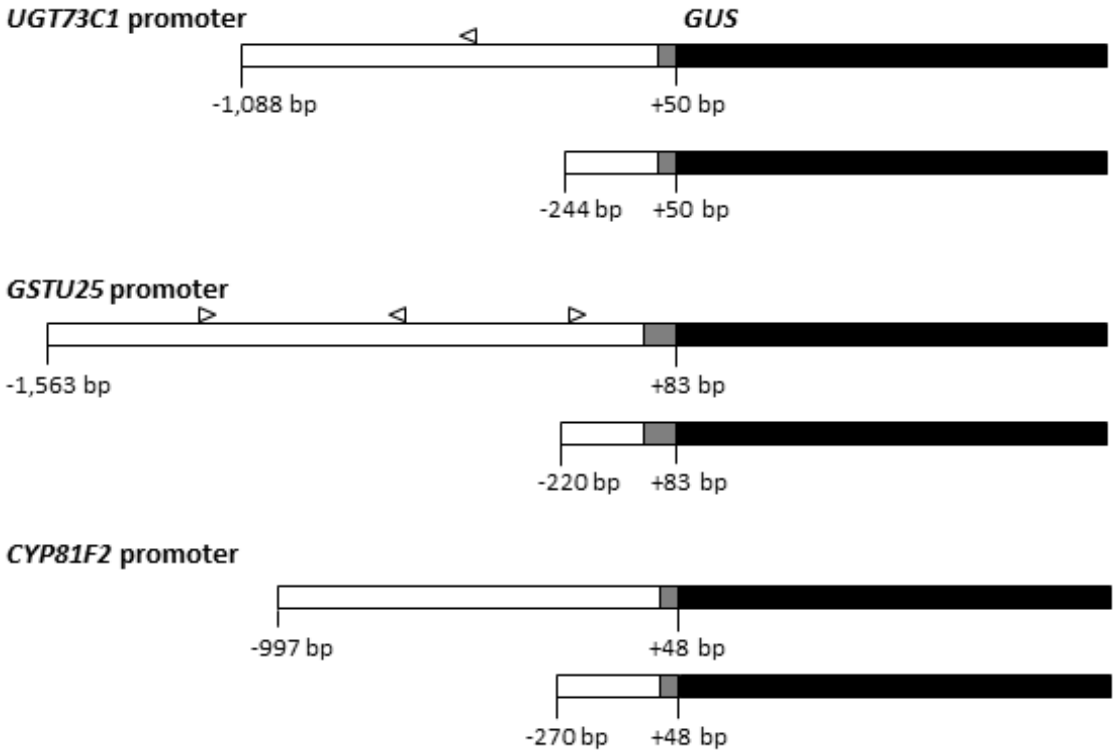

Figure 57: Promoter-reporter constructs

Black bar; *GUS* gene. Grey bar; translated region of gene. White bar; promoter region. Promoter range indicated as bp following (+) or prior (-) to gene start ATG. Arrows indicate locations of TGACG motifs in forward (▷) or reverse (◁) orientation.

5.2.7 There is an increase in glutathione following TNT treatment

As discussed in 1.5.2, various reports point to glutathione accumulation having a signalling role (Ball et al., 2004; Gomez et al., 2004; Senda and Ogawa, 2004; Li et al., 2013; Cheng et al., 2015), including in OPDA signalling; induction of OPDA response genes *GRX480*, *CYP81D11*, *GSTF8*, *GSTU19* and *HSP17.6*, is reduced in *cyclophilin 20-3* mutants, in which glutathione accumulation following OPDA treatment is abolished (Park et al., 2013).

There is a doubling in glutathione content in response to 6 h 60 µM TNT treatment, in both Col7 and *mdhar6-1*. This is statistically significant (Student's t test, P <0.05; Figure 58).

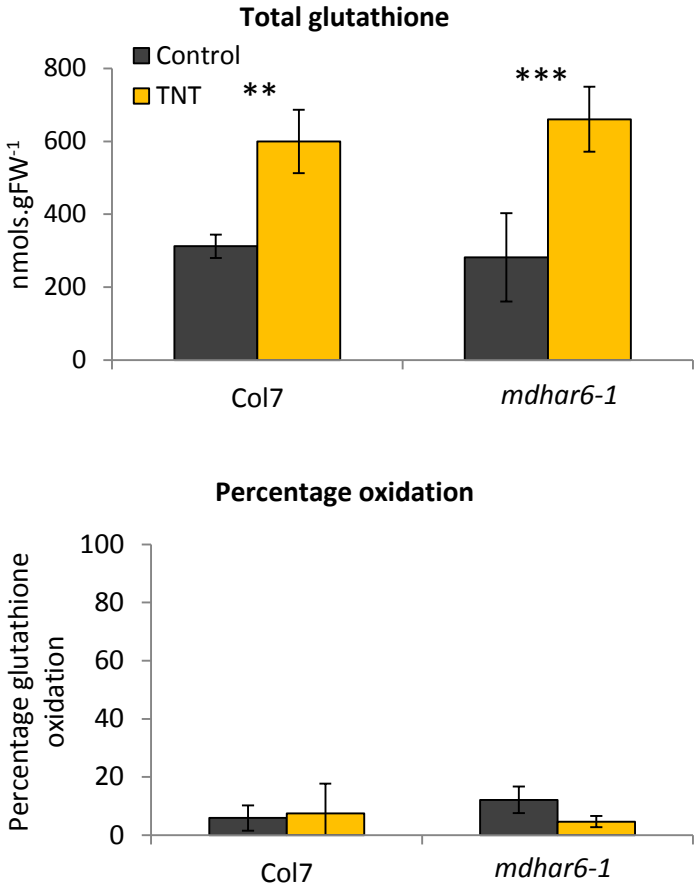

Figure 58: Changes in glutathione content in response to TNT treatment

Two-week old seedlings grown in ½ MS 20 mM sucrose, were treated with 60 µM TNT in DMF (end 0.06% v/v DMF) or DMF alone for 6 h. Mean of six biological replicates ± SD. Student's t test * P<0.05, ** P<0.01, *** P<0.001.

5.3 DISCUSSION

5.3.1 The small change in TNT tolerance in *tga2 tga5 tga6* mutants

It is surprising, considering the involvement of the target genes (OPR1 and 2, UGT73B7, 74E2, 41C1, 73C1, 73C6, 73B2 and 73B5, and GSTU25 and U24) in TNT detoxification, indicated by both enzymatic analysis and overexpression studies (Gandia-Herrero et al., 2008; Beynon et al., 2009; Gunning et al., 2014), that when expression of the corresponding genes is reduced, TNT tolerance is not compromised to a larger extent. Expression of these genes is not completely abolished however, and it is possible that functional redundancy with other enzymes mitigates the TNT toxicity; for example, *OPR3* transcript levels are unaffected in *tga2 tga5 tga6*, and OPR3 is known to reduce TNT to HADNT *in vitro* (Beynon et al., 2009).

5.3.2 Lack of requirement for MDHAR6 or phytoprostanes in the TNT response

In the presence of TNT, the transcript abundance of *CYP81D11*, *CYP81F2*, *UGT73B4* and *GSTU4* are significantly lower in *fad3-2 fad7-2 fad8* than in wild type, however when fold induction between control and TNT treatment is compared, there is no longer a significant difference between *fad3-2 fad7-2 fad8* and wild type, for all genes but *CYP81F2*. It is possible that *CYP81F2* is induced by a pathway responsive to accumulating phytoprostane levels. Additional biological replicates are required for confidence in conclusions from this experiment.

The fold induction was also unaffected in *mdhar6-1* mutants. This was unexpected, as considering the results presented in Chapter 3, less ROS might be anticipated in *mdhar6-1* compared with Col7 following TNT treatment, which would be expected to have an impact on the transcriptome. It is possible that at this early time point however, there is no difference in ROS between Col7 and *mdhar6-1*; the other MDHAR enzymes could similarly reduce TNT by one electron, and considering the relatively high K_m and low V_{max} of the reaction of MDHAR6 with TNT (522 µM and 0.143 $mmol^{-1}.min^{-1}.mg^{-1}$, respectively), and low concentration of TNT treatment (60 µM), few moles of TNT may be reduced by one electron within the 6 h treatment. Notably, this is also a very different experimental system to TNT treatment on soil or on agar; *mdhar6-1* seedlings are less tolerant to growth in liquid (hypoxic) media, and have 76 % less biomass at two-weeks of age (3.2.2). It would be of interest to clarify where there is a significant difference in ROS between the TNT and control treatment, and between Col7 and in *mdhar6-1*, using a ROS probe such as Amplex Red. Whether ROS have a role in the detoxification genes induction could be investigated by prior treatment with antioxidants such as DMTU or BHA, similar to as carried out by Garretón et al. (2002).

5.3.3 The importance of the increase in glutathione in response to TNT

As discussed in 1.5.2, numerous studies indicate a role of glutathione in defence signalling, and this study has identified a doubling in Arabidopsis glutathione content following TNT treatment (Figure 58). Of the 19 GSH-response genes found not to be induced in *glutamate receptor-like channel 3.3* mutants by Li et al. (2013), nine are also induced by TNT treatment (Gandia-Herrero et al., 2008).

The TNT-response microarray experiment reported by Gandia-Herrero et al. (2008) did not identify induction of *GSH1* (γ-glutamylcysteine synthetase) or *GSH2* (glutathione synthetase) following TNT treatment, however did identify induction of the cysteine biosynthesis genes *APR3* (adenosine 5'phosphosulphate reductase; 6-fold induction) and *SAT2.1* (serine acetyltransferase; 5-fold induction).

It would be of interest to investigate whether the increased glutathione levels in the presence of TNT are having a causative effect on the induction of detoxification genes. This could be explored by investigating whether prior treatment with BSO results in reduced detoxification gene expression in the presence of TNT. That being said, there is a similar pattern in detoxification gene induction between SA and JA, and while SA treatment results in an increase in glutathione content, JA treatment results in a decrease in glutathione content (Spoel and Loake, 2011). This argues against a role for glutathione in the regulation of these detoxification genes.

5.3.4 The involvement of class II TGA factors in mediating the TNT response

It is clear that class II TGA factors have an important role in the induction of defence and detoxification genes, following treatment with a broad range of stimuli (Table 8), including, as demonstrated by this research, TNT treatment. With regards to JA-signalling, this appears to be via regulation of a master transcriptional regulator (Zander et al., 2010, 2014), rather than via direct interaction at the *PDF1.2* promoter. It is notable that of the TNT-response detoxification genes, those with TGACG motifs most proximal to the start ATG are most reduced in transcript abundance by the *tga2 tga5 tga6* mutations (Figure 51, Table 24), which could suggest that TGA factors have a direct role at these gene promoters. That being said, *UGT74E2* and *CYP81D8* are the most TNT-induced genes, but have distal TGACG motifs. The effect of mutating TGACG motifs in the promoters of promoter-reporter constructs (Figure 57) can be used to establish whether these TFs regulate expression through direct interaction at the gene promoters.

It is also notable that transcript abundance of four genes (*GSTU25*, *GSTU24*, *CYP81D11* and *OPR2*) is reduced in *tga2 tga5 tga6* in the control treatment; this indicates that class II TGA factors are involved in the positive basal regulation of these genes, while Kesarwani et al. (2007) report basal expression of *PR-1* to be higher in *tga2 tga5 tga6* mutants. The class II TGA factors are therefore not always co-repressors as well as co-activators. Chromatin immunoprecipitation experiments could be used to investigate whether TGA factors are recruited to detoxification gene promoters upon TNT treatment.

The NPR1 and SCL14 proteins have already been demonstrated to interact with class II TGA factors, and are candidates for other proteins required in the TNT response. Comparing the TNT response with responses to SA (as reported by Blanco et al., 2009) however, only 7 % of NPR1-dependent SA-response genes are also induced by TNT treatment, while 68 % of NPR1-independent SA-response genes are induced by TNT >2-fold. This indicates that NPR1 is not likely to be involved in responses to TNT. In contrast, of the 14 genes differentially regulated in *scl14* compared with an *SCL14*-overexpressor line investigated by Fode et al. (2008), 11 are induced by TNT treatment. It is possible, therefore, that SCL14 is involved in detoxification gene activation in response to TNT, via interaction with class II TGA factors.

The Genevestigator Signature tool has provided useful insight as to treatments which similarly induce TNT-response detoxification genes. In further analysis of microarray data available on Genevestigator, the TNT-response detoxification genes are not always induced following SA, MeJA, ozone or H_2O_2 treatment, but always highly correlate with responses to antimycin A or fenclorim. Reactive Oxygen Species are produced and involved in numerous cellular processes, and presumably the location and time of ROS flux is central to directing ROS responses (Xia et al., 2015). Due to the correlations with antimycin A treatment, it is possible that the TNT response is induced by ROS flux at mitochondria. Class II TGA factors have not yet been implicated with mitochondria retrograde signalling, and this is an interesting avenue for research.

6 Final discussion

6.1 RESEARCH IN CONTEXT

This research,

i. reveals that MDHAR6 mediates TNT toxicity in Arabidopsis- a valuable contribution towards the development of phytoremediation strategies
ii. highlights a potential new herbicide target, in an environment of increasing herbicide tolerance
iii. raises questions regarding the endogenous function of MDHAR6
iv. highlights the sensitivity of the plant antioxidant system, and
v. broadens our understanding of the role of TGA factors in defence signalling

6.1.1 MDHAR6 mediates TNT toxicity in Arabidopsis- a valuable contribution towards developing phytoremediation strategies

As discussed in Chapter 1, due to the costs associated with soil removal for composting or incineration (with care for UXO), phytoremediation could be the most cost-effective and environmentally-friendly means of tackling explosives pollution. This is particularly true for military training ranges, where phytoremediation could be used to contain and degrade energetic residues *in situ*, while the land is still used for munitions testing and training of personnel.

While RDX is of top priority in explosives remediation, plants developed to degrade RDX *in situ* need at the very least tolerance to the co-pollutant TNT, and ideally, the additional capacity to degrade TNT. The CRISPR/Cas system (Sander and Joung, 2014) could be used to knockout *MDHAR6* in remediation-applicable plant species, to increase TNT tolerance.

As discussed in Rylott et al. (2015), the time and cost required to license and trial genetically modified plants is a limiting factor in the use of transgenic plants for phytoremediation; Kalaitzandonakes et al. (2007) for example, estimate the compliance cost for release of a genetically modified herbicide-tolerant maize in the US to be between $6.18 million and $14.15 million, while Baulcombe et al. (2014) report the regulatory process for commercial release of a genetically modified plant in the EU to be between €10 million and €20 million. Considering this, it is of interest to investigate the impact of inducing MDHAR6 deficiency in native plant species by mutagenesis, without use of Genetic Modification (GM) to introduce any further genes. In the US, under the Federal Food, Drug, and Cosmetic Act, crops generated using GM biotechnology do not require pre-market approval unless a gene encoding a protein significantly different to endogenous plant proteins has been introduced. The *MDHAR6* gene

could therefore be knocked out in native plant lines using CRISPR/Cas, and used *in situ* without pre-market approval. Alternatively, mutagenesis (not classed as GM technology) and TILLING (Targeting Induced Local Lesions in Genomes) could be used to identify plant lines with mutations in *MDHAR6*.

Diverse plant communities promote microbial diversity and density (Lange et al., 2015), and there is extensive evidence that metabolites in root exudates promote microbial degradation of pollutants, either through stimulating microbial growth and diversity, and/or providing co-metabolites for degradation of organic pollutants (Singer et al., 2003). It is possible that inducing MDHAR6 deficiency, and therefore TNT tolerance, without addition of transgenes, could be an effective non-GM approach. Such MDHAR6-deficient plants could then be used to contain and remove explosives pollution, stabilise soil structure, and promote microbial and plant diversity *in situ*.

A factor to keep in mind with this non-GM approach however, is that while sites could be re-vegetated with TNT-tolerant, MDHAR6-deficient plant species, if these plants lack enhanced RDX-degrading capability, water-mobile RDX may accumulate in the shoots of these plants, and be consumed by herbivores. In a study by Rylott et al. (2011), locusts had no preference between *XplA/B*-overexpressing (RDX-degrading; discussed in 1.3.6) and wild type Arabidopsis lines, while foliage of the *XplA/B* lines contained 30- to 100-fold less RDX. Impact on herbivores would need to be assessed and incorporated into risk assessment prior to deployment of this phytoremediation strategy.

6.1.2 MDHAR6 as a new herbicide target

There are >250 herbicides on the global market (Heap, 2015), however no herbicide with a new Mode of Action (MOA) has been commercialised since the 1980s (Duke, 2012), while herbicide resistance has been increasing steadily since the 1970s (Heap, 2014). Weeds have now evolved resistance to 21 of the 25 herbicide MOA (Heap, 2014).

Herbicide resistance can result from (i) target-site resistance[9], (ii) increased expression of the herbicide target, compensating for inhibition, (iii) reduced herbicide uptake, (iv) enhanced herbicide metabolism, and/or (v) increased herbicide sequestration. The most common means of cross-resistance to multiple herbicides is through stacking of target-site resistance, and there are now 65 unique cases of multiple herbicide resistance in weeds (Heap, 2014). In the UK, the most important weeds with emerging herbicide resistance are *Alopecurus myosuroides* Huds. (black-grass), *Lolium multiflorum* Lam. (Italian rye-grass), *Avena* spp. (wild-oats), *Stellaria*

[9] Occurrence of mutation(s) which prevent herbicide-binding to the target site.

media (L.) Vill (common chickweed), *Papaver rhoeas* L. (common poppy) and *Tripleurospermum inodorum* (L.) Sch.Bip. (scentless mayweed) (Hull et al., 2014).

Evolution of herbicide tolerance in weeds is a natural phenomenon, however is facilitated by year-on-year use of the same crops and weed control strategies. In 2014, three crops (wheat, barley and oilseed rape) were grown over 81 % of UK arable crop land (DEFRA, 2014), and reduced crop rotation is partially attributed to the spread of herbicide-resistant black-grass (POST, 2015). Meanwhile, year-on-year use of Roundup Ready® (Monsanto Co.) crops with reliance on glyphosate herbicide has led to widespread emergence of glyphosate-resistant weeds in the US (Heap, 2014). The uptake of herbicide-resistant crops, and subsequent devaluation of other herbicides, has been partially attributed to the lack of new herbicides in recent years (Duke, 2012). Increasing development costs could also be a contributing factor; the cost of bringing a new agrochemical active ingredient to market has increased greatly in recent years, from an estimated $184 million in 2000, to $256 million in 2008 (Phillips McDougall, 2013).

As herbicide tolerance increases, the need to destabilise evolution of herbicide resistance in weeds, through crop and herbicide MOA rotation will also increase. As MDHAR6 activity with TNT appears to induce phytotoxicity, it could be explored whether an agrochemical (more environmentally-friendly than TNT) could be designed which MDHAR6 reduces with similar phytotoxic effect. Our preliminary experiments indicate high specificity in the targets for one electron reduction by MDHAR6 however, and so this could be a challenging task.

The toxicity of the agrochemical to herbivores and humans may also be an issue; bovine lens ζ-crystallin and rat neuronal nitric oxide synthase similarly reduce TNT by one electron (Kumagai et al., 2000, 2004), and there may be enzymes in humans and herbivores which readily react with the designed MDHAR6 target in a similar way.

6.1.3 The endogenous role of MDHAR6

A surprising outcome of this research is the low impact of MDHAR6 deficiency on Arabidopsis stress tolerance. Although results in this study indicate that in Col7, MDHAR6 contributes 13 % of leaf and 32 % of root MDHAR activity, the *mdhar6-1* mutants are no more susceptible than Col7 to inhibitory levels of NaCl, sorbitol, methyl viologen or H_2O_2 in agar, although biomass when grown in liquid culture is reduced in *mdhar6-1*. Responses to further stress conditions such as high light could be characterised further. As ascorbate and dehydroascorbate levels were unchanged in the *mdhar6-1* mutant compared with wild type, it would appear that the Arabidopsis antioxidant system is robust enough to cope with a deficiency in MDHAR6.

Further insight as to the endogenous role(s) of MDHAR6 will arise from further characterisation of the enzyme location. Prior research has focussed on the mitochondria-targeted precursor protein (Chew et al., 2003), however preliminary results discussed in Chapters 3 and 4 of this thesis, indicate that a third, previously undescribed TSS is dominant, and that the majority of *MDHAR6* transcript encodes plastid-targeted precusor MDHAR6. As discussed in Chapter 3, data on public microarray repositories indicate that *MDHAR6* is induced by sucrose treatment, and also by cold night temperature, resulting in a diurnal expression pattern. Induction at night correlates with increased growth (Dowson-Day and Millar, 1999) and starch breakdown in leaf amyloplasts for carbon reallocation (Graf et al., 2010; Yazdanbakhsh and Fisahn, 2011). The MDHAR6 enzyme could have an important role in protecting amyloplasts and elaioplasts during these processes at night. This could be investigated by comparing the phenotype of wild type and *mdhar6* mutants under longer or shortened cycles of light and temperature, to disrupt the efficacy of starch regulation (Graf et al., 2010).

It is curious that while qPCR results in Chapter 4 indicate that more plastid-targeted than mitochondria-targeted MDHAR6 is likely to be produced, complementation studies carried out by Liz Rylott and Emily Beynon (Johnston et al., 2015) indicate that *m-MDHAR6* fully complements the TNT toxicity phenotype, while *p-MDHAR6* complements the TNT phenotype by approximately two-thirds. This would suggest that the (implied) low levels of MDHAR6 in mitochondria are having an especially toxic effect. Imaging subcellular distribution of ROS generation in Col7 and *mdhar6-1*, in response to TNT and other stresses, would be desirable, however there are drawbacks with most ROS probes; results can be biased by the intercellular distribution of probes, or distribution of factors required in addition to ROS for probe fluorescence (Winterbourn, 2014).

6.1.4 The sensitivity of the plant antioxidant system

Oxygenic photosynthesis arose in the ancestors of cyanobacteria around 3 billion years ago, and has had a profound effect on evolution; initially, O_2 by-product was consumed in the oxidation of metals such as iron and manganese, however when these sinks became exhausted around 2.4 billion years ago, levels of O_2 in the atmosphere began to rise steeply in what is known as the Great Oxidation Event (Buick, 2008; Planavsky et al., 2014). Aerobic respiration became dominant, which increased the ATP yield from glucose >15-fold (Halliwell, 2006). As organic compounds constructed through photosynthesis accumulated, some bacteria became to rely solely on respiration for energy, and an ozone (O_3) layer formed in the stratosphere,

protecting organisms from UV-C radiation, possibly aiding the colonisation of land (Halliwell, 2006).

Importantly, oxygen is toxic; the radical forms of oxygen are highly reactive, and the evolution of robust antioxidant systems was required to keep oxygen under control (Halliwell, 2006). These include scavengers such as ascorbate, which are metabolically cheap to produce (Gest et al., 2013), and inducible enzymes such as peroxidases and superoxide dismutases. The system is intricately balanced, as the ROS are also used as signals (Xia et al., 2015). The nature of the antioxidant system, means that, as highlighted by Noctor (2015), genetic perturbations can have unexpected effects, which are often different between species; for example, Creissen et al. (1999) overexpressed chloroplast-targeted *GSH1* in tobacco, increasing glutathione synthesis, and observed light-dependent chlorosis, while in a study by Noctor et al. (1998), overexpression of chloroplast-targeted *GSH1* in Poplar (*Populus tremula* x *Populus alba*) did not have detrimental effects. Overexpression of Arabidopsis cytosolic *MDHAR* in tobacco increased ascorbate levels in a study by Eltayeb et al. (2006), while Haroldsen et al., (2011) and Gest et al. (2013) report a decrease in ascorbate in tomato overexpressing cytosolic and peroxisomal *MDHAR*.

The results reported in this thesis are unexpected as deficiency in plastid and mitochondria MDHAR did not increase susceptibility to drought, salt and oxidative stress, and yet superoxide generation following MDHAR6 activity with TNT appears to have a highly phytotoxic consequence.

6.1.5 The role of TGA factors in defence signalling

The finding that class II TGA factors are required for detoxification gene induction in response to TNT treatment, independent of phytoprostanes, highlights the diversity of signalling pathways which are dependent on TGA factors for transcriptome responses. How often this requirement is due to interaction directly at defence and detoxification gene promoters, and how often the compromised transcriptome response in class II TGA factor mutants is due to misregulation of a master regulator, remains to be elucidated. Chromatin immunoprecipitation experiments have yielded conflicting results (Rochon et al., 2006), however it would appear that class II TGA factors are recruited to the *PR-1* promoter following SA treatment (Johnson et al., 2003). At the same time, there is evidence that TGA2 is also required for basal repression of *PR-1* (Kesarwani et al., 2007); hence much remains to be understood regarding the role of TGA factors and their regulation in defence responses.

It is also notable that the detoxification gene induction profile following TNT treatment correlates highly with responses to antimycin A treatment; it is possible that the TNT response is induced by ROS flux or other disruption at mitochondria. Class II TGA factors have not yet been implicated in mitochondria retrograde signalling, and this is an interesting avenue for research.

6.2 FUTURE DIRECTION OF RESEARCH

6.2.1 Elucidating the location and function of MDHAR6

Primarily, this research raises interesting questions regarding the function of MDHAR6; an unusual enzyme with both pro-oxidant and anti-oxidant activity. Mutagenesis and X-ray crystallography will aid in understanding this dual activity, while clarification of MDHAR6 localisation, and phenotyping *mdhar6* mutants under additional test conditions, will further elucidate the *in planta* role of MDHAR6.

While growing plants hydroponically facilitates uniform chemical treatment of roots, the hypoxic growth condition induces stress in seedlings (Fukao and Bailey-Serres, 2004). To investigate *MDHAR6* TSS preference and protein location in unstressed conditions, analysing cDNA and sections of leaf and root tissue from soil-grown seedlings would be appropriate. It is important to verify MDHAR6 location with immuno-gold labelling, and the preliminary western blot against crude extract from Col7, Nossen, *mdhar6-1* and *mdhar6-2* indicates that the anti-MDHAR6 primary antibody which has already been sourced will be appropriate for this. Sections from *mdhar6-1* seedlings can be used as a negative control.

It is ambitious to try to cause more dysfunction in one organelle than another. Differences in TSS preference could instead be investigated further by testing cDNA from different tissues (e.g. root tips, stamens), developmental stages (e.g. germination, senescence) and stress conditions (e.g. drought, heat) to gauge whether demands for MDHAR6 differ, resulting in differing TSS preference.

As qPCR data indicate that MDHAR6 is most highly expressed in root tissue, for plastid-targeting, the effect of *mdhar6* mutation on amyloplasts and elaioplasts under non-stress and stress conditions could be studied more closely using transmission electron microscopy to identify any differences in physiology. As amyloplasts in root caps have an important role in gravitropism, it would also be of interest to test whether gravitropism responses are affected by *mdhar6* mutation. Differences in tolerance to shortened or lengthened cycles of light and dark, disrupting starch regulation, may also reveal differences in amyloplast efficacy (Graf et al., 2010).

Although anecdotally there is no difference in the timing of wild type and *mdhar6* flowering and senescence, this also remains to be experimentally recorded, as well as measurement of seed number and viability as an assessment of fitness.

6.2.2 Further exploring the role of TGA factors in defence signalling

Chromatin immunoprecipitation (ChIP) experiments could provide useful insight as to whether class II TGA factors are recruited to detoxification gene promoters following TNT treatment, however prior ChIP experiments with TGA2 have yielded conflicting results, depending on the antibody used (discussed in 1.5.3). Electropheretic mobility shift assays would be useful for verifying ChIP results, while *in planta* two hybrid assays, as used by Després et al. (2003), could also provide evidence for or against TGA factor recruitment. Pre-treatment with protein synthesis inhibitor cycloheximide (Schneider-Poetsch et al., 2010) could also be used to identify whether increased translation of, for example, a transcription factor, is required for the detoxification gene induction.

A role for TGA factors in mitochondria retrograde signalling has not yet been investigated, and could be an interesting avenue of research; TNT-response detoxification gene induction correlates closely with responses to antimycin A treatment (Figure 49), while 21 of the 24 Mitochondria Dysfunction Stimulon (MDS) genes identified by Clercq et al. (2013), are also upregulated following 6 h 60 µM TNT treatment (microarray data from Gandia-Herrero et al., 2008). Fourteen of the 24 MDS genes contain one or more TGACG motifs in the promoter region +100 to -1,000 bp from the start ATG, and so it is plausible that TGA factors could have a role in the regulation of these genes. Whether gene induction following TNT and/or antimycin A treatment requires a flux in ROS or glutathione content could also be investigated, by pre-treatment of seedlings with an antioxidant or glutathione synthesis inhibitor.

6.2.3 Developing plant lines for the phytoremediation of explosives

Although overexpressing *OPR*, *UGT* and *GST* genes in Arabidopsis has been found to increase TNT tolerance (Beynon et al., 2009; Gandia-Herrero et al., 2008; Gunning et al., 2014), low transcript abundance of these TNT-response genes in *tga2 tga5 tga6* little compromises TNT tolerance, suggesting that alternative TNT detoxification pathways may be dominant and/or that a high degree of functional redundancy exists.

The impact of *mdhar6* deficiency in remediation-applicable species towards phytoremediation is of priority to be assessed; this could be an effective non-GM approach to removing explosives pollution *in situ*, and re-greening polluted areas.

Abbreviations

1/2 MS(A)(S)	half strength Murashige and Skoog medium (with 0.8 % w/v agar) (with 20 mM sucrose)
ABA	abscisic acid
ABI4	*ABSCISIC ACID INSENSITIVE 4*
ABRC	Arabidopsis Biological Resource Center
ACC	1-aminocyclopropane-1-carboxylic acid
ADNT	aminodinitrotoluene
AGI	Arabidopsis Genome Initiative reference number
AOS	*ALLENE OXIDE SYNTHASE*
AOX1a	*ALTERNATIVE OXIDASE 1A*
APX2	*ASCORBATE PEROXIDASE 2*
BHA	butylated hydroxyanisole
bHLH	basic Helix Loop Helix
BOA	benzoxazolin-2(3H)-one
bp	base pairs
BSA	bovine serum albumin
BSO	buthionine sulfoximine
bZIP	basic leucine zipper
CaMV 35S	*Cauliflower Mosaic Virus 35S promoter*
cDNA	complementary DNA
ChIP	chromatin immunoprecipitation
CMP	4-chloro-6-methyl-2-phenylpyrimidine
COI1	*CORONATINE INSENSITIVE1*
Cys	cysteine
d	days
DAMP	damage-associated molecular pattern
DEPMPO	5-diethoxyphosphoryl-5-methyl-1-pyrroline-N-oxide
DFPM	5-(3,4-Dichlorophenyl)Furan-2-yl]-Piperidin-1-ylMethanethione
DHA	dehydroascorbate
DHAR	dehydroascorbate reductase
DMF	dimethylformamide
DMPO	5,5-dimethyl-pyrroline N-oxide
DMSO	dimethyl sulfoxide
DMTU	dimethylthiourea
DNA	deoxyribonucleic acid
DTT	dithiothreitol
DW	dry weight
EMS	ethyl methanesulphonate
EPR	Electron Paramagnetic Resonance
ER	endoplasmic reticulum
ERF	*ETHYLENE RESPONSE FACTOR*
FAD	flavin adenine dinucleotide
FAD	*FATTY ACID DESATURASE*
Fd	ferredoxin
Flg22	22 amino acid concerved region of the flagellin protein

FLS2	*FLAGELLIN SENSING 2*
flu	*fluorescent*
FTR	ferredoxin-dependent Trx reductase
FW	fresh weight
gDNA	genomic DNA
GFP	Green Fluorescent Protein
GNSO	S-nitrosoglutathione
GNSOR	S-nitrosoglutathione reductase
GR	glutathione reductase
GSH	reduced glutathione
GSSG	oxidised glutathione (glutathione disulphide)
GST	glutathione-*S*-transferase
GUS	beta-glucuronidase
h	hours
HADNT	hydroxylaminodinitrotoluene
HAP1	*HEME ACTIVATOR PROTEIN 1*
HMX	High Melting Explosive
HPLC	High Performance Liquid Chromatography
HR	Hypersensitive Response
HY5	*LONG HYPOCOTYL 5*
INA	2,6-dichloroisonicotinic acid
IPTG	isopropyl β-D-1-thiogalactopyranoside
JA	jasmonate
JA-Ile	jasmonate-isoleucine
JAZ protein	jasmonate ZIM domain protein
LB	Luria Broth
LDHC	temporal expression under cycle of 12 h light, 22°C/12 h dark, 12°C
LH_LLHC	entrained to cycle of 12 h light, 22°C/12 h light, 12°C, then subjected to 24 h light, 22°C
LHCB1	*LIGHT HARVESTING CHLOROPHYLL A/B BINDING PROTEIN B1*
LLHC	temporal expression under cycle of 12 h light, 22°C/12 h light, 12°C
LRR	Leucine-Rich Repeat
MDA	monodehydroascorbate
MDHAR	monodehydroascorbate reductase
MeJA	methyl jasmonate
Mg-proto	Mg-protoporphyrin IX
m-MDHAR6	transcript variant for mitochondria-targeted MDHAR6 (*MDHAR6.2*)
MOA	Mode(s) of Action
mp-MDHAR6	region shared between *m-MDHAR6* and *p-MDHAR6*
mtETC	mitochondrion electron transport chain
Na_2EDTA	sodium ethylenediaminetetraacetic acid
NADH	nicotinamide adenine dinucleotide
NADPH	nicotinamide adenine dinucleotide phosphate
NPC	No Plant Control
NPR1	*NON-EXPRESSOR OF PR1*
NTR	NADH-dependent Trx reductase
OPDA	12-oxophytodienoic acid
ORA59	OCTADECANOID-RESPOPNSIVE ARABIDOPSIS APETALA2/EHTYLENE

	RESPONSE FACTOR protein domain59
P	Likelihood that difference in results between groups is due to chance
PAMP	Pathogen-Associated Molecular Pattern
PAP	3'phosphoadenosine 5'-phosphate
PCR	Polymerase Chain Reaction
PDF1.2	PLANT DEFENSIN 1.2
p-MDHAR6	transcript variant for plastid-targeted MDHAR6 (*MDHAR6.1*), TSS as shown in Figure 39
pB-MDHAR6	transcript variant for plastid-targeted MDHAR6 (*MDHAR6.1*), TSS as shown in Figure 39, transcript abundance determined by primer pair pB
pE-MDHAR6	transcript variant for plastid-targeted MDHAR6, from possible third TSS-transcript abundance determined by primer pair pE
PMF	phenylmethanesulfonylfluoride
PPA_1	phytoprostane AI
PR-1	*PATHOGENESIS-RELATED 1*
Prx	Peroxiredoxin
qPCR	quantitative Polymerase Chain Reaction
RDX	Royal Demolition Explosive
RLK	Receptor-Like Kinase
RNA	ribonucleic acid
RNS	Reactive Nitrogen Species
ROS	Reactive Oxygen Species
RT	room temperature
SA	salicylic acid
SAM	Sorting and Assembly Machinery
SCL14	*SCARECROW-LIKE 14*
SD	standard deviation
SEM	standard error of the mean
SOD	superoxide dismutase
TAIR	The Arabidopsis Information Resource
TEM	transmission electron microscopy
TF	transcription factor
TGA factor	TGACG-binding factor
TIBA	2,3,5-triiodobenzoic acid
TIC	Translocon at the Inner envelope Membrane
TIM	Transporter Inner Membrane
TNT	2,4,5-trinitrotoluene
TOC	Translocon at the Outer envelope Membrane
TOM	Transporter Outer Membrane
Tris	2-amino-2-hydroxymethyl-1,3-propanediol
Trx	Thioredoxin
TSS	transcription start site
US EPA	United States Environmental Protection Agency
UDP-G	uridine diphosphate-glucose
UGT	uridine diphosphate transferring glycosyltransferases
VSP2	*VEGETATIVE STORAGE PROTEIN 2*
WT	wild type
γ-ECS	γ-glutamylcysteine synthetase

References

Akhavan, J. (2004). Introduction of explosives, in: The Chemistry of Explosives, second edition. Royal Society of Chemistry Paperbacks, Cambridge, U.K. Available: http://pubs.rsc.org/en/content/ebook/978-0-85404-640-9#!divbookcontent

Alscher, R.G., Erturk, N., Heath, L.S. (2002). Role of superoxide dismutases (SODs) in controlling oxidative stress in plants. Journal of Experimental Botany. 53, 1331–1341.

Altschul, S.F., Gish, W., Miller, W., Myers, E.W., Lipman, D.J. (1990). Basic local alignment search tool. Journal of Molecular Biology 215, 403–410.

Arrigoni, O., Dipierro, S., Borraccino, G. (1981). Ascorbate free radical reductase, a key enzyme of the ascorbic acid system. FEBS Letters 125, 242–244.

ATSDR (Agency for Toxic Substances & Disease Registry) (2008). Toxicological profile for perchlorates. US Department of Health and Human Services, Public Health Service, Georgia, US. Available: http://www.atsdr.cdc.gov/toxprofiles/tp.asp?id=895&tid=181

ATSDR (Agency for Toxic Substances & Disease Registry) (1995). Toxicological profile for 2,4,6-trinitrotoluene. US Department of Health and Human Services, Public Health Service, Georgia, US. Available: http://www.atsdr.cdc.gov/ToxProfiles/TP.asp?id=677&tid=125

Baier, M., Noctor, G., Foyer, C.H., Dietz, K.-J. (2000). Antisense suppression of 2-cysteine peroxiredoxin in Arabidopsis specifically enhances the activities and expression of enzymes associated with ascorbate metabolism but not glutathione metabolism. Plant Physiology 124, 823–832.

Baker, M.E. (2005). Xenobiotics and the evolution of multicellular animals: emergence and diversification of ligand-activated transcription factors. Integrative and Comparative Biology 45, 172–178.

Bak, S., Beisson, F., Bishop, G., Hamberger, B., Höfer, R., Paquette, S., Werck-Reichhart, D. (2011). Cytochromes P450. The Arabidopsis Book 9, e0144.

Ball, L., Accotto, G.-P., Bechtold, U., Creissen, G., Funck, D., Jimenez, A., Kular, B., Leyland, N., Mejia-Carranza, J., Reynolds, H., Karpinski, S., Mullineaux, P.M. (2004). Evidence for a direct link between glutathione biosynthesis and stress defense gene expression in Arabidopsis. Plant Cell 16, 2448–2462.

Barajas-López, J. de D., Blanco, N.E., Strand, Å. (2013). Plastid-to-nucleus communication, signals controlling the running of the plant cell. Biochimica et Biophysica Acta (BBA) - Molecular Cell Research 1833, 425–437.

Baulcombe, D., Dunwell, J., Jones, J., Pickett, J., Puigdomenech, P. (2014). GM Science Update. Council for Science and Technology, CST reports on science and technology, U.K. Reference CST/14/634a. Available: https://www.gov.uk/government/publications/genetic-modification-gm-technologies

Bednarek, P., Piślewska-Bednarek, M., Svatoš, A., Schneider, B., Doubský, J., Mansurova, M., Humphry, M., Consonni, C., Panstruga, R., Sanchez-Vallet, A., Molina, A., Schulze-Lefert, P. (2009). A Glucosinolate Metabolism Pathway in Living Plant Cells Mediates Broad-Spectrum Antifungal Defense. Science 323, 101–106.

Behringer, C., Bartsch, K., Schaller, A. (2011). Safeners recruit multiple signalling pathways for the orchestrated induction of the cellular xenobiotic detoxification machinery in Arabidopsis. Plant, Cell & Environment 34, 1970–1985.

Bela, K., Horváth, E., Gallé, Á., Szabados, L., Tari, I., Csiszár, J. (2015). Plant glutathione peroxidases: Emerging role of the antioxidant enzymes in plant development and stress responses. Journal of Plant Physiology 176, 192–201.

Berglund, A.-K., Pujol, C., Duchene, A.-M., Glaser, E. (2009). Defining the Determinants for Dual Targeting of Amino Acyl-tRNA Synthetases to Mitochondria and Chloroplasts. Journal of Molecular Biology 393, 803–814.

Beynon, E. (2008). Mechanisms of trinitrotoluene transformation, tolerance and toxicity in Arabidopsis thaliana. Thesis. The University of York, Department of Biology.

Beynon, E.R., Symons, Z.C., Jackson, R.G., Lorenz, A., Rylott, E.L., Bruce, N.C. (2009). The Role of Oxophytodienoate Reductases in the Detoxification of the Explosive 2,4,6-Trinitrotoluene by Arabidopsis. Plant Physiology 151, 253 –261.

Bielski, B.H.J., Comstock, D.A., Bowen, R.A. (1971). Ascorbic acid free radicals. I. Pulse radiolysis study of optical absorption and kinetic properties. Journal of the American Chemical Society 93, 5624–5629.

Blanco, F., Garretón, V., Frey, N., Dominguez, C., Pérez-Acle, T., Van der Straeten, D., Jordana, X., Holuigue, L. (2005). Identification of NPR1-dependent and independent genes early induced by salicylic acid treatment in Arabidopsis. Plant Molecular Biology 59, 927–944.

Blanco, F., Salinas, P., Cecchini, N.M., Jordana, X., Hummelen, P.V., Alvarez, M.E., Holuigue, L. (2009). Early genomic responses to salicylic acid in Arabidopsis. Plant Molecular Biology 70, 79–102.

Borraccino, G., Dipierro, S., Arrigoni, O. (1986). Purification and properties of ascorbate free-radical reductase from potato tubers. Planta 167, 521–526.

Bouchez, D., Tokuhisa, J.G., Llewellyn, D.J., Dennis, E.S., Ellis, J.G. (1989). The *ocs*-element is a component of the promoters of several T-DNA and plant viral genes. EMBO J 8, 4197–4204.

Brentner, L.B., Mukherji, S.T., Walsh, S.A., Schnoor, J.L. (2010). Localization of hexahydro-1,3,5-trinitro-1,3,5-triazine (RDX) and 2,4,6-trinitrotoluene (TNT) in poplar and switchgrass plants using phosphor imager autoradiography. Environmental Pollution 158, 470–475.

Bruce, B.D. (2001). The paradox of plastid transit peptides: conservation of function despite divergence in primary structure. Biochimica et Biophysica Acta (BBA) - Molecular Cell Research 1541, 2–21.

Bruce, B.D. (2000). Chloroplast transit peptides: structure, function and evolution. Trends in Cell Biology 10, 440–447.

Buick, R. (2008). When did oxygenic photosynthesis evolve? Philosophical Transactions of the Royal Society London B: Biological Sciences 363, 2731–2743.

Burdette, L.J., Cook, L.L., Dyer, R.S. (1988). Convulsant properties of cyclotrimethylenetrinitramine (RDX): spontaneous audiogenic, and amygdaloid kindled seizure activity. Toxicology and Applied Pharmacology 92, 436–444.

Cairns, N.G., Pasternak, M., Wachter, A., Cobbett, C.S., Meyer, A.J. (2006). Maturation of Arabidopsis Seeds Is Dependent on Glutathione Biosynthesis within the Embryo. Plant Physiology 141, 446–455.

Camp, R.G.L. op den, Przybyla, D., Ochsenbein, C., Laloi, C., Kim, C., Danon, A., Wagner, D., Hideg, É., Göbel, C., Feussner, I., Nater, M., Apel, K. (2003). Rapid Induction of Distinct Stress Responses after the Release of Singlet Oxygen in Arabidopsis. Plant Cell 15, 2320–2332.

Cao, H., Bowling, S.A., Gordon, A.S., Dong, X. (1994). Characterization of an Arabidopsis Mutant That Is Nonresponsive to Inducers of Systemic Acquired Resistance. Plant Cell 6, 1583–1592.

Carrie, C., Small, I. (2013). A reevaluation of dual-targeting of proteins to mitochondria and chloroplasts. Biochimica et Biophysica Acta (BBA) - Molecular Cell Research 1833, 253–259.

Chang, C.C.-C., Ball, L., Fryer, M.J., Baker, N.R., Karpinski, S., Mullineaux, P.M. (2004). Induction of ASCORBATE PEROXIDASE 2 expression in wounded Arabidopsis leaves does not involve known wound-signalling pathways but is associated with changes in photosynthesis. The Plant Journal 38, 499–511.

Cheng, M.-C., Ko, K., Chang, W.-L., Kuo, W.-C., Chen, G.-H., Lin, T.-P. (2015). Increased glutathione contributes to stress tolerance and global translational changes in Arabidopsis. Plant Journal 83, 926-939.

Chen, J.-H., Jiang, H.-W., Hsieh, E.-J., Chen, H.-Y., Chien, C.-T., Hsieh, H.-L., Lin, T.-P. (2012). Drought and salt stress tolerance of an Arabidopsis glutathione S-transferase U17 knockout mutant are attributed to the combined effect of glutathione and abscisic acid. Plant Physiology 158, 340–351.

Chen, L., Song, Y., Li, S., Zhang, L., Zou, C., Yu, D. (2012). The role of WRKY transcription factors in plant abiotic stresses. Biochimica et Biophysica Acta (BBA) - Gene Regulatory Mechanisms 1819, 120–128.

Chew, O., Whelan, J., Millar, A.H. (2003). Molecular Definition of the Ascorbate-Glutathione Cycle in Arabidopsis Mitochondria Reveals Dual Targeting of Antioxidant Defenses in Plants. Journal of Biological Chemistry 278, 46869 –46877.

Chi, Y.H., Paeng, S.K., Kim, M.J., Hwang, G.Y., Melencion, S.M.B., Oh, H.T., Lee, S.Y. (2013). Redox-dependent functional switching of plant proteins accompanying with their structural changes. Frontiers in Plant Sciences 4, 277.

Choi, J., Huh, S.U., Kojima, M., Sakakibara, H., Paek, K.-H., Hwang, I. (2010). The Cytokinin-Activated Transcription Factor ARR2 Promotes Plant Immunity via TGA3/NPR1-Dependent Salicylic Acid Signaling in Arabidopsis. Developmental Cell 19, 284–295.

Chong, C.S., Sabir, D.K., Lorenz, A., Bontemps, C., Andeer, P., Stahl, D.A., Strand, S.E., Rylott, E.L., Bruce, N.C. (2014). Analysis of the xplAB-Containing Gene Cluster Involved in the Bacterial Degradation of the Explosive Hexahydro-1,3,5-Trinitro-1,3,5-Triazine. Applied and Environmental Microbiology. 80, 6601–6610.

Chuang, C.F., Running, M.P., Williams, R.W., Meyerowitz, E.M. (1999). The PERIANTHIA gene encodes a bZIP protein involved in the determination of floral organ number in Arabidopsis thaliana. Genes Dev. 13, 334–344.

Clausen, J., Robb, J., Curry, D., Korte, N. (2004). A case study of contaminants on military ranges: Camp Edwards, Massachusetts, USA. Environmental Pollution 129, 13–21.

Clay, N.K., Adio, A.M., Denoux, C., Jander, G., Ausubel, F.M. (2009). Glucosinolate Metabolites Required for an Arabidopsis Innate Immune Response. Science 323, 95–101.

de Clercq, I., Vermeirssen, V., van Aken, O., Vandepoele, K., Murcha, M.W., Law, S.R., Inzé, A., Ng, S., Ivanova, A., Rombaut, D., van de Cotte, B., Jaspers, P., van de Peer, Y., Kangasjärvi, J., Whelan, J., van Breusegem, F. (2013). The membrane-bound NAC transcription factor ANAC013 functions in mitochondrial retrograde regulation of the oxidative stress response in *Arabidopsis*. The Plant Cell 25, 3472-3490.

Clough, S.J., Bent, A.F. (1998). Floral dip: a simplified method for Agrobacterium-mediated transformation of Arabidopsis thaliana. Plant Journal 16, 735–743.

Colville, L., Smirnoff, N. (2008). Antioxidant status, peroxidase activity, and PR protein transcript levels in ascorbate-deficient Arabidopsis thaliana vtc mutants. Journal of Experimental Botany 59, 3857 –3868.

Creissen, G., Firmin, J., Fryer, M., Kular, B., Leyland, N., Reynolds, H., Pastori, G., Wellburn, F., Baker, N., Wellburn, A., Mullineaux, P. (1999). Elevated Glutathione Biosynthetic Capacity in the Chloroplasts of Transgenic Tobacco Plants Paradoxically Causes Increased Oxidative Stress. Plant Cell 11, 1277–1291.

Cui, H., Tsuda, K., Parker, J.E. (2015). Effector-Triggered Immunity: From Pathogen Perception to Robust Defense. Annual Review of Plant Biology 66, 487–511.

Cummins, I., Dixon, D.P., Freitag-Pohl, S., Skipsey, M., Edwards, R. (2011). Multiple roles for plant glutathione transferases in xenobiotic detoxification. Drug Metabolism Reviews 43, 266–280.

Dalal, A., Kumar, A., Yadav, D., Gudla, T., Viehhauser, A., Dietz, K.-J., Kirti, P.B. (2014). Alleviation of methyl viologen-mediated oxidative stress by Brassica juncea annexin-3 in transgenic Arabidopsis. Plant Science 219–220, 9–18.

Dalton, D.A., Langeberg, L., Robbins, M. (1992). Purification and characterisation of monodehydroascorbate reductase from soybean root nodules. Archives of Biochemistry and Biophysics 292, 281–286.

Dangl, J.L., Jones, J.D.G. (2001). Plant pathogens and integrated defence responses to infection. Nature 411, 826–833.

Danon, A., Miersch, O., Felix, G., op den Camp, R.G.L., Apel, K. (2005). Concurrent activation of cell death-regulating signaling pathways by singlet oxygen in Arabidopsis thaliana. The Plant Journal 41, 68–80.

DEFRA (Department for Environment, Food & Rural Affaris) (2014). Farming statistics-provisional crop areas, yields and livestock populations at 1 June 2014- UK. U.K. government. Available: https://www.gov.uk/government/statistics/farming-statistics-provisional-crop-areas-yields-and-livestock-populations-at-1-june-2014-uk.

De Leonardis, S., De Lorenzo, G., Borraccino, G., Dipierro, S. (1995). A Specific Ascorbate Free Radical Reductase Isozyme Participates in the Regeneration of Ascorbate for Scavenging Toxic Oxygen Species in Potato Tuber Mitochondria. Plant Physiology 109, 847 –851.

Després, C., Chubak, C., Rochon, A., Clark, R., Bethune, T., Desveaux, D., Fobert, P.R. (2003). The Arabidopsis NPR1 Disease Resistance Protein Is a Novel Cofactor That Confers Redox Regulation of DNA Binding Activity to the Basic Domain/Leucine Zipper Transcription Factor TGA1. Plant Cell 15, 2181–2191.

Després, C., DeLong, C., Glaze, S., Liu, E., Fobert, P.R. (2000). The Arabidopsis NPR1/NIM1 Protein Enhances the DNA Binding Activity of a Subgroup of the TGA Family of bZIP Transcription Factors. Plant Cell 12, 279–290.

Dietrich, R.A., Richberg, M.H., Schmidt, R., Dean, C., Dangl, J.L. (1997). A Novel Zinc Finger Protein Is Encoded by the Arabidopsis LSD1 Gene and Functions as a Negative Regulator of Plant Cell Death. Cell 88, 685–694.

Dietz, K.-J. (2011). Peroxiredoxins in Plants and Cyanobacteria. Antioxid Redox Signal 15, 1129–1159.

Dixon, D.P., Edwards, R. (2010). Glutathione Transferases. Arabidopsis Book 8, e0131.

Dixon, D.P., Edwards, R. (2009). Selective Binding of Glutathione Conjugates of Fatty Acid Derivatives by Plant Glutathione Transferases. The Journal of Biological Chemistry 284, 21249–21256.

Dixon, D.P., Skipsey, M., Edwards, R. (2010). Roles for glutathione transferases in plant secondary metabolism. Phytochemistry 71, 338–350.

Does, D.V. der, Leon-Reyes, A., Koornneef, A., Verk, M.C.V., Rodenburg, N., Pauwels, L., Goossens, A., Körbes, A.P., Memelink, J., Ritsema, T., Wees, S.C.M.V., Pieterse, C.M.J. (2013). Salicylic Acid Suppresses Jasmonic Acid Signaling Downstream of SCFCOI1-JAZ by Targeting GCC Promoter Motifs via Transcription Factor ORA59. Plant Cell 25, 744-761.

Dowdle, J., Ishikawa, T., Gatzek, S., Rolinski, S., Smirnoff, N. (2007). Two genes in Arabidopsis thaliana encoding GDP-L-galactose phosphorylase are required for ascorbate biosynthesis and seedling viability. Plant Journal. 52, 673–689.

Dowson-Day, M.J., Millar, A.J. (1999). Circadian dysfunction causes aberrant hypocotyl elongation patterns in Arabidopsis. Plant Journal 17, 63–71.

Drew, D.P., Lunde, C., Lahnstein, J., Fincher, G.B. (2007). Heterologous expression of cDNAs encoding monodehydroascorbate reductases from the moss, Physcomitrella patens and characterization of the expressed enzymes. Planta 225, 945–954.

Dudek, J., Rehling, P., van der Laan, M. (2013). Mitochondrial protein import: Common principles and physiological networks. Biochimica et Biophysica Acta (BBA) - Molecular Cell Research 1833, 274–285.

Duke, S.O. (2012). Why have no new herbicide modes of action appeared in recent years? Pest Management Science 68, 505–512.

Dyall, S.D., Brown, M.T., Johnson, P.J. (2004). Ancient Invasions: From Endosymbionts to Organelles. Science 304, 253–257.

Eastmond, P.J. (2007). MONODEHYROASCORBATE REDUCTASE4 Is Required for Seed Storage Oil Hydrolysis and Postgerminative Growth in Arabidopsis. The Plant Cell 19, 1376 –1387.

Eisentraeger, A., Reifferscheid, G., Dardenne, F., Blust, R., Schofer, A. (2007). Hazard characterization and identification of a former ammunition site using microarrays, bioassays, and chemical analysis. Environmental Toxicology and Chemistry 26, 634–646.

Ekman, D.R., Lorenz, W.W., Przybyla, A.E., Wolfe, N.L., Dean, J.F.D. (2003). SAGE Analysis of Transcriptome Responses in Arabidopsis Roots Exposed to 2,4,6-Trinitrotoluene. Plant Physiology 133, 1397–1406.

Ellis, J.G., Tokuhisa, J.G., Llewellyn, D.J., Bouchez, D., Singh, K., Dennis, E.S., Peacock, W.J. (1993). Does the *ocs*-element occur as a functional component of the promoters of plant genes? The Plant Journal 4, 433–443.

Eltayeb, A.E., Kawano, N., Badawi, G.H., Kaminaka, H., Sanekata, T., Shibahara, T., Inanaga, S., Tanaka, K. (2006). Overexpression of monodehydroascorbate reductase in transgenic tobacco confers enhanced tolerance to ozone, salt and polyethylene glycol stresses. Planta 225, 1255–1264.

Estavillo, G.M., Crisp, P.A., Pornsiriwong, W., Wirtz, M., Collinge, D., Carrie, C., Giraud, E., Whelan, J., David, P., Javot, H., Brearley, C., Hell, R., Marin, E., Pogson, B.J. (2011). Evidence for a SAL1-PAP Chloroplast Retrograde Pathway That Functions in Drought and High Light Signaling in Arabidopsis. Plant Cell 23, 3992–4012.

Fairlamb, A.H., Blackburn, P., Ulrich, P., Chait, B.T., Cerami, A. (1985). Trypanothione: a novel bis(glutathionyl)spermidine cofactor for glutathione reductase in trypanosomatids. Science 227, 1485–1487.

Falk, J., Munné-Bosch, S. (2010). Tocochromanol functions in plants: antioxidation and beyond. J. Exp. Bot. 61, 1549–1566.

Fan, W., Dong, X. (2002). In Vivo Interaction between NPR1 and Transcription Factor TGA2 Leads to Salicylic Acid-Mediated Gene Activation in Arabidopsis. Plant Cell 14, 1377–1389.

Farmer, E.E., Mueller, M.J. (2013). ROS-Mediated Lipid Peroxidation and RES-Activated Signaling. Annual Review of Plant Biology 64, 429-450.

Ferrari, S., Plotnikova, J.M., De Lorenzo, G., Ausubel, F.M. (2003). Arabidopsis local resistance to Botrytis cinerea involves salicylic acid and camalexin and requires EDS4 and PAD2, but not SID2, EDS5 or PAD4. The Plant Journal 35, 193–205.

Flohé, L. (2013). The fairytale of the GSSG/GSH redox potential. Biochimica et Biophysica Acta (BBA) - General Subjects 1830, 3139–3142.

Fode, B., Siemsen, T., Thurow, C., Weigel, R., Gatz, C. (2008). The Arabidopsis GRAS Protein SCL14 Interacts with Class II TGA Transcription Factors and Is Essential for the Activation of Stress-Inducible Promoters. The Plant Cell 20, 3122 –3135.

Foley, R.C., Singh, K.B. (2004). TGA5 acts as a positive and TGA4 acts as a negative regulator of ocs element activity in Arabidopsis roots in response to defence signals. FEBS Letters 563, 141–145.

Foyer, C.H., Noctor, G. (2011). Ascorbate and Glutathione: The Heart of the Redox Hub. Plant Physiology 155, 2–18.

FRTR (Federal Remediation Technologies Roundtable) (2007a). Remediation Technologies Screening Matrix and Reference Guide, Version 4.0. Section 2.10.2.2 Thermal Treatment Technologies for Explosives. Available: http://www.frtr.gov/matrix2/section2/2_10_2_2.html

FRTR, Federal Remediation Technologies Roundtable, 2007b. Remediation Technologies Screening Matrix and Reference Guide, Version 4.0. Section 2.10.2.1 Biological Treatment Technologies for Explosives. Available: http://www.frtr.gov/matrix2/section2/2_10_2_1.html

Furman, D., Kosloff, R., Dubnikova, F., Zybin, S.V., Goddard, W.A., Rom, N., Hirshberg, B., Zeiri, Y. (2014). Decomposition of Condensed Phase Energetic Materials: Interplay between Uni- and Bimolecular Mechanisms. Journal of the American Chemical Society. 136, 4192–4200.

Fu, Z.Q., Yan, S., Saleh, A., Wang, W., Ruble, J., Oka, N., Mohan, R., Spoel, S.H., Tada, Y., Zheng, N., Dong, X. (2012). NPR3 and NPR4 are receptors for the immune signal salicylic acid in plants. Nature 486, 228–232.

Fukao, T., Bailey-Serres, J. (2004). Plant responses to hypoxia- is survival a balancing act? Trend in Plant Science 9, 449-456.

Gaffney, T., Friedrich, L., Vernooij, B., Negrotto, D., Nye, G., Uknes, S., Ward, E., Kessmann, H., Ryals, J. (1993). Requirement of Salicylic Acid for the Induction of Systemic Acquired Resistance. Science 261, 754–756.

Galant, A., Preuss, M.L., Cameron, J., Jez, J.M. (2011). Plant glutathione biosynthesis: diversity in biochemical regulation and reaction products. Frontiers in Plant Science 2, 45.

Gandia-Herrero, F., Lorenz, A., Larson, T., Graham, I.A., Bowles, D.J., Rylott, E.L., Bruce, N.C. (2008). Detoxification of the explosive 2,4,6-trinitrotoluene in Arabidopsis: discovery of bifunctional O- and C-glucosyltransferases. The Plant Journal 56, 963–974.

Garretón, V., Carpinelli, J., Jordana, X., Holuigue, L. (2002). The *as-1* Promoter Element Is an Oxidative Stress-Responsive Element and Salicylic Acid Activates It via Oxidative Species. Plant Physiology 130, 1516–1526.

Gatz, C. (2013). From Pioneers to Team Players: TGA Transcription Factors Provide a Molecular Link Between Different Stress Pathways. Molecular Plant-Microbe Interactions 26, 151–159.

George, I., Eyers, L., Stenuit, B., Agathos, S.N. (2008). Effect of 2,4,6-trinitrotoluene on soil bacterial communities. Journal of Industrial Microbiology and Biotechnology 35, 225–236.

George, I.F., Liles, M.R., Hartmann, M., Ludwig, W., Goodman, R.M., Agathos, S.N. (2009). Changes in soil Acidobacteria communities after 2,4,6-trinitrotoluene contamination. FEMS Microbiology Letters 296, 159–166.

Gest, N., Garchery, C., Gautier, H., Jiménez, A., Stevens, R. (2013). Light-dependent regulation of ascorbate in tomato by a monodehydroascorbate reductase localized in peroxisomes and the cytosol. Plant Biotechnology Journal 11, 344–354.

Gest, N., Gautier, H., Stevens, R. (2012). Ascorbate as seen through plant evolution: the rise of a successful molecule? Journal of Experimental Botany 64, 33-53.

Giraud, E., Aken, O.V., Ho, L.H.M., Whelan, J. (2009). The Transcription Factor ABI4 Is a Regulator of Mitochondrial Retrograde Expression of ALTERNATIVE OXIDASE1a. Plant Physiology 150, 1286–1296.

Gómez-Gómez, L., Boller, T. (2000). FLS2: An LRR Receptor–like Kinase Involved in the Perception of the Bacterial Elicitor Flagellin in Arabidopsis. Molecular Cell 5, 1003–1011.

Gomez, L.D., Noctor, G., Knight, M.R., Foyer, C.H. (2004). Regulation of calcium signalling and gene expression by glutathione. Journal of Experimental Botany 55, 1851–1859.

Gong, P., Wilke, B.-M., Fleischmann, S. (1999). Soil-Based Phytotoxicity of 2,4,6-Trinitrotoluene (TNT) to Terrestrial Higher Plants. Archives of Environmental Contamination and Toxicology 36, 152–157.

Graf, A., Schlereth, A., Stitt, M., Smith, A.M. (2010). Circadian control of carbohydrate availability for growth in Arabidopsis plants at night. Proceedings of the National Academy of Sciences U.S.A. 107, 9458–9463.

Green, M.A., Fry, S.C. (2005). Vitamin C degradation in plant cells via enzymatic hydrolysis of 4-O-oxalyl-l-threonate. Nature 433, 83–87.

Griffith, O.W., Meister, A. (1979). Potent and specific inhibition of glutathione synthesis by buthionine sulfoximine (S-n-butyl homocysteine sulfoximine). Journal of Biological Chemistry 254, 7558–7560.

Grun, C., Berger, S., Matthes, D., Mueller, M.J. (2007). Early accumulation of non-enzymatically synthesised oxylipins in Arabidopsis thaliana after infection with Pseudomonas syringae. Functional Plant Biology 34, 65–71.

Gunning, V., Tzafestas, K., Sparrow, H., Johnston, E.J., Brentnall, A.S., Potts, J.R., Rylott, E.L., Bruce, N.C. (2014). Arabidopsis glutathione transferases U24 and U25 exhibit a range of detoxification activities with the environmental pollutant, and explosive, 2,4,6-trinitrotoluene. Plant Physiology 165, 854–865.

Hager, A., Holocher, K. (1994). Localization of the xanthophyll-cycle enzyme violaxanthin de-epoxidase within the thylakoid lumen and abolition of its mobility by a (light-dependent) pH decrease. Planta 192, 581–589.

Halliwell, B. (2006). Reactive Species and Antioxidants. Redox Biology Is a Fundamental Theme of Aerobic Life. Plant Physiology 141, 312–322.

Han, R.-M., Zhang, J.-P., Skibsted, L.H. (2012). Reaction Dynamics of Flavonoids and Carotenoids as Antioxidants. Molecules 17, 2140–2160.

Haroldsen, V.M., Chi-Ham, C.L., Kulkarni, S., Lorence, A., Bennett, A.B. (2011). Constitutively expressed DHAR and MDHAR influence fruit, but not foliar ascorbate levels in tomato. Plant Physiology and Biochemistry 49, 1244–1249.

Hatzinger, P., Lippincott, D. (2012). Final Report: In situ bioremediation of energetic compounds in groundwater. US Department of Defense Environmental Security Technology Certification Program project ER-200425. Available: https://www.serdp-estcp.org/Program-Areas/Environmental-Restoration/Contaminated-Groundwater/ER-200425

Heap, I. (2015). The International Survey of Herbicide Resistant Weeds. Online. Internet. Accessed: 17th February 2015. Available www.weedscience.org.

Heap, I. (2014). Global perspective of herbicide-resistant weeds. Pest Management Science 70, 1306–1315.

Hickman, M.J., Winston, F. (2007). Heme levels switch the function of Hap1 of Saccharomyces cerevisiae between transcriptional activator and transcriptional repressor. Molecular Cell Biology 27, 7414–7424.

Hirsch, S., Oldroyd, G.E.D. (2009). GRAS-domain transcription factors that regulate plant development. Plant Signaling and Behavior 4, 698-700.

Hossain, M.A., Asada, K. (1985). Monodehydroascorbate reductase from cucumber is a flavin adenine dinucleotide enzyme. Journal of Biological Chemistry 260, 12920 –12926.

Hossain, M.A., Nakano, Y., Asada, K. (1984). Monodehydroascorbate Reductase in Spinach Chloroplasts and Its Participation in Regeneration of Ascorbate for Scavenging Hydrogen Peroxide. Plant Cell Physiology 25, 385–395.

Hothorn, M., Wachter, A., Gromes, R., Stuwe, T., Rausch, T., Scheffzek, K. (2006). Structural basis for the redox control of plant glutamate cysteine ligase. J. Biol. Chem. 281, 27557–27565.

HRAC (Herbicide Resistance Actin Committee) (2010). The World of Herbicides. Internet. Accessed: 20th May 2015. Available: www.hracglobal.com

Hruz, T., Laule, O., Szabo, G., Wessendorp, F., Bleuler, S., Oertle, L., Widmayer, P., Gruissem, W., Zimmermann, P. (2008). Genevestigator v3: a reference expression database for the meta-analysis of transcriptomes. Advances in Bioinformatics 2008, 420747.

Huala, E., Dickerman, A.W., Garcia-Hernandez, M., Weems, D., Reiser, L., LaFond, F., Hanley, D., Kiphart, D., Zhuang, M., Huang, W., Mueller, L.A., Bhattacharyya, D., Bhaya, D., Sobral, B.W., Beavis, W., Meinke, D.W., Town, C.D., Somerville, C., Rhee, S.Y. (2001). The Arabidopsis Information Resource (TAIR): a comprehensive database and web-based information retrieval, analysis, and visualization system for a model plant. Nucleic Acids Research 29, 102–105.

Hull, R., Tatnell, L.V., Cook, S.K., Beffa, R., Moss, S.R. (2014). Current status of herbicide-resistant weeds in the UK. Aspects of Applied Biology 127, 261–272.

Imbusch, R., Mueller, M.J. (2000). Analysis of Oxidative Stress and Wound-Inducible Dinor Isoprostanes F1 (Phytoprostanes F1) in Plants. Plant Physiology 124, 1293–1304.

Ito, A., Hayashi, S., Yoshida, T. (1981). Participation of a cytochrome b5-like hemoprotein of outer mitochondrial membrane (OM cytochrome b) in NADH-semidehydroascorbic acid reductase activity of rat liver. Biochemical and Biophysical Research Communications 101, 591–598.

Ito, T., Motohashi, R., Kuromori, T., Noutoshi, Y., Seki, M., Kamiya, A., Mizukado, S., Sakurai, T., Shinozaki, K. (2005). A resource of 5,814 dissociation transposon-tagged and sequence-indexed lines of Arabidopsis transposed from start loci on chromosome 5. Plant Cell Physiology 46, 1149–1153.

Iyanagi, T., Yamazaki, I. (1969). One-electron-transfer reactions in biochemical systems. 3. One-electron reduction of quinones by microsomal flavin enzymes. Biochimica et Biophysica Acta (BBA) 172, 370–381.

Jakoby, M., Weisshaar, B., Dröge-Laser, W., Vicente-Carbajosa, J., Tiedemann, J., Kroj, T., Parcy, F. (2002). bZIP transcription factors in Arabidopsis. Trends in Plant Science 7, 106–111.

Jarvis, P. (2008). Targeting of nucleus-encoded proteins to chloroplasts in plants. New Phytologist 179, 257–285.

Jarvis, P., Chen, L.-J., Li, H., Peto, C.A., Fankhauser, C., Chory, J. (1998). An Arabidopsis Mutant Defective in the Plastid General Protein Import Apparatus. Science 282, 100–103.

Jarvis, P., López-Juez, E. (2013). Biogenesis and homeostasis of chloroplasts and other plastids. Nature Reviews in Molecular Cell Biology 14, 787–802.

Jefferson, R. (1987). Assaying chimeric genes in plants: The GUS gene fusion system. Plant Molecular Biology Reporter 5, 387–405.

Jefferson, R.A., Kavanagh, T.A., Bevan, M.W. (1987). GUS fusions: beta-glucuronidase as a sensitive and versatile gene fusion marker in higher plants. The EMBO Journal, 6, 3901-3907.

Johnson, C., Boden, E., Arias, J. (2003a). Salicylic Acid and NPR1 Induce the Recruitment of trans-Activating TGA Factors to a Defense Gene Promoter in Arabidopsis. Plant Cell 15, 1846–1858.

Johnson, C., Boden, E., Arias, J. (2003b). Salicylic Acid and NPR1 Induce the Recruitment of trans-Activating TGA Factors to a Defense Gene Promoter in Arabidopsis. Plant Cell 15, 1846–1858.

Johnston, E.J., Rylott, E.L., Beynon, E., Lorenz, A., Chechik, V., Bruce, N.C. (2015). Monodehydroascorbate reductase mediates TNT toxicity in plants. Science 349, 1072–1075.

Jupin, I., Chua, N.H. (1996). Activation of the CaMV as-1 cis-element by salicylic acid: differential DNA-binding of a factor related to TGA1a. The EMBO Journal 15, 5679–5689.

Kalaitzandonakes, N., Alston, J.M., Bradford, K.J. (2007). Compliance costs for regulatory approval of new biotech crops. Nature Biotechnology 25, 509–511.

Kampfenkel, K., Vanmontagu, M., Inze, D. (1995). Extraction and Determination of Ascorbate and Dehydroascorbate from Plant Tissue. Analytical Biochemistry 225, 165–167.

Kang, H.-G., Klessig, D.F. (2005). Salicylic acid-inducible Arabidopsis CK2-like activity phosphorylates TGA2. Plant Molecular Biology 57, 541–557.

Katagiri, F., Lam, E., Chua, N.H. (1989). Two tobacco DNA-binding proteins with homology to the nuclear factor CREB. Nature 340, 727–730.

Kavitha, K., George, S., Venkataraman, G., Parida, A. (2010). A salt-inducible chloroplastic monodehydroascorbate reductase from halophyte Avicennia marina confers salt stress tolerance on transgenic plants. Biochimie 92, 1321–1329.

Kesarwani, M., Yoo, J., Dong, X. (2007). Genetic Interactions of TGA Transcription Factors in the Regulation of Pathogenesis-Related Genes and Disease Resistance in Arabidopsis. Plant Physiology 144, 336–346.

Kindgren, P., Norén, L., Barajas López, J. de D., Shaikhali, J., Strand, Å. (2012). Interplay between HEAT SHOCK PROTEIN 90 and HY5 Controls PhANG Expression in Response to the GUN5 Plastid Signal. Molecular Plant 5, 901–913.

Kleinboelting, N., Huep, G., Kloetgen, A., Viehoever, P., Weisshaar, B. (2012). GABI-Kat SimpleSearch: new features of the Arabidopsis thaliana T-DNA mutant database. Nucleic Acids Res 40, D1211–D1215.

Koornneef, A., Leon-Reyes, A., Ritsema, T., Verhage, A., Otter, F.C.D., Loon, L.C.V., Pieterse, C.M.J. (2008). Kinetics of Salicylate-Mediated Suppression of Jasmonate Signaling Reveal a Role for Redox Modulation. Plant Physiology 147, 1358–1368.

Köster, J., Thurow, C., Kruse, K., Meier, A., Iven, T., Feussner, I., Gatz, C. (2012). Xenobiotic- and jasmonic acid-inducible signal transduction pathways have become interdependent at the Arabidopsis CYP81D11 promoter. Plant Physiology 159, 391–402.

Koussevitzky, S., Nott, A., Mockler, T.C., Hong, F., Sachetto-Martins, G., Surpin, M., Lim, J., Mittler, R., Chory, J. (2007). Signals from Chloroplasts Converge to Regulate Nuclear Gene Expression. Science 316, 715–719.

Kumagai, Y., Kikushima, M., Nakai, Y., Shimojo, N., Kunimoto, M. (2004). Neuronal nitric oxide synthase (NNOS) catalyzes one-electron reduction of 2,4,6-trinitrotoluene, resulting in decreased nitric oxide production and increased nNOS gene expression: implication for oxidative stress. Free Radical Biology and Medicine 37, 350–357.

Kumagai, Y., Wakayama, T., Li, S., Shinohara, A., Iwamatsu, A., Sun, G., Shimojo, N. (2000). ζ-Crystallin catalyzes the reductive activation of 2,4,6-trinitrotoluene to generate reactive oxygen species: a proposed mechanism for the induction of cataracts. FEBS Letters 478, 295–298.

Lachance, B., Renoux, A.Y., Sarrazin, M., Hawari, J., Sunahara, G.I. (2004). Toxicity and bioaccumulation of reduced TNT metabolites in the earthworm *Eisenia andrei* exposed to amended forest soil. Chemosphere 55, 1339–1348.

Lam, E., Benfey, P.N., Gilmartin, P.M., Fang, R.X., Chua, N.H. (1989). Site-specific mutations alter *in vitro* factor binding and change promoter expression pattern in transgenic plants. Proceedings of the National Academy of Sciences U.S.A. 86, 7890–7894.

Lam, E., Lam, Y.K. (1995). Binding site requirements and differential representation of TGF factors in nuclear ASF-1 activity. Nucleic Acids Research 23, 3778–3785.

Lange, M., Eisenhauer, N., Sierra, C.A., Bessler, H., Engels, C., Griffiths, R.I., Mellado-Vázquez, P.G., Malik, A.A., Roy, J., Scheu, S., Steinbeiss, S., Thomson, B.C., Trumbore, S.E., Gleixner, G. (2015). Plant diversity increases soil microbial activity and soil carbon storage. Nature Communications 6, 6707.

Larkin, M.A., Blackshields, G., Brown, N.P., Chenna, R., McGettigan, P.A., McWilliam, H., Valentin, F., Wallace, I.M., Wilm, A., Lopez, R., Thompson, J.D., Gibson, T.J., Higgins, D.G. (2007). Clustal W and Clustal X version 2.0. Bioinformatics 23, 2947–2948.

Lebel, E., Heifetz, P., Thorne, L., Uknes, S., Ryals, J., Ward, E. (1998). Functional analysis of regulatory sequences controlling PR-1 gene expression in Arabidopsis. The Plant Journal 16, 223–233.

Lee, D.W., Jung, C., Hwang, I. (2013). Cytosolic events involved in chloroplast protein targeting. Biochimica et Biophysica Acta (BBA) - Molecular Cell Research 1833, 245–252.

Lee, K.P., Kim, C., Landgraf, F., Apel, K. (2007). EXECUTER1- and EXECUTER2-dependent transfer of stress-related signals from the plastid to the nucleus of Arabidopsis thaliana. Proceedings of the National Academy of Sciences U.S.A. 104, 10270–10275.

Leitz, G., Kang, B.-H., Schoenwaelder, M.E.A., Staehelin, L.A. (2009). Statolith Sedimentation Kinetics and Force Transduction to the Cortical Endoplasmic Reticulum in Gravity-Sensing Arabidopsis Columella Cells. Plant Cell 21, 843–860.

Leon, J., Lawton, M.A., Raskin, I. (1995). Hydrogen Peroxide Stimulates Salicylic Acid Biosynthesis in Tobacco. Plant Physiology 108, 1673–1678.

Levine, A., Tenhaken, R., Dixon, R., Lamb, C. (1994). H_2O_2 from the oxidative burst orchestrates the plant hypersensitive disease resistance response. Cell 79, 583–593.

Li, F., Wang, J., Ma, C., Zhao, Y., Wang, Y., Hasi, A., Qi, Z. (2013). Glutamate Receptor-Like Channel3.3 Is Involved in Mediating Glutathione-Triggered Cytosolic Calcium Transients, Transcriptional Changes, and Innate Immunity Responses in Arabidopsis. Plant Physiology 162, 1497–1509.

Li, F., Wu, Q., Sun, Y., Wang, L., Yang, X., Meng, Q. (2010). Overexpression of chloroplastic monodehydroascorbate reductase enhanced tolerance to temperature and methyl viologen-mediated oxidative stresses. Physiologia Plantarum 139, 421–434.

Lindermayr, C., Sell, S., Müller, B., Leister, D., Durner, J. (2010). Redox Regulation of the NPR1-TGA1 System of Arabidopsis thaliana by Nitric Oxide. Plant Cell 22, 2894–2907.

Lin, L.S., Varner, J.E., 1991. Expression of Ascorbic Acid Oxidase in Zucchini Squash (Cucurbita pepo L.). Plant Physiol. 96, 159–165.

Lisenbee, C.S., Lingard, M.J., Trelease, R.N. (2005). Arabidopsis peroxisomes possess functionally redundant membrane and matrix isoforms of monodehydroascorbate reductase. The Plant Journal 43, 900–914.

Liu, X., Lam, E. (1994). Two binding sites for the plant transcription factor ASF-1 can respond to auxin treatments in transgenic tobacco. Journal of Biological Chemistry 269, 668–675.

Liu, Y., Ahn, J.-E., Datta, S., Salzman, R.A., Moon, J., Huyghues-Despointes, B., Pittendrigh, B., Murdock, L.L., Koiwa, H., Zhu-Salzman, K. (2005). Arabidopsis vegetative storage protein is an anti-insect acid phosphatase. Plant Physiology 139, 1545–1556.

Liu, Z., Butow, R.A. (2006). Mitochondrial Retrograde Signaling. Annual Review of Genetics 40, 159–185.

Li, X., Zhang, Y., Clarke, J.D., Li, Y., Dong, X. (1999). Identification and Cloning of a Negative Regulator of Systemic Acquired Resistance, SNI1, through a Screen for Suppressors of npr1-1. Cell 98, 329–339.

Loeffler, C., Berger, S., Guy, A., Durand, T., Bringmann, G., Dreyer, M., von Rad, U., Durner, J., Mueller, M.J. (2005). B1-Phytoprostanes Trigger Plant Defense and Detoxification Responses. Plant Physiology 137, 328 –340.

Loewus, F.A. (1999). Biosynthesis and metabolism of ascorbic acid in plants and of analogs of ascorbic acid in fungi. Phytochemistry 52, 193–210.

Lorenz, A. (2007). Bioengineering transgenic plants to detoxify nitroaromatic explosive compounds. Thesis. University of York, Department of Biology.

Lorenz, R., Bernhart, S.H., Siederdissen, C.H. zu, Tafer, H., Flamm, C., Stadler, P.F., Hofacker, I.L. (2011). ViennaRNA Package 2.0. Algorithms for Molecular Biology 6, 26.

Lunde, C., Baumann, U., Shirley, N., Drew, D., Fincher, G. (2006). Gene Structure and Expression Pattern Analysis of Three Monodehydroascorbate Reductase (MDHAR) genes in Physcomitrella patens: Implications for the evolution of the MDHAR family in plants. Plant Molecular Biology 60, 259–275.

Luwe, M., Takahama, U., Heber, U. (1993). Role of Ascorbate in Detoxifying Ozone in the Apoplast of Spinach (*Spinacia oleracea* L.) Leaves. Plant Physiology 101, 969–976.

Ma, Q. (2008). Xenobiotic-activated receptors: from transcription to drug metabolism to disease. Chemical Research in Toxicology 21, 1651–1671.

Margis, R., Dunand, C., Teixeira, F.K., Margis-Pinheiro, M. (2008). Glutathione peroxidase family – an evolutionary overview. FEBS Journal 275, 3959–3970.

Marshall, S.D.G., Putterill, J.J., Plummer, K.M., Newcomb, R.D. (2003). The carboxylesterase gene family from Arabidopsis thaliana. Journal of Molecular Evolution 57, 487–500.

Martel, R., Robertson, T.J., Doan, M.Q., Thiboutot, S., Ampleman, G., Provatas, A., Jenkins, T. (2007). 2,4,6-Trinitrotoluene in soil and groundwater under a waste lagoon at the former Explosives Factory Maribyrnong (EFM), Victoria, Australia. Environmental Geology 53, 1249–1259.

Matthes, M.C., Bruce, T.J.A., Ton, J., Verrier, P.J., Pickett, J.A., Napier, J.A. (2010). The transcriptome of cis-jasmone-induced resistance in Arabidopsis thaliana and its role in indirect defence. Planta 232, 1163–1180.

May, J.M., Cobb, C.E., Mendiratta, S., Hill, K.E., Burk, R.F. (1998). Reduction of the ascorbyl free radical to ascorbate by thioredoxin reductase. Journal of Biological Chemistry 273, 23039–23045.

May, T., Soll, J. (2000). 14-3-3 Proteins Form a Guidance Complex with Chloroplast Precursor Proteins in Plants. Plant Cell 12, 53–63.

McConn, M., Browse, J. (1996). The Critical Requirement for Linolenic Acid Is Pollen Development, Not Photosynthesis, in an Arabidopsis Mutant. Plant Cell 8, 403–416.

Mersmann, S., Bourdais, G., Rietz, S., Robatzek, S. (2010). Ethylene Signaling Regulates Accumulation of the FLS2 Receptor and Is Required for the Oxidative Burst Contributing to Plant Immunity. Plant Physiology 154, 391–400.

Meyer, Y., Reichheld, J.P., Vignols, F. (2005). Thioredoxins in Arabidopsis and other plants. Photosynthesis Research 86, 419–433.

Mhamdi, A., Noctor, G., Baker, A. (2012). Plant catalases: Peroxisomal redox guardians. Archives of Biochemistry and Biophysics, Catalases and Hydrogen Peroxide Metabolism 525, 181–194.

Miyake, C., Asada, K. (1994). Ferredoxin-Dependent Photoreduction of the Monodehydroascorbate Radical in Spinach Thylakoids. Plant Cell Physiology 35, 539–549.

Miyake, C., Michihata, F., Asada, K. (1991). Scavenging of Hydrogen Peroxide in Prokaryotic and Eukaryotic Algae: Acquisition of Ascorbate Peroxidase during the Evolution of Cyanobacteria. Plant Cell Physiology 32, 33–43.

Miyake, C., Schreiber, U., Hormann, H., Sano, S., Kozi, A. (1998). The FAD-Enzyme Monodehydroascorbate Radical Reductase Mediates Photoproduction of Superoxide Radicals in Spinach Thylakoid Membranes. Plant and Cell Physiology 39, 821 –829.

Mochizuki, N., Tanaka, R., Tanaka, A., Masuda, T., Nagatani, A. (2008). The steady-state level of Mg-protoporphyrin IX is not a determinant of plastid-to-nucleus signaling in Arabidopsis. Proceedings of the National Academy of Sciences U.S.A. 105, 15184–15189.

Mockler, T.C., Michael, T.P., Priest, H.D., Shen, R., Sullivan, C.M., Givan, S.A., McEntee, C., Kay, S.A., Chory, J. (2007). The DIURNAL project: DIURNAL and circadian expression profiling, model-based pattern matching, and promoter analysis. Cold Spring Harbor Symposia on Quantitative Biology 72, 353–363.

Moulin, M., McCormac, A.C., Terry, M.J., Smith, A.G. (2008). Tetrapyrrole profiling in Arabidopsis seedlings reveals that retrograde plastid nuclear signaling is not due to Mg-protoporphyrin IX accumulation. Proceedings of the National Academy of Sciences U.S.A. 105, 15178–15183.

Mueller, S., Hilbert, B., Dueckershoff, K., Roitsch, T., Krischke, M., Mueller, M.J., Berger, S. (2008). General Detoxification and Stress Responses Are Mediated by Oxidized Lipids through TGA Transcription Factors in Arabidopsis. The Plant Cell 20, 768 –785.

Mullineaux, P.M., Baker, N.R. (2010). Oxidative Stress: Antagonistic Signaling for Acclimation or Cell Death? Plant Physiology 154, 521–525.

Mur, L. a. J., Kenton, P., Draper, J. (2005). In planta measurements of oxidative bursts elicited by avirulent and virulent bacterial pathogens suggests that H_2O_2 is insufficient to elicit cell death in tobacco. Plant, Cell & Environment 28, 548–561.

Murmu, J., Bush, M.J., DeLong, C., Li, S., Xu, M., Khan, M., Malcolmson, C., Fobert, P.R., Zachgo, S., Hepworth, S.R. (2010). Arabidopsis Basic Leucine-Zipper Transcription Factors TGA9 and TGA10 Interact with Floral Glutaredoxins ROXY1 and ROXY2 and Are Redundantly Required for Anther Development. Plant Physiology 154, 1492–1504.

Naidu, K.A. (2003). Vitamin C in human health and disease is still a mystery ? An overview. Nutrition Journal 2, 7.

Ndamukong, I., Abdallat, A.A., Thurow, C., Fode, B., Zander, M., Weigel, R., Gatz, C. (2007). SA-inducible Arabidopsis glutaredoxin interacts with TGA factors and suppresses JA-responsive PDF1.2 transcription. The Plant Journal 50, 128–139.

Newton, G.L., Javor, B. (1985). gamma-Glutamylcysteine and thiosulfate are the major low-molecular-weight thiols in halobacteria. Journal of Bacteriology 161, 438–441.

Noctor, G. (2015). Lighting the fuse on toxic TNT. Science 349, 1052–1053.

Noctor, G., Arisi, A.-C.M., Jouanin, L., Foyer, C.H. (1998). Manipulation of Glutathione and Amino Acid Biosynthesis in the Chloroplast. Plant Physiology 118, 471–482.

Noctor, G., Mhamdi, A., Chaouch, S., Han, Y., Neukermans, J., Marquez-garcia, B., Queval, G., Foyer, C.H. (2012). Glutathione in plants: an integrated overview. Plant, Cell & Environment 35, 454–484.

Obara, K., Sumi, K., Fukuda, H. (2002). The use of multiple transcription starts causes the dual targeting of Arabidopsis putative monodehydroascorbate reductase to both mitochondria and chloroplasts. Plant and Cell Physiology 43, 697–705.

Olsen, A.N., Ernst, H.A., Leggio, L.L., Skriver, K. (2005). NAC transcription factors: structurally distinct, functionally diverse. Trends in Plant Science 10, 79-87.

Paden, N.E., Smith, E.E., Maul, J.D., Kendall, R.J. (2011). Effects of chronic 2,4,6,-trinitrotoluene, 2,4-dinitrotoluene, and 2,6-dinitrotoluene exposure on developing bullfrog (*Rana catesbeiana*) tadpoles. Ecotoxicology and Environmental Safety 74, 924–928.

Pape, S., Thurow, C., Gatz, C. (2010). The Arabidopsis *PR-1* Promoter Contains Multiple Integration Sites for the Coactivator NPR1 and the Repressor SNI1. Plant Physiology 154, 1805–1818.

Parisy, V., Poinssot, B., Owsianowski, L., Buchala, A., Glazebrook, J., Mauch, F. (2007). Identification of PAD2 as a γ-glutamylcysteine synthetase highlights the importance of glutathione in disease resistance of Arabidopsis. The Plant Journal 49, 159–172.

Park, J.-H., Halitschke, R., Kim, H.B., Baldwin, I.T., Feldmann, K.A., Feyereisen, R. (2002). A knock-out mutation in allene oxide synthase results in male sterility and defective wound signal transduction in Arabidopsis due to a block in jasmonic acid biosynthesis. The Plant Journal 31, 1–12.

Park, S.K., Jung, Y.J., Lee, J.R., Lee, Y.M., Jang, H.H., Lee, S.S., Park, J.H., Kim, S.Y., Moon, J.C., Lee, S.Y., Chae, H.B., Shin, M.R., Jung, J.H., Kim, M.G., Kim, W.Y., Yun, D.-J., Lee, K.O., Lee, S.Y. (2009). Heat-Shock and Redox-Dependent Functional Switching of an h-Type Arabidopsis Thioredoxin from a Disulfide Reductase to a Molecular Chaperone. Plant Physiology 150, 552–561.

Park, S.-W., Li, W., Viehhauser, A., He, B., Kim, S., Nilsson, A.K., Andersson, M.X., Kittle, J.D., Ambavaram, M.M.R., Luan, S., Esker, A.R., Tholl, D., Cimini, D., Ellerström, M., Coaker, G., Mitchell, T.K., Pereira, A., Dietz, K.-J., Lawrence, C.B. (2013). Cyclophilin 20-3 relays a 12-oxo-phytodienoic acid signal during stress responsive regulation of cellular redox homeostasis. Proceedings of the National Academy of Sciences U.S.A. 110, 9559–9564.

Pascussi, J.-M., Gerbal-Chaloin, S., Duret, C., Daujat-Chavanieu, M., Vilarem, M.-J., Maurel, P. (2008). The Tangle of Nuclear Receptors that Controls Xenobiotic Metabolism and Transport: Crosstalk and Consequences. Annual Review of Pharmacology and Toxicology 48, 1–32.

Peer, W.A., Brown, D.E., Tague, B.W., Muday, G.K., Taiz, L., Murphy, A.S. (2001). Flavonoid Accumulation Patterns of Transparent Testa Mutants of Arabidopsis. Plant Physiology 126, 536–548.

Pennington, J.C., Hayes, C.A., Myers, K.F., Ochman, M., Gunnison, D., Felt, D.R., McCormick, E.F. (1995). Fate of 2,4,6-trinitrotoluene in a simulated compost system. Chemosphere 30, 429–438.

Pennington, J.C., Jenkins, T.F., Ampleman, G., Thiboutot, S., Brannon, J.M., Hewitt, A.D., Lewis, J., Brochu, S., Diaz, E., Walsh, M.R., Walsh, M.E., Taylor, S., Lynch, J.C., Clausen, J., Ranney, T.A., Ramsey, C.A., Hayes, C.A., Grant, C.L., Collins, C.M., Bigl, S.R., Yost, S., Dontsova, K. (2006). Distribution and fate of energetics on DoD test and training ranges: final report. US Army Corps of Engineers, Engineer Research and Development Center. Report ERDC TR-06-13/ER-1155-FR. Available: https://www.serdp-estcp.org/Program-Areas/Environmental-Restoration/Contaminants-on-Ranges/Characterizing-Fate-and-Transport/ER-1155/ER-1155-FR/%28modified%29/15May2015

Perry, A.J., Hulett, J.M., Likić, V.A., Lithgow, T., Gooley, P.R. (2006). Convergent Evolution of Receptors for Protein Import into Mitochondria. Current Biology 16, 221–229.

Phillips McDougall (2013). R&D trends for chemical crop protection products and the position of the European Market. A consultancy study undertaken for the European Crop Protection Agency. Available: http://www.ecpa.eu/information-page/regulatory-affairs/publications-regulatory-affairs.

Pichtel, J. (2012). Distribution and Fate of Military Explosives and Propellants in Soil: A Review. Applied and Environmental Soil Science 2012, e617236.

Pignocchi, C., Foyer, C.H. (2003). Apoplastic ascorbate metabolism and its role in the regulation of cell signalling. Current Opinion in Plant Biology 6, 379–389.

Pitsch, N.T., Witsch, B., Baier, M. (2010). Comparison of the chloroplast peroxidase system in the chlorophyte *Chlamydomonas reinhardtii*, the bryophyte *Physcomitrella patens*, the lycophyte *Selaginella moellendorffii* and the seed plant *Arabidopsis thaliana*. BMC Plant Biology 10, 133.

Planavsky, N.J., Asael, D., Hofmann, A., Reinhard, C.T., Lalonde, S.V., Knudsen, A., Wang, X., Ossa Ossa, F., Pecoits, E., Smith, A.J.B., Beukes, N.J., Bekker, A., Johnson, T.M., Konhauser, K.O., Lyons, T.W., Rouxel, O.J. (2014). Evidence for oxygenic photosynthesis half a billion years before the Great Oxidation Event. Nature Geosciences 7, 283–286.

POST (Parliamentary Office of Science and Technology) (2015). POSTNOTE Herbicide Resistance. Reference POST-PN-0501. Available: http://researchbriefings.parliament.uk/ResearchBriefing/Summary/POST-PN-0501.

Prescott, A.G., John, P. (1996). DIOXYGENASES: Molecular Structure and Role in Plant Metabolism. Annual Review of Plant Physiology and Plant Molecular Biology 47, 245–271.

Qin, X.F., Holuigue, L., Horvath, D.M., Chua, N.H. (1994). Immediate early transcription activation by salicylic acid via the cauliflower mosaic virus *as-1* element. Plant Cell 6, 863–874.

Queval, G., Noctor, G. (2007). A plate reader method for the measurement of NAD, NADP, glutathione, and ascorbate in tissue extracts: Application to redox profiling during Arabidopsis rosette development. Analytical Biochemistry 363, 58–69.

Radhamony, R.N., Theg, S.M. (2006). Evidence for an ER to Golgi to chloroplast protein transport pathway. Trends in Cell Biology 16, 385–387.

Ramel, F., Sulmon, C., Serra, A.-A., Gouesbet, G., Couée, I. (2012). Xenobiotic sensing and signalling in higher plants. Journal of Experimental Botany 63, 3999-4014.

Rea, P.A., Vatamaniuk, O.K., Rigden, D.J., 2004. Weeds, Worms, and More. Papain's Long-Lost Cousin, Phytochelatin Synthase. Plant Physiology 136, 2463–2474.

Rentel, M.C., Lecourieux, D., Ouaked, F., Usher, S.L., Petersen, L., Okamoto, H., Knight, H., Peck, S.C., Grierson, C.S., Hirt, H., Knight, M.R. (2004). OXI1 kinase is necessary for oxidative burst-mediated signalling in Arabidopsis. Nature 427, 858–861.

Rochon, A., Boyle, P., Wignes, T., Fobert, P.R., Després, C. (2006). The Coactivator Function of Arabidopsis NPR1 Requires the Core of Its BTB/POZ Domain and the Oxidation of C-Terminal Cysteines. Plant Cell 18, 3670–3685.

Ross, A.F. (1961). Systemic acquired resistance induced by localized virus infections in plants. Virology 14, 340–358.

Ross, J., Li, Y., Lim, E., Bowles, D.J. (2001). Higher plant glycosyltransferases. Genome Biology 2, reviews3004.

Rouhier, N. (2010). Plant glutaredoxins: pivotal players in redox biology and iron-sulphur centre assembly. New Phytologist 186, 365–372.

Rylott, E.L., Bruce, N.C. (2009). Plants disarm soil: engineering plants for the phytoremediation of explosives. Trends in Biotechnology 27, 73–81.

Rylott, E.L., Budarina, M.V., Barker, A., Lorenz, A., Strand, S.E., Bruce, N.C. (2011a). Engineering plants for the phytoremediation of RDX in the presence of the co-contaminating explosive TNT. New Phytologist 192, 405–413.

Rylott, E.L., Jackson, R.G., Edwards, J., Womack, G.L., Seth-Smith, H.M., Rathbone, D.A., Strand, S.E., Bruce, N.C. (2006). An explosive-degrading cytochrome P450 activity and its targeted application for the phytoremediation of RDX. Nature Biotechnology 24, 216–219.

Rylott, E.L., Johnston, E.J., Bruce, N.C. (2015). Harnessing microbial gene pools to remediate persistent organic pollutants using genetically modified plants—a viable technology? Journal of Experimental Botany, online ahead of print.

Rylott, E.L., Lorenz, A., Bruce, N.C. (2011b). Biodegradation and biotransformation of explosives. Current Opinion in Biotechnology 22, 434–440.

Sakihama, Y., Mano, J., Sano, S., Asada, K., Yamasaki, H. (2000). Reduction of Phenoxyl Radicals Mediated by Monodehydroascorbate Reductase. Biochemical and Biophysical Research Communications 279, 949–954.

Sander, J.D., Joung, J.K. (2014). CRISPR-Cas systems for editing, regulating and targeting genomes. Nature Biotechnology 32, 347–355.

Sandermann Jr., H. (1992). Plant metabolism of xenobiotics. Trends in Biochemical Sciences 17, 82–84.

Sano, S., Miyake, C., Mikami, B., Asada, K. (1995). Molecular Characterization of Monodehydroascorbate Radical Reductase from Cucumber Highly Expressed in Escherichia coli. Journal of Biological Chemistry 270, 21354 –21361.

Sano, S., Tao, S., Endo, Y., Inaba, T., Hossain, M.A., Miyake, C., Matsuo, M., Aoki, H., Asada, K., Saito, K. (2005). Purification and cDNA cloning of chloroplastic monodehydroascorbate reductase from spinach. Bioscience, Biotechnology, and Biochemistry 69, 762–772.

Schlaeppi, K., Bodenhausen, N., Buchala, A., Mauch, F., Reymond, P. (2008). The glutathione-deficient mutant pad2-1 accumulates lower amounts of glucosinolates and is more susceptible to the insect herbivore *Spodoptera littoralis*. The Plant Journal 55, 774–786.

Schmidt, O., Harbauer, A.B., Rao, S., Eyrich, B., Zahedi, R.P., Stojanovski, D., Schönfisch, B., Guiard, B., Sickmann, A., Pfanner, N., Meisinger, C. (2011). Regulation of mitochondrial protein import by cytosolic kinases. Cell 144, 227–239.

Schneider, C.A., Rasband, W.S., Eliceiri, K.W. (2012). NIH Image to ImageJ: 25 years of image analysis. Nature Methods 9, 671–675.

Schneider-Poetsch, T., Ju, J., Eyler, D.E., Dang, Y., Bhat, S., Merrick, W.C., Green, R., Shen, B., Liu, J.O. (2010). Inhibition of eukaryotic translation by cycloheximide and lactimidomycin. Nature Chemical Biology 6, 209-217.

Schoenmuth, B.W., Pestemer, W. (2004). Dendroremediation of trinitrotoluene (TNT) Part 2: Fate of radio-labelled TNT in trees. Environmental Science & Pollution Research 11, 331–339.

Schwarzländer, M., Fricker, M.D., Sweetlove, L.J. (2009). Monitoring the in vivo redox state of plant mitochondria: Effect of respiratory inhibitors, abiotic stress and assessment of recovery from oxidative challenge. Biochimica et Biophysica Acta (BBA) - Bioenergetics, Mitochondrial Physiology and Pathology 1787, 468–475.

Schwarzländer, M., König, A.-C., Sweetlove, L.J., Finkemeier, I. (2012). The impact of impaired mitochondrial function on retrograde signalling: a meta-analysis of transcriptomic responses. Journal of Experimental Botany 63, 1735–1750.

Sekito, T., Thornton, J., Butow, R.A. (2000). Mitochondria-to-nuclear signaling is regulated by the subcellular localization of the transcription factors Rtg1p and Rtg3p. Molecular Biology of the Cell 11, 2103–2115.

Senda, K., Ogawa, K. (2004). Induction of PR-1 Accumulation Accompanied by Runaway Cell Death in the *lsd1* Mutant of Arabidopsis is Dependent on Glutathione Levels but Independent of the Redox State of Glutathione. Plant Cell Physiology 45, 1578–1585.

Sens, C., Scheidemann, P., Klunk, A., Werner, D. (1998). Distribution of ^{14}C-TNT and derivatives in different biochemical compartments of *Phaseolus vulgaris*. Environmental Science and Pollution Research International 5, 202–208.

Senthil-Kumar, M., Mysore, K.S. (2013). Nonhost Resistance Against Bacterial Pathogens: Retrospectives and Prospects. Annual Review of Phytopathology 51, 407–427.

Sevilla, F., Camejo, D., Ortiz-Espín, A., Calderón, A., Lázaro, J.J., Jiménez, A. (2015). The thioredoxin/peroxiredoxin/sulfiredoxin system: current overview on its redox function in plants and regulation by reactive oxygen and nitrogen species. Journal of Experimental Botany 66, 2945–2955.

Shaikhali, J., Heiber, I., Seidel, T., Ströher, E., Hiltscher, H., Birkmann, S., Dietz, K.-J., Baier, M. (2008). The redox-sensitive transcription factor Rap2.4a controls nuclear expression of 2-Cys peroxiredoxin A and other chloroplast antioxidant enzymes. BMC Plant Biology 8, 48.

Shaikhali, J., Norén, L., Barajas-López, J. de D., Srivastava, V., König, J., Sauer, U.H., Wingsle, G., Dietz, K.-J., Strand, Å. (2012). Redox-mediated Mechanisms Regulate DNA Binding Activity of the G-group of Basic Region Leucine Zipper (bZIP) Transcription Factors in Arabidopsis. Journal of Biological Chemistry 287, 27510–27525.

Shearer, H.L., Cheng, Y.T., Wang, L., Liu, J., Boyle, P., Després, C., Zhang, Y., Li, X., Fobert, P.R. (2012). Arabidopsis Clade I TGA Transcription Factors Regulate Plant Defenses in an NPR1-Independent Fashion. Molecular Plant-Microbe Interactions 25, 1459–1468.

Singer, A.C., Crowley, D.E., Thompson, I.P. (2003). Secondary plant metabolites in phytoremediation and biotransformation. Trends in Biotechnology 21, 123–130.

Skipsey, M., Knight, K.M., Brazier-Hicks, M., Dixon, D.P., Steel, P.G., Edwards, R. (2011). Xenobiotic Responsiveness of Arabidopsis thaliana to a Chemical Series Derived from a Herbicide Safener. Journal of Biological Chemistry 286, 32268 –32276.

Spoel, S.H., Loake, G.J. (2011). Redox-based protein modifications: the missing link in plant immune signalling. Current Opinion in Plant Biology, Biotic interactions 14, 358–364.

Stael, S., Kmiecik, P., Willems, P., Van Der Kelen, K., Coll, N.S., Teige, M., Van Breusegem, F. (2015). Plant innate immunity– sunny side up? Trends in Plant Science 20, 3–11.

Stotz, H.U., Mueller, S., Zoeller, M., Mueller, M.J., Berger, S. (2013). TGA transcription factors and jasmonate-independent COI1 signalling regulate specific plant responses to reactive oxylipins. Journal of Experimental Botany 64, 963-975.

Tada, Y., Spoel, S.H., Pajerowska-Mukhtar, K., Mou, Z., Song, J., Wang, C., Zuo, J., Dong, X. (2008). Plant Immunity Requires Conformational Charges of NPR1 via S-Nitrosylation and Thioredoxins. Science 321, 952–956.

TAIR (The Arabidopsis Information Resource) (2015). Online resource. Available: https://www.arabidopsis.org/

Taira, Y., Okegawa, Y., Sugimoto, K., Abe, M., Miyoshi, H., Shikanai, T. (2013). Antimycin A-like molecules inhibit cyclic electron transport around photosystem I in ruptured chloroplasts. FEBS Open Bio 3, 406–410.

Takahama, U. (1993). Redox state of ascorbic acid in the apoplast of stems of *Kalanchoë daigremontiana*. Physiologia Plantarum 89, 791–798.

Taki, N., Sasaki-Sekimoto, Y., Obayashi, T., Kikuta, A., Kobayashi, K., Ainai, T., Yagi, K., Sakurai, N., Suzuki, H., Masuda, T., Takamiya, K.-I., Shibata, D., Kobayashi, Y., Ohta, H. (2005). 12-Oxo-Phytodienoic Acid Triggers Expression of a Distinct Set of Genes and Plays a Role in Wound-Induced Gene Expression in Arabidopsis. Plant Physiology 139, 1268–1283.

Taylor, S., Hewitt, A., Lever, J., Hayes, C., Perovich, L., Thorne, P., Daghlian, C. (2004). TNT particle size distributions from detonated 155-mm howitzer rounds. Chemosphere 55, 357–367.

Thoma, I., Loeffler, C., Sinha, A.K., Gupta, M., Krischke, M., Steffan, B., Roitsch, T., Mueller, M.J. (2003). Cyclopentenone isoprostanes induced by reactive oxygen species trigger defense gene activation and phytoalexin accumulation in plants. The Plant Journal 34, 363–375.

Tolson, A.H., Wang, H. (2010). Regulation of drug-metabolizing enzymes by xenobiotic receptors: PXR and CAR. Advanced Drug Delivery Reviews, Development of Novel Therapeutic Strategy by Regulating the Nuclear Hormone Receptors 62, 1238–1249.

Torres, M.A., Dangl, J.L., Jones, J.D.G. (2002). Arabidopsis gp91phox homologues AtrbohD and AtrbohF are required for accumulation of reactive oxygen intermediates in the plant defense response. Proceedings of the National Academy of Sciences U.S.A. 99, 517–522.

Travis, E.R., Bruce, N.C., Rosser, S.J. (2008a). Short term exposure to elevated trinitrotoluene concentrations induced structural and functional changes in the soil bacterial community. Environmental Pollution 153, 432–439.

Travis, E.R., Bruce, N.C., Rosser, S.J. (2008b). Microbial and plant ecology of a long-term TNT-contaminated site. Environmental Pollution 153, 119–126.

Trumpolt, C.W., Crain, M., Cullison, G.D., Flanagan, S.J.P., Siegel, L., Lathrop, S. (2005). Perchlorate: Sources, uses, and occurrences in the environment. Remediation 16, 65–89.

United States General Accountability Office (2004). Department of Defense Operational Ranges, More Reliable Cleanup Cost Estimates and a Proactive Approach to Identifying Contamination Are Needed (Report to Congressional Requesters). Reference GAO-04-601. Available: http://www.gao.gov/products/GAO-04-601

US EPA (Environmental Protection Agency) (2014a). Technical Fact Sheet- 2,4,6-Trinitrotoluene (TNT). Reference EPA 505-F-14-009. Available: http://www2.epa.gov/fedfac/technical-fact-sheet-246-trinitrotoluene-tnt

US EPA (Environmental Protection Agency) (2014b). Technical Fact Sheet- Hexahydro-1,3,5-trinitro-1,3,5-triazine (RDX). Reference EPA 505-F-14.008. Available: http://www2.epa.gov/fedfac/technical-fact-sheet-hexahydro-135-trinitro-135-triazine-rdx

US EPA (Environmental Protection Agency) (2014c). Technical Fact Sheet- Perchlorate. Reference EPA 505-F-14-003. Available: http://www2.epa.gov/fedfac/technical-fact-sheet-perchlorate

US EPA (Environmental Protection Agency) (2012). Technical Fact Sheet - 2,4,6-trinitrotoluene (TNT). Reference EPA 505-F-11-011.

US EPA (Environmental Protection Agency) (2015a). Regional Screening Level Summary Table. Updated Jan 2015. Available: http://www.epa.gov/reg3hwmd/risk/human/rb-concentration_table/Generic_Tables/docs/master_sl_table_run_JAN2015.pdf.

US EPA (Environmental Protection Agency) (2015b). Using Phytoremediation to Clean Up Sites. Internet resource. Accessed 22nd July 2015. Available: http://www.epa.gov/superfund/accomp/news/phyto.htm

Valério, L., De Meyer, M., Penel, C., Dunand, C. (2004). Expression analysis of the Arabidopsis peroxidase multigenic family. Phytochemistry 65, 1331–1342.

Vanacker, H., Carver, T.L.W., Foyer, C.H. (1998). Pathogen-Induced Changes in the Antioxidant Status of the Apoplast in Barley Leaves. Plant Physiology 117, 1103–1114.

Vanderauwera, S., Zimmermann, P., Rombauts, S., Vandenabeele, S., Langebartels, C., Gruissem, W., Inzé, D., Breusegem, F.V. (2005). Genome-Wide Analysis of Hydrogen Peroxide-Regulated Gene Expression in Arabidopsis Reveals a High Light-Induced Transcriptional Cluster Involved in Anthocyanin Biosynthesis. Plant Physiology 139, 806–821.

van Loon, L.C., Rep, M., Pieterse, C.M.J. (2006). Significance of Inducible Defense-related Proteins in Infected Plants. Annual Review of Phytopathology 44, 135–162.

Verrier, P.J., Bird, D., Burla, B., Dassa, E., Forestier, C., Geisler, M., Klein, M., Kolukisaoglu, U., Lee, Y., Martinoia, E., Murphy, A., Rea, P.A., Samuels, L., Schulz, B., Spalding, E.J., Yazaki, K., Theodoulou, F.L. (2008). Plant ABC proteins- a unified nomenclature and updated inventory. Trends in Plant Science 13, 151–159.

Vivancos, P.D., Dong, Y., Ziegler, K., Markovic, J., Pallardó, F.V., Pellny, T.K., Verrier, P.J., Foyer, C.H. (2010). Recruitment of glutathione into the nucleus during cell proliferation adjusts whole-cell redox homeostasis in Arabidopsis thaliana and lowers the oxidative defence shield. The Plant Journal 64, 825–838.

Wagner, D., Przybyla, D., Camp, R. op den, Kim, C., Landgraf, F., Lee, K.P., Würsch, M., Laloi, C., Nater, M., Hideg, E., Apel, K. (2004). The Genetic Basis of Singlet Oxygen–Induced Stress Responses of Arabidopsis thaliana. Science 306, 1183–1185.

Wasternack, C., Hause, B. (2013). Jasmonates: biosynthesis, perception, signal transduction and action in plant stress response, growth and development. An update to the 2007 review in. Annals of Botany. Annals of Botany 111, 1021–1058.

Waters, M.T., Wang, P., Korkaric, M., Capper, R.G., Saunders, N.J., Langdale, J.A. (2009). GLK Transcription Factors Coordinate Expression of the Photosynthetic Apparatus in Arabidopsis. Plant Cell 21, 1109–1128.

Weigel, D., Ahn, J.H., Blázquez, M.A., Borevitz, J.O., Christensen, S.K., Fankhauser, C., Ferrándiz, C., Kardailsky, I., Malancharuvil, E.J., Neff, M.M., Nguyen, J.T., Sato, S., Wang, Z.-Y., Xia, Y., Dixon, R.A., Harrison, M.J., Lamb, C.J., Yanofsky, M.F., Chory, J. (2000). Activation Tagging in Arabidopsis. Plant Physiology 122, 1003–1014.

Wheeler, G., Ishikawa, T., Pornsaksit, V., Smirnoff, N. (2015). Evolution of alternative biosynthetic pathways for vitamin C following plastid acquisition in photosynthetic eukaryotes. eLife Sciences 4, e06369.

White, R.F. (1979). Acetylsalicylic acid (aspirin) induces resistance to tobacco mosaic virus in tobacco. Virology 99, 410–412.

Williams, R.E., Bruce, N.C. (2002). New uses for an Old Enzyme- the Old Yellow Enzyme family of flavoenzymes. Microbiology 148, 1607–1614.

Winterbourn, C.C. (2014). The challenges of using fluorescent probes to detect and quantify specific reactive oxygen species in living cells. Biochimica et Biophysica Acta 1840, 730–738.

Woodson, J.D., Chory, J. (2008). Coordination of gene expression between organellar and nuclear genomes. Nature Reviews Genetics 9, 383–395.

Wood, Z.A., Poole, L.B., Karplus, P.A. (2003). Peroxiredoxin Evolution and the Regulation of Hydrogen Peroxide Signaling. Science 300, 650–653.

Xia, D., Yu, C.A., Kim, H., Xia, J.Z., Kachurin, A.M., Zhang, L., Yu, L., Deisenhofer, J. (1997). Crystal structure of the cytochrome bc1 complex from bovine heart mitochondria. Science 277, 60–66.

Xiang, C., Miao, Z.-H., Lam, E. (1996). Coordinated activation of as-1-type elements and a tobacco glutathione S-transferase gene by auxins, salicylic acid, methyl-jasmonate and hydrogen peroxide. Plant Molecular Biology 32, 415–426.

Xia, X.-J., Zhou, Y.-H., Shi, K., Zhou, J., Foyer, C.H., Yu, J.-Q. (2015). Interplay between reactive oxygen species and hormones in the control of plant development and stress tolerance. Journal of Experimental Botany, erv089v1 online

Yamazaki, I., Piette, L.H. (1961). Mechanism of free radical formation and disappearance during the ascorbic acid oxidase and peroxidase reactions. Biochimica et Biophysica Acta 50, 62–69.

Yan, X., Khan, S., Hase, T., Emes, M.J., Bowsher, C.G. (2006). Differential uptake of photosynthetic and non-photosynthetic proteins by pea root plastids. FEBS Letters 580, 6509–6512.

Yazdanbakhsh, N., Fisahn, J. (2011). Mutations in leaf starch metabolism modulate the diurnal root growth profiles of *Arabidopsis thaliana*. Plant Signaling and Behavior 6, 995–998.

Yin, L., Wang, S., Eltayeb, A.E., Uddin, M.I., Yamamoto, Y., Tsuji, W., Takeuchi, Y., Tanaka, K. (2010). Overexpression of dehydroascorbate reductase, but not monodehydroascorbate reductase, confers tolerance to aluminum stress in transgenic tobacco. Planta 231, 609–621.

Yogev, O., Pines, O. (2011). Dual targeting of mitochondrial proteins: Mechanism, regulation and function. Biochimica et Biophysica Acta (BBA) - Biomembranes 1808, 1012–1020.

Yu, X.-Z., Gu, J.-D., Li, T.-P., 2008. Availability of Ferrocyanide and Ferricyanide Complexes as a Nitrogen Source to Cyanogenic Plants. Archives of Environmental Contamination and Toxicology 55, 229–237.

Zander, M., La Camera, S., Lamotte, O., Métraux, J.-P., Gatz, C. (2010). *Arabidopsis thaliana* class-II TGA transcription factors are essential activators of jasmonic acid/ethylene-induced defense responses. The Plant Journal 61, 200–210.

Zander, M., Thurow, C., Gatz, C. (2014). TGA Transcription Factors Activate the Salicylic Acid-Suppressible Branch of the Ethylene-Induced Defense Program by Regulating ORA59 Expression. Plant Physiology 165, 1671–1683.

Zechmann, B., Müller, M. (2010). Subcellular compartmentation of glutathione in dicotyledonous plants. Protoplasma 246, 15–24.

Zechmann, B., Stumpe, M., Mauch, F. (2011). Immunocytochemical determination of the subcellular distribution of ascorbate in plants. Planta 233, 1–12.

Zhang, Y., Fan, W., Kinkema, M., Li, X., Dong, X. (1999). Interaction of NPR1 with basic leucine zipper protein transcription factors that bind sequences required for salicylic acid induction of the PR-1 gene. Proceedings of the National Academy of Sciences U.S.A. 96, 6523–6528.

Zhang, Y., Tessaro, M.J., Lassner, M., Li, X. (2003). Knockout Analysis of Arabidopsis Transcription Factors TGA2, TGA5, and TGA6 Reveals Their Redundant and Essential Roles in Systemic Acquired Resistance. Plant Cell 15, 2647–2653.

Zheng, X., Spivey, N.W., Zeng, W., Liu, P.-P., Fu, Z.Q., Klessig, D.F., He, S.Y., Dong, X. (2012). Coronatine Promotes *Pseudomonas syringae* Virulence in Plants by Activating a Signaling Cascade that Inhibits Salicylic Acid Accumulation. Cell Host & Microbe 11, 587–596.

Zhou, J.-M., Trifa, Y., Silva, H., Pontier, D., Lam, E., Shah, J., Klessig, D.F. (2000). NPR1 Differentially Interacts with Members of the TGA/OBF Family of Transcription Factors That Bind an Element of the *PR-1* Gene Required for Induction by Salicylic Acid. Molecular Plant-Microbe Interactions 13, 191–202.

Zipfel, C. (2014). Plant pattern-recognition receptors. Trends in Immunology 35, 345–351.

Zitting, A., Szumańska, G., Nickels, J., Savolainen, H. (1982). Acute toxic effects of trinitrotoluene on rat brain, liver and kidney: role of radical production. Archives of Toxicology 51, 53–64.